

In the Name of God

Journal of Information Systems & Telecommunication

Vol. 7, No. 1, January-March 2019, Serial Number 25

Research Institute for Information and Communication Technology
Iranian Association of Information and Communication Technology
Affiliated to: Academic Center for Education, Culture and Research (ACECR)

Manager-in-Charge: Habibollah Asghari, ACECR, Iran

Editor-in-Chief: Masoud Shafiee, Amir Kabir University of Technology, Iran

Editorial Board

Dr. Abdolali Abdipour, Professor, Amirkabir University of Technology, Iran

Dr. Mahmoud Naghibzadeh, Professor, Ferdowsi University, Iran

Dr. Zabih Ghasemlooy, Professor, Northumbria University, UK

Dr. Mahmoud Moghavvemi, Professor, University of Malaya (UM), Malaysia

Dr. Ali Akbar Jalali, Professor, Iran University of Science and Technology, Iran

Dr. Alireza Montazemi, Professor, McMaster University, Canada

Dr. Ramezan Ali Sadeghzadeh, Professor, Khajeh Nasireddin Toosi University of Technology, Iran

Dr. Hamid Reza Sadegh Mohammadi, Associate Professor, ACECR, Iran

Dr. Sha'ban Elahi, Associate Professor, Tarbiat Modares University, Iran

Dr. Shohreh Kasaei, Professor, Sharif University of Technology, Iran

Dr. Mehrnoush Shamsfard, Associate Professor, Shahid Beheshti University, Iran

Dr. Ali Mohammad-Djafari, Associate Professor, Le Centre National de la Recherche Scientifique (CNRS), France

Dr. Rahim Saeidi, Assistant Professor, Aalto University, Finland

Executive Manager: Shirin Gilaki

Executive Assistants: Ali Mokhtarani, Mahdokht Ghahari

Print ISSN: 2322-1437

Online ISSN: 2345-2773

Publication License: 91/13216

Editorial Office Address: No.5, Saeedi Alley, Kalej Intersection., Enghelab Ave., Tehran, Iran,

P.O.Box: 13145-799

Tel: (+9821) 88930150 Fax: (+9821) 88930157

E-mail: infojist@gmail.com

URL: www.jist.ir

Indexed by:

- SCOPUS

www.Scopus.com

- Index Copernicus International

www.indexcopernicus.com

- Islamic World Science Citation Center (ISC)

www.isc.gov.ir

- Directory of open Access Journals

www.Doaj.org

- Scientific Information Database (SID)

www.sid.ir

- Regional Information Center for Science and Technology (RICEST)

www.ricest.ac.ir

- Iranian Magazines Databases

www.magiran.com

Publisher:

Regional Information Center for Science and Technology (RICEST)

Islamic World Science Citation Center (ISC)

This Journal is published under scientific support of
Advanced Information Systems (AIS) Research Group and
Digital & Signal Processing Research Group, ICTRC

Acknowledgement

JIST Editorial-Board would like to gratefully appreciate the following distinguished referees for spending their valuable time and expertise in reviewing the manuscripts and their constructive suggestions, which had a great impact on the enhancement of this issue of the JIST Journal.

(A-Z)

- Minaei, Behrooz, University of Science and Technology, Tehran, Iran
- Akbari, Mohammad, Amirkabir, Tehran, Iran
- Arabi, Somaye, Kharazmi University, Tehran, Iran
- Alizadeh, Sasan, Qazvin Islamic Azad University, Qazvin, Iran
- Bahrepour, Davoud, Islamic Azad University, Mashhad Branch, Iran
- Balali, Ali, Tehran University, Tehran, Iran
- Bateni, Zohreh, University of Science and Culture, Tehran, Iran
- Dashtbani, Majid, Razi University, Kermanshah, Iran
- Emami, Hodjjat, University of Bonab, East Azarbaijan, Iran
- Fouladi, Kazim, Tehran University, Tehran, Iran
- Farsijani, Hasan, Shahid Beheshti University, Tehran, Iran
- Ghanbari, Hamed, ACECR, Tehran, Iran
- Haghbin, Afrooz, Islamic Azad University, Science and Research Branch, Tehran
- Hosseini, Monireh, K. N. Toosi University of Technology, Tehran, Iran
- Hamidi, Hodjat, K. N. Toosi University of Technology, Tehran, Iran
- Haghighi, Hassan, Shahid Beheshti University, Tehran, Iran
- Kashef, Seyed Sadra, Urmia University, Urmia, Iran
- Mohammadi Zanjireh, Morteza, Imam Khomeini International University, Qazvin, Iran
- Moradi, Parham, University of Kurdistan, Kurdistan, Iran
- Mohammadpour, Davoud, Zanjan University, Zanjan, Iran
- Momen, Amir, Islamic Azad University of Shahr Rey, Tehran, Iran
- Mirza Momen, Zahra, Shahid Rajaei Teacher Training University, Tehran, Iran
- Mansoorizadeh, Muharram, Bu-Ali Sina University, Hamedan, Iran
- Nasersharif, Babak, K. N. Toosi University of Technology, Tehran, Iran
- Nilforoushan, Zahra, Kharazmi University, Tehran, Iran
- Naderan Tahan, Marjan, Shahid Chamran University of Ahvaz, Iran
- Pirgazi, Jamshid, Zanjan University, Zanjan, Iran
- Rahmati, Alireza, University of Waterloo, Ontario, Canada
- Rezakhani, Afshin, Ayatollah Ozma Borujerdi University, Lorestan, Iran
- Reshadat, Malek-Ashtar University of Technology, Tehran, Iran
- Sa' doon, Azizi, University of Kurdistan, Kurdistan, Iran
- Saeb, Armin, Stellenbosch University, Stellenbosch, South Africa
- Sarmady, Siamak, Urmia University of technology
- Talebi Mazraeh Shahi, Mohammad Sadegh, KTH Royal Institute of Technology, Sweden, Stockholm
- Yadollahzadeh Tabari, Meisam, Shahrood University Of Technology, Iran

Table of Contents

• A Bias-reduced Solution for Target Localization with Distance-dependent Noises in Illuminator of Opportunity Passive Radar	1
Habib Rasi and Maryam Shirzadian Gilan	
• A Game Theory Based Dynamic Transmission Opportunity Adjustment in WLANs	12
Mahdiah Ghazvini, Naser Movahedinia and Kamal Jamshidi	
• Farsi Conceptual Text Summarizer: A New Model in Continuous Vector Space	23
Mohammad Ebrahim Khademi, Mohammad Fakhredanesh and Seyed Mojtaba Hoseini	
• Graph Based Feature Selection Using Symmetrical Uncertainty in Microarray Dataset	35
Soodeh Bakhshandeh, Reza Azmi and Mohammad Teshnehlab	
• A Novel Approach for Cluster Self-Optimization Using Big Data Analytics	50
Abbas Mirzaei and Amir Rahimi	
• Assessing the Company's E-Readiness for implementing Mobile-CRM System: Case A Nationwide Distribution Company	65
Alireza Kamanghad, Gholamreza Hashemzadeh Khorasgani, Mohammadali Afsharkazemi and Nosratollah Shadnoosh	
• A New VAD Algorithm using Sparse Representation in Spectro-Temporal Domain	74
Mohadese Eshaghi, Farbod Razzazi and Alireza Behrad	

A Bias-reduced Solution for Target Localization with Distance-dependent Noises in Illuminator of Opportunity Passive Radar

Habib Rasi

Department of Electrical and Electronic Engineering, Shiraz University of Technology, Shiraz, Iran
h.rasi@sutech.ac.ir

Maryam Shirzadian Gilan*

Department of Electrical Engineering, Kermanshah Branch, Islamic Azad University, Kermanshah, Iran
maryam.shirzadian@gmail.com

Received: 19/Nov/2018

Revised: 19/Mar/2019

Accepted: 07/May/2019

Abstract

A closed-form solution for target localization based on the realistic distance-dependent noises in illuminator of opportunity passive radar and the reduction method of the bias which exists in the two-stage weighted least squares (2SWLS) method is proposed. 2SWLS is a classic method for time-of-arrival (TOA) and frequency-of-arrival (FOA) localization problem and has a couple of improved solutions over the years. The 2SWLS and its improved solutions have great localization performances in their established location scenarios on the basis of two approximations that setting the noise to a constant and ignoring the high-order terms of TOA and FOA measurement noises. It is these two approximations that lead to a sub-optimal solution with bias. The bias of 2SWLS has a significant influence on the target localization in illuminator of opportunity passive radar that has lower measurement accuracy and higher noises than active radar. Therefore, this paper starts by taking into consideration of the realistic distance-dependent characteristics of TOA/-FOA noises and improving 2SWLS method. Then, the bias of the improved 2SWLS method is analyzed and a bias-reduced solution based on weighted least squares (WLS) is developed. Numerical simulations demonstrate that, compared to the existing improved solutions of the 2SWLS, the proposed method effectively reduces the bias and achieves higher localization accuracy.

Keywords: TOA; FOA; Target localization; Distance-dependent noises; Bias reduction; Illuminator of opportunity passive radar.

1. Introduction

The illuminator of opportunity passive radar has a unique advantage in terms of security and anti-stealth characteristics [1, 2]. Target localization with an illuminator of opportunity passive radar is a fundamental problem in the target reconnaissance field, which has received extensive attention in recent years [3-5].

Time-of-arrival (TOA) and frequency-of-arrival (FOA) measurements [6, 7] are mostly used in target localization methods. In Ho et al. [8], the classic two-stage weighted least squares (2SWLS) method is proposed. After transforming the measurement equations to a set of linear equations by introducing nuisance parameters and ignoring the second-order error, Ho et al. [8] applied weighted least squares (WLS) to obtain the estimated value of nuisance parameters, and get the estimates of position and velocity by using WLS again. Taking into account the accuracy drop of targets located on or near the axes, Xu et al. [9] proposed Turbo-2SWLS based on the anchor reference selection and coordinate rotation, thus achieving higher accuracy. However, the coordinate rotation process of Turbo-2SWLS required much higher computational complexity, especially as the number of transmitters and receivers increases. In Yang et al. [10], an auxiliary variable was introduced in the second stage of 2SWLS, and the new method is called Aux-2SWLS for short in this paper. By selecting the appropriate auxiliary

variables, Aux-2SWLS could enhance the localization accuracy without increasing computational complexity. Amiri et al. [11, 12] proposed Ami-2SWLS method, which considered the realistic distance-dependent noises model [13], and achieved some improvement in most cases. However, it was demonstrated by our extensive calculations that there was a significant accuracy drop of velocity when the target was located on or near the axes.

In Ho et al. [8], Xu et al. [9], Yang et al. [10] and Amiri et al. [11], the high-order terms of noises were always ignored to reduce the computational complexity, but this ignores would bring an increasing bias in localization results as the TOA/FOA measurement noises got larger. Different from the situation of passive illuminators in Ho et al. [8], Xu et al. [9], Yang et al. [10] and Amiri et al. [11], the illuminators of passive radar is often non-cooperative and their signal waveform, frequency and phase cannot be obtained exactly most of the time. As a result, the TOA/FOA measurement noises are larger and signal-to-noise ratios are lower, and then the bias of localization is large enough to be taken into account to improve the localization accuracy [14]. Analyzed the bias in time-differences-of-arrival (TDOA) only and proposed a bias reduction method. However, aiming at the distance-

*Corresponding Author

dependent noises and the bias caused by higher TOA/FOA noises in this paper concerns, we will seek a more simple and effective method.

In this paper, the distance-dependent noises, which actually exist in the TOA/FOA measurements, are introduced first, and an improved method is derived based on Aux-2SWLS. Then, a bias-reduced solution of the improved method for TOA/FOA localization is proposed.

Finally, numerical simulations are carried out and the results show that this method could extremely attain the Cramer-Rao lower bound (CRLB) and lower the bias at higher noise levels.

2. An Improved 2SWLS With Distance-Dependent Noises

We consider the illuminator of opportunity passive radar system consisting of N_t illuminators expressed by I_1, I_2, \dots, I_5 and N_r receivers expressed by R_1, R_2, \dots, R_5 in N_s -dimensional space. Figure 1 shows a localization scenario of 5 illuminators and 5 receivers in 3-D space.

The position and velocity of the i th illuminator are denoted as $\mathbf{x}_{t,i} = [x_{t,i}^{(1)}, \dots, x_{t,i}^{(N_s)}]^T$ and $\dot{\mathbf{x}}_{t,i} = [\dot{x}_{t,i}^{(1)}, \dots, \dot{x}_{t,i}^{(N_s)}]^T$, and as $\mathbf{x}_{r,j} = [x_{r,j}^{(1)}, \dots, x_{r,j}^{(N_s)}]^T$ and $\dot{\mathbf{x}}_{r,j} = [\dot{x}_{r,j}^{(1)}, \dots, \dot{x}_{r,j}^{(N_s)}]^T$ denote the position and velocity of the j th receiver. The target position and velocity are represented by $\mathbf{x}_0 = [x_0^{(1)}, \dots, x_0^{(N_s)}]^T$ and $\dot{\mathbf{x}}_0 = [\dot{x}_0^{(1)}, \dots, \dot{x}_0^{(N_s)}]^T$.

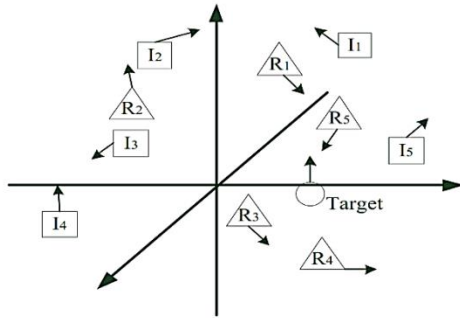


Fig. 1. Localization in 3-D space.

Each receiver can get N_t bistatic range (BR) and N_t bistatic range rate (BRR) measurements by Range-Doppler processing, that is, N_t TOA and N_t FOA data. Accordingly, there is a total of $2N_t N_r$ data that can be used for localization. Furthermore, the BR and BRR for the pair of the i th illuminator and the j th receiver can be computed from

(1)

$$\begin{aligned} d_{i,j} &= d_i^t + d_j^r \\ \dot{d}_{i,j} &= \dot{d}_i^t + \dot{d}_j^r \end{aligned}$$

Where d_i^t and \dot{d}_i^t are the range and range-rate between the i th illuminator and the target, and similarly, d_j^r and \dot{d}_j^r the

range and range-rate between the j th receiver and the target. They are given by

(2)

$$\begin{aligned} d_i^t &= \|\mathbf{x}_0 - \mathbf{x}_{t,i}\| \\ \dot{d}_i^t &= (\mathbf{x}_0 - \mathbf{x}_{t,i})^T (\dot{\mathbf{x}}_0 - \dot{\mathbf{x}}_{t,i}) / d_i^t \\ d_j^r &= \|\mathbf{x}_0 - \mathbf{x}_{r,j}\| \\ \dot{d}_j^r &= (\mathbf{x}_0 - \mathbf{x}_{r,j})^T (\dot{\mathbf{x}}_0 - \dot{\mathbf{x}}_{r,j}) / d_j^r \end{aligned}$$

2.1 Distance-dependent noises

The measurement noises of BR and BRR, which are always considered to obey zero mean Gaussian distribution and independent of each other [10], are denoted as

(3)

$$\begin{aligned} q &= [q_{1,1}, q_{1,2}, \dots, q_{N_t, N_r}]^T \\ \dot{q} &= [\dot{q}_{1,1}, \dot{q}_{1,2}, \dots, \dot{q}_{N_t, N_r}]^T \end{aligned}$$

Thus, the noisy measurements of BR and BRR can be expressed as

(4)

$$r_{i,j} = d_{i,j} + q_{i,j}$$

$$\dot{r}_{i,j} = \dot{d}_{i,j} + \dot{q}_{i,j}$$

The measurements of BR and BRR are always estimated by correlation processing in illuminator of opportunity passive radar. According to Stein [15], the standard deviations of BR and BRR noises are

(5)

$$\sigma_{i,j} = \frac{1}{f_{rms}} \frac{1}{\sqrt{BT \left(\frac{S}{N}\right)}}$$

(6)

$$\dot{\sigma}_{i,j} = \frac{1}{T_{rms}} \frac{1}{\sqrt{BT \left(\frac{S}{N}\right)}}$$

Where B is the noise bandwidth, T is the integration time, T_{rms} and f_{rms} are the root mean square integration time and the root mean square radian frequency, S/N is the effective input signal-to-noise ratio. The four parameters B , T , T_{rms} and f_{rms} depend on transmitted signal or receiver characteristics, while the parameter S/N depends on the distance and spatial geometry of illuminators, receivers and target. Hence S/N in (5) and (6) is the origin of the distance-dependent characteristics of BR and BRR noises. And then, from the bistatic radar equation [16], we have

(7)

$$\frac{S}{N} \propto 1/(d_i^t d_j^r)^2$$

That is to say,

(8)

$$\sigma_{i,j}^2 \propto \dot{\sigma}_{i,j}^2 \propto (d_i^t d_j^r)^2$$

Where α is a symbol of the proportional relationship. So we can see that the noises are actually distance-dependent. In order to describe and analyze the problem conveniently,

we assume that the illuminators have the same radiant power and the bistatic radar cross-section of the target is constant. This assumption will not affect the derivation and usability of the method to be proposed. Based on the above assumption, we denote the variances corresponding to $(d_i^t d_j^r)_{\max}^2$ as σ_0^2 and $\dot{\sigma}_0^2$. Then, the variances for the pair of i th illuminator and the j th receiver can be denoted as

$$\begin{aligned}\sigma_{i,j}^2 &= \sigma_0^2 (d_i^t d_j^r)^2 / (d_i^t d_j^r)_{\max}^2 \\ \dot{\sigma}_{i,j}^2 &= \dot{\sigma}_0^2 (d_i^t d_j^r)^2 / (d_i^t d_j^r)_{\max}^2\end{aligned}\quad (9)$$

And the BR and BRR covariance matrix is considered to be

$$\mathbf{Q} = \text{diag}\{\sigma_{1,1}^2, \sigma_{1,2}^2, \dots, \sigma_{N_t, N_r}^2, \dot{\sigma}_{1,1}^2, \dot{\sigma}_{1,2}^2, \dots, \dot{\sigma}_{N_t, N_r}^2\} \quad (10)$$

Where $\text{diag}\{*\}$ denotes the diagonal matrix whose diagonal entries are the elements in braces.

Consequently, compared to the simple form of the covariance matrix without regard for the distance-dependent characteristics of noises,

$$\mathbf{Q}_{\text{simple}} = \text{diag}\{\sigma_s^2, \sigma_s^2, \dots, \sigma_s^2, \dot{\sigma}_s^2, \dot{\sigma}_s^2, \dots, \dot{\sigma}_s^2\} \quad (11)$$

Where σ_s^2 and $\dot{\sigma}_s^2$ are constant variances of BR and BRR, covariance matrix in (10) is more realistic and complicated, and will be further researched.

2.2 An improved 2SWLS method

Aux-2SWLS is a creative and excellent improved version of the classic 2SWLS method, which enhances the localization performance to a great extent by introducing an auxiliary variable. Thus, we will derive an improved 2SWLS method with distance-dependent noises based on Aux-2SWLS method introduced in Yang et al. [10].

- Stage 1:

The estimate of $\boldsymbol{\theta}_0 = [\mathbf{x}_0^T, d_1^t, \dot{\mathbf{x}}_0^T, \dot{d}_1^t]^T$ is

$$\hat{\boldsymbol{\theta}}_a = (\mathbf{G}_a^T \mathbf{W}_a^{-1} \mathbf{G}_a)^{-1} \mathbf{G}_a^T \mathbf{W}_a^{-1} \mathbf{h}_a \quad (12)$$

Where

$$\begin{aligned}\mathbf{G}_a &= [\mathbf{G}_{a,1}^T, \mathbf{G}_{a,2}^T, \dot{\mathbf{G}}_{a,1}^T, \dot{\mathbf{G}}_{a,2}^T]^T \\ [\mathbf{G}_a]_{j,:} &= [2(\mathbf{x}_{r,j} - \mathbf{x}_{t,1})^T, -2r_{1,j}, \mathbf{0}] \\ [\mathbf{G}_a]_{k,:} &= [2(\mathbf{x}_{t,i} - \mathbf{x}_{t,1})^T, 2(r_{i,j} - r_{1,j}), \mathbf{0}] \\ &\quad k = (i-2)N_r + j \\ &\quad i = 2, \dots, N_t, \quad j = 1, \dots, N_r \\ \mathbf{W}_a &\approx \mathbf{T}_a \mathbf{Q} \mathbf{T}_a^T \\ \mathbf{T}_a &= \begin{bmatrix} 2\mathbf{T}_{a,1}\boldsymbol{\Lambda}_a & \mathbf{0} \\ \mathbf{T}_{a,1}\boldsymbol{\Lambda}_a & \mathbf{T}_{a,1}\mathcal{A}_a \end{bmatrix}\end{aligned}\quad (13)$$

$$\begin{aligned}\mathbf{T}_{a,1} &= \begin{bmatrix} \mathbf{T}_{1,1} & \mathbf{0} \\ \mathbf{0} & \mathbf{T}_{1,2} \end{bmatrix} \\ \boldsymbol{\Lambda}_a &= (\mathbf{I}_{N_t} + (\mathbf{e}_1 - \mathbf{1}_{N_t})\mathbf{e}_1^T) \otimes \mathbf{I}_{N_r}\end{aligned}$$

$$\begin{aligned}\mathbf{T}_{1,1} &= \text{diag}\{d_1^t - r_{1,1}, \dots, d_1^t - r_{1,N_r}\} \\ \mathbf{T}_{1,2} &= \text{diag}\{r_{1,1} - r_{2,1} - d_1^t, \dots, r_{1,N_r} - r_{N_t, N_r} - d_1^t\}\end{aligned}$$

$$\mathbf{h}_a = [\mathbf{h}_{a,1}^T, \mathbf{h}_{a,2}^T, \dot{\mathbf{h}}_{a,1}^T, \dot{\mathbf{h}}_{a,2}^T]^T,$$

$$[\mathbf{h}_a]_j = \mathbf{x}_{r,j}^T \mathbf{x}_{r,j} - \mathbf{x}_{t,1}^T \mathbf{x}_{t,1} - r_{1,j}^2,$$

$$[\mathbf{h}_a]_k = \mathbf{x}_{t,i}^T \mathbf{x}_{t,i} - \mathbf{x}_{t,1}^T \mathbf{x}_{t,1} - (r_{i,j} - r_{1,j})^2$$

Here, \mathbf{I}_{N_t} is an identity matrix of size N_t , $\mathbf{1}_{N_t}$ is a N_t -dimensional column vector whose elements are all 1, and \mathbf{e}_1 denotes a unit column vector proper in size, of which first element is 1 and other elements are 0. Besides, $[*]_k$ denotes the k th row of the matrix in square brackets, $[*]_k$ denotes the k th element of the vector in square brackets and \otimes denotes the Kronecker product.

\mathbf{W}_a is not known in practice as \mathbf{T}_a and \mathbf{Q} contain the true distances between illuminators, receivers and target. Further approximation is necessary to get \mathbf{W}_a . Normally, each d_i^t and \dot{d}_i^t is approximately at a similar level of magnitude as others, so that $\sigma_{i,j}$ and $\dot{\sigma}_{i,j}$ are close to σ_0 and $\dot{\sigma}_0$, respectively. Therefore, we have rough approximations

$$\mathbf{T}_a \approx d_0 \mathbf{I}_{2N_t N_r}$$

$$\mathbf{Q} \approx \sigma_0^2 \text{diag}\{1, 1, \dots, 1, \eta^2, \eta^2, \dots, \eta^2\}$$

Where $\eta = \dot{\sigma}_0 / \sigma_0$, which represents the ratio of standard deviation of BRR noises to BR noises. Admittedly, this approximation will be controversial, but it can be used to obtain an initial solution to estimate \mathbf{W}_a . Then, the initial $\hat{\boldsymbol{\theta}}_a$ is computed from (12), and \mathbf{T}_a , \mathbf{Q} and \mathbf{W}_a can be corrected by the computed $\hat{\boldsymbol{\theta}}_a$. Finally, using (12) again, we can get the final estimate of $\hat{\boldsymbol{\theta}}_a$.

- Stage 2:

Since d_1^t and \dot{d}_1^t are dependent on \mathbf{x}_0 and $\dot{\mathbf{x}}_0$ respectively, we need to incorporate this relationship to get an improved estimate. In accordance with Yang et al. [10], the auxiliary variables $\boldsymbol{\alpha} = [\hat{\boldsymbol{\theta}}_a]_{1:N_s} - \gamma \mathbf{1}_{N_s}$ and $\dot{\boldsymbol{\alpha}} = [\hat{\boldsymbol{\theta}}_a]_{N_s+2:2N_s+1}$ are introduced, where can be any constant larger than several times or tens of times of \hat{d}_1^t , and we set

$$\boldsymbol{\theta}_b = \left(\begin{bmatrix} [\boldsymbol{\theta}]_{1:N_s} \\ [\boldsymbol{\theta}]_{1:N_s} \end{bmatrix} - \begin{bmatrix} \boldsymbol{\alpha} \\ \dot{\boldsymbol{\alpha}} \end{bmatrix} \right) \odot (\boldsymbol{\theta} - \begin{bmatrix} \boldsymbol{\alpha} \\ \dot{\boldsymbol{\alpha}} \end{bmatrix}) \quad (15)$$

Where \odot denotes element-wise product.

Then the estimate of (15) can be calculated by

$$\hat{\boldsymbol{\theta}}_b = (\mathbf{G}_b^T \mathbf{W}_b^{-1} \mathbf{G}_b)^{-1} \mathbf{G}_b^T \mathbf{W}_b^{-1} \mathbf{h}_b \quad (16)$$

where

$$\begin{aligned}\mathbf{G}_b &= \mathbf{I}_2 \otimes [\mathbf{I}_{N_s}, \mathbf{1}_{N_s}]^T \\ \mathbf{W}_b &\approx \mathbf{T}_b (\mathbf{G}_a^T \mathbf{W}_a^{-1} \mathbf{G}_a)^{-1} \mathbf{T}_b^T \\ \mathbf{T}_b &= \begin{bmatrix} 2\mathbf{T}_{b,1} & \mathbf{0} \\ \mathbf{T}_{b,2} & \mathbf{T}_{b,1} \end{bmatrix}\end{aligned}$$

$$\begin{aligned} \mathbf{T}_{b,1} &= \text{diag}\{[\widehat{\boldsymbol{\theta}}_a]_{1:N_s+1} - [\boldsymbol{\alpha}^T, 0]^T\} \\ &\quad + \mathbf{e}_{N_s+1}[(\mathbf{x}_{t,1} - \boldsymbol{\alpha})^T, 0] \\ \mathbf{T}_{b,2} &= \text{diag}\{[\widehat{\boldsymbol{\theta}}_a]_{N_s+2:2N_s+2} - [\dot{\boldsymbol{\alpha}}^T, 0]^T\} \\ &\quad + \mathbf{e}_{N_s+1}[(\dot{\mathbf{x}}_{t,1} - \dot{\boldsymbol{\alpha}})^T, 0] \end{aligned} \quad (17)$$

$$\mathbf{h}_b = \begin{bmatrix} ([\widehat{\boldsymbol{\theta}}_a]_{1:N_s} - \boldsymbol{\alpha}) \odot ([\widehat{\boldsymbol{\theta}}_a]_{1:N_s} - \boldsymbol{\alpha}) \\ [\widehat{\boldsymbol{\theta}}_a]_{N_s+1}^2 - \mathbf{x}_{t,1}^T \mathbf{x}_{t,1} + \boldsymbol{\alpha}^T \boldsymbol{\alpha} + 2(\mathbf{x}_{t,1} - \boldsymbol{\alpha})^T [\widehat{\boldsymbol{\theta}}_a]_{1:N_s} \\ ([\widehat{\boldsymbol{\theta}}_a]_{1:N_s} - \boldsymbol{\alpha}) \odot ([\widehat{\boldsymbol{\theta}}_a]_{N_s+2:2N_s+1} - \dot{\boldsymbol{\alpha}}) \\ \left(\begin{array}{l} [\widehat{\boldsymbol{\theta}}_a]_{N_s+1} [\widehat{\boldsymbol{\theta}}_a]_{2N_s+2} - \dot{\mathbf{x}}_{t,1}^T \mathbf{x}_{t,1} + \dot{\boldsymbol{\alpha}}^T \boldsymbol{\alpha} \\ + (\dot{\mathbf{x}}_{t,1} - \dot{\boldsymbol{\alpha}})^T [\widehat{\boldsymbol{\theta}}_a]_{1:N_s} + (\mathbf{x}_{t,1} - \boldsymbol{\alpha})^T [\widehat{\boldsymbol{\theta}}_a]_{N_s+2:2N_s+1} \end{array} \right) \end{bmatrix}$$

$$\text{Then, the final estimate of } \boldsymbol{\theta} = [\mathbf{x}^T, \dot{\mathbf{x}}^T]^T \quad (18)$$

$$\widehat{\boldsymbol{\theta}} = \begin{bmatrix} \text{diag}\{\text{sgn}([\widehat{\boldsymbol{\theta}}_a]_{1:N_s} - \boldsymbol{\alpha})\} \sqrt{[\widehat{\boldsymbol{\theta}}_b]_{1:N_s} + \boldsymbol{\alpha}} \\ [\widehat{\boldsymbol{\theta}}_b]_{N_s+1:2N_s} \oslash (\dot{\mathbf{x}} - \dot{\boldsymbol{\alpha}}) + \dot{\boldsymbol{\alpha}} \end{bmatrix}$$

Where $\text{sgn}(\ast)$ denotes the sign function and \oslash denotes element-wise division. The details of the derivation and expression of (12) and (16) can be referred to Yang et al. [10].

For the convenience of the description, we will abbreviate the improved 2SWLS method with distance-dependent noises as Ddn-2SWLS in this paper.

Ddn-2SWLS has strong robustness and relatively accurate results as the Aux-2SWLS method under low noise levels, but it will deviate from CRLB quickly like the measurement noise increases. This is due in large part to the fact that with the increase of noise, the reasonable approximation of ignoring high-order error terms becomes less reasonable [17]. That is, the high-order error will bring significant bias and need to be considered.

3. Bias-Reduced Solution

3.1 Bias Analysis

In order to analyze the high-order error and localization bias, we should compute the error in each stage of the Ddn-2SWLS. According to Yang et al. [10], the error of the stage 1 is

$$\begin{aligned} \Delta \boldsymbol{\theta}_a &= (\mathbf{G}_a^T \mathbf{W}_a^{-1} \mathbf{G}_a)^{-1} \mathbf{G}_a^T \mathbf{W}_a^{-1} (\mathbf{h}_a - \mathbf{G}_a \boldsymbol{\theta}_a) \\ &= (\mathbf{G}_a^T \mathbf{W}_a^{-1} \mathbf{G}_a)^{-1} \mathbf{G}_a^T \mathbf{W}_a^{-1} \boldsymbol{\varepsilon}_a \end{aligned} \quad (19)$$

Where

$$\mathbf{W}_a = \mathbf{E}(\boldsymbol{\varepsilon}_a \boldsymbol{\varepsilon}_a^T), \boldsymbol{\varepsilon}_a = \mathbf{T}_a \begin{bmatrix} \mathbf{q} \\ \dot{\mathbf{q}} \end{bmatrix} + \begin{bmatrix} \boldsymbol{\Lambda}_a \mathbf{q} \\ \boldsymbol{\Lambda}_a \dot{\mathbf{q}} \end{bmatrix} \odot \begin{bmatrix} \boldsymbol{\Lambda}_a \mathbf{q} \\ \boldsymbol{\Lambda}_a \dot{\mathbf{q}} \end{bmatrix} \quad (20)$$

Here, $\mathbf{E}(\ast)$ denotes the expectation operator. \mathbf{T}_a is related to the $\widehat{\mathbf{d}}_1^t$ and $\widehat{\mathbf{d}}_1^{\dot{t}}$ which are the elements of the initial $\widehat{\boldsymbol{\theta}}_a$ and independent of \mathbf{q} and $\dot{\mathbf{q}}$. In this paper, we are only

concerned with the bias brought by the high-order terms of noises and the error caused by the initial estimate of $\widehat{\boldsymbol{\theta}}_a$ will be the content to be studied in the future.

For convenience of expression, we set

$$\begin{aligned} \mathbf{q}^2 &= \mathbf{q} \odot \mathbf{q}, \dot{\mathbf{q}}^2 = \dot{\mathbf{q}} \odot \dot{\mathbf{q}}, \quad \mathbf{q} \dot{\mathbf{q}} = \mathbf{q} \odot \dot{\mathbf{q}} \\ (21) \quad (\mathbf{G}_a^T \mathbf{W}_a^{-1} \mathbf{G}_a)^{-1} \mathbf{G}_a^T \mathbf{W}_a^{-1} &= \mathbf{A} = \begin{bmatrix} \mathbf{A}_1 & \mathbf{A}_2 \\ \mathbf{A}_3 & \mathbf{A}_4 \end{bmatrix} \\ (\mathbf{G}_b^T \mathbf{W}_b^{-1} \mathbf{G}_b)^{-1} \mathbf{G}_b^T \mathbf{W}_b^{-1} &= \mathbf{B} = \begin{bmatrix} \mathbf{B}_1 & \mathbf{B}_2 \\ \mathbf{B}_3 & \mathbf{B}_4 \end{bmatrix} \end{aligned} \quad (22)$$

where $\mathbf{A}_1, \mathbf{A}_2, \mathbf{A}_3$ and \mathbf{A}_4 are matrices of equal size; $\mathbf{B}_1, \mathbf{B}_2, \mathbf{B}_3$ and \mathbf{B}_4 are matrices of equal size. $\mathbf{q}^2, \dot{\mathbf{q}}^2$, and $\mathbf{q} \dot{\mathbf{q}}$ are the second-order terms of noises, which is always ignored by 2SWLS methods for the assumption of small noise level. However, the second order terms of noises actually have a growing significant contribution to the bias with the increase of noises. Consequently, the effect of $\mathbf{q}^2, \dot{\mathbf{q}}^2$, and $\mathbf{q} \dot{\mathbf{q}}$ will be considered in this paper.

By taking expectations of $\Delta \boldsymbol{\theta}_a$, the bias of $\widehat{\boldsymbol{\theta}}_a$ is

$$\mathbf{E}(\Delta \boldsymbol{\theta}_a) = \mathbf{D}_a [\mathbf{E}(\mathbf{q}^2)^T, \mathbf{E}(\dot{\mathbf{q}}^2)^T]^T \quad (24)$$

Where

$$\mathbf{D}_a = \begin{bmatrix} \mathbf{A}_1 & |\boldsymbol{\Lambda}_a| & \mathbf{0} \\ \mathbf{A}_3 & |\boldsymbol{\Lambda}_a| & \mathbf{0} \end{bmatrix} \quad (25)$$

and $|\ast|$ denotes the absolute value operator.

Similarly, the error of the stage 2 is

$$\Delta \boldsymbol{\theta}_b = (\mathbf{G}_b^T \mathbf{W}_b^{-1} \mathbf{G}_b)^{-1} \mathbf{G}_b^T \mathbf{W}_b^{-1} (\mathbf{h}_b - \mathbf{G}_b \boldsymbol{\theta}_b) = \mathbf{B} \boldsymbol{\varepsilon}_b \quad (26)$$

Where

$$\boldsymbol{\varepsilon}_b = \mathbf{T}_b \Delta \boldsymbol{\theta}_a - \begin{bmatrix} [\Delta \boldsymbol{\theta}_a]_{1:N_s+1} \\ [\Delta \boldsymbol{\theta}_a]_{1:N_s+1} \end{bmatrix} \odot \Delta \boldsymbol{\theta}_a \quad (27)$$

Substituting (19) into (26) gives

$$\begin{aligned} \Delta \boldsymbol{\theta}_b &= \mathbf{B} \mathbf{T}_b \mathbf{A} \mathbf{T}_a \begin{bmatrix} \mathbf{q} \\ \dot{\mathbf{q}} \end{bmatrix} + \mathbf{B} \mathbf{T}_b \mathbf{A} \begin{bmatrix} \boldsymbol{\Lambda}_a \mathbf{q} \\ \boldsymbol{\Lambda}_a \dot{\mathbf{q}} \end{bmatrix} \odot \begin{bmatrix} \boldsymbol{\Lambda}_a \mathbf{q} \\ \boldsymbol{\Lambda}_a \dot{\mathbf{q}} \end{bmatrix} \\ &- \mathbf{B} \left(\begin{bmatrix} \mathbf{A}_1 & \mathbf{A}_2 \\ \mathbf{A}_3 & \mathbf{A}_4 \end{bmatrix} \mathbf{T}_a \begin{bmatrix} \mathbf{q} \\ \dot{\mathbf{q}} \end{bmatrix} \right) \odot \left(\mathbf{A} \mathbf{T}_a \begin{bmatrix} \mathbf{q} \\ \dot{\mathbf{q}} \end{bmatrix} \right) + \boldsymbol{\Theta}_3 \left(\begin{bmatrix} \mathbf{q} \\ \dot{\mathbf{q}} \end{bmatrix} \right) \end{aligned} \quad (28)$$

Where $\boldsymbol{\Theta}_3([\mathbf{q}^T, \dot{\mathbf{q}}^T]^T)$ denotes a vector of size $2N_t N_r$, whose each element contains $q_{1,1}^{t_1} q_{1,2}^{t_2} \dots q_{N_t N_r}^{t_{N_t N_r}}$ $\dot{q}_{1,1}^{t_{N_t N_r+1}} \dot{q}_{1,2}^{t_{N_t N_r+2}} \dots \dot{q}_{N_t N_r}^{t_{2N_t N_r}}$, where $t_1, t_2, \dots, t_{2N_t N_r}$ are natural numbers and $t_1 + t_2 + \dots + t_{2N_t N_r} \geq 3$. In this

paper, $\mathbf{E} (q_{1,1}^{t_1} \quad q_{1,2}^{t_2} \quad \dots \quad q_{N_t N_r}^{t_{N_t N_r}} \quad \dot{q}_{1,1}^{t_{N_t N_r+1}} \quad \dot{q}_{1,2}^{t_{N_t N_r+2}} \dots \dot{q}_{N_t N_r}^{t_{N_t N_r}}) = 0$

when $t_1 + t_2 + \dots + t_{2N_t N_r} = 3$, and $\mathbf{E} (q_{1,1}^{t_1} \quad q_{1,2}^{t_2} \dots q_{N_t N_r}^{t_{N_t N_r}} \quad \dot{q}_{1,1}^{t_{N_t N_r+1}} \quad \dot{q}_{1,2}^{t_{N_t N_r+2}} \dots \dot{q}_{N_t N_r}^{t_{2N_t N_r}})$ will be extremely small when $t_1 + t_2 + \dots + t_{2N_t N_r} \geq 4$. That is to say $\Theta_3([\mathbf{q}^T, \dot{\mathbf{q}}^T]^T)$ can be neglected and $\mathbf{E}(\Theta_3([\mathbf{q}^T, \dot{\mathbf{q}}^T]^T))$ is considered to be $\mathbf{0}$ in the derivation of bias.

Taking expectations of $\Delta\theta_b$ yields

$$\mathbf{E}(\Delta\theta_b) \approx \mathbf{D}_b[\mathbf{E}(\mathbf{q}^2)^T, \mathbf{E}(\dot{\mathbf{q}}^2)^T]^T \quad (29)$$

Where

$$\mathbf{D}_b = \mathbf{B}\mathbf{T}_b\mathbf{D}_a - \mathbf{B} \left(\begin{bmatrix} \mathbf{A}_1 & \mathbf{A}_2 \\ \mathbf{A}_1 & \mathbf{A}_2 \end{bmatrix} \mathbf{T}_a \right) \Theta(\mathbf{A}\mathbf{T}_a) \quad (30)$$

Furthermore, we can Taylor expand

$$\theta = \begin{bmatrix} \text{diag}\{\text{sgn}([\hat{\theta}_a]_{1:N_s} - \alpha)\} \sqrt{[\theta_b]_{1:N_s} + \alpha} \\ [\theta_b]_{N_s+1:2N_s} \odot (\hat{\mathbf{x}} - \alpha) + \dot{\alpha} \end{bmatrix} \quad (31)$$

around $\hat{\theta}_b$, and the error of $\hat{\theta}$ is found to be

$$\Delta\theta = \text{diag}\{\text{sgn}([\hat{\theta}_a]_{1:N_s} - \alpha), \text{sgn}([\hat{\theta}_a]_{1:N_s} - \alpha)\} \quad (32)$$

$$\begin{bmatrix} [\Delta\theta_b]_{1:N_s} \odot (2[\hat{\theta}_b]_{1:N_s}^{\frac{1}{2}}) + [\Delta\theta_b]_{1:N_s} \odot [\Delta\theta_b]_{1:N_s} \odot (8[\hat{\theta}_b]_{1:N_s}^{3/2}) + \mathbf{R}_3([\Delta\theta_b]_{1:N_s}) \\ \left(\begin{array}{l} [\Delta\theta_b]_{1:N_s} \odot [\Delta\theta_b]_{N_s+1:2N_s} \odot (-2[\hat{\theta}_b]_{1:N_s}^{3/2}) + [\Delta\theta_b]_{N_s+1:2N_s} \odot [\hat{\theta}_b]_{1:N_s}^{1/2} \\ + [\Delta\theta_b]_{1:N_s} \odot [\Delta\theta_b]_{1:N_s} \odot (-3[\hat{\theta}_b]_{N_s+1:2N_s}) \odot (8[\hat{\theta}_b]_{1:N_s}^{\frac{5}{2}}) \\ + [\Delta\theta_b]_{1:N_s} \odot [\Delta\theta_b]_{N_s+1:2N_s} \odot (2[\hat{\theta}_b]_{1:N_s}^{3/2}) + \mathbf{R}'_3(\Delta\theta_b) \end{array} \right) \end{bmatrix}$$

where $\mathbf{R}_3([\Delta\theta_b]_{1:N_s})$ and $\mathbf{R}'_3(\Delta\theta_b)$ are Lagrange remainder terms of $[\theta]_{1:N_s}$ and $[\theta]_{N_s+1:2N_s}$ respectively. Since $\mathbf{R}_3([\Delta\theta_b]_{1:N_s})$ and $\mathbf{R}'_3(\Delta\theta_b)$ are two specific forms of $\Theta_3([\mathbf{q}^T, \dot{\mathbf{q}}^T]^T)$ they are neglected and their mathematical expectations are considered to be $\mathbf{0}$.

The bias will then be

$$\mathbf{E}(\Delta\theta) \approx \mathbf{C} \begin{bmatrix} E([\Delta\theta_b]_{1:N_s}) \\ E([\Delta\theta_b]_{N_s+1:2N_s}) \\ E([\Delta\theta_b]_{1:N_s} \odot [\Delta\theta_b]_{1:N_s}) \\ E([\Delta\theta_b]_{1:N_s} \odot [\Delta\theta_b]_{N_s+1:2N_s}) \end{bmatrix} = \mathbf{D}_c \begin{bmatrix} \mathbf{E}(\mathbf{q}^2) \\ \mathbf{E}(\dot{\mathbf{q}}^2) \end{bmatrix} \quad (33)$$

Where

$$\mathbf{D}_c \approx \mathbf{C} \begin{bmatrix} \mathbf{D}_b \\ [\mathbf{B}_1, \mathbf{B}_2] \mathbf{T}_b \mathbf{A} \mathbf{T}_a \odot [\mathbf{B}_1, \mathbf{B}_2] \mathbf{T}_b \mathbf{A} \mathbf{T}_a \\ [\mathbf{B}_1, \mathbf{B}_2] \mathbf{T}_b \mathbf{A} \mathbf{T}_a \odot [\mathbf{B}_3, \mathbf{B}_4] \mathbf{T}_b \mathbf{A} \mathbf{T}_a \end{bmatrix} \quad (34)$$

C

$$= \begin{bmatrix} \text{diag}\{\beta \odot (2[\hat{\theta}_b]_{1:N_s}^{1/2})\} & \text{diag}\{\beta \odot [\hat{\theta}_b]_{N_s+1:2N_s} \odot (-2[\hat{\theta}_b]_{1:N_s}^{3/2})\} \\ \mathbf{0} & \text{diag}\{\beta \odot [\hat{\theta}_b]_{1:N_s}^{1/2}\} \\ \text{diag}\{\beta \odot (8[\hat{\theta}_b]_{1:N_s}^{3/2})\} & \text{diag}\{\beta \odot (-3[\hat{\theta}_b]_{N_s+1:2N_s}) \odot (8[\hat{\theta}_b]_{1:N_s}^{5/2})\} \\ \mathbf{0} & \text{diag}\{\beta \odot (2[\hat{\theta}_b]_{1:N_s}^{3/2})\} \end{bmatrix}^T$$

$$\beta = \text{sgn}([\hat{\theta}_a]_{1:N_s} - \alpha)$$

We do not know the exact value of $[\mathbf{q}^T, \dot{\mathbf{q}}^T]^T$ in practice, so we cannot calculate $\Delta\theta$ directly. However, the bias $\mathbf{E}(\Delta\theta)$ consisting of the second-order term of $[\mathbf{q}^T, \dot{\mathbf{q}}^T]^T$ is linearly related to $[\mathbf{E}(\mathbf{q}^2)^T, \mathbf{E}(\dot{\mathbf{q}}^2)^T]^T$, which is actually a vector consisting of the main diagonal elements of \mathbf{Q} and can be estimated by $\hat{\theta}$. In addition, the first-order error term $\Delta\theta_1 = [\Delta x_1^T, \Delta \dot{x}_1^T]^T$ in $\Delta\theta$ can be introduced in 2SWLS and derived by solving the new linear equations without the second-order and higher-order error terms. In this way, we can derive the first-order error term $\Delta\theta_1$ and the second-order error term $\Delta\theta_2 = \mathbf{E}(\Delta\theta)$ and subtract them from $\hat{\theta}$ to improve accuracy and reduce the bias.

3-2- Bias Reduction

On the basis of the former analysis, we firstly derive the first-order error term $\Delta\theta_1$.

we set $\mathbf{x}_0 = \mathbf{x} - \Delta\mathbf{x}_1$ and $\dot{\mathbf{x}}_0 = \dot{\mathbf{x}} - \Delta\dot{\mathbf{x}}_1$. Then the distance between the j th receiver and target can be approximated by the Taylor expansion without the second-order and higher-order error terms as

$$d_j^r = \|\mathbf{x} - \Delta\mathbf{x}_1 - \mathbf{x}_{r,j}\| \approx d_j^{(0)} + \mathbf{d}_j^{(1)T} \Delta\mathbf{x}_1 \quad (35)$$

where

$$d_j^{(0)} = \|\mathbf{x} - \mathbf{x}_{r,j}\| \quad (36)$$

$$\mathbf{d}_j^{(1)} = -(\mathbf{x} - \mathbf{x}_{r,j}) / \|\mathbf{x} - \mathbf{x}_{r,j}\|$$

Moreover, substituting $\mathbf{x}_0 = \mathbf{x} - \Delta\mathbf{x}_1$ and $d_{i,j} = r_{i,j} - q_{i,j}$ into $\|\mathbf{x}_0 - \mathbf{x}_{t,i}\|^2 = (d_{i,j} - d_j^r)^2$ and ignoring the second-order error term give

$$\mathbf{x}_{r,j}^T \mathbf{x}_{r,j} - \mathbf{x}_{t,i}^T \mathbf{x}_{t,i} + r_{i,j}^2 + 2(\mathbf{x}_{t,i} - \mathbf{x}_{r,j})^T \mathbf{x} - 2r_{i,j} d_j^{(0)} \quad (37)$$

$$-2(r_{i,j} \mathbf{d}_j^{(1)} + \mathbf{x}_{t,i}^T - \mathbf{x}_{r,j}^T) \Delta\mathbf{x}_1 \approx 2(r_{i,j} - d_j^{(0)}) q_{i,j}$$

(37) can be expressed in matrix form,

$$\boldsymbol{\varepsilon}_{c,1} = \mathbf{h}_{c,1} - \mathbf{G}_{c,1} \Delta\theta_1 \quad (38)$$

Where

$$\mathbf{G}_{c,1} = [2\mathbf{G}_1, \mathbf{0}_{N_r \times N_r, N_s}]$$

$$[\mathbf{G}_1]_{n,1:N_s} = (r_{i,j} \mathbf{d}_j^{(1)} + \mathbf{x}_{t,i} - \mathbf{x}_{r,j})^T \quad (39)$$

$$\begin{aligned}
[\mathbf{h}_{c,1}]_n &= \mathbf{x}_{r,j}^T \mathbf{x}_{r,j} - \mathbf{x}_{t,i}^T \mathbf{x}_{t,i} + r_{i,j}^2 + 2(\mathbf{x}_{t,i} - \mathbf{x}_{r,j})^T \mathbf{x} \\
&\quad - 2r_{i,j} d_j^{(0)} \\
n &= (i-1)N_r + j \\
\boldsymbol{\varepsilon}_{c,1} &\approx \mathbf{T}_{c,1} [\mathbf{q}^T, \dot{\mathbf{q}}^T]^T \\
\mathbf{T}_{c,1} &= [2\mathbf{T}_1, \mathbf{0}_{N_r \times N_r, N_r \times N_r}]
\end{aligned} \tag{45}$$

$$\mathbf{T}_1 = \text{diag}\{r_{1,1} - d_1^{(0)}, \dots, r_{1,N_r} - d_{N_r}^{(0)}, \dots, r_{N_t, N_r} - d_{N_r}^{(0)}\}$$

Differentiating both sides of (37) with respect to time, we obtain

$$\begin{aligned}
&\dot{\mathbf{x}}_{r,j}^T \mathbf{x}_{r,j} - \dot{\mathbf{x}}_{t,i}^T \mathbf{x}_{t,i} + \dot{r}_{i,j} r_{i,j} + (\dot{\mathbf{x}}_{t,i} - \dot{\mathbf{x}}_{r,j})^T \mathbf{x} \\
&\quad + (\mathbf{x}_{t,i} - \mathbf{x}_{r,j})^T \dot{\mathbf{x}} - \dot{r}_{i,j} d_j^{(0)} - r_{i,j} \dot{d}_j^{(0)} \\
&- 2(\dot{r}_{i,j} \mathbf{d}_j^{(1)} + r_{i,j} \dot{\mathbf{d}}_j^{(1)} + \dot{\mathbf{x}}_{t,i} - \dot{\mathbf{x}}_{r,j})^T \Delta \mathbf{x}_1 - 2(r_{i,j} \mathbf{d}_j^{(1)} + \\
&\mathbf{x}_{t,i} - \mathbf{x}_{r,j})^T \Delta \dot{\mathbf{x}}_1 \\
&\approx 2(\dot{r}_{i,j} - \dot{d}_j^{(0)}) q_{i,j} + 2(r_{i,j} - d_j^{(0)}) \dot{q}_{i,j}
\end{aligned} \tag{40}$$

where

$$\begin{aligned}
\dot{d}_j^{(0)} &= (\dot{\mathbf{x}} - \dot{\mathbf{x}}_{r,j})^T (\mathbf{x} - \mathbf{x}_{r,j}) / d_j^{(0)} \\
\dot{\mathbf{d}}_j^{(1)} &= (\mathbf{x} - \mathbf{x}_{r,j}) \dot{d}_j^{(0)} / (d_j^{(0)})^2 - (\dot{\mathbf{x}} - \dot{\mathbf{x}}_{r,j}) / d_j^{(0)}
\end{aligned}$$

Similarly, (40) can be expressed in matrix form,

$$\boldsymbol{\varepsilon}_{c,2} = \mathbf{h}_{c,2} - \mathbf{G}_{c,2} \Delta \boldsymbol{\theta}_1 \tag{42}$$

where

$$\begin{aligned}
\mathbf{G}_{c,2} &= [\dot{\mathbf{G}}_1, \mathbf{G}_1] \\
[\dot{\mathbf{G}}_1]_{n,1:N_s} &= (\dot{r}_{i,j} \mathbf{d}_j^{(1)} + r_{i,j} \dot{\mathbf{d}}_j^{(1)} + \dot{\mathbf{x}}_{t,i} - \dot{\mathbf{x}}_{r,j})^T \\
[\mathbf{h}_{c,2}]_n &= \dot{\mathbf{x}}_{r,j}^T \mathbf{x}_{r,j} - \dot{\mathbf{x}}_{t,i}^T \mathbf{x}_{t,i} + \dot{r}_{i,j} r_{i,j} + (\dot{\mathbf{x}}_{t,i} - \dot{\mathbf{x}}_{r,j})^T \mathbf{x} \\
&\quad + (\mathbf{x}_{t,i} - \mathbf{x}_{r,j})^T \dot{\mathbf{x}} - \dot{r}_{i,j} d_j^{(0)} - r_{i,j} \dot{d}_j^{(0)} \\
\boldsymbol{\varepsilon}_{c,2} &\approx \mathbf{T}_{c,2} [\mathbf{q}^T, \dot{\mathbf{q}}^T]^T \\
\mathbf{T}_{c,2} &= [\dot{\mathbf{T}}_1, \mathbf{T}_1] \\
\dot{\mathbf{T}}_1 &= \text{diag}\{\dot{r}_{1,1} - \dot{d}_1^{(0)}, \dots, \dot{r}_{1,N_r} - \dot{d}_{N_r}^{(0)}, \dots, \dot{r}_{N_t, N_r} - \dot{d}_{N_r}^{(0)}\}
\end{aligned} \tag{43}$$

In (37) and (40), \mathbf{x} and $\dot{\mathbf{x}}$ are replaced by the result $\hat{\boldsymbol{\theta}}$ in (18). From (38) and (42), the integrated equation can be expressed in the matrix form as

$$\boldsymbol{\varepsilon}_c = \mathbf{h}_c - \mathbf{G}_c \Delta \boldsymbol{\theta}_1 \tag{44}$$

Where

$$\mathbf{G}_c = [\mathbf{G}_{c,1}^T, \mathbf{G}_{c,2}^T]^T$$

$$\mathbf{h}_c = [\mathbf{h}_{c,1}^T, \mathbf{h}_{c,2}^T]^T$$

$$\boldsymbol{\varepsilon}_c \approx \mathbf{T}_c [\mathbf{q}^T, \dot{\mathbf{q}}^T]^T$$

$$\mathbf{T}_c = [\mathbf{T}_{c,1}^T, \mathbf{T}_{c,2}^T]^T$$

The solution of (44) is calculated using WLS as

$$= (\mathbf{G}_c^T \mathbf{W}_c^{-1} \mathbf{G}_c)^{-1} \mathbf{G}_c^T \mathbf{W}_c^{-1} \mathbf{h}_c \tag{46}$$

Where $\mathbf{W}_c \approx \mathbf{T}_c Q \mathbf{T}_c^T$.

The derivation process of $\Delta \hat{\boldsymbol{\theta}}_1$ ignores the second-order error terms, so the derived $\Delta \hat{\boldsymbol{\theta}}_1$ is the first-order error term of Ddn-2SWLS, which needs to be eliminated from the original estimate $\hat{\boldsymbol{\theta}}$.

Then, we recalculate Ta, Wa and Wb by (13) and (17) on the basis of $\hat{\boldsymbol{\theta}}$, and get the second-order error term $\Delta \boldsymbol{\theta}_2$ from (24), (29) and (33). Finally, the bias-reduced solution of $\hat{\boldsymbol{\theta}}_0 = [\hat{\mathbf{x}}_0^T, \hat{\dot{\mathbf{x}}}_0^T]^T$ can be given by

$$\hat{\boldsymbol{\theta}}_0 = \hat{\boldsymbol{\theta}} - \Delta \hat{\boldsymbol{\theta}}_1 - \Delta \boldsymbol{\theta}_2 \tag{47}$$

This paper is concerned with the root mean square position error (RMSPE), the root mean square velocity error (RMSVE), the position bias (Pbias) and the velocity bias (Vbias) to evaluate the performance of target localization. RMSPE, RMSVE, Pbias and Vbias are defined as

$$RMSPE = \sqrt{E(\|\mathbf{x}_0 - \hat{\mathbf{x}}_0\|^2)}$$

$$RMSVE = \sqrt{E(\|\dot{\mathbf{x}}_0 - \hat{\dot{\mathbf{x}}}_0\|^2)}$$

$$Pbias = \|\mathbf{E}(\mathbf{x}_0 - \hat{\mathbf{x}}_0)\|$$

$$Vbias = \|\mathbf{E}(\dot{\mathbf{x}}_0 - \hat{\dot{\mathbf{x}}}_0)\|$$

respectively. From the former part of bias analysis, we can see that the elimination of the second-order error term $\mathbf{E}(\Delta \boldsymbol{\theta})$ can lower the Pbias and Vbias. At the same time, At the same time, the bias-reduced solution eliminating the first-order and second-order error terms in (48) can theoretically improve the performance of RMSPE and RMSVE very well.

4. Numerical Simulations

The simulations are performed to compare the relative localization accuracy and bias value of different methods. To evaluate the comprehensive performance of different methods, we simulate the near-field localization and the far-field localization, respectively. The near-field case means the target position is roughly in the spatial structure formed by the illuminators and receivers, while the far-field case refers to the target located outside the spatial structure formed by the illuminators and receivers.

For near-field case in this paper, we set the target randomly within a sphere, of which center is the coordinate origin and radius is $R/2$. The illuminators and receivers are placed randomly between the two spherical surfaces whose centers are the origin and radii are $R/2$ and R , respectively, as shown in Figure 2, where cubes, tetrahedron and, sphere represent illuminators, receivers and target respectively. Meanwhile, the velocities of the target, the illuminators and, the receivers are random vectors whose lengths are not greater than V . Here, R and V are two constants to represent distance and velocity respectively.

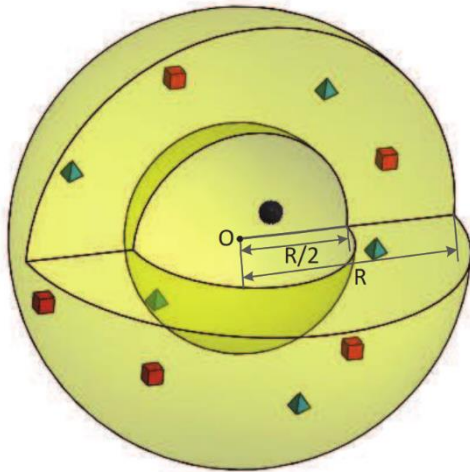


Fig. 2 An example of spatial structure in near-field case.

For the far-field case in this paper, we set the target randomly between the two spherical surfaces with radius $R/2$ and R respectively, and the illuminators and receivers randomly within the sphere with radius $R/2$, as shown in Figure 3. The velocities are random vectors no greater than V .

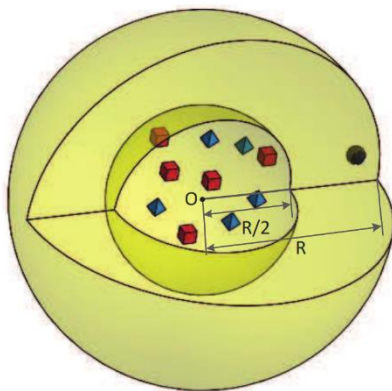
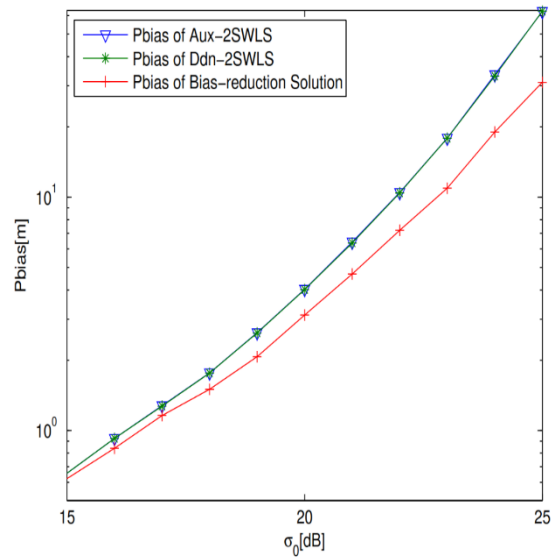
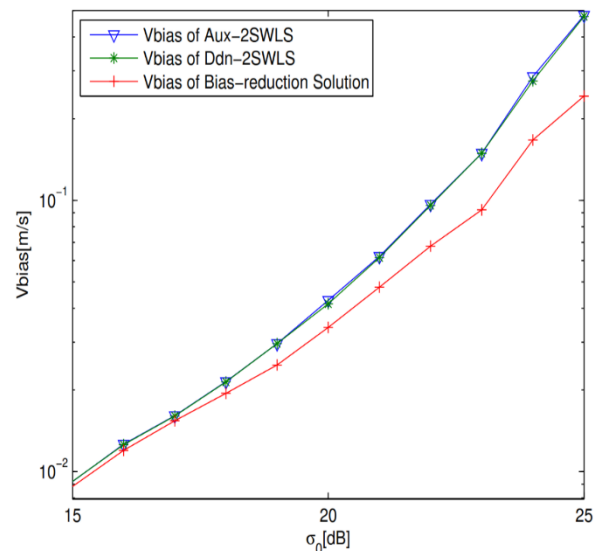


Fig. 3 An example of spatial structure in far-field case.

Considering an illuminator of opportunity passive radar consisting of five illuminators and five receivers in 3-D space, we set $R=2000m$, $V=20m/s$ and, $\eta = 0.01$. The simulation results are obtained via 10000 Monte Carlo runs. The simulation results of RMSPE, RMSVE, Pbias and Vbias of Aux-2SWLS, Ddn-2SWLS and the proposed bias-reduction solution concerning σ_0 in different cases are given in Figure 4, 5, 6 and 7.

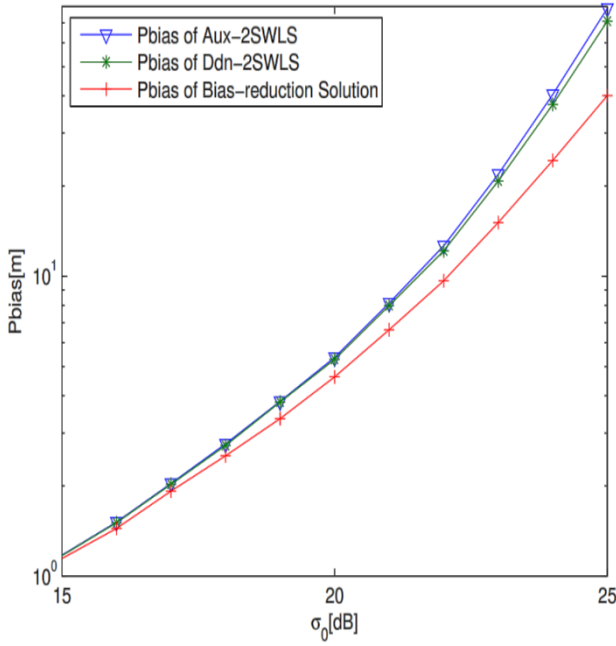


(a) Comparison of the Pbias.

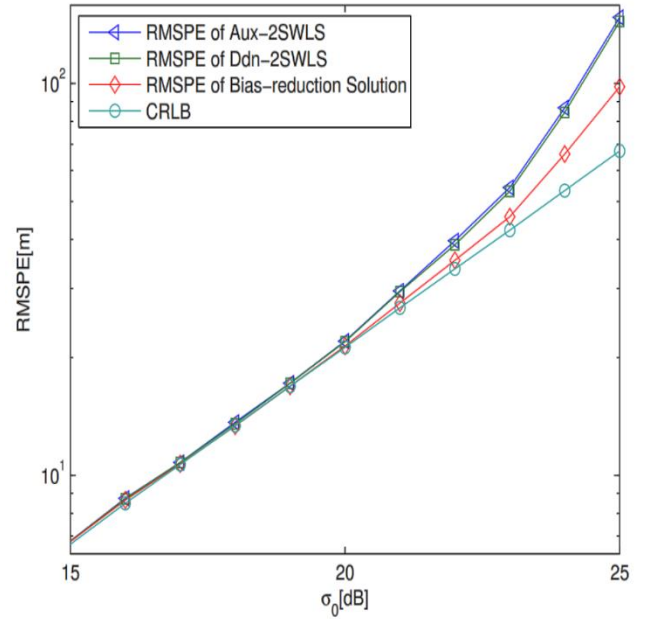


(b) Comparison of the Vbias

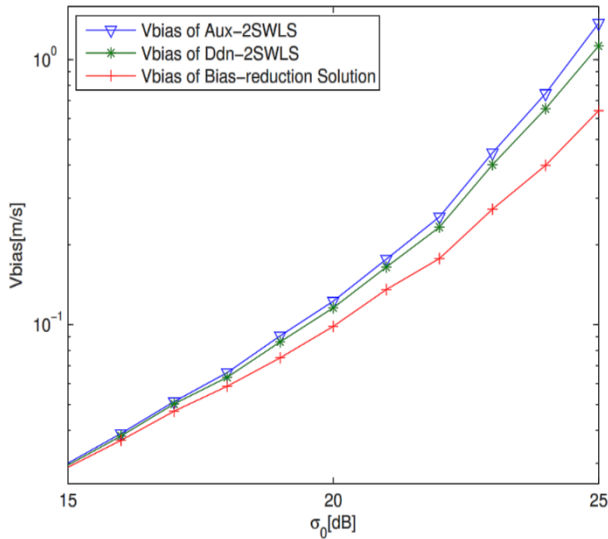
Fig. 4 Comparison of the bias of Aux-2SWLS, Ddn-2SWLS and the proposed bias-reduction solution with regard to σ_0 in the near-field case: (a) Pbias and (b) Vbias.



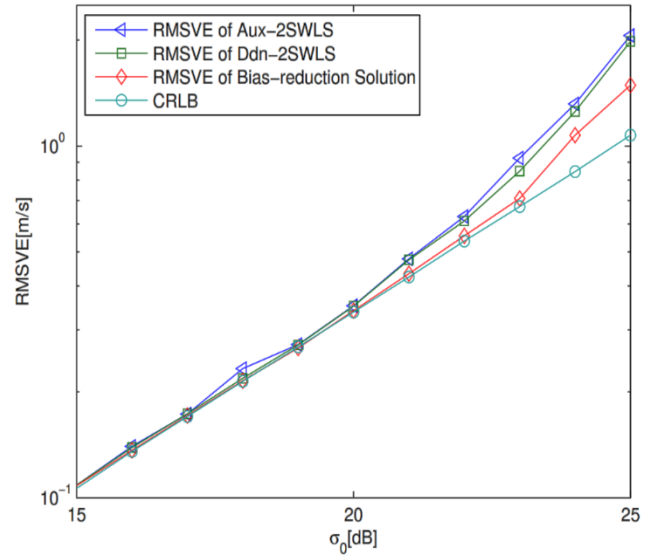
(a) Comparison of the Pbias.



(a) Comparison of the RMSPE.



(b) Comparison of the Vbias.



(b) Comparison of the RMSVE.

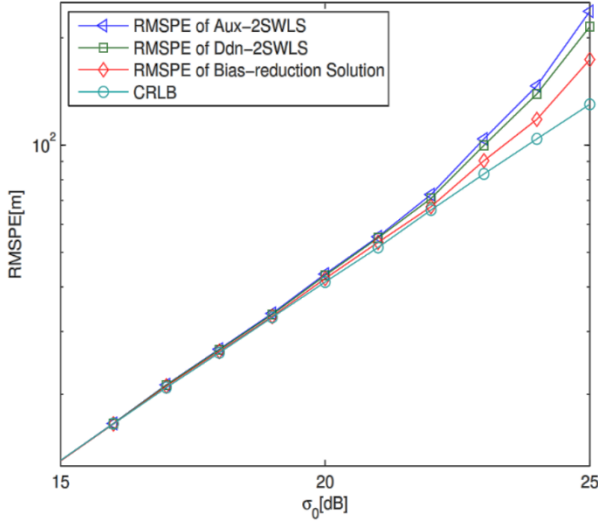
Fig. 5 Comparison of the bias of Aux-2SWLS, Ddn-2SWLS and the proposed bias-reduction solution with regard to σ_0 in the far-field case: (a) Pbias and (b) Vbias.

Fig. 6 Comparison of the RMSPE and RMSVE of Aux-2SWLS, Ddn-2SWLS and the proposed bias-reduction solution with regard to σ_0 in the near-field case: (a) RMSPE and (b) RMSVE.

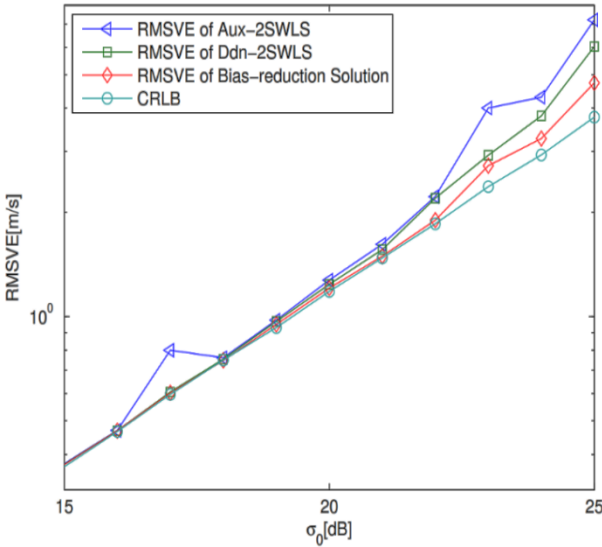
Figure 4 and Figure 5 illustrate the bias of the Aux-2SWLS method, the Ddn-2SWLS method and the proposed bias-reduction method at different noise levels. As we can see from Figure 4 and Figure 5, both in near-field and far-field cases, Aux-2SWLS and Ddn-2SWLS have a similar bias, while the bias-reduction solution could reduce the bias to a considerable extent compared to Aux-2SWLS and Ddn-2SWLS, especially at higher noise levels. For instance, when σ_0 is 25dB, the Pbias and Vbias of the bias-reduction solution are about half of these of Aux-2SWLS and Ddn-2SWLS. This proves the effectiveness of the proposed bias-reduction solution.

We can see from Figure 6 and Figure 7 that there is an apparent difference between CRLB curves and simulation results of different methods since σ_0 is above 20dB. When σ_0 is larger than 20dB, not at all times but in general, the RMSPE and RMSVE curves of Ddn-2SWLS are obviously closer to the CRLB than Aux-2SWLS for the consideration of distance-dependent noises, especially for the far-field case. The locations of illuminators, receivers, and targets in this simulation are limited in different spheres while, theoretically, the difference between the curves of Aux-2SWLS and Ddn-2SWLS will be bigger when the spatial

geometry of illuminators, receivers, and target is more complicated. Furthermore, through bias reduction, the localization accuracy has been greatly improved, and it implies the practical significance of the bias-reduction solution at high noise levels.



(a) Comparison of the RMSPE.



(b) Comparison of the RMSVE.

Fig. 7 Comparison of the RMSPE and RMSVE of Aux-2SWLS, Ddn-2SWLS and the proposed bias-reduction solution with regard to σ_0 in the far-field case: (a) RMSPE and (b) RMSVE.

To Find the CRLB for estimating the phase we need the PDF:

$$P(x; \phi) = \frac{1}{(2\pi\delta^2)^{\frac{N}{2}}} \exp\left[-\frac{\sum_{n=0}^{N-1} (x[n] - 2\pi fn + \phi)^2}{2\delta^2}\right] \quad (49)$$

Now taking the log gets rid of the exponential, then taking partial derivative gives:

$$(50)$$

$$\frac{\partial \ln p(x; \phi)}{\partial \phi} = \frac{-A}{\delta^2} \sum_{n=0}^{N-1} (x[n] \sin(2\pi fn + \phi) - \frac{A}{2} \sin(4\pi fn + 2\phi))^2$$

Taking partial derivative again:

$$\frac{\partial^2 \ln p(x; \phi)}{\partial \phi^2} = \frac{-A}{\delta^2} \sum_{n=0}^{N-1} (x[n] \cos(2\pi fn + \phi) - A \cos(4\pi fn + 2\phi))^2$$

Still depends on random vector x so need $E\{\}$

Taking the expected value:

$$-E\left\{\frac{\partial^2 \ln p(x; \phi)}{\partial \phi^2}\right\} = E\left\{\frac{-A}{\delta^2} \sum_{n=0}^{N-1} (x[n] \cos(2\pi fn + \phi) - A \cos(4\pi fn + 2\phi))^2\right\} = \frac{-A}{\delta^2} (E\{x[n]\} \cos(2\pi fn + \phi) - A \cos(4\pi fn + 2\phi))$$

$$E\{x[n]\} = A \cos(2\pi fn + \phi)$$

So, plug that in, get a \cos^2 term, use trig identity, and get

$$-E\left\{\frac{\partial^2 \ln p(x; \phi)}{\partial \phi^2}\right\} = \frac{A^2}{2\delta^2} \left[\sum_{n=0}^{N-1} 1 - \sum_{n=0}^{N-1} \cos(4\pi fn + 2\phi)\right] \approx \frac{NA^2}{2\delta^2} = N \times SNR$$

f not near to 0 or $\frac{1}{2}$

Now, invert to get CRLB:

$$\text{Var}\{\hat{\phi}\} = \frac{1}{N \times SNR} \quad (54)$$

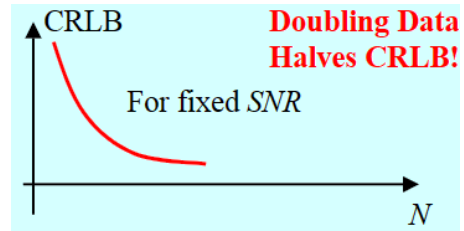


Fig. 8 Doubling data halves CRLB

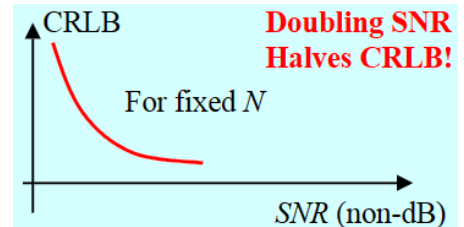


Fig. 9 Halve CRLB for every 3B in SNR

Does an efficient estimator exist for this problem? The CRLB theorem says there is only if

$$\frac{\partial \ln p(x; \phi)}{\partial \phi} = I(\theta)[g(x) - \theta] \quad (55)$$

Our earlier result was:

$$(56)$$

$$\frac{\partial \ln p(x; \phi)}{\partial \phi} = \frac{-A}{\partial^2} \sum_{n=0}^{N-1} (x[n] \sin(2\pi f n + \phi) - \frac{A}{2} \sin(4\pi f n + 2\phi))^2$$

We will see later though, an estimator for which $\text{Var}\{\hat{\phi}\} \rightarrow \text{CRLB}$ as $N \rightarrow \infty$ or as $\text{SNR} \rightarrow \infty$

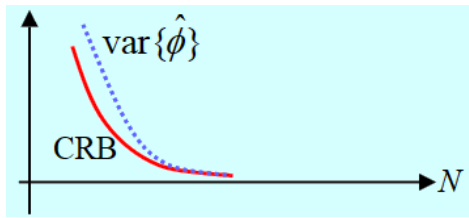


Fig. 10 $\text{Var}\{\hat{\phi}\} \rightarrow \text{CRLB}$ as $N \rightarrow \infty$ or as $\text{SNR} \rightarrow \infty$

Such an estimator is called an asymptotically efficient estimator

5. Conclusions

Considering the realistic distance-dependent noises and the bias in 2SWLS methods, we developed a bias-reduced solution for target localization in illuminator of opportunity passive radar. This solution is proved by numerical simulations to be effective to reduce the bias and attain the CRLB, especially at higher noise levels. The theoretical performance of the proposed method is derived via second-order error analysis, demonstrating theoretically the effectiveness of the proposed method in reducing the bias and achieving the CRLB under moderate noise. That is to say, the proposed bias-reduced solution is useful for the illuminator of opportunity passive radar localization problem.

References

- [1] Palmer J, Palumbo S, Cao V, et al. A new illuminator of opportunity bistatic radar research project at DSTO. Defence Science and Technology Organisation Edinburgh (Australia) Electronic Warfare and Radar Division. 2009.
- [2] H. Ma, M. Antoniou, D. Pastina, F. Santi, F. Pieralice, M. Bucciarelli and M. Cherniakov, "Maritime moving target indication using passive GNSS-based bistatic radars," *IEEE Transactions on Aerospace and Electronic Systems*. 54(1):115-130, 2018.
- [3] J. Palmer, S. Palumbo, A. Summers, D. Merrett, S. Searle and S. Howard, "An overview of an illuminator of opportunity passive radar research project and its signal processing research directions," *Digital Signal Processing*. 21(5):593-599, 2011.
- [4] M. Malanowski and K. Kulpa, "Two Methods for Target Localization in Multistatic Passive Radar," *IEEE Transactions on Aerospace and Electronic Systems*. 48(1):572-580, 2012.
- [5] S. Wu, D. Xu, J. Tan, et al. "Two base station location techniques with adjusted measurements in circular scattering environments," *International Journal of Communication Systems*. 29(6):1073-1083, 2016.
- [6] N. H. Nguyen, "Multistatic Target Tracking and Localization: Waveform Adaptation, Geometry Optimization, and Pseudolinear Estimation," *University of South Australia*. 2016.
- [7] A. Ali, G. Shah, M. Aslam, "Model for autonomous agents in machine-to-machine navigation networks," *International Journal of Communication Systems*. 31(4): e3491, 2018.
- [8] K.C. Ho and W. Xu, "An accurate algebraic solution for moving source location using TDOA and FDOA measurements," *IEEE Transactions on Signal Processing*. 52(9):2453-2463, 2004.
- [9] B. Xu, W. D. Qi, L. Wei and P. Liu, "Turbo-TSWLS: enhanced two-step weighted least squares estimator for TDOA-based localization," *Electronics Letters*. 48(25): 1597-1598, 2012.
- [10] H. Yang and J. Chun, "An improved algebraic solution for moving target localization in noncoherent MIMO radar systems," *IEEE Transactions on Signal Processing*. 64(1):258-270, 2016.
- [11] R. Amiri, F. Behnia and M.A.M Sadr, "Efficient positioning in MIMO radars with widely separated antennas," *IEEE Communications Letters*. 21(7):1569-1572, 2017.
- [12] R. Amiri, F. Behnia and M.A.M Sadr, "Positioning in MIMO radars based on constrained least squares

estimation,” *IEEE Communications Letters*. 21(10):2222-2225, 2017.

[13] B. Huang, L. Xie and Z. Yang, “TDOA-based source localization with distance-dependent noises,” *IEEE Transactions on Wireless Communications*. 14(1):468-480, 2015.

[14] K. C. Ho, “Bias reduction for an explicit solution of source localization using TDOA,” *IEEE Transactions on Signal Processing*. 60(5): 2101-2114, 2012.

[15] S. Stein, “Algorithms for ambiguity function processing,” *IEEE Transactions on Acoustics, Speech, and Signal Processing*. 29(3):588-599, 1981.

[16] M. Cherniakov, “Bistatic radars: emerging technology,” *John Wiley & Sons*. 2008.

[17] Y. T. Chan and K. C. Ho, “A simple and efficient estimator for hyperbolic location,” *IEEE Transactions on signal processing*,” 42(8):1905-1915, 1994.

Habib rasi received the B.Sc. in Electrical and Electronic Engineering in 2009 in Sattari university, Tehran, Iran, M.Sc. of radar signal processing in 2012 in Islamic azad university of Shahr-e Rey branch in Tehran province, He received PhD degree in Electrical Engineering from Shiraz university of technology Shiraz, Iran, in 2019. His research interests include Radar Signal Processing, Radar Signal Design, Statistical Signal Processing, Electronic Warfare Systems.

Maryam Shirzadian Gilan received both B.Sc. and M.Sc. Degrees in Electrical Engineering in Electronics and Telecommunications fields respectively in 2010 and 2012 from Shahid Beheshti University, Tehran, Iran. She received her PhD degree in Telecommunications Engineering from Islamic Azad University, Science Research Branch, Tehran, Iran in 2019 and currently works as an assistant professor at Islamic Azad University of Kermanshah, Iran. Her research interests include Antennas, Radar, Radio Networks, and Nanotechnology in electromagnetics, signal processing and wave propagation.

A Game Theory Based Dynamic Transmission Opportunity Adjustment in WLANs

Mahdieh Ghazvini*

Department of Computer Engineering, Faculty of Engineering, Shahid Bahonar University of Kerman, Kerman, Iran
mghazvini@uk.ac.ir

Naser Movahedinia

Faculty of Computer Engineering, University of Isfahan, Isfahan, Iran
naserm@eng.ui.ac.ir

Kamal Jamshidi

Faculty of Computer Engineering, University of Isfahan, Isfahan, Iran
jamshidi@eng.ui.ac.ir

Received: 04/Oct/2018

Revised: 18/May/2019

Accepted: 28/Sep/2019

Abstract

IEEE 802.11e is standardized to enhance real-time multimedia applications' Quality of Service. This standard introduces four access categories for different types of applications. Each access category has four adjustable parameters: Arbitrary Inter-Frame Space Number, minimum Size of Contention Window, maximum size of Contention Window, and a Transmission Opportunity limit. A Transmission Opportunity limit is the time interval, in which a wireless station can transmit a number of frames consecutively, without releasing the channel and any further contention with other wireless stations. Transmission Opportunity improves network throughput as well as service differentiation. Proper Transmission Opportunity adjustment can lead to better bandwidth utilization and Quality of Service provisioning. This paper studies the dynamic adjustment of Transmission Opportunity in IEEE 802.11e using a game-theory based approach called Game Theory Based Dynamic Transmission Opportunity. Based on the proposed method, each wireless node chooses its appropriate Transmission Opportunity according to its queue length and media access delay. Simulation results indicate that the proposed approach improves channel utilization, while preserving efficiency in WLANs and minimizing selfishness behaviors of stations in a distributed environment.

Keywords: Transmission Opportunity (TXOP); Game Theory; WLAN, IEEE 802.11e; EDCA.

1. Introduction

The IEEE 802.11 standard supports only the best effort service, providing the same access probability to wireless media for all applications [1]. In practice, however, delay-sensitive traffic applications such as voice and video need to experience limited delays; therefore, IEEE 802.11e is standardized to improve Quality of Service (QoS) of real-time multimedia applications. This standard defines a medium access method called Hybrid Coordination Function (HCF) with two access mechanisms called Enhanced distributed channel access (EDCA) and HCF Controlled Channel Access (HCCA) [2]. The HCCA and EDCA are contention-free and contention-based channel access mechanisms, respectively. Each mechanism has four Access Categories (ACs) for different types of traffic. These ACs are known as voice (AC_VO), video (AC_VI), best-effort (AC_BE) and background (AC_BK). AC_VO and AC_VI have queues with the highest priorities, AC_BE has medium priority and AC_BK is the one with the lowest priority. Each AC in the EDCA mode which uses Carrier Sense Multiple Access (CSMA), has four adjustable parameters: Arbitrary Inter-Frame Space Number(AIFSN), the minimum Size of Contention Window(CWmin), the maximum size of Contention Window (CWmax), and TXOP_limit [3].

AIFS determines the time interval a wireless station should wait before the start of channel-access negotiation. Different AIFSNs are assigned to each AC based on the AC to improve QoS differentiation. In case of unsuccessful access, a backoff procedure starts and the wireless station chooses a random value called backoff time, in the range of zero and CWmin. The CWmin is doubled each time a collision occurs until it achieves the CWmax. The AC with higher priority has a shorter CWmin. A short CW decreases the channel access delay but increases the collision probability. Eventually, TXOP_limit (TXOP) describes the maximum duration a wireless station can transmit and it is assigned per AC. The ACs can be prioritized by adjusting these four parameters. The major challenge is how to adjust these parameters dynamically in order to support the QoS of multimedia applications. Researches show that proper TXOP adjustment may significantly improve channel utilization and media access delay [4].

The main contribution of this paper is presenting a heuristic non-cooperative game to dynamic adjustment of TXOP. On the one hand, Game theory is a mathematical tool exploited to analyse the circumstances in which multiple participants (players) interact or affect each other. In other words, in game theory, a player's payoff is depended on not its decisions but also others' decisions.

* Corresponding Author

Besides, Game theory is a tool to investigate systems' behaviors as well as to optimize their performance in multi-agent environments. Although optimization theory cannot consider interactions between different players, game theory is a useful tool to study and analyse these interactions. Because of the competing nature of such an interaction, in order to make a decision, each player should analyse the effect of others' reactions and decide how to behave to gain the most benefit.

On the other hand, choosing a long TXOP by a station has negative effects on the neighbouring stations and the repetition of this action by the other stations may lead to violation of QoS requirements of the stations. Therefore, each station should consider the effect of its TXOP adjustment on the other stations and the overall network performance. Therefore, every long-sighted and rational station should consider the possibility of retaliation from the other stations in order to improve channel utilization along with providing proportional fairness [5] without any need to solve a global optimization problem.

Table 1. List of Acronyms and Abbreviations

AC	Access Category
AIFSN	Arbitrary Inter-Frame Space Number
ATXOP	Adaptive TXOP
CSMA/CA	Carrier Sense Multiple Access/Collision Avoidance
CW	Contention Window
CW_{max}	Maximum Contention Window
CW_{min}	Minimum Contention Window
DCF	Distributed Coordination Function
DIFS	Distributed Inter-Frame Space
EDCA	Enhanced Distributed Channel Access
GDTXOP	Game Theoretic Dynamic TXOP
GTXOP	Game Theoretic TXOP
HCCA	HCF Controlled Channel Access
HCF	Hybrid Coordination Function
MAC	Media Access Control
PCF	Point Coordination Function
QoS	Quality of Service
TXOP	Transmission Opportunity
WLANs	Wireless Local Area Networks

Although, TXOP tuning in terms of the number of stations using game theory is presented in [6], different types of traffic, including voice, video, and best effort as well as network load, mean data rate, maximum burst size, user priorities, delay bound, channel conditions, etc. have not been considered in that study. In our proposed game model, TXOP will be determined according to the station's traffic types, stations' load, and different delay bounds. The payoff function of [6] is defined based on analytical models. It includes some equations with complex solutions in order to achieve suitable TXOP for each transmission. However, in the current study the payoff function is simple and requires little computing as

well as no need to know the number of active stations. A list of abbreviations and acronyms used throughout the paper is given in Table 1.

Investigation of related work is given in Section 2. The proposed method and its evaluation are included in Section 3 and Section 4, respectively. Finally, the paper is concluded in Section 5.

2. Related Work

Studies show that TXOP adjustment may improve the channel utilization, performance and media access delay in IEEE 802.11e based WLANs, significantly [4]. The studies on dynamic TXOP can be divided into two main categories. The first category is dynamic TXOP determination in multiple-rate networks. Since there are different transmission rates, some approaches have been proposed to establish fairness. In the second category, by considering different characteristics of stations, such as arrival rate and type of traffic, some solutions have been proposed to improve the channel utilization.

In the first category, it is supposed that stations support multi-rate transmission, and the amount of transmitted frames in a specific period of time for a multi-rate network depends on the data transfer rate in that specific time period. Hence, in an IEEE 802.11e based multi-rate WLAN, a constant TXOP causes unfairness. In other words, in case of constant TXOP, the stations with higher data rates transmit more data than those with lower data rates. To fix this problem, some mechanisms are proposed to generate adaptive TXOPs, according to network conditions. For example, to ensure temporal fairness in multi-rate WLAN the studies in [6] have shown that equalization of channel access time results in granting an adapting throughput according to the data transmission rate of stations. Guo in [7] proposed Dynamic TXOP Assignment for Fairness, (DTAF) in order to keep fairness in multi-rate 802.11e networks. In DTAF, prior to transmission and based on the amount of collision, network traffic conditions are estimated, then the TXOP parameter is adjusted according to the load condition of the network. In [7], it is assumed that the network is in saturation condition and there are only three stations with various rates.

In [8] Adaptive TXOP (ATXOP) is proposed, in which longer TXOPs are allocated to those stations with lower data rates and vice versa. As a result, initially, the average transmission rate for each wireless station is calculated, and then the current transmission rate of each station is compared to the current rate. If the current rate is lower or higher than the average rate, the TXOP will be changed according to the ratio of the current rate to the average rate. Although the unfairness due to modification to the transmission rate is investigated in [8], TXOP allocation for different multimedia and data traffics is not analysed correctly. In addition, simulations indicate that this solution works well merely for small-sized packets and does not always lead to a better solution than the standard. Additionally, since this algorithm does not take into account the number of stations and the amount of contention in case

of proliferation of stations and collisions, the efficiency of this method declines. Authors of [8], in [9], also entailed packet size in the calculation of new TXOPs and by doing so, have improved their former work in terms of fairness.

Nevertheless, with an increase in the number of stations and consequently in collisions, the performance degrades. In order to cope with the problem of performance decline due to channel faults. In [10] dynamic allocation of TXOP is proposed based on accurate predictions of channel conditions and allocating different TXOPs to different traffic. To cope with the unfairness problem due to different data rates, Yazdani et al. [11] proposed a mechanism for TXOP determination, which considers data rate, channel error rate, and data packet size to calculate adaptive TXOPs.

The main characteristic of multimedia traffic is that they are bursting and self-similar which indicates a frequent massive burst of frames. Hence, TXOPs must be adjusted according to traffic characteristics dynamically [12], so in the second group of studies, this issue is considered. In [12] each station adjusts its TXOP according to the state of its transmission queue. According to his approach, if a queue is not long enough and set to a limit, its TXOP is set to default values. In the case of the queue length exceeding the limit, the TXOP is reinforced by a new value, which is bigger than the default value (double of the default value). Simulations and numerical analysis indicate that the value of TXOP must be chosen according to buffer size [13-19]. Fang et al [20] have adjusted the value of TXOP through a Random Early Detection (RED) mechanism. They used queue length, which reflects the network load at the moment. The RED algorithm is a buffer management method in which the probability of packet loss increases in relation to the average queue size in a linear manner. Through this solution, traffic load conditions in QAP and stations are monitored. In the case of queue size, being less than the lower threshold (Tl) a smaller value is set for TXOP and if queue length exceeds this threshold, TXOP increases according to queue length in a linear manner. If queue length exceeds the high threshold level (Th), the maximum value for TXOP is used. This algorithm relies on improving QoS of video streams similar to [21].

In ETXOP [10], assuming that input traffic follows Poisson distribution, TXOP values is calculated based on the priority of ACs and its stream data rate whenever an AC wins the contention. Whenever a stream gets access to the channel, ETXOP algorithm reviews MAC queue and estimates the queue length and frame average size. Then, it calculates the most appropriate TXOP, which satisfies QoS requirements. In fact, the TXOP limit is determined based on the existing frames in the queues of AC2 and AC3. For AC0 and AC1, however, the default values of EDCA are used. ETXOP provides more flexibility by adapting network streams' QoS requirements, regardless of their individual bit rate.

In case of heavy traffic, by assigning long TXOPs to high priority ACs, low-priority traffics will suffer from starvation. Liu and Zhao [22], have allocated TXOP values in variable bit rate conditions. Their solution tunes TXOPs

according to the size of incoming frames, variable-rate video prediction algorithms, and current queue length. TXOP is predicted as the total required time to transmit the next incoming frame and all the existing frames in the transmission queue as well as their ACKs. The main drawback of this solution is the computational complexity due to using a wavelet estimator for dynamic estimation of TXOP. Another dynamic TXOP allocation scheme [23] assigns the variable length of TXOP to different traffics based on the number of Service Data Units (SDUs) to be transmitted. It is claimed that this approach improves the packet delivery ratio, throughput, and end-to-end delay [23]. Al-Maqri et al [24] used piggybacked information about the size of the subsequent video frames of the uplink traffic to assign the TXOP according to the fast changes in the VBR profile. In [26], the TXOP dependency on the maximum number of VOIP calls in 802.11 networks is studied. In this approach, the highest priority is given to QAP by assigning longer TXOPs to it. However, this increase in TXOP causes a bottleneck to shift from QAP to stations, long waiting to access the channel and consequently causes long delays for stations. In addition, it has been shown that there is an optimum value for TXOP and voice capacity in WLANs. It will not be improved if values greater than TXOP higher band are used.

The impact of TXOP on video streams has been studied, and it is acknowledged that TXOP mechanism is not suitable for audio streams with a constant bit rate [25]. In [26], a QoS-capable mechanism is proposed to guarantee both inter-AC and intra-AC differentiations. In [26], each traffic class monitors the MAC queue and then based on the queue length, it calculates TXOP at runtime. An admission control function is also proposed to maintain accepted streams and network scalability. This method does not consider the frames, which are received during transmission. In [27], a distributed policy is presented in which each station measures its throughput in a temporal window and then compares its value to the target throughput and finally determines the TXOP based on the result of that comparison. In [28] the dynamic TXOP allocation scheme (DTAS) is presented. DTAS includes link lifetime estimation and dynamic TXOP allocation tasks, which dynamically allocate TXOPs to vehicles to enhance the efficiency of non-safety applications. It assigns TXOPs based on the number of competing providers, the number of packets to be transmitted and link lifetime between providers and their users. In addition, in order to improve the performance of TXOP scheduling and channel resource utilization, a game-theory-based optimization framework is proposed [29]. For every station according to the current channel capacity and transmission requirements of the stations, the optimal TXOP is determined. In another study [4], the authors proposed the Enhanced QoS with Q-Learning (EQQ) based on users' channel state estimations in order to enhance the QoS of multimedia services by adjusting TXOP and service interval (SI).

In IEEE 802.11 based Wireless mesh networks (WMNs), the fairness problem makes users in different locations of

the WMN experience a different QoE and QoS [30]. Authors of [31] presented an approach to mitigate the unfairness problem in WMNs by tuning the TXOP at each intermediate node according to the number of flows served. A dynamic TXOP allocation approach based on a weighted fair queuing solution and average traffic rate of the ACs in WMNs is proposed in [32]. The approach improves fairness in wireless multi-hop networks.

Based on our knowledge, although a lot of researches from different points of view has been done to adjust TXOP dynamically, the impacts of choosing TXOP by a station on the other stations have been taken into account in only two works [6, 29]. At first, In [6] according to the number of stations in a network, a game-theoretic approach called GTXOP is proposed to determine TXOP dynamically. GTXOP is defined based on analytical models of EDCA. In GTXOP, each station can adjust its TXOP dynamically by taking the interaction between stations and impact of them on one another into account[6]. In addition, in order to improve the performance of TXOP scheduling and channel resource utilization, A game theory based optimization framework is proposed [29] where, for every station according to the current channel capacity and transmission requirements of the stations, the optimal TXOP is determined.

3. The proposed method for dynamic TXOP Adjustment

Ad hoc networks rely on the cooperation of stations. As such, they are susceptible to selfish attacks that abuse network mechanisms [33]. In all situations with two or more players that involve known payouts or quantifiable consequences, game theory can be used to help determine the most likely outcomes. WLANs are an example of such environments. In fact, game theory is a common tool for examining and analysing the problems of wireless networks. It is able to model the characteristics or limitations of wireless networks; such as lack of coordination. The theory of non-cooperative games can model conflict situations between individual players, where the payoffs of each player depend not only on its own actions but also on the actions of the other player. Non-cooperative game theory studies the optimum behaviour of rational players when cost(s) and utility(s) of each rational player depending on its own choice as well as the others. IEEE 802.11 based wireless networks are typical examples of such systems, in which communicating nodes access the channel through the CSMA method influencing the other neighbouring nodes' access. There are several parameters, which have significant effects on the performance of WLANs such as contention window, transmission power, transmission rate, transmission opportunity, etc. Game theory is widely used in CSMA based wireless networks, for different objectives such as contention window adjustment, media access control, transmission power, and rate tuning, TXOP control and etc. [6, 34-36].

In EDCA mode of 802.11e, which uses CSMA, it is seen that when an AC takes over the channel, its transmission time (TXOP) affects the other ACs' queue delay as well as the other stations. In the case of numerous active stations, this can cause frame starvation. Transmission with long TXOP reduces contention chances for channel and consequently, other stations will have little chance to transmit their frames. Hence, TXOP parameter must be set carefully and rigorously. In fact, choosing a long TXOP by a station has a negative effect on neighbouring stations, and if other stations imitate and repeat this action, it may lead to violating QoS requirements of those stations. Therefore, each station must consider the effect of its action on the others prior to adjusting it. However, in the methods that have been proposed so far for dynamic determination of TXOP, the effects of stations on one another have not been taken into account.

Therefore, to incorporate the effects of other stations, it would be helpful to model this problem within game theory framework. Game theory examines decision making in a shared environment for multiple rational decision makers with different goals. In other words, this theory plays an important role in cooperation and contention analysis among diverse rational agents. Rationality is one of the most common assumptions made in game theory. It means that every player always maximizes his utility, thus being able to perfectly calculate the probabilistic result of every action. Therefore, a rational player is goal-oriented, reflective and consistent.

The main characteristic of making a decision in game conditions is analyzing the others' reactions prior to choosing an action by an agent. After this analysis, it must take an action, which is the best one for it and gains the highest amount of payoff by taking other opponents' reactions into account. The environment in which there is such an effect and mutual reaction among decision makers is called a strategic environment and each decision maker in this environment is called a player. A game is comprised of a set of players, existing actions for the players and a set of payoff functions. Usually, a payoff function is defined in each game, which is the subtraction between a utility function and a cost function for players. The payoff function is a mapping from the action space of players to a set of real numbers. Its definition plays an important role in a game. The solution to a game is displayed by an array of a user's strategies in the game. Generally, in game theory, the goal is to find equilibrium in a game, where each player employs a strategy, which is the best response to the other players' strategies. Nash equilibrium is a solution to a game in which none of the players gains by changing their strategy in a one-way manner [2-8]. Hence, the idea of the game is to form a decision set (for each player) in which a user's strategy is the best response for her/ him and the other players choose their best strategy as well. In other words, each player chooses the best reaction to what the others

have done, and each player should obtain a fair share of payoff at equilibrium.

Additionally, resistance against selfish behavior is another characteristic, which has to be taken into account in order to maintain security. In fact, in autonomous wireless networks, instead of a cooperative behavior, players may implement a strategy to maximize their own interest and utility through a selfish action regardless of the harms they will cause to the others. Therefore, it cannot be implicitly assumed that players will follow designed protocols. To do so, suitable and efficient protocols are required that are able to lead players to an equilibrium even in such conditions. In other words, the proposed method should incorporate a strategy in which none of the selfish stations has any intention to disobey the protocol. In this paper, the TXOP dynamic determination is modeled as a non-cooperative game called GDTXOP. In this game, each player implements its own strategy, including TXOP period, in order to maximize its own payoff function. A distributed and dynamic mechanism to improve TXOP, based on delay and the number of stations and the existing frames in queues, is proposed.

3.1 System Model and Problem Statement

The problem of controlling TXOP in multiple-access contention-based networks deals with the determination of the period to take over the media after winning the contention. Within the Game theory, each active station is considered as a network agent that must decide on adjusting its TXOP each time it accesses the channel. Each station makes decisions based on maximizing a payoff function that is defined in the station's decision space and indicates the amount of utility by a station in the environment.

The goal is to reach an efficient equilibrium point for the whole network when the stations maximize their payoff functions locally. It is obvious that the utilization of environment by a station is maximized when the mentioned station does its transmission in all time slots. Such selfishness behaviour causes unfairness for the adjacent stations and decreases the network throughput dramatically. Thus, the payoff function has to be defined in a way that each player makes decisions in order to maximize the whole network utilization. Therefore, in order to achieve this, the payoff function is, to use the resources of the shared environment including time and frequency, each station must pay some costs. It is clear that in a shared channel network; only one station is able to transmit its frames in TXOP period after winning the contention. Therefore, if a station increases its TXOP period selfishly, regardless of the other stations, it will increase channel access delays of the other stations. This increment causes the number of the existing frames to increase in the station's buffers and ultimately buffer-overflow. Therefore, the other stations, through a countermeasure to prevent buffer overflow, increase their own TXOPs. In the case of repeating this action by all stations, all the stations will be harmed and consequently the overall network throughput

decline. Thus, choosing long intervals for TXOP by some stations causes violation of QoS and unfairness for the others. Therefore, for adjusting TXOP, each station must consider its effect on the others and chooses it is suitable TXOP regarding the arrival traffic, transmission rate and also the feedback of its former behaviours. Media access delay can be a suitable criterion to evaluate the others' behaviours and also the amount of network traffic. In other words, each station can evaluate its former behaviours' feedback by calculating its own media access delay. Thus, media access delay, which can be calculated easily for each station, can help stations to choose a suitable TXOP.

On the one hand, each station is different in terms of incoming traffic rate and must incorporate queue length in determining TXOP. Therefore, each station attempts to increase its TXOP whenever it notices an increase in its buffer queue length. A station can increase its throughput by increasing its TXOP and consequently transmitting more frames without involving further in the contention process. Thus, in this case, TXOP results in throughput improvement. On the other hand, media access delay for each station can be considered as a kind of cost in media access. This cost, informs each station about traffic volume and network load. By observing an undesirable increase in media access delay, each station notices that there has been an increase in either traffic volume or the number of active stations. Since the goal of all stations is to cooperate with one another and improve network performance, on the observation of delay increase, they tune their TXOP proportional to the observed delay and their former TXOP in order to prevent their QoS requirements violation. As a result, each station attempts to establish an appropriate trade-off between queue length and arrival traffic.

3.2 GDTXOP Game Definition

Let us assume that $G = [N, \{TXOP_i\}, \{u_i(\cdot)\}]$ indicates the GDTXOP game where $N = \{1, 2, \dots, n\}$ is the set of active stations in the network and $TX_i = [TXOP_{min}, TXOP_{max}]$ is the strategy space of the station i . The payoff function of the MAC layer for the station i is shown as $u_i(TXOP_i, TXOP_{-i})$. This function indicates satisfaction level of station i when choosing $TXOP_i$ to transmit its frames. The TXOP vector of the other network stations other than station i is shown as $TXOP_{-i}$. The mathematical definition of GDTXOP game is as follows:

$$GDTXOP \max_{TXOP_i \in TX_i} u_i(TXOP_i) \quad \forall j \in N \quad (1)$$

Various payoff functions can be defined for this game, but the defined function must be a continuous, strictly increasing and concave function. To guarantee proportional fairness, a logarithmic function is used in defining the payoff function. The goal is to maximize the throughput of each station so that media access delay decreases and fairness of media access will be achieved. According to the analysis of EDCA, average media access time can be expressed as follows [15, 37-40]:

$$E[A_i] = T_{ci}\varphi_i + \bar{\sigma}_i\delta_i \quad (2)$$

Where, T_{ci} is the average collision time and $\bar{\sigma}_i$ indicates the average time interval observed by each station. φ_i and δ_i variables show the number of collisions before a successful transmission and the average number of time intervals that station i was deferred in back off, respectively [15, 37-40].

$$\varphi_i = \sum_{l=0}^m \frac{lpc_i^l(1-pc_i)}{(1-pc_i)^{m+1}} \quad (3)$$

$$\delta_i = \sum_{l=0}^m \sum_{h=0}^1 \frac{\min(2^h CW_{\min}, CW_{\max}) - 1}{2} \frac{pc_i^l(1-pc_i)}{1-pc_i^{m+1}} \quad (4)$$

Where, pc_i is collision probability and CW_{\min}, CW_{\max} are the minimum and maximum size of contention window, respectively. The reasonable time interval would be [15, 37-40]:

$$\bar{\sigma}_i = (1-pb_i)\sigma + \sum_{r=1}^N ps_i^r T_s^r + pc_i T_c \quad (5)$$

Where σ is the length of a physical time interval and T_s^r shows the average amount of time for a successful burst transmission for a station in class r . In addition, pb_i and ps_i^r indicate the probability of the channel being busy and the probability of successful access for class r . Given that only the logical time interval is a function of $TXOP_i$, the average media access time can be expressed as follows [15, 37-40]:

$$\begin{aligned} E[A_i] &= T_c\varphi_i + \bar{\sigma}_i\delta_i \\ &= T_c\varphi_i + \delta_i \left[(1-pb_i)\sigma + \sum_{r=1}^N ps_i^r T_s^r + pc_i T_c \right] \\ &= T_c\varphi_i + \delta_i \left[(1-pb_i)\sigma + ps_i T_s \right. \\ &\quad \left. + \sum_{r=1}^{N-1} ps_i^r T_s^r + pc_i T_c \right] \\ &= T_c\varphi_i + \delta_i \left[(1-pb_i)\sigma + pc_i T_c + ps_i TXOP_i \right. \\ &\quad \left. + \sum_{r=1}^{N-1} ps_i^r TXOP_r \right] \end{aligned} \quad (6)$$

Therefore, the average media access delay can be as:

$$E[A_i] = \Psi_i + f_i(TXOP_i, TXOP_{-i}) \quad (7)$$

Where,

$$\Psi_i = T_c\varphi_i + \delta_i[(1-pb_i)\sigma + pc_i T_c] \quad (8)$$

And,

$$f_i(TXOP_i, TXOP_{-i}) = \delta_i \left[ps_i TXOP_i + \sum_{r=1}^{N-1} ps_i^r TXOP_r \right] \quad (9)$$

According to these definitions, $u_i(\cdot)$, the payoff function for station i can be defined as follows:

$$\begin{aligned} u_i(TXOP_i, TXOP_{-i}) &= \alpha_i Q_i \log(TXOP_i) \\ &\quad + \beta_i (\mu_i - [\Psi_i + f_i(TXOP_i, TXOP_{-i})])^2 \end{aligned} \quad (10)$$

Where, μ_i and Q_i show the most tolerable delay (delay threshold) and queue length of the station, respectively. In addition, $\alpha_i > 0$ and $0 < \beta_i$ are constant weights to normalize the payoff function. Choosing a logarithmic function in the payoff function ensures the efficient solution to fairness [41]. GDTXOP game with the payoff function defined in (10) is a heuristic game. The first statement in equation (10) indicates that the higher the value of TXOP and the queue length of a station, the higher the media utilization by that station will be. The second statement shows the effect of controlling TXOP on the payoff function, which guarantees the maximum amount of media access delay that is μ , for station i as a barrier function. In additions, β_i is the weight of the barrier function. Therefore, each link attempts to maximize its TXOP while adjusting its MAC delay to experience the minimum delay. This term somehow shows the cost function in the payoff function. It can be seen that the payoff function is a function of each station's TXOP, the other station's TXOP and also the number of network stations. The cost function considered in the payoff function is used to coordinate selfish decisions of stations in order to use network resources efficiently.

It is assumed that it is not possible to transmit fake frames. Stations' utilization is reduced in proportional to the delay it experiences. That is, each station decreases its utilization by the amount of difference between its delay and the delay threshold. Thus, the stations, which experience higher delay, reduce their utilization by a lower amount factor and as a result achieve longer TXOPs. However, the stations, which tolerate longer delays, set shorter TXOPs. In addition, increasing queue length has positive effects on increasing TXOPs.

3.3 Analysis of GDTXOP Game

There is Nash equilibrium in GDTXOP game if $\alpha_i > 0$ and $0 < \beta_i$. It should be proved that the strategy space of each user is a convex and compact subset and $u_j(TXOP_j)$ is continuous and concave. As that the strategy space of each user is an infinite subset of R , it is compact and convex. In addition, the payoff function in TXOP is continuous. The Hessian of this payoff function is as follows:

$$\begin{aligned} & \nabla^2_{TXOP_i} u_i(\cdot) \\ & = -\alpha_i \frac{Q_i}{TXOP_i^2} + 2\beta_i (ps_i \delta_i)^2 < 0, \\ & (0 < \alpha_i, \beta_i \ll 1) \end{aligned} \quad (11)$$

On the one hand $0 < TXOP_i \ll 1$ and $1 < Q_i$, and on the other hand $0 < ps_i \ll 1$ and $(0 < \alpha_i, \beta_i)$. Thus, assuming $\beta_i \rightarrow 0$, the Hessian function will be negative. If Hessian function is negative, the mentioned payoff function will be a concave function. The best solution from the viewpoint of the station i is obtained by local optimization of Equation (10). With respect to faster convergence of the Gradient method, each station, according to the Gradient method, updates its TXOP as follows:

$$\begin{aligned} TXOP_i(t+1) &= TXOP_i(t) \\ &+ \gamma_i \frac{du_i(TXOP_i, TXOP_{-i})}{dTXOP_i} \end{aligned} \quad (12)$$

$$\begin{aligned} TXOP_i(t+1) &= TXOP_i(t) \\ &+ \gamma_i \left(\alpha_i \frac{Q_i}{TXOP_i(t)} - 2\beta_i ps_i \delta_i (\mu \right. \\ &\left. - [\Psi_i + f_i(TXOP_i, TXOP_{-i})]) \right) \end{aligned} \quad (13)$$

Suppose we identify the delay by $MD_i(t)$ ¹. Thus, by substituting this delay in (13), the TXOP scheme turns into a following access latency problem then TXOP is calculated as follows:

$$\begin{aligned} TXOP_i(t+1) &= TXOP_i(t) + \\ &\gamma_i \left(\alpha_i \frac{Q_i}{TXOP_i(t)} - 2\beta_i ps_i \delta_i (\mu - MD_i(t)) \right) \end{aligned} \quad (14)$$

3.4 Distributed GDTXOP Algorithm

According to GDTXOP game, each station in every media access (probably successful) measures its current queue length and the maximum amount of MAC delay. Then based on them, it sets its TXOP. The GDTXOP algorithm proposed for dynamic TXOP determination is shown in Table 2. In addition to the existence and uniqueness of the solution, the efficiency of the proposed method is also important. The GDTXOP can be analysed from efficiency point of view by comparing the proposed method with other former methods and also the standard method. In the next section, the proposed approach is simulated and compared with existing solutions.

4. Evaluation of the Proposed Method

Since the goal of this research is to increase throughput and maintain delay threshold and fairness within different

traffic categories, the most relevant work to the current research is the one by Min et al (called TBD-TXOP) [12]. Hence, the proposed method is compared with TBD-TXOP and also with original EDCA. To do so, several scenarios with different number of stations and three kinds of different traffic type; voice, video and best effort are used.

Table 2. GDTXOP Algorithm

<p>1. Initialization:</p> <p>For each station $j \in N$, the initial TXOP value is the same as the specified value in the 802.11e standard i.e. $TXOP_j(t_0) \in TXOP_i$.</p> <p>2. Measuring:</p> <p>2. A. Measuring the maximum media access delay of the station j</p> <p>2. B. Measuring the queue length of the station j</p> <p>3. Updating TXOP:</p> <p>Each station updates its TXOP using (14)</p> <p>4. Transmission.</p>

In order to obtain more clarity and do a better comparison, it is assumed that each station supports only one type of traffic. In the first scenario, three stations are used and each one supports one type of traffic. In real environments, voice traffic and video traffic have a bursting nature, so these two traffic types are defined in a self-similar manner (ON-OFF type with Pareto distribution and exponential arrival rate). Best effort traffic, however, is transmitted with a constant bit rate service. The arrival rate of the stations is random and the scenario is simulated with 3, 6, 9, 12, 15 stations. The network capacity is assumed to be 5.5 Mbps. The number of stations for each traffic type in all scenarios is the same but the traffic flow is different.

The desired delay for voice, video, and best effort traffic were set to 200, 300, 500 milliseconds respectively. In addition, to increase reliability, the simulations for each scenario are repeated several times using different seeds and finally, the average is calculated from the result of different iterations. The results are compared in terms of throughput, delay and drop rate.

4.1 Throughput Comparisons

Throughput is evaluated from the viewpoint of different ACs and in terms of overall throughput. Throughput for each ACs, is equal to the amount of payload received by the physical layer and delivered to the higher level for that ACs by the MAC sublayer of each station. Of course, it is noteworthy that repeated and incomplete frames are not considered in throughput. Fig.1 illustrates the comparison of voice, video and best effort traffic in different scenarios (different number of stations).

In TBD-TXOP and EDCA methods, the network has become saturated for BE traffic in the scenario with 12 stations and consequently, the throughput declined in these two methods. GDTXOP, however, provides good

¹ MAC Delay

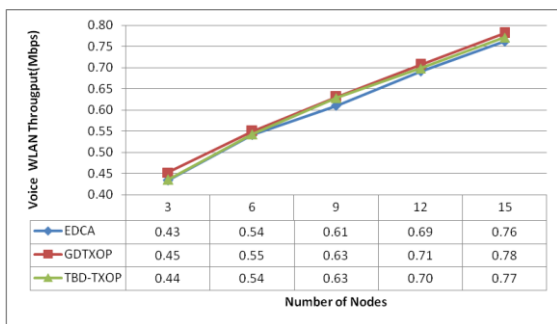
conditions in terms of throughput ceaselessly for the stations. The network stability area in GDTXOP has increased and the saturation boundary is postponed. In GDTXOP, upon entering the saturated region, this method attempts to maintain the throughput of low-priority traffics within acceptable limits in order to establish higher fairness by applying a little delay. The overall throughput (Fig.1(d)) is equal to the total number of bits transmitted from the MAC layer of every station in network to higher layers regardless of their ACs. Clearly, by setting TXOP appropriately and dynamically, the GDTXOP improves the throughput of each traffic type especially the traffic with low priority.

The GDTXOP is more flexible than TBD-TXOP, in turn; it is more compatible with network conditions. In addition, in TBD-TXOP, similar to EDCA, TXOP is used for high-priority ACs. In GDTXOP, however, TXOP mechanism is used for every ACs, by choosing different delay thresholds.

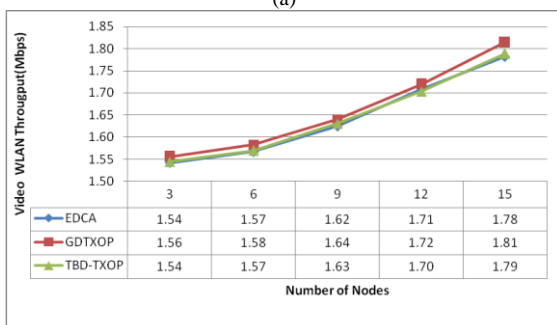
4.2 Delay Comparisons

End-to-end delay includes queuing delay, media access delay and packet transmission and receiving delay. In other words, this delay is equal to the average delay of all packets received and submitted to higher layers, by the MAC layer of all the network stations. Fig.2.(a) illustrates the comparison of voice traffic delay, which shows the result of the simulation of the three methods.

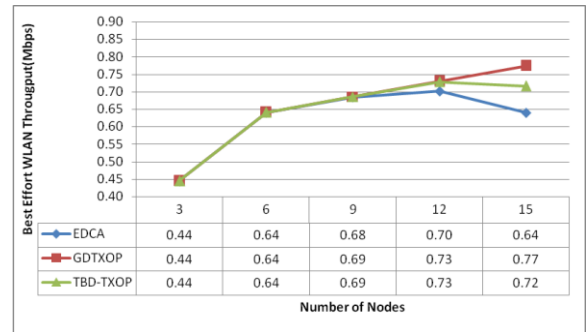
It is clear that TBD-TXOP and GDTXOP impose less delay on the stations carrying voice traffic than EDCA. The delay in GDTXOP, however, is a little higher than TBD-TXOP method. This increase in delay is the cost that GDTXOP imposes on stations with audio applications in order to improve traffics with low priority. Since voice traffic's delay tolerability is about 400 milliseconds, this slight delay will not be troublesome.



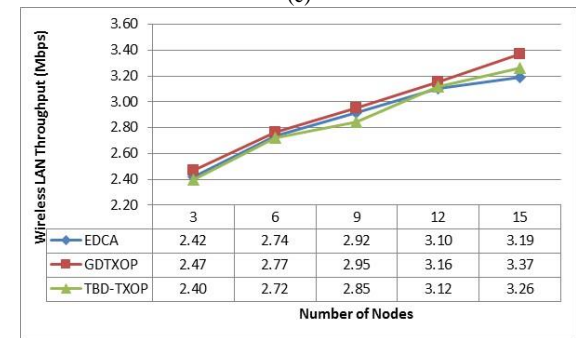
(a)



(b)



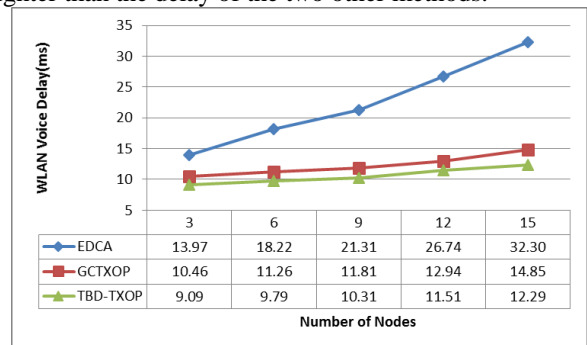
(c)



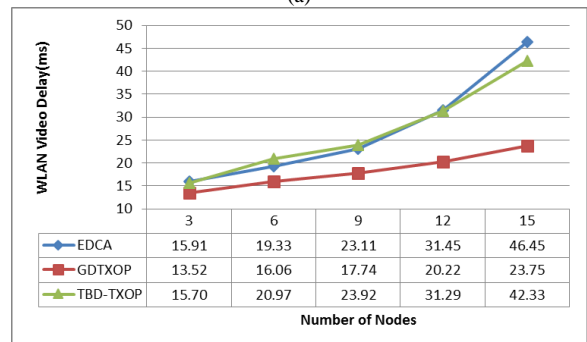
(d)

Fig.1. Throughput comparison of (a). Voice traffic (b). Video traffic (c). Best effort traffic (d). Network throughput

However, in comparison to the voice traffic which has the highest priority and gets access to the channel ahead of all other traffics, the delay of GDTXOP for video traffic (Fig.2.(b)) and best effort traffic (Fig.2.(c)) is much slighter than the delay of the two other methods.



(a)



(b)

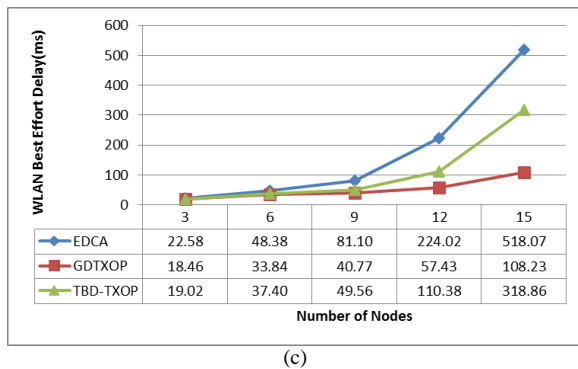


Fig.2. Delay comparison (a). Voice traffic (b). Video traffic (c). Best effort traffic

4.3 Drop Comparisons

The amount of packet drop caused by buffer overflow is illustrated in Fig.3.(a). In the simulation, the size of MAC layer buffer is considered to be finite (256000 bits, approximately 32 KB). Therefore, overflow occurs when a packet is received from the higher layers and a full buffer is encountered. In bursting traffics in which several packets arrive frequently from higher layers, buffer overflow is more probable. Hence, the approach to prevent this problem is burst transmission that is proportional to the length of the buffer. Since, the number of existing packets in a queue is taken into account in both TBD-TXOP and GDTXOP when determining TXOP, in these two methods, the stations experience much fewer buffer overflows than EDCA.

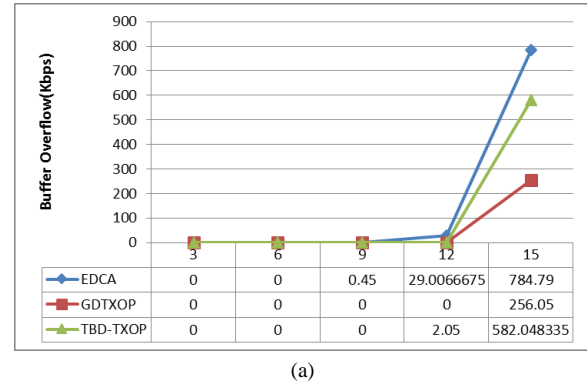
In addition, GDTXOP causes fewer overflows than TBD-TXOP due to the more flexibility it features in determining TXOP. Moreover, a considerable amount of the overflow is concerned with low-priority traffics. These traffic types, in TBD-TXOP and EDCA, do not get the chance to access the channel, transmit their frames, and as a result suffer from overflow.

However, another reason for packet loss is packet drop due to exceeding the retry limit. In case an ACK frame is not received by the transmitter, it is assumed that the transmission encountered a problem and has to be retransmitted.

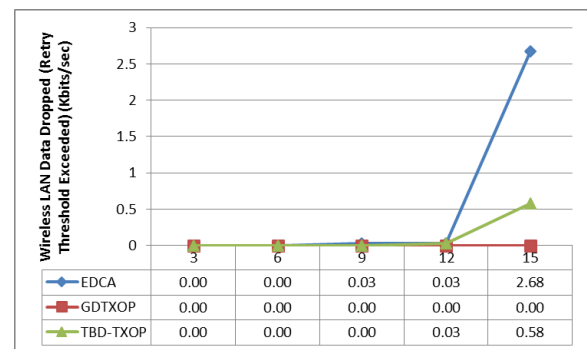
The retransmission is repeated until the packet is transmitted successfully or the number of retrials exceeds the allowed retry limit, which is usually 7 times, in which case the frame is disposed. The comparison of packet drop due to exceeding the retry limit is illustrated in Fig.3.(b). The important factor, which affects the amount of packet loss due to re-transmission, is the size of contention window. In case of saturation, in which each station always has a packet to transmit in its queue, the size of contention window is so important and plays a determining role in the probability of packet loss.

The size of contention window must increase according to the number of stations, and re-transmissions should repeat with longer periods to decrease the probability of packet loss due to successive collisions, significantly. Since the appropriate determination of

TXOP results in increasing the network stability area, and consequently postponing the saturation region, it reduces the number of transmissions and decreases the collision probability.



(a)



(b)

Fig.3. Drop Comparison (a). Packet drop due to buffer overflow (b). Packet drop due to exceeding retry limit

Therefore, in the simulation, packet drop has not occurred in GDTXOP due to exceeding the re-transmission limit. In addition, in TBD-TXOP fewer drops are observed than EDCA, again due to postponing the saturation region up to 12 stations.

5. Conclusion

In this paper, Transmission Opportunity (TXOP) was allocated using game theory. TXOP is a limited period of time allocated to each station in which the station can transmit any possible number of frames without contention with the other stations. TXOP improves network throughput as well as service differentiation. Choosing long TXOP by some stations causes unfairness and QoS violations for the others. Thus, in the proposed non-cooperative game, GDTXOP, the payoff function is defined in a way that each station chooses its appropriate TXOP according to its queue length and media access delay. Using the results of the game, an algorithm was obtained to control and determine TXOP dynamically. The resulting algorithm was simulated and its accuracy was evaluated and verified. The results of the simulation

indicate that tuning TXOP appropriately improves both channel utilization for all levels of traffic priority and fairness. This improvement does not impair the QoS of high-priority applications.

References

- [1] A. Malik, J. Qadir, B. Ahmad, K.-L. A. Yau, and U. Ullah, "QoS in IEEE 802.11-based wireless networks: a contemporary review," *Journal of Network and Computer Applications*, vol. 55, pp. 24-46, 2015.
- [2] H. I. Zawia, R. Hassan, and D. P. Dahnil, "A survey of medium access mechanisms for providing robust audio video streaming in IEEE 802.11 standard," *IEEE Access*, vol. 6, pp. 27690-27705, 2018.
- [3] A. Banchs and P. Serrano, "Analysis and Configuration of IEEE 802.11e," in *Medium Access Control in Wireless Networks*: Nova Science Publishers, 2008.
- [4] H. Ghazanfar, R. Taheri, and S. Nejatian, "Application of Learning Methods for QoS Provisioning of Multimedia Traffic in IEEE802.11e," in *Fundamental Research in Electrical Engineering*: Springer, 2019, pp. 369-383.
- [5] L. Li, M. Pal, and Y. R. Yang, "Proportional fairness in multi-rate wireless LANs," in *IEEE INFOCOM 2008-The 27th Conference on Computer Communications*, 2008: IEEE, pp. 1004-1012.
- [6] M. Ghazvini, N. Movahedinia, and K. Jamshidi, "GTxOP: A game theoretic approach for QoS provisioning using transmission opportunity tuning," *PloS one*, vol. 8, no. 5, p. e62925, 2013.
- [7] N. Guo, C. Chen, and C. Pei, "Dynamic TXOP Assignment for Fairness (DTAF) in IEEE 802.11 e WLAN under Heavy Load Conditions," in *Parallel and Distributed Computing, Applications and Technologies, 2006. PDCAT'06. Seventh International Conference on*, 2006: IEEE, pp. 80-85.
- [8] E. K. Kim and Y. J. Suh, "ATxOP: an adaptive TXOP based on the data rate to guarantee fairness for IEEE 802.11 e wireless LANs," in *60th Vehicular Technology Conference, 2004. VTC2004-Fall.*, 2005, vol. 4: IEEE, pp. 2678-2682.
- [9] E. Kim and Y. J. Suh, "A Rate Adaptive Transmission Opportunity for Fairness over IEEE 802.11 e Wireless LANs," in *IEEE International Conference on Communications, ICC '07 2007*: IEEE, pp. 4523-4528.
- [10] K. Ju, D. Lee, and K. Chung, "Dynamic TXOP allocation to support QoS based on channel conditions in wireless networks," in *8th International Conference on Computing Technology and Information Management (ICCM)*, 2012, vol. 2: IEEE, pp. 721-724.
- [11] M. Yazdani, M. Kamali, N. Moghim, and M. Ghazvini, "A fair access mechanism based on TXOP in IEEE 802.11 e wireless networks," *International Journal of Communication Networks and Information Security (IJCNIS)*, vol. 8, no. 1, 2016.
- [12] G. Min, J. Hu, and M. E. Woodward, "A dynamic IEEE 802.11e txop scheme in wlan under self-similar traffic: Performance enhancement and analysis," in *International Conference on Communications, ICC '08, 2008*: IEEE, pp. 2632-2636.
- [13] L. Romdhani and C. Bonnet, "Performance analysis and optimization of the 802.11 e EDCA transmission opportunity (TXOP) mechanism," in *Third IEEE International Conference on Wireless and Mobile Computing, Networking and Communications, WiMOB 2007.*, 2007: IEEE, pp. 68-75.
- [14] Y. P. Fallah and H. M. Alnuweiri, "Modeling and Performance Evaluation of Frame Bursting in Wireless LANs," in *IWCMC '06: Proceeding of the 2006 International Conference on Communications and Mobile Computing*, New York, NY, USA, 2006, pp. 869-874.
- [15] J. Hu, G. Min, and M. E. Woodward, "Analysis and Comparison of Burst Transmission Schemes in Unsaturated 802.11e WLANs," in *Global Telecommunications Conference (Globecom)*, Washington, DC, USA, 2007, pp. 5133-5137.
- [16] F. Peng, H. M. Alnuweiri, and V. C. M. Leung, "Analysis of burst transmission in IEEE 802.11 e wireless LANs," in *Communications, 2006. ICC'06. IEEE International Conference on*, 2006, vol. 2: IEEE, pp. 535-539.
- [17] S. Selvakennedy, "The Influence of MAC Buffer on the Contention Based Access Scheme with Bursting Option for IEEE 802.11e Wireless Networks," *Journal of Engineering Science and Technology (JESTEC)*, vol. 1, no. 2, pp. 119-138, 2006.
- [18] Rashwand S. and J. Mišić, "Stable operation of IEEE 802.11e EDCA: Interaction between offered load and MAC parameters," *Ad Hoc Networks*, vol. 10, pp. 162-173, 2012.
- [19] S. Rashwand and J. Misić, "IEEE 802.11e EDCA under Bursty Traffic-How Much TXOP Can Improve Performance," *IEEE Transactions on Vehicular Technology*, vol. 60, no. 3, pp. 1099-1115, 2011.
- [20] Z. Feng, G. Wen, Z. Zou, and F. Gao, "RED-TXOP scheme for video transmission in IEEE802.11e EDCA WLAN," in *Communications Technology and Applications, 2009. ICCTA'09. IEEE International Conference on*, 2009: IEEE, pp. 371-375.
- [21] J. Majkowski and F. C. Palacio, "Dynamic TXOP configuration for QoS enhancement in IEEE 802.11 e wireless LAN," in *International Conference on Software in Telecommunications and Computer Networks, SoftCOM'06.*, Barcelona 2006: IEEE, pp. 66-70.
- [22] H. Liu and Y. Zhao, "Adaptive EDCA algorithm using video prediction for multimedia IEEE 802.11 e WLAN," in *Wireless and Mobile Communications, 2006. ICWMC'06. International Conference on*, 2006: IEEE, pp. 10-10.
- [23] K. Ju and K. Chung, "Dynamic TXOP allocation for multimedia QoS providing over wireless networks," in *Information Networking (ICOIN), 2013 International Conference on*, 2013: IEEE, pp. 397-401.
- [24] M. A Al-Maqri, M. Othman, B. Mohd Ali, and Z. Mohd Hanapi, "Providing Dynamic TXOP for QoS Support of Video Transmission in IEEE 802.11 e WLANs," *Journal of Networks*, vol. 10, no. 9, pp. 501-511, 2015.
- [25] N. Cranley, T. Debnath, and M. Davis, "An Experimental Investigation of Parallel Multimedia Streams Over IEEE 802.11e WLAN Networks Using TXOP," in *IEEE International Conference on " in International Conference on Communications, ICC'07, Glasgow, Scotland, 2007*, pp. 1740-1746.
- [26] A. Ksentini, A. Nafaa, A. Gueroui, and M. Naimi, "ETxOP: A resource allocation protocol for QoS-sensitive services provisioning in 802.11 networks," *ELSEVIER's Performance Evaluation (PEVA)*, vol. 64, no. 5, pp. 419-443, 2007.
- [27] J. Y. Lee, H. Y. Hwang, J. Shin, and S. Valaee, "Distributed optimal TXOP control for throughput requirements in IEEE 802.11 e wireless LAN," in *22nd International Symposium on Personal Indoor and Mobile*

- Radio Communications (PIMRC)*, 2011: IEEE, pp. 935-939.
- [28] M. A. Togou and G.-M. Muntean, "A Dynamic Transmission Opportunity Allocation Scheme to Improve Service Quality of Vehicle-to-Vehicle Non-Safety Applications," in *2018 IEEE 87th Vehicular Technology Conference (VTC Spring)*, 2018: IEEE, pp. 1-5.
- [29] Z. Zhu, F. Cao, and Z. Fan, "WLAN throughput management: A game theoretic TXOP scheduling approach," in *Computer Aided Modelling and Design of Communication Links and Networks (CAMAD), 2015 IEEE 20th International Workshop on*, 2015: IEEE, pp. 161-164.
- [30] C.-H. Lin, C.-K. Shieh, W.-S. Hwang, and W.-T. Huang, "Proportional bandwidth allocation with consideration of delay constraint over IEEE 802.11 e-based wireless mesh networks," *Wireless Networks*, vol. 24, no. 5, pp. 1575-1592, 2018.
- [31] J. Lee, H. Yoon, and I. Yeom, "Distributed fair scheduling for wireless mesh networks using IEEE 802.11," *IEEE transactions on vehicular technology*, vol. 59, no. 9, pp. 4467-4475, 2010.
- [32] M. Namazi, N. Moghim, M. Ghazvini, and A. Askarian, "Dynamic TXOP Assignment in IEEE802.11e Multi-hop Wireless Networks Based on an Admission Control Method," *Wireless Personal Communications*, vol. 97, no. 1, pp. 749-772, 2017.
- [33] S. Szott and J. Konorski, "Traffic remapping attacks in ad hoc networks," *IEEE Communications Magazine*, vol. 56, no. 4, pp. 218-224, 2018.
- [34] I. Ahmad, Z. Kaleem, R. Narmeen, L. D. Nguyen, and D.-B. Ha, "Quality-of-service aware game theory-based uplink power control for 5G heterogeneous networks," *Mobile Networks and Applications*, vol. 24, no. 2, pp. 556-563, 2019.
- [35] Y. Jiang, H. Ge, M. Bennis, F.-C. Zheng, and X. You, "Power control via Stackelberg game for small-cell networks," *Wireless Communications and Mobile Computing*, vol. 2019, 2019.
- [36] H. Jang, S.-Y. Yun, J. Shin, and Y. Yi, "Game theoretic perspective of optimal CSMA," *IEEE Transactions on Wireless Communications*, vol. 17, no. 1, pp. 194-209, 2018.
- [37] J. Hu, G. Min, W. Jia, and M. E. Woodward, "Comprehensive QoS Analysis of Enhanced Distributed Channel Access in Wireless Local Area Networks," *Information Sciences*, pp. 20-34, 2012.
- [38] J. Hu, G. Min, and M. E. Woodward, "Performance analysis of the TXOP burst transmission scheme in single-hop ad hoc networks with unbalanced stations," *Computer Communications*, vol. 34, no. 13, pp. 1593-1603, 2011.
- [39] G. Min, J. Hu, W. Jia, and M. E. Woodward, "Performance analysis of the TXOP scheme in IEEE 802.11 e WLANs with bursty error channels," in *Wireless Communications and Networking Conference, 2009. WCNC 2009. IEEE*, 2009: IEEE, pp. 1-6.
- [40] J. Hu, G. Min, M. E. Woodward, and W. Jia, "A comprehensive analytical model for IEEE 802.11 e QoS differentiation schemes under unsaturated traffic loads," in *Communications, 2008. ICC'08. IEEE International Conference on*, 2008: IEEE, pp. 241-245.
- [41] F. Kelly, "Charging and rate control for elastic traffic," *European transactions on telecommunications*, vol. 8, no. 1, pp. 33-37, 1997.

Mahdieh Ghazvini received her B.Sc. from Shahid Bahonar University of Kerman, Iran in 2000, and her M.Sc. and Ph.D. from the University of Isfahan, Isfahan, Iran in 2004 and 2013, in Computer Architecture Engineering, respectively. Currently she is assistant professor of Computer Engineering Department at Shahid Bahonar University of Kerman. She is the author of several technical papers in signal processing and telecommunications journals and conferences. Her research interests are wireless networks, game theory, signal processing and neural networks.

Naser Movahedinia received his B.Sc. from Tehran University, Tehran, Iran in 1987, and his M.Sc. from Isfahan University of Technology, Isfahan, Iran in 1990, and his Ph.D. degree from Carleton University, Ottawa, Canada in 1997, in Electrical and Computer Engineering. Currently he is a full professor at the Faculty of Computer Engineering, University of Isfahan. His research interests are wireless networks, Internet Technology and Intelligent Systems.

Kamal Jamshidi received his B.Sc. in Electrical Engineering from Isfahan University of Technology, Isfahan, Iran, in 1988, and his M.Sc. from Department of Electrical Engineering, Anna University, Madras, India, in 1992. He got his Ph.D. in Electrical Engineering from Indian Institute of Technology (IIT), Madras, India, in 1995. Currently, he is an associate professor at the Faculty of Computer Engineering, University of Isfahan. His research interests are wireless networks, digital control, fuzzy logic, cyber-physical system, digital signal and image processing.

Farsi Conceptual Text Summarizer: A New Model in Continuous Vector Space

Mohammad Ebrahim Khademi

Faculty of Electrical and Computer Engineering, Malek Ashtar University of Technology, Iran
khademi@mut.ac.ir

Mohammad Fakhredanesh*

Faculty of Electrical and Computer Engineering, Malek Ashtar University of Technology, Iran
fakhredanesh@mut.ac.ir

Seyed Mojtaba Hoseini

Faculty of Electrical and Computer Engineering, Malek Ashtar University of Technology, Iran
mojtabahoseini@aut.ac.ir

Received: 04/Feb/2019

Revised: 24/Aug/2019

Accepted: 08/Sep/2019

Abstract

Traditional methods of summarization were very costly and time-consuming. This led to the emergence of automatic methods for text summarization. Extractive summarization is an automatic method for generating summary by identifying the most important sentences of a text. In this paper, two innovative approaches are presented for summarizing the Farsi texts. In these methods, using a combination of deep learning and statistical methods (TFIDF), we cluster the concepts of the text and, based on the importance of the concepts in each sentence, we derive the sentences that have the most conceptual burden. In these methods, we have attempted to address the weaknesses of representation in repetition-based statistical methods by exploiting the unsupervised extraction of association between vocabulary through deep learning. In the first unsupervised method, without using any hand-crafted features, we achieved state-of-the-art results on the Pasokh single-document corpus as compared to the best supervised Farsi methods. In order to have a better understanding of the results, we have evaluated the human summaries generated by the contributing authors of the Pasokh corpus as a measure of the success rate of the proposed methods. In terms of recall, these have achieved favorable results. In the second method, by giving the coefficient of title effect and its increase, the average ROUGE-2 values increased to 0.4% on the Pasokh single-document corpus compared to the first method and the average ROUGE-1 values increased to 3% on the Khabir news corpus.

Keywords: Extractive Text Summarization; Unsupervised Learning; Language Independent Summarization; Continuous Vector Space; Word Embedding.

1. Introduction

Automatic text summarization of a large corpus has been a source of concern over the years, from two areas of information retrieval and natural language processing. The primary studies in this field began in 1950s. Baxendale, Edmundson and Luhn have done research in those years[1]–[3]. Automatic generation of summaries provides a short version of documents to help users in capturing the important contents of the original documents in a tolerable time [4]. Now humans produce summaries of documents in the best way. Today, with the growth of data, especially in the big data domain, it is not possible to generate all of these summaries manually, because it's neither economical nor feasible.

There are two approaches to text summarization based on the chosen process of generating the summary [5]:

- Extractive summarization: This approach of summarization selects a subset of existing words, phrases, or sentences in the original text to form the summary. There are, of course, limitations on choosing these pieces. One of these limitations,

which is common in summarization, is output summary length.

- Abstractive summarization: This approach builds an internal semantic representation and then uses natural language generation techniques to create a summary that is expected to be closer to what the text wants to express.

Based on the current limitations of natural language processing methods, extractive approach is the dominant approach in this field. Almost all extractive summarization methods encounter two key problems in [6]:

- assigning scores to text pieces
- choosing a subset of the scored pieces

Traditional methods of summarization were very costly and time-consuming. This led to the emergence of automatic methods for text summarization. Extractive summarization is an automatic method for generating summary by identifying the most important sentences of a text. Hitherto text summarization has traveled a very unpaved path to address this challenge unsupervisedly. In the beginning, frequency based approaches were utilized for text summarization. Then, lexical chain based

* Corresponding Author

approaches came to succeed with the blessing of using large lexical databases such as WordNet [7] and FarsNet [8], [9]. Since the most common subject in the text has an important role in summarization, and lexical chain is a better criterion than word frequency for identifying the subject of text; as a result, a more discriminating diagnosis of the subject of text was made possible which was a further improvement in summarization. However the great reliance of these methods on lexical databases such as WordNet or FarsNet is the main weakness of these methods. For the success of these methods depends on enriching and keeping up to date the vocabulary of these databases that is very costly and time consuming, removing this weakness is not feasible.

Hence, valid methods such as Latent Semantic Analysis (LSA) based approaches that do not use dedicated static sources -which requires trained human forces for producing them- became more prominent. Latent Semantic Analysis is a valid unsupervised method for an implicit representation of the meaning of the text based on the co-occurrence of words in the input document. This method is unsupervised and it is considered an advantage. But this method has many other problems:

- The dimensions of the matrix changes very often (new words are added very frequently and corpus changes in size).
- The matrix is extremely sparse since most words do not co-occur.
- The matrix is very high dimensional in general ($\approx 10^6 \times 10^6$)
- Quadratic cost to train (i.e. to perform SVD)

With the advent of machine learning methods in recent years, training more complex models on much larger datasets has become possible. Lately, the advancement in computing power of GPUs and new processors have made it possible for hardware to implement these more advanced models. One of the most successful of these cases in recent years is the use of the distributed representation of vocabularies [10].

Word Embedding model was developed by Bengio et al. more than a decade ago [11]. The word embedding model W , is a function that maps the words of a language into vectors with about 200 to 500 dimensions. To initialize W , random vectors are assigned to words. This model learns meaningful vectors for doing some tasks.

In lexical semantics, Linear Dimension Reduction methods such as Latent Semantic Analysis have been widely used [12]. Non-linear models can be used to train word embedding models [13], [14]. Word embedding models not only have a better performance, but also lacks many problems of Linear Dimension Reduction methods such as Latent Semantic Analysis.

Distributed representation of vocabularies (Word Embedding) is one of the important research topics in the field of natural language processing [10], [12]. This method, which in fact is one of the deep learning branches, has been widely used in various fields of

natural language processing in recent years. Among these, we can mention the following:

- Neural language model [11], [15]
- Sequence tagging [16], [17]
- Machine translation [18], [19]
- Contrasting meaning [20]

Bengio et al. [11], Mikolov et al. [21], and Schwenk [15] have shown that Neural network based language models have produced much better results than N-gram models.

In this paper, a novel method of extractive generic document summarization based on perceiving the concepts present in sentences is proposed. Therefore after unsupervised learning of the target language word embedding, input document concepts are clustered based on the learned word feature vectors (hence the proposed method is language independent). After allocating scores to each conceptual cluster, sentences are ranked and selected based on the significance of the concepts present in each sentence. Ultimately we achieved promising results on Pasokh benchmark corpus.

The structure of the paper is as follows. Section two describes some related works. Section three presents the summary generation process. Section four outlines evaluation measures and experimental results. Section five concludes the paper and discusses the avenues for future research.

2. Related Works

Although many text summarization methods are available for languages such as English, little work is done in devising methods of summarizing Farsi texts.

In general these methods can be categorized as supervised and unsupervised, while most of the Farsi proposed methods so far have been of the former type. Supervised summarization methods presented for Farsi documents are divided into four categories of heuristic, lexical chain based, graph based, and machine learning or mathematical based methods:

- Heuristic method:
 - Hassel and Mazdak proposed FarsiSum as a heuristic method [22]. It is one of the first attempts to create an automatic text summarization system for Farsi. The system is implemented as a HTTP client/server application written in Perl. It has used modules implemented in SweSum (Dalianis 2000), a Farsi stop-list in Unicode format and a small set of heuristic rules.
- Lexical chain based methods:
 - Zamanifar et al. [23] proposed a new hybrid summarization technique that combined “term co-occurrence property” and “conceptually related feature” of Farsi language. They consider the relationship between words and use a synonym dataset to

- eliminate similar sentences. Their results show better performance in comparison with FarsiSum.
- Shamsfard et al. [24] proposed Parsumist. They presented single-document and multi-document summarization methods using lexical chains and graphs. To rank and determine the most important sentence, they consider the highest similarity with other sentences, the title and keywords. They achieved better performance than FarsiSum.
 - Zamanifar and Kashefi [25] proposed AZOM, a summarization approach that combines statistical and conceptual text properties and in regards of document structure, extracts the summary of text. AZOM performs better than three common structured text summarizers (Fractal Yang, Flat Summary and Co-occurrence).
 - Shafiee and Shamsfard [26] proposed a single/multi-document summarizer using a novel clustering method to generate text summaries. It consists of three phases: First, a feature selection phase is employed. Then, FarsNet, a Farsi WordNet, is utilized to extract the semantic information of words. Finally, the input sentences are clustered. Their proposed method is compared with three known available text summarization systems and techniques for Farsi language. Their method obtains better results than FarsiSum, Parsumist and Ijaz.
 - Graph based method:
 - Shakeri et al. [27] proposed an algorithm based on the graph theory to select the most important sentences of the document. They explain their objective as “The aim of this method is to consider the importance of sentences independently and at the same time the importance of the relationship between them. Thus, the sentences are selected to attend in the final summary contains more important subjects, and also have more contact with other sentences.” [27] Evaluation results indicate that the output of proposed method improves precision, recall and ROUGE-1 metrics in comparison with FarsiSum.
 - Hosseinikhah et al.[28]proposed an extractive method by combining natural language processing and text mining techniques. Part of speech tagging is used for calculating coefficient of words’ importance and graph similarity’s methods are used to select sentences without redundancy problem.
 - Machine learning and mathematical based methods:
 - Kiyomarsi and Rahimi [29] proposed a new method for summarizing Farsi texts based on features available in Farsi language and the use of fuzzy logic. Their method obtains better results as compared with four previous methods.
 - Tofighy et al. [30] proposed a new method for Farsi text summarization based on fractal theory whose main goal is using hierarchical structure of document to improve the summarization quality of Farsi texts. Their method achieved a better performance than FarsiSum, but weaker than AZOM.
 - Bazghandi et al. [31] proposed a textual summarization system based on sentence clustering. Collective intelligence algorithms are used for optimizing the methods. These methods rely on semantic aspect of words based on their relations in the text. Their results is comparable to traditional clustering approaches.
 - Tofighi et al. [32] proposed an Analytical Hierarchy Process (AHP) technique for Farsi text summarization. The proposed model uses the analytical hierarchy as a base factor for an evaluation algorithm. Their results show better performance in comparison with FarsiSum.
 - Pourmasoumi et al. [33] proposed a Farsi single-document summarization system called Ijaz. It is based on weighted least squares method [34]. Their results proved a better performance as compared with FarsiSum. They also proposed Pasokh [35], a popular corpus for evaluation of Farsi text summarizers.
 - Farzi and Kianian [36] proposed a Farsi summarizer based on a semi-supervised summarization approach, which is a combination of co-training and self-training algorithms. Co-training is a machine learning algorithm used when there are only small amounts of labeled data and large amounts of unlabeled data. They took a semi-supervised approach to overcome the absence of sufficient labeled data.

As an unsupervised method, Honarpisheh et al. [37] proposed a new multi-document multi-lingual text summarization method, based on singular value decomposition (SVD) and hierarchical clustering.

Success of Lexical chain based methods and supervised machine learning methods depends on enriching and keeping up to date lexical databases and training labeled datasets respectively, that is very costly and time consuming. These methods often use language-dependent features and cannot be generalized to other languages. On the other hand unsupervised methods such as SVD based methods have many problems that are mentioned in the previous section.

The proposed generic extractive method is a novel method that not only is unsupervised, but also does not have many problems of SVD-based methods and without using any hand-crafted features, achieves much better performance compared to supervised methods.

Although many text summarization methods are available for languages such as English

As to the related works done for English language, two of the latest research accomplished in the realm of deep learning are:

- Joshi et al. [38] proposed SummCoder, a methodology for generic extractive text summarization of single documents. The approach generates a summary according to three sentence selection metrics:
 - The sentence content relevance is measured using a deep auto-encoder network,
 - The novelty metric is derived by exploiting the similarity among sentences represented as embeddings.
 - The sentence position relevance metric is a hand-designed feature, which assigns more weight to the first few sentences through a dynamic weight calculation function.
 Finally Sentence Ranking & Selection module fuses the three scores and computes the final ranks for each sentence to select high-ranked sentences for the final document summary.
- Nallapati et al. [39] proposed a Recurrent Neural Network (RNN) based sequence model for extractive summarization of documents and show that it achieves performance better than or comparable to state-of-the-art.

3. Proposed Method

In this section we propose a novel method of extractive generic document summarization based on perceiving the concepts present in sentences. It is an unsupervised and language independent method that does not have many problems of SVD-based methods. For this purpose, firstly, the necessary preprocesses are performed on the Hamshahri2 [40] corpus texts. Subsequently, the Farsi word embedding is created by unsupervised learning of Hamshahri2 corpus. Then the input document keywords are extracted. Afterward the input document concepts are clustered based on the learned word feature vectors (hence the proposed method can be generalized to other languages), and the score of each of these conceptual clusters are calculated. Finally, the sentences are ranked and selected based on the significance of the concepts present in each sentence. The chart of this method is presented in **Error! Reference source not found.** The following sections will be described based on this chart.

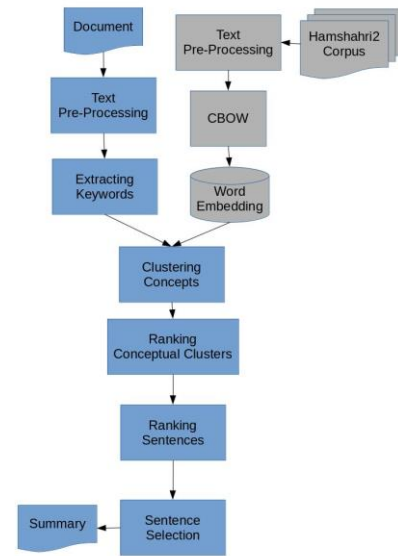


Fig. 1 Conceptual text summarizer

3.1 Text Pre-Processing

To learn a Farsi language model, we use Hamshahri2 [40] corpus. We need to produce a dictionary of vocabularies of Hamshahri2 corpus. To do this, we tokenize the words of each text file of the corpus using Hazm word_tokenize function[41] library. Hazm is an applicable open source natural language processing library in Farsi. Then we compose a dictionary out of these words by counting the frequency of each word throughout the corpus. This dictionary will be used in succeeding steps.

We constitute a complete list of Farsi stopwords out of frequent words in the prepared dictionary along with stopword lists in other open source projects.

3.2 Unsupervised Learning of Farsi Word Embedding

The Hamshahri2 [40] corpus has 3206 text files in unlabeled text sections. Each of these files is a concatenation of hundreds of news and articles. These news and articles are from different fields of cultural, political, social, etc.

To construct a suitable Farsi word embedding set, we use CBOW model [42]. This model is a neural network with one hidden layer. To learn the model a small window moves across the corpus texts and the network tries to predict *the central word of the window* using the words around it.

We assume a window with nine words length and it goes across the unlabeled texts of Hamshahri2 corpus to learn the weights of the network as Farsi word embedding vectors. The first and the last four words of each window is assumed to be the input of the network. The central word of the window is assumed to be the label of the output. Thus we have a rich labeled dataset.

Completing the learning process of network weights on all windows of Hamshahri2 corpus, we will have a suitable Farsi word embedding set, whose words' dimension is equal to the size of the hidden layer of the

network. The hidden layer size is assumed to be 200 in this work.

The Farsi word embedding generated at this stage, maps every words of the Hamshahri2 corpus to a vector in a 200 dimensional vector space. The generated Farsi word embedding set contains 300,000 words.

The t-SNE method for visualization can be used to better understand the word embedding environment.



Fig. 2 A Persian word embedding visualization using t-SNE method. Part of the words of one of the texts of the Pasokh corpus visualized in this figure

In the proposed method, using the relationship between words, the concepts of the input document are represented. In this method, the importance of sentences is determined using semantic and syntactic similarities between words. And Instead of using single words to express concepts, multiple similar words are used. For example, the occurrence of words: computer, keyboard, display, mouse and printer, even though they are not frequently repeated singly in the input document, express a certain concept.

As stated in the introduction, the great reliance of lexical chain based methods on lexical databases is the main weakness of these methods. At this stage, to remove this weakness, an appropriate word embedding for summarization is created that encompasses the semantic and syntactic communication of the words in a broader and more up to date lexical range than databases that of lexical.

The word embedding presented in this work is able to discover relationships present in the outside world that do not exist in common vocabulary databases. For example, this word embedding can detect the relation between the words of Mashhad, Neyshabur and Khorasan (**Error! Reference source not found.**). Mashhad is the capital of Khorasan province and Neyshabur is one of the cities of this province. (The common vocabulary databases that cannot discover such relationships, are comprehensive lexical databases that carry different meanings for each word along with relationships between them such as: synonyms, antonyms, part of / containing, or more general / more specific relationships. But their construction is manual, costly and time-consuming.)

In the mapping of the words in **Error! Reference source not found.**, similar words are closer to each other. This issue can also be examined from other dimensions, as another example in **Error! Reference source not found.**, the closest vocabularies to the header terms is given (using the proposed Farsi word embedding generated in this work).

Isfahan	Semnan	Ahvaz	Mashhad	Darab
Shiraz	Zanjan	Abadan	Shiraz	Fasa
Tabriz	Yazd	Shiraz	Isfahan	Kazerun
Yazd	Qazvin	Tabriz	Tabriz	Firuzabad
Mashhad	Hamedan	Khuzestan	Sabzevar	Jahrom
kerman	kermanshah	Rasht	Qom	Bavanat
Hamedan	Ardabil	Mahshahr	Rasht	Behbahan
Zanjan	Lorestan	Sepahan	Tehran	Dashtestan
Qazvin	Ilam	Isfahan	Khorasan	Lamerd
Kermanshah	Kerman	Omidyeh	Neyshabur	Estahban

Fig. 3 The closest vocabulary to the header terms is given (using the proposed Persian word embedding generated in this work)

3.3 Extracting the Keywords of the Document

For extracting the keywords of the input document, we first tokenized the words of the document using Hazm tokenizer [41]. Then we excluded stopwords from input document tokens. The score of each word of the input document calculated using equation (1) [43]:

$$point(w) = TF_{ij} \times IDF_i \quad (1)$$

where w is the intended word, TF calculated from equation (2):

$$TF_{ij} = \frac{f_{ij}}{\max_k f_{kj}} \quad (2)$$

where f_{ij} is frequency of the i -th word in the j -th document and $\max_k f_{kj}$ is maximum frequency of the words in the input document. The TF is normalized using this division.

Finally, IDF in equation (1) was calculated from equation (3):

$$IDF_i = \log_2(N/n_i) \quad (3)$$

where N is the number of documents of the Hamshahri2 corpus and n_i is the number of documents in the corpus that the i -th word has been observed there.

If a word is not in the Hamshahri2 corpus, there will not be a score for it. Also due to the absence of a vector in

the continuous vector space for this word, it is deleted from the decision making cycle. Therefore, learning word embedding on a richer Farsi corpus will cause to increase the accuracy of the method.

3.4 Clustering Concepts

In this phase, the concepts present in the input document are constructed using the Farsi word embedding obtained in section 3.2. For this purpose:

1. First we sort the keywords of the previous phase according to their calculated scores.
2. Then we map all input document terms into a 300-dimensional space using the prepared Farsi word embedding
3. We cluster the concepts of this document into ten different clusters using K-means algorithm:
 - To select the initial centroids, we used the top keywords selected in Section 3.3, starting with the top keyword and selecting it as the first centroid. Then, using the cosine distance criterion, we extract 150 of the words most similar to this keyword from the word embedding found in Section 3.2. To select a second centroid, we go to the next keyword selected in Section 3.3 and check to see if it is among the most similar words to the previously selected centroids. If available, we will skip this keyword and move on to the next keyword. Otherwise we choose this keyword as the next centroid. We continue these steps until we have extracted the first 10 centroids suitable for clustering. Excluding keywords that are among the words similar to the preceding centroids makes the selected centroids of the most important keywords of the text less semantically similar. The selected initial centroids thus help to differentiate created clusters conceptually.
 - Then we cluster the entire words of the input document using the obtained initial centroids.
 - Each obtained cluster can be considered as a concept. Thus ten key concepts of the document are constructed.
 - Finally, we consider the nearest word to each cluster center as the criterion word for that cluster or concept.
 - The total score of each concept is calculated using the equation (4):

$$point(C) = \sum_{w \in C} (point(w) \times nearness(w)) \quad (4)$$

where w is the word, C is the concept and $point(w)$ is the total score of each word that was calculated based on equation (1).

The $nearness(w)$ indicates the closeness of each word in the intended concept to the concept's criterion

word. Therefore the words nearer to the concept's criterion word will have larger linear coefficients and the words farther to that criterion word will have smaller linear coefficients. Thus the nearness of each word to its concept's criterion word affects the final score of the concept. Hence, repetition of more closely situated words in the input document will result in a higher score than repetition of farther words.

3.5 Sentence Ranking

For ranking sentences, the following steps are taken:

- First, the input document is read line by line and the sentences of each line are separated using Hazm sentence tokenizer.
- For scoring extracted sentences, equation (5) is used:

$$score(S) = \frac{\sum_{w \in S} point(C)}{N} \quad (5)$$

where S is a sentence, N is its number of words and $point(C)$ is the score of the intended word's concept.

- By dividing the sentence score into its number of words, we normalized the obtained score, so that shorter and longer sentences would have equal chance of selection.
- Sentences are sorted according to their normalized scores.
- According to the desired summary length, some sentences with the highest score are selected, and are displayed in the order they appear in the document.

3.6 Taking advantage of titles

As discussed in the previous section, the first method presented in this article does not exploit the benefits of the title of the text in the summarization process. The text title usually contains the most important text message. So the concepts mentioned in the title can earn more points and the title explanatory sentences in the text thus gain more prominence in the summary. This section examines the importance of the title in the second proposed method. For this purpose, in the first step of the summarization process, the coefficient of title effect has been added to the calculation of the score of each of the words of the input document (using equation 1). This change highlights the effect of the words in the title when calculating TF_{ij} (using equation 2):

$$TF_{ij} = \frac{f_{ij} + CTE_i}{\max_k f_{kj}} \quad (6)$$

In the above equation, CTE_i is the coefficient of title effect. This coefficient in the case of presence of the i -th word in the title, is equal to the positive constant value, and in the absence of it, is equal to zero. By increasing the coefficient of title effect, the words that appear in the title are scored more and, in the next step (clustering) are more likely to be considered as the primary cluster centers. Given that in the next steps in order to score the words of

each sentence, the score of the cluster containing the word is considered as the score of each word, the score of the words in the title affects the score of the cluster and in fact the clusters containing the words that are in the title will score more points and the sentences containing their words will also earn more points.

The results of the second proposed method are reported in Table 1, Table 2, Table 3.

4. Experimental Results

In this section using ROUGE criterion, our system generated summaries on single-document Pasokh corpus is evaluated and the obtained results are compared with other available Farsi summarizers.

4.1 Evaluation Measures

ROUGE-N is a measure for evaluation of summarizations [44]. This recall based measure is very close to human evaluation of summaries. This measure calculates the number of common n-grams between the system generated summaries and the reference human made summaries. It's therefore a suitable measure for automatically evaluating summaries produced in all languages. For this work, two public ROUGE evaluation tools are studied:

1. ROUGE: Is a Perl implementation of ROUGE measure that was developed by Mr. C. Lin et al. at the University of Southern California [44]. This implementation does not support unicode and it generates unrealistic results for the Farsi summary evaluation. After obtaining the exaggerated results of this tool for Farsi summaries, we realized this great weakness.
2. ROUGE 2: Is a Java implementation of ROUGE-N measure developed by Rxnlp team and is publicly accessible [45]. This tool supports unicode and the obtained results are accurate, but it has only implemented ROUGE-N and not any other variations of ROUGE measure.

In this work, a python implementation of ROUGE-N was developed based on Mr. C. Lin's paper [44]. This tool supports unicode and verifies the results of the ROUGE-2 implementation [45]. According to the above descriptions, the ROUGE-2 is used for summary evaluation in this study.

4.2 Pasokh Corpus

Pasokh [35] is a popular corpus for the evaluation of Farsi text summarizers. This dataset consists of a large number of Farsi news documents on various topics. It contains human-written summaries of the documents in the forms of single-document, multi-document, extractive and abstractive summaries.

The single-document dataset of Pasokh contains 100 Farsi news texts that five extractive and five abstractive summaries for each of these news are generated by different human agents.

One hundred news texts of the single-document Pasokh dataset were summarized using the proposed algorithm in this work. The compression ratio of our system summaries was 25 percent. Then we needed to calculate ROUGE-N between each of our system generated summaries and the related 5 Pasokh extractive reference summaries (human-made summaries). For this purpose, ROUGE 2.0 (Java implementation) tool was used, which is mentioned in Evaluation tool section earlier. The average of the 5 ROUGE-N is considered as the evaluation of each of our system summaries. Finally, the average of 100 system summary evaluations was calculated as the final evaluation result.

It should be noted that the news headlines of Pasokh corpus has not been used in summarization process and the results are obtained without taking advantage of headlines.

Pourmasoumi et al. [33] presented Ijaz as an extractive single-document summarizer of Farsi news in 2014 which is available online. In this experiment one hundred news texts of the Pasokh corpus were summarized using Ijaz summarizer. The compression ratio was 25 percent, and the results were obtained without using headlines.

The results are reported in Table 1, Table 2, Table 3..

Table 1 ROUGE-1 scores (percent) on Pasokh single-document dataset

<i>Systems</i>	<i>ROUGE-1</i>		
	<i>Avg_Recall</i>	<i>Avg_Precision</i>	<i>Avg_F-Score</i>
Shafiee and Shamsfard method [26]	38.8	42.5	39.1
Ijaz [33]	39.3	44.8	40.5
Our First Proposed Method (without using titles)	45.4	52.4	46.8
Our Second Proposed Method (Coefficient of Title Effect: 100)	45.6	53.1	47.2
Pasokh Authors	53.9	53.9	49.7

Table 2 ROUGE-2 scores (percent) on Pasokh single-document dataset

<i>Systems</i>	<i>ROUGE-2</i>		
	<i>Avg_Recall</i>	<i>Avg_Precision</i>	<i>Avg_F-Score</i>
Shafiee and Shamsfard method [26]	21.6	24.7	22.1
Ijaz [33]	22.6	27.6	15.4
Our First Proposed Method (without using titles)	30.1	37.3	31.9
Our Second Proposed Method (Coefficient of Title Effect: 100)	30.5	38.2	32.6
Pasokh Authors	39.7	40.4	36.5

Table 3 ROUGE-3 scores (percent) on Pasokh single-document dataset

<i>Systems</i>	<i>ROUGE-3</i>		
	<i>Avg_Recall</i>	<i>Avg_Precision</i>	<i>Avg_F-Score</i>
Shafiee and Shamsfard method [26]	16.7	19.3	17.1
Ijaz [33]	18.0	22.4	19.3
Our First Proposed Method (without using titles)	26.7	34.0	28.5
Our Second Proposed Method (Coefficient of Title Effect: 100)	27.1	35.0	29.2
Pasokh Authors	35.1	12.11	17.59

Thus our proposed method in this work has the following advantages over Pourmasoumi et al. method:

- Our proposed method achieves much better results than the proposed method of Pourmasoumi et al. in all ROUGE-1, ROUGE-2 and ROUGE-3 measures.
- The method proposed by Pourmasoumi et al. [33] has taken a supervised learning approach, while our learning approach is unsupervised. As defined by authorities supervised learning requires that the algorithm's possible outputs are already known and that the data used to train the algorithm is already labeled with correct answers. While, unsupervised machine learning is more closely aligned with what some call true artificial intelligence, the idea that a computer can learn to identify complex processes and patterns without a human to provide guidance along the way. Although unsupervised learning is prohibitively complex for some simpler enterprise use cases, it opens the doors to solving

problems that humans normally would not tackle.

- Their proposed method is a Farsi specific method, while our proposed method can be generalized to other languages.

Shafiee and Shamsfard [26] proposed an approach in extractive single-document Farsi summarization in 2017.

Unfortunately, neither their summarizer nor summaries generated by their proposed algorithm are available for comparison, therefore, the algorithm has been implemented.

In this experiment one hundred news texts of the Pasokh corpus were summarized using developed summarizer. The compression ratio was 25 percent, and the results were obtained using headlines. The results are reported in Table 1, Table 2, Table 3.

Our approach has the following advantages over Shafiee and Shamsfard's approach:

- Our proposed method achieves much better results than the "number of similar and related sentences" method of Shafiee and Shamsfard in all ROUGE-1, ROUGE-2 and ROUGE-3 measures.
- Shafiee and Shamsfard's method is supervised, while ours is unsupervised. In order to calculate a feature's weight, they utilize one-third of the Pasokh single-document corpus. To compute a feature's weight, the mean of F-measure scores is calculated to be considered as the final weight of the selected feature for single-document summarization.
- Their proposed method depends on enriching and keeping up to date the FarsNet lexical database, that is very costly and time consuming, while our method depends on unsupervised learning of the target language word embedding.
- Their proposed method is a Farsi specific method, while our proposed method can be generalized to other languages.
- Their method has used the news headlines in the summarization process, while our method has obtained the results without using headlines.

In order to have a better understanding of the results, we have evaluated the human summaries generated by the contributing authors of the Pasokh corpus as a measure of the success rate of the proposed method. Assuming that the best summaries are produced by human factors (the various authors of the Pasokh corpus), these summaries should be the most ideal in the evaluation. For this purpose, we compared the summaries generated by each of the authors of the Pasokh corpus with summaries from other authors of this corpus (with the ROUGE-N criterion). Given the varying number of texts summarizing by different authors, we consider the weighted average of evaluations made by all authors as the final evaluation of the corpus authors. The results obtained in Table 1, Table 2, Table 3 show that:

- In terms of recall, our proposed method has achieved favorable results.
- In terms of accuracy, based on ROUGE-1 and ROUGE-2 our proposed method yielded results close to the results of the authors of the corpus and in the ROUGE-3 criterion, it reached a much higher accuracy than the authors of this corpus (2.8 times).
- In terms of F-Score, ROUGE-1 and ROUGE-2 our proposed method also yielded results close to the results of the authors of the Pasokh corpus and in the ROUGE-3 criterion, it achieved a much higher score than the authors of this corpus (1.6 times).

The comparison of the results of our proposed methods and the authors of the Pasokh corpus shows that the results obtained in this paper are close to the ideal results and, in some cases, outweigh the human abstracts.

Hassel and Mazdak created FarsiSum [22] in 2004 as one of the first Farsi text summarizers reported in related literature. The available version of FarsiSum summarizer in their website has a number of bugs. For example, the length of the summary FarsiSum produces has a significant difference with the requested compression ratio percentage. According to previous studies [26], [33], the results of our proposed method on Pasokh corpus are much higher than the results obtained by FarsiSum summarizer.

4.3 Taking advantage of titles

Now, we examine the effect of the coefficient of title effect on the summaries generated in two corpuses of the Pasokh and the Khabir news corpus: As shown in **Error! Reference source not found.**, by applying different values of the coefficient of title effect and summarizing all the records of the Pasokh corpus by this coefficient, it can be seen that the overall observed behavior is that by increasing the coefficient of title effect, the mean of the F-Score values is Gradually increased. Noteworthy, the exception is the overall behavior in the range of 0 to 12, and the observation of the gradual decrease of the F-Score values. In fact, the sentences selected in this method are sentences that relate more to clusters containing title words. By factoring in the words of the title, we actually increase the weight of clusters associated with them.

For example, if the coefficient of title effect in the Pasokh corpus is considered 25, the mean value of the F-Score for all the summarized texts of the corpus is approximately equal to that of the zero coefficient. In this case, 54 summarized texts are exactly the same as

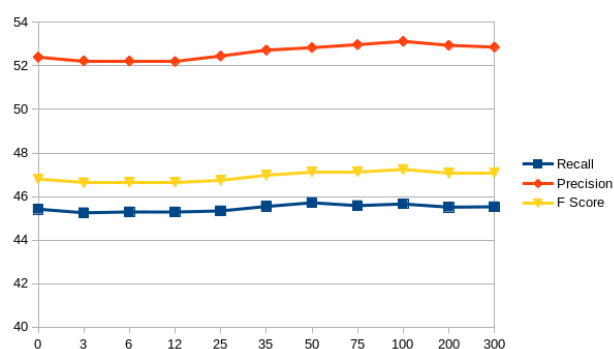


Fig. 4 Average score of all summarized texts of the Pasokh corpus for various coefficients of title effect

generated abstracts with a zero coefficient and 46 other texts are often created with a little difference. By analyzing the differences, it can be said that most of the sentences with more literal similarity to the title have been selected. In many cases, this has caused a weaker statement. In some cases, with a marginal content is selected as the title, the selected sentences are closer to the content of the headline and have been removed from the original content of the text.

Since the small number of texts of the Pasokh corpus and the observation of the results made it difficult to make the final conclusion, we repeated this experiment on the Khabir corpus. This corpus is made up of 80 thousand Farsi news and the lead of them is considered as a summary of the news. The abundance of abstracted texts in the Khabir corpus eliminates the influence of the rare factors in the final results. In this experiment, summaries with a length of 10% were produced in separate experiments. As shown in **Error! Reference source not found.**, this test was performed for various coefficients of title effect and the average score of all generated summaries in each test was calculated. By increasing the value of the coefficient of the title, the average of recall based ROUGE-1 measure initially grows linearly. After the growth of the coefficient of title effect up to 400, this linear growth is significantly reduced and the results tend to be a constant number. It is therefore clear that the increase in the coefficient of title effect in the Khabir corpus is a 3% improvement in the recall based ROUGE-1 measure of the generated summaries.

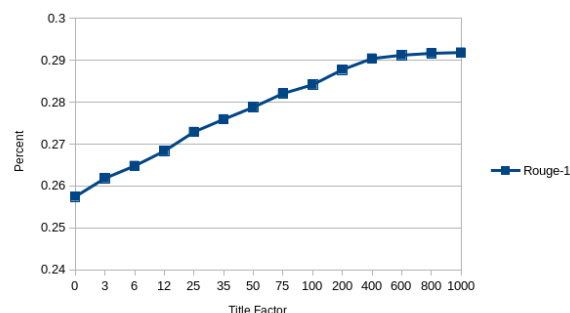


Fig. 5 Average score of all Khabir corpus texts for various coefficients of title effect

5. Conclusion

In this paper, two novel methods of extractive generic document summarization based on perceiving the concepts present in sentences are proposed. Therefore after unsupervised learning of the target language word embedding, input document concepts are clustered based on the learned word feature vectors (hence the proposed methods can be generalized to other languages). After allocating scores to each conceptual cluster, sentences are ranked and selected based on the significance of the concepts present in each sentence.

One of the most important challenges in recent researches in the field of summarizing Farsi texts is the lack of a rich lexical database in Farsi language that can be used to measure semantic similarities. In this research, by constructing a Farsi word embedding using Hamshahri2 corpus, we were able to correctly answer this shortage and provide two new methods for summarizing the texts according to the semantic and syntactic relations learned.

Using the relationship between words, the concepts discussed in the input document are represented. In these methods, the importance of sentences is determined using semantic and syntactic similarities between words. Instead of using single words to express concepts, different related words are used. We evaluated the proposed methods on Pasokh single-document dataset using the ROUGE evaluation measure. Without using any hand-crafted features, our proposed methods achieved state-of-the-art results. For system summaries generated with 25 percent compression ratio on Pasokh single-document corpus using our first method, ROUGE-1, ROUGE-2 and ROUGE-3 recall scores were 45, 30 and 27 percent, respectively.

In the second proposed method in this paper, by applying various coefficients of title effect and summarizing all the records of the Pasokh corpus by this coefficient, the overall observed behavior is the gradual increase of the mean value of the F-Score by increasing the coefficient of title effect. The comparison of the results of our proposed methods and the authors of the Pasokh corpus also demonstrates that the results obtained in this paper are close to the ideal results, and even in some cases, outweigh the human abstracts.

Evaluation of our proposed methods for summarization of other languages is suggested for future works. Learning word embedding on richer Farsi corpuses may be effective in increasing the accuracy of our methods. Using PageRank [46] algorithm to produce the concept similarity graph and to find more significant concepts may also increase the accuracy of our concept selection algorithm. Using exploited MMR (Maximum Marginal Relevance) [47] greedy algorithm in sentence selection process may decrease the redundancy of the selected sentences in our proposed methods.

References

- [1] P. B. Baxendale, "Machine-made index for technical literature—an experiment," *IBM J. Res. Dev.*, vol. 2, no. 4, pp. 354–361, 1958.
- [2] H. P. Edmundson, "New methods in automatic extracting," *J. ACM JACM*, vol. 16, no. 2, pp. 264–285, 1969.
- [3] H. P. Luhn, "The automatic creation of literature abstracts," *IBM J. Res. Dev.*, vol. 2, no. 2, pp. 159–165, 1958.
- [4] H. Khanpour, "Sentence extraction for summarization and notetaking," University of Malaya, 2009.
- [5] W. Song, L. C. Choi, S. C. Park, and X. F. Ding, "Fuzzy evolutionary optimization modeling and its applications to unsupervised categorization and extractive summarization," *Expert Syst. Appl.*, vol. 38, no. 8, pp. 9112–9121, 2011.
- [6] F. Jin, M. Huang, and X. Zhu, "A comparative study on ranking and selection strategies for multi-document summarization," in *Proceedings of the 23rd International Conference on Computational Linguistics: Posters*, 2010, pp. 525–533.
- [7] G. A. Miller, "WordNet: a lexical database for English," *Commun. ACM*, vol. 38, no. 11, pp. 39–41, 1995.
- [8] M. Shamsfard, "Developing FarsNet: A lexical ontology for Persian," in *4th Global WordNet Conference, Szeged, Hungary*, 2008.
- [9] M. Shamsfard *et al.*, "Semi automatic development of farsnet; the persian wordnet," in *Proceedings of 5th global WordNet conference, Mumbai, India*, 2010, vol. 29.
- [10] G. E. Hinton, J. L. McClelland, and D. E. Rumelhart, *Distributed representations, Parallel distributed processing: explorations in the microstructure of cognition, vol. 1: foundations*. MIT Press, Cambridge, MA, 1986.
- [11] Y. Bengio, R. Ducharme, P. Vincent, and C. Jauvin, "A neural probabilistic language model," *J. Mach. Learn. Res.*, vol. 3, no. Feb, pp. 1137–1155, 2003.
- [12] P. D. Turney and P. Pantel, "From frequency to meaning: Vector space models of semantics," *J. Artif. Intell. Res.*, vol. 37, pp. 141–188, 2010.
- [13] S. T. Roweis and L. K. Saul, "Nonlinear dimensionality reduction by locally linear embedding," *science*, vol. 290, no. 5500, pp. 2323–2326, 2000.
- [14] J. B. Tenenbaum, V. De Silva, and J. C. Langford, "A global geometric framework for nonlinear dimensionality reduction," *science*, vol. 290, no. 5500, pp. 2319–2323, 2000.
- [15] H. Schwenk, "Continuous space language models," *Comput. Speech Lang.*, vol. 21, no. 3, pp. 492–518, 2007.
- [16] R. Collobert, J. Weston, L. Bottou, M. Karlen, K. Kavukcuoglu, and P. Kuksa, "Natural language

- processing (almost) from scratch,” *J. Mach. Learn. Res.*, vol. 12, no. Aug, pp. 2493–2537, 2011.
- [17] R. Collobert and J. Weston, “A unified architecture for natural language processing: Deep neural networks with multitask learning,” in *Proceedings of the 25th international conference on Machine learning*, 2008, pp. 160–167.
- [18] J. Devlin, R. Zbib, Z. Huang, T. Lamar, R. M. Schwartz, and J. Makhoul, “Fast and Robust Neural Network Joint Models for Statistical Machine Translation,” in *ACL (1)*, 2014, pp. 1370–1380.
- [19] I. Sutskever, O. Vinyals, and Q. V. Le, “Sequence to sequence learning with neural networks,” in *Advances in neural information processing systems*, 2014, pp. 3104–3112.
- [20] Z. Chen *et al.*, “Revisiting Word Embedding for Contrasting Meaning,” in *ACL (1)*, 2015, pp. 106–115.
- [21] T. Mikolov, A. Deoras, S. Kombrink, L. Burget, and J. Černocký, “Empirical evaluation and combination of advanced language modeling techniques,” in *Twelfth Annual Conference of the International Speech Communication Association*, 2011.
- [22] M. Hassel and N. Mazdak, “FarsiSum: a Persian text summarizer,” in *Proceedings of the Workshop on Computational Approaches to Arabic Script-based Languages*, 2004, pp. 82–84.
- [23] A. Zamanifar, B. Minaei-Bidgoli, and M. Sharifi, “A new hybrid farsi text summarization technique based on term co-occurrence and conceptual property of the text,” in *Software Engineering, Artificial Intelligence, Networking, and Parallel/Distributed Computing, 2008. SNPD’08. Ninth ACIS International Conference on*, 2008, pp. 635–639.
- [24] M. Shamsfard, T. Akhavan, and M. E. Joorabchi, “Persian document summarization by PARSUMIST,” *World Appl. Sci. J.*, vol. 7, pp. 199–205, 2009.
- [25] A. Zamanifar and O. Kashefi, “AZOM: a Persian structured text summarizer,” *Nat. Lang. Process. Inf. Syst.*, pp. 234–237, 2011.
- [26] F. Shafiee and M. Shamsfard, “Similarity versus relatedness: A novel approach in extractive Persian document summarisation,” *J. Inf. Sci.*, p. 0165551517693537, 2017.
- [27] H. Shakeri, S. Gholamrezazadeh, M. A. Salehi, and F. Ghadamyari, “A new graph-based algorithm for Persian text summarization,” in *Computer science and convergence*, Springer, 2012, pp. 21–30.
- [28] T. Hosseinikhah, A. Ahmadi, and A. Mohebi, “A new Persian Text Summarization Approach based on Natural Language Processing and Graph Similarity,” *Iran. J. Inf. Process. Manag.*, vol. 33, no. 2, pp. 885–914, 2018.
- [29] F. Kiyomarsi and F. R. Esfahani, “Optimizing persian text summarization based on fuzzy logic approach,” in *2011 International Conference on Intelligent Building and Management*, 2011.
- [30] M. Tofighy, O. Kashefi, A. Zamanifar, and H. H. S. Javadi, “Persian text summarization using fractal theory,” in *International Conference on Informatics Engineering and Information Science*, 2011, pp. 651–662.
- [31] M. Bazghandi, G. T. Tabrizi, M. V. Jahan, and I. Mashahd, “Extractive Summarization Of Farsi Documents Based On PSO Clustering,” *jiA*, vol. 1, p. 1, 2012.
- [32] S. M. Tofighy, R. G. Raj, and H. H. S. Javad, “AHP techniques for Persian text summarization,” *Malays. J. Comput. Sci.*, vol. 26, no. 1, pp. 1–8, 2013.
- [33] P. Asef, K. Mohsen, T. S. Ahmad, E. Ahmad, and Q. Hadi, “IJAZ: AN OPERATIONAL SYSTEM FOR SINGLE-DOCUMENT SUMMARIZATION OF PERSIAN NEWS TEXTS,” vol. 0, no. 121, pp. 33–48, Jan. 2014.
- [34] T. Strutz, *Data fitting and uncertainty: A practical introduction to weighted least squares and beyond*. Vieweg and Teubner, 2010.
- [35] B. B. Moghaddas, M. Kahani, S. A. Toosi, A. Pourmasoumi, and A. Estiri, “Pasokh: A standard corpus for the evaluation of Persian text summarizers,” in *Computer and Knowledge Engineering (ICCKE), 2013 3th International eConference on*, 2013, pp. 471–475.
- [36] S. Farzi and S. Kianian, “Katibeh: A Persian news summarizer using the novel semi-supervised approach,” *Digit. Scholarsh. Humanit.*, vol. 34, no. 2, pp. 277–289, 2018.
- [37] M. A. Honarpisheh, G. Ghassem-Sani, and S. A. Mirroshandel, “A Multi-Document Multi-Lingual Automatic Summarization System,” in *IJCNLP*, 2008, pp. 733–738.
- [38] A. Joshi, E. Fidalgo, E. Alegre, and L. Fernández-Robles, “SummCoder: An unsupervised framework for extractive text summarization based on deep auto-encoders,” *Expert Syst. Appl.*, vol. 129, pp. 200–215, 2019.
- [39] R. Nallapati, F. Zhai, and B. Zhou, “Summarunner: A recurrent neural network based sequence model for extractive summarization of documents,” in *Thirty-First AAAI Conference on Artificial Intelligence*, 2017.
- [40] A. AleAhmad, H. Amiri, E. Darrudi, M. Rahgozar, and F. Oroumchian, “Hamshahri: A standard Persian text collection,” *Knowl.-Based Syst.*, vol. 22, no. 5, pp. 382–387, 2009.
- [41] *hazm: Python library for digesting Persian text*. Sobhe, 2017.
- [42] T. Mikolov, I. Sutskever, K. Chen, G. S. Corrado, and J. Dean, “Distributed Representations of Words and Phrases and their Compositionality,” in *Advances in Neural Information Processing Systems 26*, C. J. C. Burges, L. Bottou, M. Welling,

- Z. Ghahramani, and K. Q. Weinberger, Eds. 2013, pp. 3111–3119.
- [43] J. Leskovec, A. Rajaraman, and J. D. Ullman, *Mining of massive datasets*. Cambridge university press, 2014.
- [44] C.-Y. Lin, “Rouge: A package for automatic evaluation of summaries,” in *Text summarization branches out: Proceedings of the ACL-04 workshop*, 2004, vol. 8.
- [45] *ROUGE-2.0: Java implementation of ROUGE for evaluation of summarization tasks. Stemming, stopwords and unicode support*. 2017.
- [46] L. Page, S. Brin, R. Motwani, and T. Winograd, “The PageRank citation ranking: Bringing order to the web.,” Stanford InfoLab, 1999.
- [47] J. Carbonell and J. Goldstein, “The use of MMR, diversity-based reranking for reordering documents and producing summaries,” in *Proceedings of the 21st annual international ACM SIGIR conference*

on Research and development in information retrieval, 1998, pp. 335–336.

Mohammad Ebrahim Khademi received his M.S. degree in computer engineering from the Malek Ashtar University of Technology, Iran, in 2013. He is currently a PhD candidate in computer engineering there. His research interests include machine learning (deep learning) and natural language processing.

Mohammad Fakhredanesh received his B.S., M.S. and PhD degree in computer science and Engineering from the Amirkabir University of Technology (Tehran Polytechnic), Iran, in 2005, 2007, and 2014 respectively. He is currently an assistant professor at the Malek Ashtar University of Technology. His research interests are the fields of artificial intelligence, pattern recognition, and text summarization.

Seyed Mojtaba Hoseini received his B.S. degree in Electronic Engineering from Malek Ashtar University of Technology in 1991. He also received his M.S. and PhD degrees in Computer Architecture Engineering from Amirkabir University of Technology in 1995 and 2011 respectively. His research interests include Wireless sensor Networks, with an emphasis on target coverage and tracking applications, image and signal processing, and evolutionary computing.

Graph Based Feature Selection Using Symmetrical Uncertainty in Microarray Dataset

Soodeh Bakhshandeh

Department of Computer Engineering, Science and Research Branch, Islamic Azad University, Tehran, Iran
soodeh.bakhshandeh@gmail.com

Reza Azmi*

Department of Computer Engineering, Alzahra University, Tehran, Iran
azmi@alzahra.ac.ir

Mohammad Teshnehlab

Department of Control Engineering, K. N. Toosi University, Tehran, Iran
teshnehlab@kntu.ac.ir

Received: 30/Apr/2019

Revised: 25/Sep/2019

Accepted: 04/Nov/2019

Abstract

Microarray data using small samples and thousands of genes provides a difficult challenge for researchers. Utilizing gene selection helps to select the most relevant genes from original dataset with the purpose of dimensionality reduction of microarray data as well as increasing the prediction performance. In this paper, a new gene selection method based on community detection technique and ranking the best genes, is proposed. In order to select the best genes, Symmetric Uncertainty calculates the similarity between two genes, and between gene and its class label. In the first phase, this leads to representation of search space in form of graph. In the second phase, the proposed graph is divided into several clusters, using community detection algorithm. Finally, after ranking the genes, the ones with maximum ranks are selected as the best genes. This approach is a supervised/unsupervised filter-based gene selection method, which not only minimizes the redundancy between genes, but also maximizes the relevance of genes and their class labels. Performance of the proposed method is compared with twelve well-known unsupervised/supervised gene selection approaches over twelve microarray datasets using four classifiers including SVM, DT, NB and k-NN. The results illustrate the advantages of the proposed approach.

Keywords: Gene Selection; Microarray Data; Filter Method; Graph-Based Clustering; Feature Selection.

1. Introduction

In recent years, a new research path has been opened in Bioinformatics and machine learning field. This field contains monitoring thousands of gene expressions for detecting or classifying the specific type of tumor in DNA microarray datasets. Applying machine learning techniques to microarray data results extracting valuable information from dataset and building a model for classifying data into different categories based on the data classes. In training and testing phase, the researchers deal with small samples consisting of thousands of genes which may lead to “curse of dimensionality” [1]. In high dimensional data, many features are irrelevant and redundant which requires large storage space and consequently, have impact on performance and increasing the cost of learning process [2]. For improving the performance of learning model, the dimensionality reduction methods have been introduced in several papers. These methods reduce the cost and risk of over-fitting, but on the other hand they increase the ability of learning model for classifying the high-dimensionality data in different classes.

For reducing the dimensionality of features (genes), data could be transformed from the original space, with

data dimension, into a new space with lower dimension, using feature (gene) extraction techniques. Another technique for reducing the dimensionality of features (genes) is feature (gene) selection. If there are n features (genes), the whole search space size will be 2^n . Therefore, the time complexity of feature selection process is 2^n , which is NP hard problem [3]. In past years, some methods, such as feature selection method, have been introduced to find a near-optimal feature (gene) subset. Feature selection is a preprocessing step that identifies and removes irrelevant and redundant genes from the training data. In classification phase, the gene selection method leads to increasing the influence of training data.

The gene selection methods can be classified into filter, wrapper, embedded, and hybrid categories. The goal of filter, which is independent of any learning algorithm, is to reduce the data dimensionality based on the statistical properties of data. Univariate and multivariate strategies are used for evaluating the relevance of each gene to others in filter method. While univariate methods rank the genes individually and independent of other genes, the multivariate methods consider the correlation between genes. Therefore, because the univariate methods ignore the relation

* Corresponding Author

between genes, they are rather fast but with low accuracy compared to multivariate methods [4]. While Laplacian score [5], term variance [6], mutual information [7], and information gain [8] are popular univariate methods, the well-known multivariate methods are mRMR [9], FCBF [10], RRFS [11], UFSACO [12], RSM [13].

The wrapper method optimizes a predictor for selection process. The predictor evaluates the quality of the selected genes iteratively. Greedy and stochastic search strategies are two categories of wrapper methods. Sequential forward selection and sequential backward selection are two classical greedy search methods and ant colony optimization (ACO) [14], particle swarm optimization (PSO) [15] are two stochastic search methods. Greedy strategy searches based on single track and stochastic method uses the randomness nature of data. The performance of wrapper method is better comparing to filter method because of using learning model, however the computational cost is higher.

The embedded methods work on training a learning model for classification and using it for building the optimal subset of features. Since the embedded approach uses all the genes for training the classifier, the training phase is so time consuming. Kernel penalized SVM (KP-SVM) [16], First Order Inductive Learner (FOIL) [17] and SVM-RFE [18] are three examples of the embedded methods.

The last category of gene selection methods is hybrid methods. This method combines the advantages of filter and wrapper methods for improving the performance of the selected genes in classifying phase. Combining of SVM-RFE and mRMR [19], combining correlation-based feature selection (CFS) and Taguchi-genetic algorithm [20] and combining Fisher score with a GA and PSO [21], are some hybrid methods that are introduced during recent years.

In this paper, a filter-based gene selection method is introduced that uses class label and the correlation between the genes for removing the redundant and irrelevant genes. The proposed method works in three steps; graph representation, gene clustering and selecting the best features from each cluster. In the first step, the gene search space is represented as a graph, corresponding to the similarity between features and also the similarity between feature and its class label. Afterwards, in the second step, a clustering algorithm is applied to the constructed graph to divide the genes into several clusters. Finally, the best genes from each cluster are selected as the final gene subset. The proposed method is compared with other feature/gene selection methods (Mutual correlation (MC), fast clustering-based feature selection algorithm (FAST), Graph Clustering with Node Centrality for unsupervised feature selection (GCNC), Unified-Feature Association Map (U-FAM), Feature Selection method with Joint Maximal Information Entropy between features and class (FS-JMIE), a Correlation based Memetic Algorithm (MA-C), Dense Subgraph Finding with Feature Clustering (DSFFC),

Distributed dCor-based FS (D²CORFS), a ReliefF and ACO-based gene selection (RFACO-GS), A hybrid algorithm for feature subset selection in high-dimensional datasets using FICA and IWSSr algorithm (FICA-IWSSr), Greedy Randomized Adaptive Search Procedure (GRASP), and Support Vector Machine Recursive Feature Elimination (FCSVM-REF)). The comparison is done in terms of classification accuracy, number of selected genes, feature reduction, parameter effects and execution time. The novelties of the proposed method lie in the following aspects:

1. Using Symmetric Uncertainty (SU) for representing the search space as a graph: In this paper, a new method is introduced for calculating the weights of graph based on the similarity between two genes and between each gene and its class label by using SU. Changing the value of the parameters in the first step of the proposed method, leads to supervised or unsupervised gene selection method. If class of dataset samples is available, supervised method is used, otherwise unsupervised method is applied. By using this selection method, the results are considerably improved.

2. Using a new ranking method for determining the important nodes in a graph: In this paper a new ranking method is used for identifying the selection of the influential genes in the third step. After applying the ranking method, a meta-heuristic method is used for selecting the best genes in the third step, resulting minimum redundancy between selected genes in the proposed method.

The rest of the paper is organized as follows: Section 2 contains a brief review on other related works. In Section 3, the materials and concepts, which are used in the proposed method, are explained in more detail. In Section 4, the proposed method is presented. In Section 5, in order to demonstrate the advantages of the proposed method, experimental results on some datasets using different classifiers are presented. Additionally, the reasons backing up the efficiency of the proposed method is described. At the end, in Section 6, the conclusion part is provided.

2. Related Works

As the information of redundant genes presents in other genes, these genes do not help the prediction result. The irrelevant genes do not contribute in increasing the predictive accuracy either. Therefore, the goal of gene selection is removing the redundant and irrelevant genes from gene subset. In past years, some gene/feature selection methods have been introduced considering these goals. Some of them have been successful in removing irrelevant features like [22-24] and some others on eliminating both irrelevant and redundant features ([25, 26]).

As mentioned in section 1, filter gene selection methods are successful in case of dealing with large

number of features. There have been also some graph-based feature selection methods, which work on the relation between different features.

In [27], a fast clustering based feature selection algorithm (FAST) for high dimensional data is proposed, which works in two main steps. In the first step, by using graph-theoretic clustering methods, features are divided into different clusters. In the second step, the relationship between all features and the target class is calculated and based on storage of the relation, some features are selected. In this paper, after eliminating irrelevant features, a minimum spanning tree is constructed, which after partitioning it, the representative features are selected.

In [28], an unsupervised feature selection is presented that works based on graph theory. First, a graph is constructed based on the dissimilarity of features. Then the densest subgraph by maximum average weight is identified. As the reduced subgraph contains the features with less average correlation, these features are the selected features. As in constructing the graph, feature dissimilarity is taken into account, so the feature relevancy does not influence the graph.

In [29], for eliminating both redundant and irrelevant features, the densest subgraph and feature clustering are combined. For removing the redundant features, the densest subgraph like [28] is obtained, and for eliminating the irrelevant features, a specific feature clustering is applied to the feature set.

In [30], ant colony optimization (ACO) with a new fitness function is used for a new unsupervised gene selection method that is called MGSACO. In this method, first a graph represents the search space, using similarity between genes. After that, ACO with new fitness function is used for gene selection.

In [31], a graph is constructed using Pearson correlation coefficient measure for representation the features relationship. Then Louvain community detection algorithm is used for clustering the features. In the last phase, a novel ACO-based search strategy is proposed for selecting a feature subset from the cluster group.

In [32], a new feature selection method called Probabilistic Attribute-Value for Class Distinction (Pavicd), is introduced for removing irrelevant and redundant genes. It works on the space of feature values instead of the features' space. It only requires an evaluation function, for estimating the prediction of class label by one or more features, and a threshold for analysis of relevance.

In [33], by combining Genetic Algorithm (GA) and Local Search (LS), a correlation based memetic framework is introduced. For tuning the population of GA, symmetrical uncertainty measure is used.

In [34], a joint maximal information entropy between features and their classes is used for feature selection process. For measuring the feature subset, a joint maximal information entropy is defined, and a binary particle swarm optimization searches the feature space for finding the best feature subset.

3. Materials and Methods

The proposed approach is based on graph-theoretic principles, clustering and ranking concepts which have been covered in this section.

3.1 Symmetric Uncertainty (SU)

Entropy is the uncertainty measure in the distribution of variable and is defined as:

$$H(X) = -\sum_i P(x_i) \log_2(P(x_i)) \quad (1)$$

Where X and $P(X)$ are discrete variable and probability mass function of X , respectively and $H(X)$ indicates entropy of variable X . After observing values of another variable Y , the entropy of X is defined as:

$$H(X|Y) = -\sum_j P(y_j) \sum_i P(x_i|y_j) \log_2(P(x_i|y_j)) \quad (2)$$

Where $P(X)$ and $P(X|Y)$ denote the prior probabilities for all value of X and the posterior probabilities of X given the value of Y , respectively. Information gain between two variables X and Y reflects additional information about X provided by Y , by which the entropy of X decreases. Information gain is the decrease of the uncertainty of X after observing Y , and is defined as:

$$IG(X|Y) = H(X) - H(X|Y) \quad (3)$$

Where $H(X)$ and $H(X|Y)$ have been defined in equation 1 and 2. If $IG(X|Y) > IG(Z|Y)$, the correlation between features Y and Z is more than correlation between features Y and X . Information gain is a symmetrical measure and therefore for two features X and Y , the order of them does not affect the value of IG ($IG(X|Y) = IG(Y|X)$). As IG is symmetry, it can be used for measuring the correlation between two features.

For normalizing the value of IG, IG should be divided by feature entropies and is known as Symmetric Uncertainty (SU). In some researches, SU is used to evaluate the goodness of features for classification.

The symmetric uncertainty is defined as follows:

$$SU(X, Y) = \frac{2 \times IG(X|Y)}{H(X) + H(Y)} \quad (4)$$

SU value is in range [0, 1]. For two features X and Y , if the value of SU is 1, it indicates that knowing the value of each feature, the value of other feature is predictable. If the value of SU is 0, it indicates the two variables are independent.

For calculating SU in continues features, the discretization process should be done before [35]. In [27], F-Correlation and T-Relevance are defined as following:

F-Correlation: The correlation between any pair of features F_i and F_j ($(F_i, F_j \in F) \wedge (i \neq j)$) is called the F-Correlation of F_i and F_j and denoted by $SU(F_i, F_j)$.

T-Relevance: The relevance between the feature $F_i \in F$ and the target concept C is referred to as T-Relevance of F_i and C and denoted by $SU(F_i, C)$.

Following these definitions, the below items are realized:

1. The correlation between irrelevant feature and target concept is very weak.

2. For redundant features, the value of F-Correlation will be near 1.

3.2 Community Detection

In real system, the graph representation of nodes and vertices is not regular. Using clustering approaches, in the real systems, improves our perception of the relations between patterns. In past decades, some clustering approaches have been introduced for detecting clusters (communities) in complex patterns. k -means is one of the classical clustering approaches that is very sensitive to initialized parameters. To compensate for its weakness, the novel clustering approaches are focused on community detection ([36]). Community detection is used for grouping nodes, which are shared common or similar property to one community (also called cluster or module). Therefore, community detection field refers to finding groups of nodes that are more internally connected than externally. Based on [37], using community detection leads to information regarding the network structure, its functionality and its compact representation. Community detection concept is used in some fields such as social networks, recommendation systems, Ad-hoc networks and so on.

Louvain community detection method is one of the popular community detection methods that uses [38]. This method is a heuristic method that works based on modularity function maximization. Modularity has been used to compare the partition quality in different methods, and is an objective function, which its optimization is computationally difficult.

Louvain method is used for finding high modularity partitions in a short period of time. The algorithm steps are intuitive and easy to implement. The computational complexity of the algorithm, for n nodes in the graph, is $O(n \log n)$, therefore for large scale networks with some nodes, the algorithm will be rather quick.

Iterative Louvain method is started with a weighted network as input. In the first step, each node of the network is assigned to a community (community No. has the same value of node No. in the beginning). Then, for each node, the gain modularity is calculated based on removing a node from its community to the other community. In the second phase, a new network, based on modularity, is generated. These two steps are repeated till the significant improvement of the network modularity is obtained. The below equation is used for calculating the gain in modularity by moving one node (i^{th} node) into a community C :

$$\Delta Q = \left[\left(\frac{\sum_{in} + k_{i,in}}{2m} \right) - \left(\frac{\sum_{tot} + k_i}{2m} \right)^2 \right] - \left[\left(\frac{\sum_{in}}{2m} \right) - \left(\frac{\sum_{tot}}{2m} \right)^2 - \left(\frac{k_i}{2m} \right)^2 \right] \quad (5)$$

Where \sum_{in} is the summation of all the weights of the links inside the community C , where i is moving into, \sum_{tot} is the sum of all the weights of the links to nodes in the community C , where i is moving into, k_i is the

weighted degree of i , $k_{i,in}$ is the sum of the weights of the links between i and other nodes in the community that i is moving into, and m is the sum of all of the edge weights in the network.

3.3 Identifying influential nodes

In complex networks, node importance is a basic measure for characterizing and identifying the structure of them, which is also an open issue ([39]). Centrality is a common measure for ranking the nodes of graphs [40]. Different centrality measures have been proposed such as degree centrality, closeness centrality, betweenness centrality, and eigenvector centrality [41]. Although these centrality measures are used in complex networks, however there are some disadvantages [42].

In [42], a new evaluation method is introduced for determining the important nodes based on Technique for Order Performance by Similarity to Ideal Solution (TOPSIS) approach. In this method, Multiple Attribute Decision Making (MADM) for exploring how to identify important nodes is introduced. TOPSIS method chooses the alternatives that have the shortest distance from the positive ideal solution and the farthest distance from the negative-ideal solution, and it operates in four steps. In the first step, the network is constructed based on the connection of nodes. After that, different centrality values are calculated based on network topology. In the third step, based on Euclidean distance, the separation from the positive ideal alternative S_i^+ and the separation from the negative ideal alternative S_i^- of nodes is calculated as follow:

$$S_i^+ = \sqrt{\sum_{j=1}^n (v_j^+ - v_{ij})^2}, \quad i = 1, \dots, m; j = 1, \dots, m \quad (6)$$

$$S_i^- = \sqrt{\sum_{j=1}^n (v_j^- - v_{ij})^2}, \quad i = 1, \dots, m; j = 1, \dots, m \quad (7)$$

In the final step, the relative closeness to the ideal alternatives (C_i) is calculated and the alternatives with higher C_i are considered as important alternatives.

$$C_i = \frac{S_i^-}{S_i^- + S_i^+}, \quad i = 1, \dots, m \quad (8)$$

4. Proposed Method

In this paper, a novel gene selection method is introduced which can remove irrelevant and redundant genes in the selection process. The proposed method consists of three steps. In the following sections, these three steps are described in more detail.

4.1 Graph Representation

In all graph-based feature selection methods, the first step is to represent the search space as an undirected graph. In the constructed graph, each feature represents a node in graph. The gene search space is mapped to a fully connected undirected weighted graph $G = \langle F, E, w_F \rangle$. In this graph, $F = \{F_1, F_2, \dots, F_n\}$ denotes a set of original genes (features) and $E = \{(F_i, F_j); F_i, F_j \in F\}$ is the graph

edge and w_{ij} contains the similarity between two features F_i and F_j , which are connected by edge (F_i, F_j) .

So far, the methods expressed in different papers have been emphasizing on improving performance of graph-based gene selection algorithm. In this paper, on the other hand, a new measurement based on Symmetrical Uncertainty (SU) is proposed. As it was already explained in 3.1, in SU the similarity value between genes and between genes and their class labels are measured. According to SU, for two features, T-Relevance should be as great as possible, and F-Correlation should be as small as possible. In this case, w_{ij} is defined as follows:

$$w_{ij} = \begin{cases} \beta SU(F_i, C) + \gamma SU(F_j, C) - \alpha SU(F_i, F_j), \\ \alpha + \beta + \gamma = 1, \text{ if } i \neq j \\ 1, \text{ otherwise} \end{cases} \quad (9)$$

Where $SU(F_i, F_j)$ is F-Correlation between two genes (F_i and F_j) and $SU(F_i, C)$ and $SU(F_j, C)$ are T-Relevance values between feature F_i and F_j and target class C , respectively.

Based on [43], the measure that is sensitive to rotation is not desirable in many applications. As above formula, if $\beta \neq \gamma$, therefore the value of w_{ij} is not equal to w_{ji} ($w_{ij} \neq w_{ji}$). For this reason, γ should be equal to β ($\gamma = \beta$). Therefore, the equation 8 could be changed as follows:

$$w_{ij} = \begin{cases} \frac{(1-\alpha)}{2} (SU(F_i, C) + SU(F_j, C)) - \alpha SU(F_i, F_j), \\ 0 \leq \alpha \leq 1, \text{ if } i \neq j \\ 1, \text{ otherwise} \end{cases} \quad (10)$$

w_{ij} is in the range $[-1, 1]$. For scaling the edge weight into the range $[0, 1]$, softmax scaling is used as follows [6]:

$$\hat{w}_{ij} = \frac{1}{1 + \exp(-\frac{w_{ij} - \bar{w}}{\sigma})} \quad (11)$$

Where w_{ij} is the edge weight between node F_i and F_j and, \bar{w} and σ are the mean and variance of all edge weights in the graph, respectively. After applying this equation, \hat{w}_{ij} is the normalized edge weight that represents the similarity between two genes, as well as each gene and its class label on the two sides of the edge.

4.2 Gene Clustering

The clustering methods try to group the existing data into different clusters. Therefore, the similarity array is inputted to the proposed algorithm, and the output of clustering method is some clusters that each of them contains the seeds with maximum similarity. Over the past few years, some community detection methods are introduced, which could apply the clustering as well. As mentioned in 3.2, Louvain community detection algorithm, performance wise, is one of the fastest community detection algorithms that has been used in the past. Additionally, this method is reasonably easy to implement. Due to these advantages, the method is used in this paper in the gene clustering step. Therefore, in the second step, after constructing the graph, Louvain community detection algorithm is applied to the graph for

grouping the nodes (genes) to different clusters based on the normalized weight of graph edges.

4.3 Selecting the Best Genes

After grouping the genes in different clusters, selecting the best genes in each cluster is a major step by removing irrelevant and redundant genes. Therefore, in this step, the main goal is removing the features that have no influence on the result.

According to subsection 3.3, the technique for order performance by similarity to ideal solution (TOPSIS) approach is introduced for determining the important nodes in a graph. In the proposed method, after constructing the graph in the first step and applying community detection in the second step, for selecting the influential nodes in each cluster, TOPSIS is used. TOPSIS method is very efficient and practical for evaluating the importance of nodes.

For using TOPSIS, a new ranking method is used to rank each gene. After ranking each gene, the best genes are selected and used as final gene subset. For selecting the best genes, two rank parameters are used:

1. Ranking each gene without considering its cluster (Total Rank Score - TRS) and
2. Ranking the genes with considering its cluster (Cluster Rank Score - CRS)

TRS is independent of the second phase and CRS is dependent to the result of the second phase.

For calculating the first rank value (TRS), TOPSIS runs over all genes, based on the graph that is constructed in the first step. By running TOPSIS over all genes, the rank of each gene is compared to the other genes. After that, the total rank score is calculated by dividing the distance between $[0, 1]$ to equal intervals, depending on the number of genes. For example, assuming there are five genes F_1, F_2, F_3, F_4 and F_5 in the dataset. If after applying TOPSIS, the gene ranks are 4, 2, 5, 1 and 3, respectively, then the total rank score (TRS) of each gene is calculated as Table 1.

For calculating the second rank value (CRS), TOPSIS runs over each cluster. In this calculation, the subgraphs, which were constructed after applying community detection in the second phase, are used. Applying TOPSIS in each subgraph results the rank of each gene in comparison to the other genes, within each community. Thereafter, for each cluster, the rank of each gene is calculated independent of other clusters and, looking like

Gene	F_1	F_2	F_3	F_4	F_5
Gene rank	4	2	5	1	3
TRS	0.4	0.8	0.2	1	0.6

Algorithm 1 shows the pseudo-code of calculating CRS and TRS.

For selecting the best genes, two methods are used in this paper. The first method is selecting based on TRS and CRS (TC). The second method is based on TRS, CRS and Simulated Annealing (TCS).

1. Selecting the best genes based on only TRS and CRS (TC):

As it was described in 3.2, the features in one cluster have maximum similarity. Therefore, in this step, selecting genes from one cluster leads to selecting the genes with maximum redundancy. To reach such a target, a gene with maximum TRS value is selected. In this case, the selected gene would not have lower CRS in compare to other genes from the same cluster. If CRS of the new candidate gene is less than the CRS of other selected genes in its cluster, the new gene, depends on the comparison result of ΔTV_{norm} and θ . Term Variance (TV) is to represent valuable information; the larger value this parameter has, the more valuable information the gene contains. TV for gene F_i is defined as follows:

$$TV(F_i) = \frac{1}{|n|} \sum_{j=1}^{|n|} (F_{ij} - \bar{F}_i) \quad (12)$$

Where $|n|$ is the number of samples, F_{ij} shows the value of gene i for sample j and \bar{F}_i is the average value of all samples for gene F_i .

ΔTV is the result of dividing the TV of picking a gene from its cluster by TV of not picking it at all. ΔTV for gene i in cluster C is calculated as:

$$\Delta TV(F_i) = \frac{\sum_k TV(F_k)}{\sum_l TV(F_l)} \quad (13)$$

Where $|m|$ is the number of selected genes in cluster C , $\sum_k TV(F_k)$ and $\sum_l TV(F_l)$ are the summation of TV s of the genes in the cluster, $k \in \{1 \dots |m|\}$ and $l \in \{1 \dots |m|\}$ with the condition of $k \neq l$.

By normalizing $\Delta TV(F_i)$ in range $[0, 1]$, $\Delta TV_{norm}(F_i)$ is obtained.

For selecting the gene with lower CRS compared to another CRS in its cluster, $\Delta TV_{norm}(F_i)$ is calculated for the gene and if $\Delta TV_{norm}(F_i)$ is greater than θ , F_i will be selected.

Algorithm 2 shows the pseudo-code of using TRS and CRS (TC) to select the final subset.

2. Selecting the best genes based on TRS, CRS and Simulated Annealing (TCS):

Simulated Annealing (SA) is a probabilistic non-greedy algorithm that explores search space of a problem by annealing from a high to a low temperature state [44]. In this algorithm, moving to better state is accepted in any case but moving to the worse state is accepted only with a variable probability. This probability is high at the beginning, but is getting decreased along with the temperature, and thus the algorithm becomes greedier. If a solid heated past melting point and then cooled down, the solid's structural properties will vary depending on the rate of cooling. By cooling down the liquid slow enough, large crystals will be formed. On the other hand, if the cooling is done quickly (quenched) the crystals will contain defects and imperfections. The algorithm

- α : Relevance threshold.

output:

- CRS : Set of CRS.

- TRS : Set of TRS.

```

1: for  $i = 1$  to  $n$  do
2:   for  $j = 1$  to  $n$  do
3:      $w_{ij} \leftarrow \frac{(1-\alpha)}{2} (SU(F_i, C) + SU(F_j, C)) - \alpha SU(F_i, F_j)$ 
4:   end for
5: end for
6:  $\hat{w} \leftarrow \text{Softmax-scaling}(w)$ 
7:  $\{cluster_1, cluster_2, \dots, cluster_c\} \leftarrow \text{Louvian}(\hat{w})$ 
8: for  $i = 1$  to  $n$  do
9:    $TRS_i \leftarrow \text{Scale}(\text{TOPSIS}(F_i))$ 
10: end for
11: for  $k = 1$  to  $C$  do
12:   for  $j = 1$  to  $nC$  do
13:      $CRS_{kj} \leftarrow \text{Scale}(\text{TOPSIS}(F_{kj}))$ 
14:   end for
15: end for

```

Algorithm 2: Selecting the best genes using TRS and CRS - TC

input:

- CRS : Set of CRS;

- TRS : Set of TRS.

output:

- S_{OPT} : Set of final selected features.

```

1:  $TRS_S \leftarrow \text{Sort-Descending}(TRS)$ 
2: for  $i = 1$  to  $n$  do
3:    $temp \leftarrow TRS_{S_i}$ 
4:    $k \leftarrow \text{Check-Cluster}(temp)$ 
5:   if  $CRS(temp) > CRS(\text{all features in cluster } k)$  then
6:      $S_{OPT} \leftarrow S_{OPT} \cup temp$ 
7:   else
8:     if  $\Delta TV_{norm}(temp) > \theta$  then
9:        $S_{OPT} \leftarrow S_{OPT} \cup temp$ 
10:    end if
11:  end if
12: end for

```

terminates when the final temperature reaches, or sufficient number of consecutive moves have been rejected.

In SA, at first an initial solution is randomly selected, and it is assumed to be the optimal solution. Subsequently, the cost of the initial solution is computed using the $Cost$ function. While temperature T does not satisfy the termination condition, a neighboring solution of the current optimal solution is selected, and its cost is calculated. If the cost of the newly selected neighboring solution is less than or equal to current optimal solution, the current optimal solution is replaced with a newly selected neighbor solution. If the cost of the neighboring solution is greater than the current optimal solution, a random value q is chosen in the range of $[0, 1]$. In this case, the replacement of the optimal solution is permitted only if a random value q is less than $e^{-\frac{Cost(v_n) - Cost(v_b)}{T}}$. After temperature T is reduced based on $g(T)$, the same process is continued until T satisfies the termination condition.

Definition of $Cost$ function is the main step of SA. For this purpose, Sum $CRS(SCRS)$ is used as $Cost$ function in this paper, which is calculated as follows:

$$SCRS = \sum_{i=1}^C ICRS_i \quad (14)$$

Algorithm 1: CRS-TRS-Calculating Algorithm

input:

- F : $p \times n$ matrix, p patterns of n features;

Where

$$ICRS = \frac{\sum_{j=1}^m CRS}{m} \quad (15)$$

Where c and m are the number of cluster and the number of genes in each cluster, respectively and $ICRS$ is summation of CRSs in each cluster.

The goal of this algorithm is reaching maximum value on $SCRS$ applied to the sorted TRS .

For using SA, the inputs are FB and T_0 . FB is an array of 0 and 1. fb_i is 0 when the gene is not selected and 1 when gene is selected. For calculating FB , TRSs are sorted in descending manner, and fb_i represents the index of each variable in FB , which is calculated based on the sorted TRSs.

T is the initial temperature. This initial temperature should be large enough to allow sufficient transitions to be accepted. The temperature reduction function is defined as a simple iterative function which is the product of T multiplied by a constant r ($g(T) = r \times T$). In some references, this value is in range [0.5 0.99].

Algorithm 3 shows the pseudo-code of using SA, TRS and CRS (TCS) for selecting the final subset.

In the last step, for selecting the final subset, two mentioned methods could be used. When using only TRS and CRS in the selection process, θ parameter should be set, and when using SA, then it is added to the selection process. The main advantages of using SA are the flexibility and ability to approach global optimality in this step. However, the selection process is slower comparing to when using only CRS and TRS. On the other hand, selecting the best value for θ in the first method, makes it very sensitive and could affect the results.

Fig. 1 shows the schematic diagram of the proposed method.

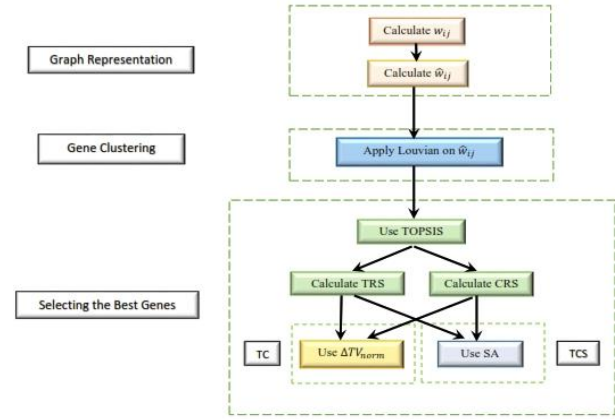


Fig. 1: Illustrating the proposed method on a schematic diagram

Algorithm 3: Selecting the best genes using TRS, CRS and SA – TCS

input:

- $FB = \langle fb_1 \dots fb_n \rangle$ where $fb_i \in \{0,1\}$;
- T_0 : The initial temperature;
- r : temperature reduction constant.

output:

- v_b : Combination of genes.

- 1: Generate an initial solution, v_i
- 2: $v_b \leftarrow v_i$
- 3: Calculate the cost of initial solution, $Cost(v_b)$
- 4: **while** ($T > T_{min}$) or ($iteration < itr_{max}$) **do**
- 5: Randomly select a neighbor solution, v_n , of v_b which have one bit different from v_b
- 6: $\Delta Cost = Cost(v_b) - Cost(v_n)$
- 7: **if** ($\Delta Cost \leq 0$) **then**
- 8: $v_b \leftarrow v_n$
- 9: **else**
- 10: Generate a random number q uniformly in the range [0,1]
- 11: **if** ($q < e^{-\frac{\Delta Cost}{T}}$) **then**
- 12: $v_b \leftarrow v_n$
- 13: **end if**
- 14: **end if**
- 15: $T \leftarrow g(T)$
- 16: **end while**

5. Experimental Results and Discussion

In this section, the performance of the proposed method is compared to twelve other frequently used gene/feature selection methods upon twelve well-known microarray datasets.

For comparing the proposed method with other methods, twelve different DNA microarray datasets are selected. The selected datasets cover a wide spectrum of cancer types and are already used in some other papers. Datasets include nine binary classification types (Blastom, Colon, Gastric, Central Nervous System (CNS), Leukemia 2-class, Diffuse Large-B-Cell Lymphoma (DLBCL), Prostate Tumor, Ovarian, and Brain) and three multi-class (Lymphoma, SRBCT, and Lung Cancer) that are available at [45-47]. Table 2 displays the brief description of used datasets.

Table 2: Description of the datasets used in the experiments

Dataset	Sample (Pattern)		Class
	NO	NO	
Blastom	23	1,465	2
Colon	62	2,000	2
Gastric	30	4,522	2
CNS	60	7,129	2
ALL-AML	72	7,129	2
DLBCL	77	7,129	2
Prostate Tumor	102	10,509	2
Ovarian	253	15,154	2
Brain	21	12,625	2
Lymphoma	62	4,026	3
SRBT	83	2,308	4
Lung Cancer	203	12,600	5

The other gene/feature selection methods that are used for comparing the results are Mutual correlation (MC) [48], FAST [27], Graph Clustering with Node Centrality for unsupervised feature selection (GCNC) [49], Unified-Feature Association Map (U-FAM) [50], Feature Selection method with Joint Maximal Information Entropy between features and class (FS-JMIE) [34], A Correlation based Memetic Algorithm (MA-C) [33], Dense Subgraph Finding with Feature Clustering (DSFFC) [29], Distributed dCor-based FS (D²CORFS) [51], a ReliefF and ACO-based gene

selection (RFACO-GS) [52], A hybrid algorithm for feature subset selection in high-dimensional datasets using FICA and IWSSr algorithm (FICA-IWSSr) [53], Greedy Randomized Adaptive Search Procedure (GRASP) [54], and Support Vector Machine Recursive Feature Elimination (FCSVM-REF) [55].

Since the proposed method is a filter-based gene selection and is independent of using any classifier in the gene selection process, for evaluating the performance, the different types of classifiers are used in experiment phase. Different classifiers that are considered in this paper are Support Vector Machine (SVM) [56], Decision Tree (DT) [57], Naïve Bayes (NB) [6] and k-Nearest Neighbor (kNN) [58].

For obtaining the accurate and stable experiment results, the average classification accuracy rate (%), over ten independent runs, is considered. In each run, for training/testing the classifier, 70%/30% of the dataset is used in train/test phase. In the training phase, the final feature subsets are selected using training sets and the learning model is evaluated in the test phase, using testing sets. All experiment results are obtained on a machine with 2.70 GHz CPU and 4GB of RAM.

5.1 Experimental Results

To demonstrate the performance of the proposed method, in this section, the experimental results have been presented in terms of classification accuracy term, feature reduction, and the parameters' effect and the execution time. In all results, α is 0.4 when calculating the weights of the graph.

The last step in the proposed algorithm is where selecting the best genes by using two methods; TC and TCS. Where ever TC is used, θ is set to 0.7, and where TCS is applied initial temperature (T_0), temperature reduction constant (r) and termination condition of SA are 100,000, 0.95 and $T < 0.01$, respectively.

The accuracy in the selection process of FCSVM-REF is reported by SVM, since that is the mechanism used in the selection process.

5.1.1 Classification accuracy

To demonstrate the advantages of the proposed methods (TC and TCS), the average classification accuracy of it has been compared with other well-known gene selection methods. Table 3 shows the comparison results between the proposed method with twelve gene selection methods. The results are averaged over ten runs of different gene selection methods, using SVM, DT, NB and kNN classifiers. For each classifier in Table 3, the rank of each algorithm in comparison to other methods is presented in parentheses.

As it is indicated in the results, in average, the proposed method using TC achieves the second rank with 87.33%, 87.29%, and 86.03%, using SVM, DT, and kNN, respectively. In average, the proposed method using TCS, obtains the best rank with 89.08%, 87.5%, and 87.14%, using SVM, DT, and kNN classifiers, respectively.

5.1.2 Feature reduction

In Table 4, feature reduction of the proposed method (TC and TCS) has been compared with other feature selection methods over different datasets. As it is presented, that the proposed method (TC or TCS) feature reductions are 83.81%, 84.75%, 83.19%, 84.78%, 81.90%, 75.65%, 89.25%, 83.36%, 83.74%, 94.97%, 85.23%, 94.18% and 85.27% over Blastom, Colon, Gastric, CNS, Leukemia, DLBCL, Prostate Tumor, Ovarian, Lymphoma, Brain, SRBT, Lung Cancer and in average. The average reduction for the proposed method is the highest one with 83.80% for TC and 85.27% for TCS.

5.1.3 Parameters

In the proposed method, α is a user-specified parameter that is used for calculating the graph weights in equation 10. If $\alpha = 0$, the equation 10 will be changed to:

$$w_{ij} = \frac{1}{2} \times (SU(F_i, C) + SU(F_j, C)) \quad (16)$$

In this situation, only T-Relevance (the correlation between each gene and its target class) affects the graph weights, and so, the method will be a supervised graph-based gene selection. While $\alpha = 1$, the graph weights are calculated as follow:

$$w_{ij} = -SU(F_i, F_j), \quad (17)$$

Therefore, only F-Correlation between two genes determines the weight of the edge between two nodes and the effect of its target class will be ignored. This leads to changing the proposed method to an unsupervised graph-based gene selection.

In other situation, the value of $\frac{1-\alpha}{2}$ depends on the value of α , and so if the value of α is 0.3, the value of $\frac{1-\alpha}{2}$ is 0.35. Figure 2 and Figure 3 show the average classification accuracy of the proposed method using TCS over ten runs with different α values using SVM and DT classifiers. In these figures, for different values of α (which cause change on the $\frac{1-\alpha}{2}$ value), the average classification accuracy is calculated and represented. For example, using SVM, and $\alpha = 0.4$, for Colon, Leukemia, Prostate Tumor, Brain, SRBT, Lung Cancer and average, the classification accuracy is 88.53%, 90.54%, 89.67%, 80.70%, 77.73%, 82.31% and 84.91%, respectively. Using DT and $\alpha = 0.4$, for Colon, Leukemia, Prostate Tumor, Brain, SRBT, Lung Cancer and average, the classification accuracy is 78.48%, 88.92%, 83.45%, 80.67%, 82.88%, 88.27% and 83.78%, respectively.

In Fig. 2, the maximum classification accuracy, for Colon, Leukemia, Prostate Tumor, Brain, SRBT, Lung Cancer and in average is 88.53% ($\alpha = 0.4$), 90.54% ($\alpha = 0.4$), 89.67% ($\alpha = 0.4$), 81.61% ($\alpha = 0.5$), 78.45% ($\alpha = 0.3$), 84.48% ($\alpha = 0.5$) and 84.91% ($\alpha = 0.4$), respectively.

Table 4: Comparison of feature reduction of different feature selection methods over different datasets.

Dataset	Proposed Method		MC	FAS T	GC NC	U-FAM	MA -C	DSF FC
	TC	ITCS						
Blastom	83.8%	75.4%	63.9%	71.4%	69.3%	72.0%	76.9%	70.4%
Colon	84.7%	82.4%	71.3%	87.5%	81.2%	59.2%	79.1%	73.3%
Gastric	83.1%	83.1%	65.4%	80.4%	75.9%	70.4%	74.0%	75.9%
CNS	81.6%	84.7%	72.0%	73.2%	70.9%	70.8%	72.2%	75.4%
Leukemia	79.9%	81.9%	63.9%	73.0%	80.3%	76.4%	85.4%	74.3%
DLBCL	70.2%	75.6%	61.4%	60.8%	66.7%	70.4%	75.2%	58.2%
Prostate Tumor	88.1%	89.2%	76.9%	97.4%	78.9%	81.6%	79.5%	57.1%
Ovarian	81.5%	83.3%	78.4%	80.6%	76.9%	90.1%	79.4%	73.4%
Lymphoma	80.1%	83.7%	68.9%	78.9%	80.4%	73.8%	71.7%	79.1%
Brain	92.7%	94.9%	81.9%	74.1%	75.3%	80.8%	80.4%	71.3%
SRBT	85.1%	85.2%	83.5%	78.3%	87.1%	87.2%	70.4%	59.9%
Lung Cancer	94.1%	93.4%	54.3%	92.4%	83.9%	86.6%	71.0%	80.2%
Average	83.8%	85.2%	70.7%	79.7%	78.0%	77.0%	76.2%	73.5%

In Fig. 3, the maximum classification accuracy, for Colon, Leukemia, Prostate Tumor, Brain, SRBT, Lung Cancer and in average is 79.35% ($\alpha = 0.3$), 88.92% ($\alpha = 0.4$), 84.28% ($\alpha = 0.3$), 80.67% ($\alpha = 0.4$), 83.92% ($\alpha = 0.6$), 88.27% ($\alpha = 0.4$) and 83.78% ($\alpha = 0.4$), respectively.

θ is other parameter that is used in the proposed method for selecting the best genes in the final step (Algorithm 2). Selecting the best value for θ is very sensitive and could affect the results. Fig. 4 shows the average classification accuracy of the proposed method using TC over ten runs with different θ values using SVM classifier. Therefore, the maximum classification accuracy, for Colon, Leukemia, Prostate Tumor, Brain, SRBT, Lung Cancer and in average is 83.46% ($\theta = 0.7$), 87.30% ($\theta = 0.7$), 89.94% ($\theta = 0.7$), 81.97% ($\theta = 0.8$), 81.74% ($\theta = 0.9$), 81.06% ($\theta = 0.7$) and 83.59% ($\theta = 0.7$), respectively.

5.1.4 Execution time

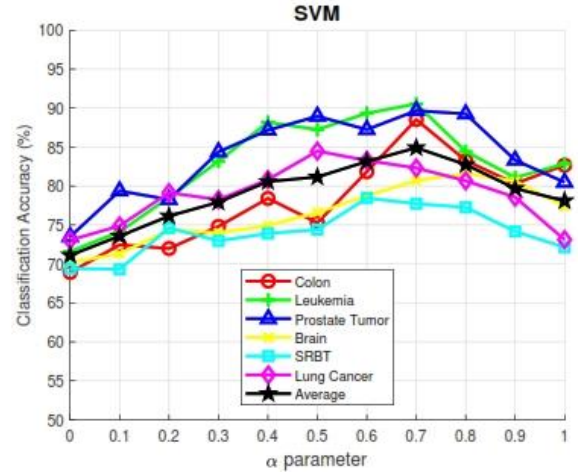
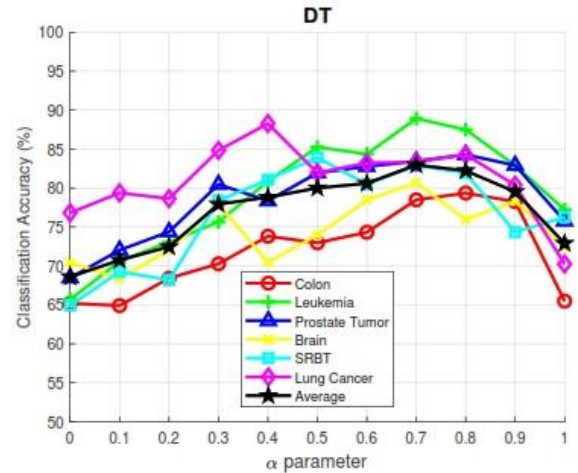
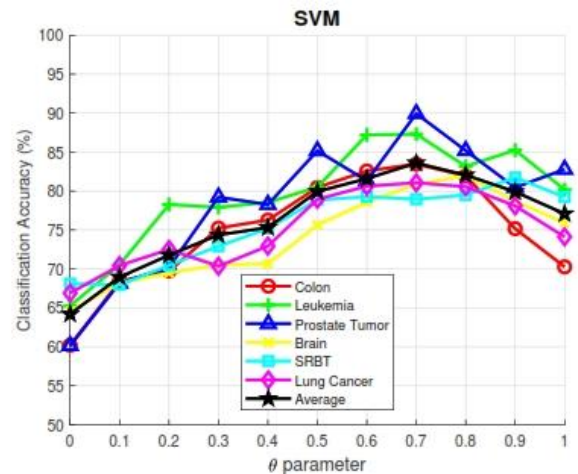
To analyze the complexity of the proposed method, the computational complexity should be estimated. The proposed method consists of three steps: graph representation, gene clustering and selecting the best genes from each cluster. Therefore, computational complexity of the proposed method could be estimated as follows:

Step 1: For n genes and p samples, calculating the graph edges for all pairs of genes has a computational cost of $O(n^2p)$.

Step 2: For clustering the genes, Louvain community detection algorithm is used with computational cost of $O(n \log n)$.

Step 3: based on [59], the time complexity of TOPSIS could be calculated as: $O(n^2)$ for the first step, $O(n)$ for the second step, $O(n)$ for the third step and $O(1)$ for the final step. This means the computational cost of TOPSIS is $O(n^2 + n + n + 1) = O(n^2)$.

In the proposed method, the TOPSIS is used for ranking the genes without considering their clusters with $O(n^2)$ computational cost, and considering their clusters

Fig. 2: Average classification accuracy over ten runs with different α values using SVM classifier.Fig. 3: Average classification accuracy over ten runs with different α values using DT classifier.Fig. 4: Average classification accuracy over ten runs with different θ values using SVM classifier.

In the proposed method, the TOPSIS is used for ranking the genes without considering their clusters with

$O(n^2)$ computational cost, and considering their clusters with $O(mk)$ computational cost, where m ($m \leq n$) is the number of genes in each cluster and k is the number of clusters ($O(mk) \leq O(n^2)$).

After applying TOPSIS, for selecting the best genes, two different methods are used. For the first method (Algorithm 2), all genes will be traced based on TRS and CRS values. Therefore, the computational cost of this method is $O(n)$.

For the second method (Algorithm 3), because of using the selected temperature reduction function and the stop condition of SA, the computational cost of this method is $O(\log \frac{T}{T_{min}}) \gg O(\log n)$.

Consequently, the total computational complexity of the proposed method is $O(n^2p + n \log n + n^2 + n^2 + (n \vee \log n)) = O(n^2p)$.

For comparing the execution time of the proposed method (TC and TCS) with other gene selection methods, the average execution times (in milliseconds) of different methods are shown in Table 5. As for filter based gene selection, where the gene selection process is independent of the classifier, only the execution time of the feature selection process is reported. As described in section 2, for univariate feature selection, the dependency between genes will be ignored and so each gene is evaluated independently. For multivariate gene selection, on the other hand, the dependency between genes will affect the gene selection process. Therefore, for univariate gene selection (i.e., FS, ReliefF), the execution time is greater than multivariate (i.e., mRMR, and GCNC).

5.2 Discussion

In the past subsections, the performance of the proposed method was compared to other gene selection methods in different experiments. In this section, the reasons behind the efficiency of the proposed method are described briefly.

Increasing the performance of gene selection in microarray data with high-dimensional genes depends on

how well the irrelevant and redundant genes are ignored when dealing with a dataset. If the gene selection method handles both the irrelevant and redundant genes efficiently, then it would obtain better results. That is why when using univariate methods (i.e., LS, FS and ReliefF), since they ignore the gene dependency in their gene selection processes, they are not successful in removing redundant genes. In the proposed method, the symmetric uncertainty concept takes into consideration the relation between genes and also between each gene and its class label. The higher relation between different genes has a negative impact in the gene selection process, but on the other hand the effect of relation between each gene and class label is positive. Therefore, in the proposed method, using SU leads to ignoring the redundant and irrelevant genes, when selecting the genes in the first phase of the process. But using SU for calculating the graph weights in the first step of the proposed method may be time consuming for the datasets with huge number of features.

When it comes to the second phase by using graph clustering algorithm, not only the similar genes within a cluster are grouped, but also genes with minimum dependency to other genes within a cluster are selected. This helps selecting the genes with minimum redundancy, in the proposed method. By ranking the genes in third step and selecting the genes with highest rank on the global and lowest rank inside the cluster, the genes with similar attributes are ignored. Therefore, the redundant and irrelevant genes have a low chance for being picked up to the final feature subsets. In the proposed method, for selecting the best genes in third step, two different methods are used. The first method selects the genes within a cluster based on its probability. In order to calculate the probability, TV have been used. If a gene has greater TV, it means it contains valuable information. Therefore, using ΔTV (comparing between TV of when the gene is selected and when it is not) as probability of

Table 5: Average execution time (in ms) of different gene selection methods over ten independent runs.

Method	Colon	Leukemia	Prostate Tumor	Brain	SRBT	Lung Cancer	Average
TC	109,532	189,472	183,944	247,936	140,368	218,629	181,647
TCS	118,945	210,490	286,701	404,618	172,184	291,309	247,375
ReliefF	1,978	2,591	2,671	2,734	2,080	2,695	2,458
FS	89	103	176	217	91	205	147
LS	1,368	1,498	3,527	8,926	1,395	6,719	3,906
mRMR	9,763	11,261	13,893	14,789	10,428	14,735	12,478
RSM	68	71	128	459	73	193	165
MC	27	64	124	278	59	161	119
FAST	117,591	162,814	168,436	283,612	154,31	220,581	190,607
GCNC	116,831	193,477	205,716	259,332	124,821	238,900	189,846
U-FAM	43,953	61,704	72,136	121,742	51,826	91,491	73,809
FS-JMIE	186,947	261,955	37,827	450,970	190,333	480,729	268,127
MA-C	143,218	205,007	291,476	386,445	178,593	307,906	252,108
DSFFC	121,487	218,706	197,467	390,041	120,963	378,117	237,797
FCSVM-REF	147,281	269,405	293,863	458,052	193,924	394,589	292,852

selecting or ignoring a gene, results picking up only those genes which would lead to improve the method's performance.

In the second method, for selecting the best genes, SA is used, in the proposed method. SA is a probabilistic technique for approximating the global optimum of a given function. Specifically, it is a meta-heuristic to approximate global optimization in a large search space. It is often used when the search space is discrete. For problems where finding an approximate global optimum is more important than finding a precise local optimum in a fixed amount of time, SA may be preferable to alternatives. Using Sum CRS (SCRS) as SA cost function leads to decreasing the redundancy between selected genes and increasing the performance of proposed method. The experimental results show that using SA in the third step of the proposed method (TCS) actually improves the results, however the selection process is slower than TC.

The proposed method uses class label in the first step with parameter α . This parameter is used for determining the effect of the class label and the relation between different genes. By changing the value of α , different conditions will be created and so, different results will be achieved. For example, if $\alpha = 1$, the class label will be ignored, and the algorithm will be changed to an unsupervised algorithm. This condition would be used when the label of the class is not reliable in the dataset. The Figure 2 and Figure 3 show that if the value of α is in range $[0.3, 0.5]$ ($\frac{1-\alpha}{2}$ in range $[0.25, 0.35]$), the best results are obtained.

5.3 Statistical Analysis

The Friedman test is a non-parametric equivalent that can be used for illustrating the statistical significance of the results over multiple datasets. The test ranks each classifier accuracy over different datasets, separately. Therefore, the best performing algorithm gets the first rank, the second best gets the second rank and so on. After ranking each classifier over different datasets, χ_F^2 and F_F could be calculated. For N datasets and k methods:

$$\chi_F^2 = \frac{12N}{k(k+1)} \times \left[\sum_{i=1}^k R_j^2 - \frac{k(k+1)^2}{4} \right] \quad (18)$$

$$F_F = \frac{(N-1)\chi_F^2}{N(k-1)-\chi_F^2} \quad (19)$$

Where R_j^2 is the average rank of the j^{th} method over all datasets and which is distributed according to the Fisher distribution with $k-1$ and $(k-1) \times (N-1)$ degrees of freedom. In Friedman test, using significance level α , the null hypothesis means all methods perform equivalently at level α .

In our experiments, using SVM, with $N = 12$ and $k = 14$, the critical value of Fisher distribution with 13 and degrees of freedom 143, for $\alpha = 0.05$, $F(13, 143)$ is near 1.8. Therefore, if the gene selection method is incorporated with a classifier and the value of F_F is

greater than 1.836, the null hypothesis will be rejected, and the result is statistically significant.

For other classifiers, with $N = 12$ and $k = 13$, the critical value of Fisher distribution with 12 and degrees of freedom 132, for $\alpha = 0.05$, $F(12, 132)$ is near 1.8. Therefore, if the gene selection method is incorporated with a classifier and the value of F_F is greater than 1.874, the null hypothesis will be rejected, and the result is statistically significant.

For comparing the results of Friedman test between the proposed method (TC and TCS) and other gene selection methods, after ranking different gene selection method, the results of Friedman test are shown in Table 7. For all classifiers, it is demonstrated that when the gene selection methods are incorporated with different classifiers, the value of F_F is greater than 1.8. Therefore, the null hypothesis will be rejected, and it can be concluded that these results are statistically significant.

For demonstrating the distribution of accuracies for different treatments based on the obtained ranks, the distribution of accuracies for twelve datasets are investigated. It conclusion the distribution of all accuracies are near normal. In Fig. 5 and Fig. 6, Quantile-Quantile (Q-Q) plot for five datasets (i.e., Colon, Gastric, Ovarian, SRBT and Lung Cancer) are shown. In this plot the linearity of the points suggests the data are normally distributed [60].

6. Conclusion

In this paper, a new supervised/unsupervised filter gene selection was proposed, which was based on the graph clustering and ranking the genes and it selects the best subset of genes from the microarray data. For selecting the genes with minimum redundancy to other genes and maximum relevance to the class label, some concepts were used; Symmetric Uncertainty for creating graph, community detection for grouping the genes in different clusters, and a new method for ranking the genes. It did not use any learning model in the selection process which led to decrease the time complexity. The performance of the proposed method was compared to different gene/feature selection methods including Mutual correlation (MC), fast clustering-based feature selection algorithm (FAST), Graph Clustering with Node Centrality for unsupervised feature selection (GCNC), Unified- Feature Association Map (U-FAM), Feature

Table 7: The results of Friedman test

Classifier	χ_F^2		F_F		Significant	
	TC	TCS	TC	TCS	TC	TCS
SVM	47.30293	45.08423	8.7425	8.0451	+	+
DT	47.38560	48.65455	11.7498	11.7208	+	+
NB	52.84612	50.19547	12.4287	12.8106	+	+
kNN	48.98744	50.04512	11.7298	11.4925	+	+

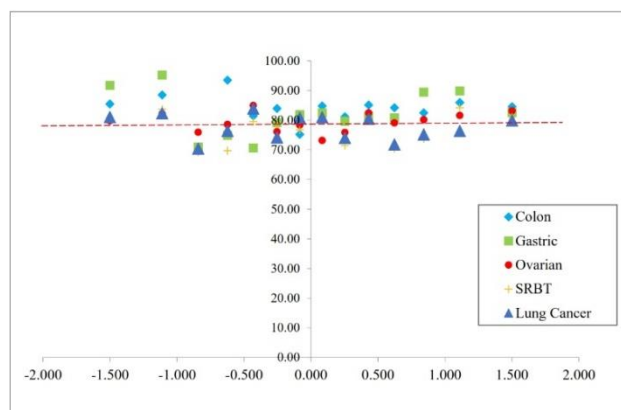


Fig. 5: Distribution of accuracies for different classification accuracies of TCS for five datasets using SVM classifier.

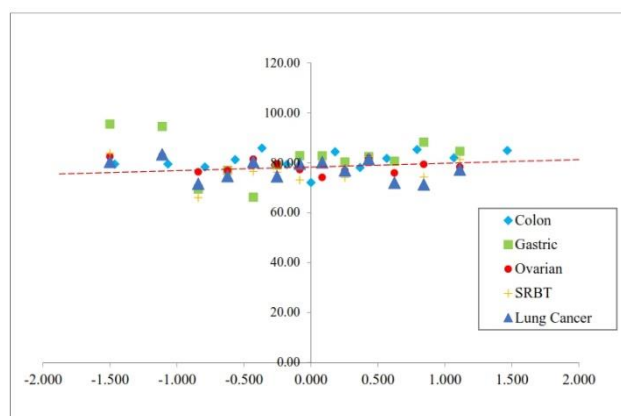


Fig. 6: Distribution of accuracies for different classification accuracies of TCS for five datasets using DT classifier.

Selection method with Joint Maximal Information Entropy between features and class (FS-JMIE), a Correlation based Memetic Algorithm (MA-C), Dense Subgraph Finding with Feature Clustering (DSFFC), Distributed dCor-based FS (D2CORFS), a ReliefF and ACO-based gene selection (RFACO-GS), A hybrid algorithm for feature subset selection in high-dimensional datasets using FICA and IWSSr algorithm (FICA-IWSSr), Greedy Randomized Adaptive Search Procedure (GRASP), and Support Vector Machine Recursive Feature Elimination (FCSVM-REF). The performance comparison was done over twelve microarray datasets using four different classifiers including Support Vector Machine (SVM), Decision Tree (DT), Naïve Bayes (NB) and k-Nearest Neighbor (kNN).

The experimental results showed that the proposed method using three steps for selecting the best gene subset, was able to select a subset of genes with minimum redundancy between genes and maximum relevance to class label. The results indicated that the proposed method obtained significantly better result in comparison to the other well-known supervised and unsupervised feature/gene selection approaches. The results also confirmed that the proposed method achieved satisfying

performance over different classifiers for different microarray datasets.

References

- [1] A. Salimi, M. Ziaii, A. Amiri, M. H. Zadeh, S. Karimpouli, and M. Moradkhani, "Using a feature subset selection method and support vector machine to address curse of dimensionality and redundancy in hyperion hyperspectral data classification," *The Egyptian Journal of Remote Sensing and Space Science*, vol. 21, no. 1, pp. 27–36, 2018.
- [2] T. R. Golub, D. K. Slonim, P. Tamayo, C. Huard, M. Gaasenbeek, J. P. Mesirov, H. Coller, M. L. Loh, J. R. Downing, M. A. Caligiuri et al., "Molecular classification of cancer: class discovery and class prediction by gene expression monitoring," *science*, vol. 286, no. 5439, pp. 531–537, 1999.
- [3] H. Liu and H. Motoda, *Computational Methods of Feature Selection* (Chapman & Hall/Crc Data Mining and Knowledge Discovery Series). Chapman and Hall, 2007.
- [4] A. Jovi'c, K. Brki'c, and N. Bogunovi'c, "A review of feature selection methods with applications," in *2015 38th International Convention on Information and Communication Technology, Electronics and Microelectronics (MIPRO)*. IEEE, 2015, pp. 1200–1205.
- [5] B. Liao, Y. Jiang, W. Liang, W. Zhu, L. Cai, and Z. Cao, "Gene selection using locality sensitive laplacian score," *IEEE/ACM Transactions on Computational Biology and Bioinformatics*, vol. 11, no. 6, pp. 1146–1156, Nov 2014.
- [6] S. Theodoridis and K. Koutroubas, *Pattern Recognition*, fourth edition. Academic Press, Oxford, 2008.
- [7] R. Cai, Z. Hao, X. Yang, and W. Wen, "An efficient gene selection algorithm based on mutual information," *Neurocomputing*, vol. 72, no. 4, pp. 991 – 999, 2009.
- [8] L. E. Raileanu and K. Stoffel, "Theoretical comparison between the gini index and information gain criteria," *Annals of Mathematics and Artificial Intelligence*, vol. 41, no. 1, pp. 77–93, May 2004.
- [9] H. Peng, F. Long, and C. Ding, "Feature selection based on mutual information criteria of max-dependency, max relevance, and min-redundancy," *IEEE Transactions on Pattern Analysis and Machine Intelligence*, vol. 27, pp. 1226– 1238, Aug 2005.
- [10] L. Yu and H. Liu, "Efficient feature selection via analysis of relevance and redundancy," *Journal of Machine Learning Research*, vol. 5, pp. 1205–1224, 2004.
- [11] A. J. Ferreira and M. A. Figueiredo, "Efficient feature selection filters for high-dimensional data," *Pattern Recognition Letters*, vol. 33, no. 13, pp. 1794 – 1804, 2012.
- [12] S. Tabakhi, P. Moradi, and F. Akhlaghian, "An unsupervised feature selection algorithm based on ant colony optimization," *Engineering Applications of Artificial Intelligence*, vol. 32, no. Supplement C, pp. 112 – 123, 2014.
- [13] C. Lai, M. J. Reinders, and L. Wessels, "Random subspace method for multivariate feature selection," *Pattern Recognition Letters*, vol. 27, no. 10, pp. 1067 – 1076, 2006.
- [14] R. J. Manoj, M. A. Praveena, and K. Vijayakumar, "An aco- ann based feature selection algorithm for big data," *Cluster Computing*, pp. 1–8, 2018.
- [15] I. Jain, V. K. Jain, and R. Jain, "Correlation feature selection based improved-binary particle swarm optimization for gene selection and cancer classification," *Applied Soft Computing*, vol. 62, pp. 203–215, 2018.
- [16] S. Maldonado, R. Weber, and J. Basak, "Simultaneous feature selection and classification using kernel-penalized

- support vector machines,” *Information Sciences*, vol. 181, no. 1, pp. 115 – 128, 2011.
- [17] G. Wang, Q. Song, B. Xu, and Y. Zhou, “Selecting feature subset for high dimensional data via the propositional foil rules,” *Pattern Recognition*, vol. 46, no. 1, pp. 199 – 214, 2013.
- [18] J. Canul-Reich, L. O. Hall, D. Goldgof, J. N. Korecki, and S. Eschrich, “Iterative feature perturbation as a gene selector for microarray data,” vol. 26, 08 2012.
- [19] P. A. Mundra and J. C. Rajapakse, “Svm-rfe with mrmr filter for gene selection,” *IEEE Transactions on NanoBioscience*, vol. 9, no. 1, pp. 31–37, March 2010.
- [20] L.-Y. Chuang, C.-H. Yang, K.-C. Wu, and C.-H. Yang, “A hybrid feature selection method for dna microarray data,” *Computers in Biology and Medicine*, vol. 41, no. 4, pp. 228 – 237, 2011.
- [21] W. Zhao, G. Wang, H. Wang, H. Chen, H. Dong, and Z. Zhao, “A novel framework for gene selection,” vol. 3, pp. 184–191, 04 2011.
- [22] G. Forman, “An extensive empirical study of feature selection metrics for text classification,” *J. Mach. Learn. Res.*, vol. 3, pp. 1289–1305, march 2003.
- [23] K. Kira and L. A. Rendell, “The feature selection problem: Traditional methods and a new algorithm,” in *Proceedings of the Tenth National Conference on Artificial Intelligence*, ser. AAAI’92, 1992, pp. 129–134.
- [24] I. Kononenko, *Estimating attributes: Analysis and extensions of RELIEF*.
- [25] L. Yu and H. Liu, “Feature selection for high-dimensional data: A fast correlation-based filter solution,” in *Proceedings, Twentieth International Conference on Machine Learning*, vol. 2, 01 2003, pp. 856–863.
- [26] R. Battiti, “Using mutual information for selecting features in supervised neural net learning,” *IEEE Transactions on Neural Networks*, vol. 5, no. 4, pp. 537–550, July 1994.
- [27] Q. Song, J. Ni, and G. Wang, “A fast clustering-based feature subset selection algorithm for high-dimensional data,” *IEEE Trans. on Knowl. and Data Eng.*, vol. 25, pp. 1–14, jan 2013.
- [28] M. Mandal and A. Mukhopadhyay, *Unsupervised Nonredundant Feature Selection: A Graph-Theoretic Approach*. Springer Berlin Heidelberg, 2013, pp. 373–380.
- [29] S. Bandyopadhyay, T. Bhadra, P. Mitra, and U. Maulik, “Integration of dense subgraph finding with feature clustering for unsupervised feature selection,” *Pattern Recognition Letters*, vol. 40, no. Supplement C, pp. 104 – 112, 2014.
- [30] S. Tabakhi, A. Najafi, R. Ranjbar, and P. Moradi, “Gene selection for microarray data classification using a novel ant colony optimization,” *Neurocomputing*, vol. 168, no. Supplement C, pp. 1024 – 1036, 2015.
- [31] P. Moradi and M. Rostami, “Integration of graph clustering with ant colony optimization for feature selection,” *Knowledge-Based Systems*, vol. 84, no. Supplement C, pp. 144 – 161, 2015.
- [32] A. Pino Angulo, “Gene selection for microarray cancer data classification by a novel rule-based algorithm,” *Information*, vol. 9, no. 1, p. 6, 2018.
- [33] S. S. Kannan and N. Ramaraj, “A novel hybrid feature selection via symmetrical uncertainty ranking based local memetic search algorithm,” *Knowledge-Based Systems*, vol. 23, no. 6, pp. 580–585, 2010.
- [34] K. Zheng and X. Wang, “Feature selection method with joint maximal information entropy between features and class,” *Pattern Recognition*, vol. 77, pp. 20–29, 2018.
- [35] U. M. Fayyad and K. B. Irani, “Multi-interval discretization of continuous-valued attributes for classification learning,” in *IJCAI*, 1993, pp. 1022–1029.
- [36] C. Shi, Y. Cai, D. Fu, Y. Dong, and B. Wu, “A link clustering based overlapping community detection algorithm,” *Data and Knowledge Engineering*, vol. 87, no. Supplement C, pp. 394 – 404, 2013.
- [37] E. Le Martelot and C. Hankin, “Fast multi-scale detection of relevant communities in large-scale networks,” *The Computer Journal*, vol. 56, no. 9, pp. 1136–1150, 2013.
- [38] V. D. Blondel, J. loup Guillaume, R. Lambiotte, and E. Lefebvre, “Fast unfolding of communities in large networks,” pp. 1–12, 2008.
- [39] C. Gao, D. Wei, Y. Hu, S. Mahadevan, and Y. Deng, “A modified evidential methodology of identifying influential nodes in weighted networks,” *Physica A: Statistical Mechanics and its Applications*, vol. 392, no. 21, pp. 5490–5500, 2013.
- [40] M. R. G. R. . V. L. V. Nicosia, R. Criado, “Controlling centrality in complex networks,” *Scientific Reports* 2, no. 218, pp. 218–223, 2012.
- [41] M. Campiteli, A. Holanda, L. Soares, P. Soles, and O. Kinouchi, “Lobby index as a network centrality measure,” *Physica A: Statistical Mechanics and its Applications*, vol. 392, pp. 5511 – 5515, 2013.
- [42] Y. Du, C. Gao, Y. Hu, S. Mahadevan, and Y. Deng, “A new method of identifying influential nodes in complex networks based on topsis,” *Physica A: Statistical Mechanics and its Applications*, vol. 399, no. Supplement C, pp. 57 – 69, 2014.
- [43] P. Mitra, C. A. Murthy, and S. K. Pal, “Unsupervised feature selection using feature similarity,” *IEEE Trans. Pattern Anal. Mach. Intell.*, vol. 24, no. 3, pp. 301–312, March 2002.
- [44] M. P. V. S. Kirkpatrick, C. D. Gelatt Jr., “Optimization by simulated annealing,” *American Association for the Advancement of Science*, vol. 220, no. 4598, pp. 671–680, may 1983.
- [45] K. R. B. D. S. Repository, kent ridge bio-medical dataset, <http://datam.i2r.a-star.edu.sg/datasets/krbd/>.
- [46] B. institute, Cancer Program Data Sets, 2014, <http://www.broadinstitute.org/cgi-bin/cancer/datasets.cgi>.
- [47] I. T. G. A. Statnikov, C.F. Aliferis, *Gene Expression Model Selector*, 2005, <http://www.gems-system.org>.
- [48] M. Haindl, P. Somol, D. Ververidis, and C. Kotropoulos, *Feature Selection Based on Mutual Correlation*. Springer Berlin Heidelberg, 2006, pp. 569–577.
- [49] P. Moradi and M. Rostami, “A graph theoretic approach for unsupervised feature selection,” *Engineering Applications of Artificial Intelligence*, vol. 44, no. Supplement C, pp. 33 – 45, 2015.
- [50] A. K. Das, S. Goswami, A. Chakrabarti, and B. Chakraborty, “A new hybrid feature selection approach using feature association map for supervised and unsupervised classification,” *Expert Systems with Applications*, vol. 88, no. Supplement C, pp. 81 – 94, 2017.
- [51] A. Brankovic, M. Hosseini, and L. Piroddi, “A distributed feature selection algorithm based on distance correlation with an application to microarrays,” *IEEE/ACM transactions on computational biology and bioinformatics*, 2018.
- [52] L. Sun, X. Kong, J. Xu, R. Zhai, S. Zhang et al., “A hybrid gene selection method based on relieff and ant colony

optimization algorithm for tumor classification,” *Scientific Reports*, vol. 9, no. 1, p. 8978, 2019.

- [53] M. Moradkhani, A. Amiri, M. Javaherian, and H. Safari, “A hybrid algorithm for feature subset selection in high dimensional datasets using fica and iwssr algorithm,” *Applied Soft Computing*, vol. 35, pp. 123–135, 2015.
- [54] P. Bermejo, J. A. Gamez, and J. M. Puerta, “A grasp algorithm for fast hybrid (filter-wrapper) feature subset selection in high dimensional datasets,” *Pattern Recognition Letters*, vol. 32, no. 5, pp. 701–711, 2011.
- [55] X. Huang, L. Zhang, B. Wang, F. Li, and Z. Zhang, “Feature clustering based support vector machine recursive feature elimination for gene selection,” *Applied Intelligence*, vol. 48, no. 3, pp. 594–607, 2018.
- [56] I. Guyon, J. Weston, S. Barnhill, and V. Vapnik, “Gene selection for cancer classification using support vector machines,” *Machine Learning*, vol. 46, pp. 389–422, Jan 2002.
- [57] J. R. Quinlan, “Induction of decision trees,” *Mach. Learn.*, vol. 1, March 1986.
- [58] D. W. Aha, D. Kibler, and M. K. Albert, “Instance-based learning algorithms,” *Machine Learning*, vol. 6, pp. 37–66, Jan 1991.
- [59] Hamdani and R. Wardoyo, “The complexity calculation for group decision making using topsis algorithm,” *AIP Conference Proceedings*, vol. 1755, pp. 0700071 – 0700077, 2016.
- [60] T. J. Cleophas and A. H. Zwinderman, “Quantile-quantile plots, a good start for looking at your medical data (50 cholesterol measurements and 58 patients),” in *Machine Learning in Medicine-a Complete Overview*. Springer, 2015, pp. 253– 259.

Soodeh Bakhshandeh received his BS degree in Computer Engineering (Software) from Alzahra University, Tehran, Iran in 2007. She graduated in Artificial Intelligence from Science and Research Branch, Islamic Azad University, Tehran, Iran. Her research areas are pattern recognition, feature selection, big data analysis, and data mining.

Reza Azmi received his BS degree in Electrical Engineering from Amirkabir University of technology, Tehran, Iran in 1990 and his MS and PhD degrees in Electrical Engineering from Tarbiat Modares University, Tehran, Iran in 1993 and 1999, respectively. He is a faculty member of Computer Engineering Department of Alzahra University of Technology since 2001. He is conducting research activities in the areas of big data analysis, machine learning and cloud computing.

Mohammad Teshnehlab is a faculty member of Electrical Eng. Department of K. N. Toosi University of Technology. His main research interests focus on Intelligent Systems and Control. Professor Teshnehlab is a member of Industrial Control Center of Excellence and founder of Intelligent Systems Laboratory (ISLab). He also is head and Co-founder of Intelligent Systems Scientific Society of Iran (ISSSI) and member of editorial board of International Journal of Information and Communication Technology Research (IJICTR).

A Novel Approach for Cluster Self-Optimization Using Big Data Analytics

Abbas Mirzaei*

Department of Computer Engineering, Islamic Azad University, Ardabil Branch, Ardabil, Iran
a.mirzaei@iauardabil.ac.ir

Amir Rahimi

Department of Computer Engineering, Islamic Azad University, Ardabil Branch, Ardabil, Iran
dramr@ihemardabili.ac.ir

Received: 05/Feb/2019

Revised: 28/Aug/2019

Accepted: 28/Sep/2019

Abstract

One of the current challenges in providing high bitrate services in next generation mobile networks is limitation of available resources. The goal of proposing a self-optimization model is to maximize the network efficiency and increase the quality of services provided to femto-cell users, considering the limited resources in radio access networks. The basis for our proposed scheme is to introduce a self-optimization model based on neighbouring relations. Using this model, we can create the possibility of controlling resources and neighbouring parameters without the need of human manipulation and only based on the network's intelligence. To increase the model efficiency, we applied the big data technique for analyzing data and increasing the accuracy of the decision-making process in a way that on the uplink, the sent data by users is to be analyzed in self-optimization engine. The experimental results show that despite the tremendous volume of the analyzed data – which is hundreds of times bigger than usual methods – it is possible to improve the KPIs, such as throughput, up to 30 percent by optimal resource allocation and reducing the signaling load. Also, the presence of feature extraction and parameter selection modules will reduce the response time of the self-optimization model up to 25 percent when the number of parameters is too high. Moreover, numerical results indicate the superiority of using support vector machine (SVM) learning algorithm. It improves the accuracy level of decision making based on the rule-based expert system. Finally, uplink quality improvement and 15-percent increment of the coverage area under satisfied SINR conditions can be considered as outcome of the proposed scheme.

Keywords: Self-Optimization Networking; Big Data; Quality of service (QoS); Resource Allocation; Load Balancing.

1. Introduction

Over the last four years, annual mobile data traffic has increased more than 130%. It is predicted to continue to increase from 2016 to 2020 at an accumulated annual rate of 78%. Despite the technical and economic advantages of using femto-cell layer in new generation of mobile network, establishing the femto-cell layer for the operators entails some challenges. In order to reach the expected spectrum efficiency, the macro and femto layers must operate at a single bandwidth, which will make interference more erratic and its control more difficult. The responsibility of the resource management center (RMC) will become more complex than for conventional cellular networks. In this regard, SON is introduced as the only viable solution for controlling and managing this type of huge data networks [1].

The control and management of various nodes in mobile networks require self-organization and smart organization.

2. Related Works

The most recently-proposed structures for current mobile networks are combinations of the functions of the base station [4]. These products require a data connection such as

DSL through which to connect to the main network of the mobile operator. Its capabilities should include a maximum transfer strength of about 20 dBm, coverage of high-speed packet access and the ability to establish a certain number of simultaneous voice calls or data sessions. Basic functions of the PnP, such as self-configuration and activation, are carried out in a very limited manner.

Researchers have proposed numerous methods based on automatic neighbour relations (ANR) for optimization in large scale networks. A number of schemes have been developed based on the selection of automatic neighbour relations [5], [6], [7].

Authors [8] proposed a solution for increasing the quality of the service which is to reduce the number of periodical errors during connection. Reducing the number of drop rates and increasing the HOSR increases the QoS in the cellular networks. The authors proposed a framework for determining the neighbour cell list (NCL) to increase the call maintenance indicator and the HOSR. They showed that improving the efficiency of the network relates directly to the NCL. One problem with this scheme is the imbalance in the level of cell coverage with the changes in the NCLs. This has no significant influence under ordinary conditions, but can lead to failure of service provision.

* Corresponding Author

In [9] Authors found that an automatic NCL scheme is more reliable than similar schemes. It is implemented by adding a management register called a network management system to the network core to allow scalability of the network. When a new entity is added to the network, it connects without problem and can be introduced to other parts of the network through a logical procedure during service provision.

In [10] a scheme for third-generation mobile networks has been considered where the requirements of load balancing are considered in the design phase. The authors considered the transmission power of the downlink as well as measures which influence the effective coverage area of the cell. In this scheme, prediction error due to the fallibility of GIS and the probability of incorrect mapping of the data can increase the rate of unsuccessful handovers. The high fallibility of this scheme means it cannot be considered a highly efficiency pattern.

Authors in [11] proposed a scheme where UTRA FDD-based networks provide good ability for configuring and adjusting inter-frequency handovers between cells based on assessment of the NCLs. While this scheme is advantageous from some aspects, the failure to consider inter-frequency handovers in next-generation mobile networks decreases its value to a great degree. The scheme proposed in [12] introduces big data technology to optimize fifth-generation mobile networks. Despite the suitability of this technique for next-generation mobile networks, it is only loosely introduced and no output is provided to compare with similar schemes.

Some authors [13] proposed a self-optimization scheme for optimizing neighbour relation indicators by covering the gaps present in the coverage area of the network. Despite the positive and efficient aspects of this scheme, it only considers optimization for determining ANR. As seen from the algorithms in this scheme, it can only be used under static conditions to increase the level of successful neighbour connections between cells. Assessments show that the previous patterns have some disadvantages. The next section describes our proposed model, which addresses the shortages seen in previous schemes.

The proposed approach is a self-optimization model based on capacity/coverage index management by controlling the network parameters and considering events, timing factors, limited network resources and population distribution of the coverage area. The proposed self-optimization engine comprises four main modules. Big data technology is applied to make the proposed model smart and increase its decision-making capability. The challenge of managing big data in mobile networks has been significantly addressed. Extracting useful and structured data requires the use of a great chunk of information in a very short timeframe

and the ability to extract meaningful information from insignificant data. Reaching a logical relationship between telecommunication and statistical parameters and events can improve decision-making in the mobile network about the use of power and frequency resources in the handover among components.

3. The Move Towards Distributed Intelligence: Big Data based SON

The basis of the proposed approach is to provide a self-optimization model which allows for control of resources and measures related to neighbourhood relations in the mobile network without human interference and by reliance solely on network intelligence. To increase efficiency, big data techniques will be used for the data analysis and decision-making of the network regarding resource allocation. The need to optimal resource supply in areas covered by the network and ensuring the user QoS require control enormous volume of data and manage the configuration characteristics of new generation wireless networks [14]. This will result in an exponential increase in the functional complexity of the design and optimization for this type of network. Self-optimization techniques are the only viable solution for controlling and managing this type of networks that allows control of resources and key performance indicators (KPI) of the mobile network without human intervention based solely on the intelligence of the network [15]. The main objective behind such a self-optimization model is to maximize network efficiency and increase the quality of service (QoS) provided to macro-cell and femto-cell users with the limited network resources. Although some methods such as Learning, Fuzzy Logic, and Convex Optimization approaches have been used to make self-optimization models intelligent but in next-generation networks, such non-intelligent methods don't provide acceptable functionality because of their computational complexity restrictions. Also, their computational complexity depends to scale of network and it will increase dramatically with the increasing volume of data exchanged. Data in these networks require high volume, high speed, and variety, which are the main features of a powerful data management technology called big data so, this study proposes an approach that uses a self-optimization framework based on this technology [16].

In order to satisfy the QoS requirements in multimedia services, resource allocation algorithms must be modified and adjusted to clarify the distinction among services and network conditions [17]. Previous studies have shown that demand side management increases the efficiency and effectiveness of the network to supply resource demand considering user utility and cost [18]. A proper efficient resource allocation based on peak reduction has been presented by [19] in which reducing the network operational

cost was considered, as well as resource supplier’s cost. The optimality of most current distributed optimization schemes are based on achieve a single objective for example utility of user side does not guarantee satisfaction of hard QoS constraints, although; they rely on optimization schemes to apply the proper scheme to minimize cost functions [20], [21].

4. BD-SON Configuration

The way to utilize the self-optimization technology in next-generation mobile networks is through a specific change in the architecture of these networks. The first section added to the structure of the networks is to the data gathering unit, which must be able to receive data from parts and sections and classify the data. The data gathered must be filtered to extract the correlation and meaning and that with the more important meaning will be entered into the self-optimization engine [22]. As you can see in the architecture of the proposed self-optimization networking model (Figure 1), we need to apply at least two additional section through the architecture of current generation mobile networks. The first register by the name of Big Data Gateway is responsible for collecting data from Femto-cell level and send it to the core for further evaluation. Also, another register is Big Data SON Engine which will be applied to making decision based on network condition and the level of resources and customer behaviors which it is in communication with some other parts of the core registers such as MME and S-GW. You can take a look at the introduced architecture as the Figure (1):

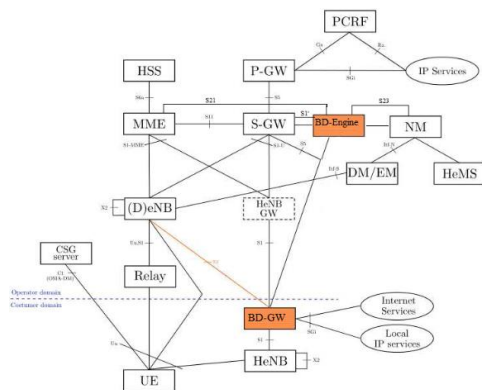


Figure 1. The modified structure of NGMN using BD-SON

The proposed scheme provides a framework for overcoming challenges to 4G and 5G networks using self-organizing networks (SONs) which is consistent with the characteristics of next-generation multi-carrier mobile networks. A general framework for reinforcing the SON using big data is proposed to improve the decision-making resource of the intelligent self-optimization system and the general efficiency of the network. Different data analysis techniques are used and pre-processing before decision-making are the logical methods for decreasing the state

space of decision-making and the response time.

We have introduced the configuration of the proposed Self-Optimization Networking in previous part. As mentioned, automatic controller engine and the resource controller are the most important part of all self-organized networks. So, in order to more accurate investigation of the functionality of this model, we describe all parts of the proposed model in detail. In this regard, you can find the various characteristics and their interfaces in the Figure (2).

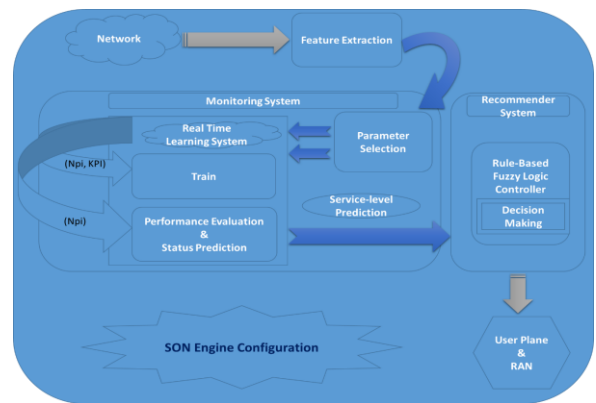


Figure 2. The component of SON Engine

After analyzing the input data and making decision, we have two external command follow which the first commands is relevant to Resource Management Center (RMC) for adjustment of resource level of each network entities and another command sequences which applied to modification of all decision-making thresholds and various applied timing factors. Also, in order to describe the SON configuration better, we should consider the relation of engine with other parts of the radio access networks.

Figure 3 demonstrates the functioning of the self-optimization model. The flowchart records the data from the access network layer, events and user-level data in a register. After the pre-processing phase, which involves the classification of the data, filtration, rating and checking the level of correlation between data, the data enters the efficacy assessment unit. In this unit, the status of the network for a certain time period is predicted and, if the efficiency levels are satisfactory, after a time delay, it returns to monitoring the status of the network. If the efficiency levels are not satisfactory, the self-optimization engine will be activated. After analysis of the proven relations between the efficiency indicators and the network parameters, network decision-making is initiated. The results are sent to the RMC. The control information transferred between the self-optimization engine and the RMC includes details about the allocation of resources to various components of the network for a specific time period in the future.

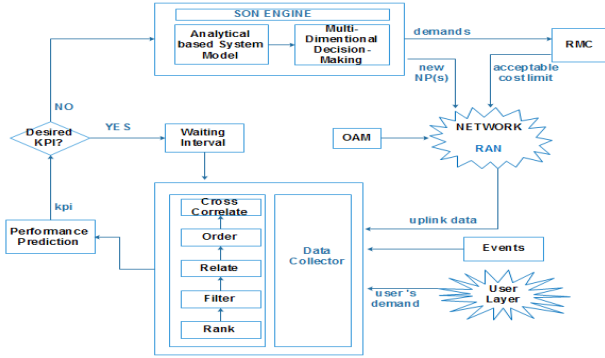


Figure 3. The proposed BD-SON architecture

In the RMC, the response to the self-optimization engine request is provided such that resource allocation accrues the lowest possible cost. The working algorithm attempts to optimally allocate resources based on requests from the SON engine using a pre-defined function. The control messages related to resource allocation and commands for readjustment of the threshold levels in neighbour relations are sent to the MME unit of the network core. The resource allocation commands are executed in accordance with the handover operators in the network.

5. Optimal Resource Allocation in the Distributed Self-Optimization Model

One of the factors influencing the level of service quality is the ideal allocation of the resources based on the network's load distribution approach. In order to minimize the load variance, the proposed self-optimization model utilizes an intelligent resource allocation pattern. Moreover, while allocating resources to users, cost limitations and the upper limitation of the total power of the network must also be considered.

In this part of the assessment for the proposed self-optimization model, the level of efficiency for femto-cell networks based on the proposed method and other resource allocation patterns will be evaluated. Accordingly, the quality of communication channels regarding the SINR indicator, the coverage area, the throughput, and the uplink/downlink quality will be discussed.

In order to use this power allocation framework in the self-optimization model, the resource distribution approach is presented as a three-part online algorithm that converges to optimal values after a number of iterations. The various steps of the algorithm are as follows: The constant coefficients related to the optimization relations based on the current conditions of the user and the received service are determined through the analysis of uplink data. Using this approach in the resource allocation process in the self-optimization model, the quality requirements of the users

will be met by considering the costs and with a low computational load.

Ideal resource allocation based on the network load distribution is a main QoS affecting factor [23]. In order to minimize load variance, the proposed self-optimizing model utilizes an intelligent resource allocation pattern. Cost constraints and the upper bound of network power limitation must be considered when distributing resources among entities. In order to allocate power to users over time intervals $t = [1, 2, \dots, T]$, information related to flexibility $\omega_i(t)$ and cost component $c(t)$ must be determined by the big data processing engine through analysis of the received data. $P_i(t)$ denotes the power consumption by user i at moment t and P denotes the restriction on network total power. The problem of real time resource assignment can be formulated as follows:

$$\max: \sum_{i=1}^T \sum_{i \in N} \left[U(P_i(t), \omega_i(t)) - f\left(\sum_{i \in N} P_i(t)\right) P_i(t) \right] - \frac{\alpha T}{2} \text{Var}\left(\sum_{i \in N} \bar{P}_i\right) \quad (1)$$

where:

$$P_i(t) \geq P_{i,\min}(t), \forall i \in N, t \in \{1, 2, \dots, T\} \quad (2)$$

$$C\left(\sum_{i \in N} P_i(t)\right) \leq c(t), \forall t \in \{1, 2, \dots, T\} \quad (3)$$

where $\text{Var}(\cdot)$ denotes the variance of the network total power, $f(\cdot)$ denotes the cost function and $U(\cdot)$ denotes the utilization function. To provide consistency between the network load variance and satisfaction of user QoS constraints, parameter α is defined as a positive value. $P_{i,\min}(t)$ is the user's i^{th} minimum power request at t . In this framework, N denotes the node set of the network.

Formulation (1) expresses the goal function of the model. Actually, this formulation is included a utilization function denoted by $U(P_i(t), \omega_i(t))$ a cost function which is shown as $f(\sum_{i \in N} P_i(t)) P_i(t)$ in addition to load balancing part which has been formulated based on variance function $(\frac{\alpha T}{2} \text{Var}(\sum_{i \in N} \bar{P}_i))$.

The proposed approach is expressed in the form of a three-step optimization model which has a unique solution. This real-time algorithm converges to optimal values after a number of iterations as follows:

Step 1: Begin $\forall i \in N$, initialize $\hat{P}_i(0) \in \mathbb{P}$.

Step 2: During consecutive iterations: for time slot t , the below convex optimization problem has been solved by SON engine (mentioned Probe-On):

$$\max: \sum_{i \in N} U(p_i(t), \omega_i(t)) - f\left(\sum_{i \in N} p_i(t)\right) \sum_{i \in N} p_i(t) - \frac{\alpha}{2} \sum_{i \in N} (p_i(t) - \hat{p}_i(t-1))^2 \quad (4)$$

where:

$$p_i(t) \geq p_{i,\min}(t), \forall i \in N \quad (5)$$

$$c \left(\sum_{i \in \mathbb{N}} p_i(t) \right) \leq c(t), \forall t \in \{1, 2, \dots, T\} \quad (6)$$

Which $\hat{P}_i(0) \in \mathbb{P}$ shows the set of primary power vector relevant to all network's entities. Note that the sum of the dedicated powers should not be more than the limitation of the upper bound of the power. The solution of Probe-On is shown by $\vec{p}^*(t)$, where in these formulation $p_i^*(t)$ indicates the optimal assigned power to user i .

Step 3: In each time slot t for all $\forall i \in \mathbb{N}$, Update $\hat{p}_i(t)$ using following equation:

$$\hat{p}_i(t) = \hat{p}_i(t-1) + \frac{\alpha}{t+\alpha} \cdot (p_i^*(t) - \hat{p}_i(t-1)) \quad (7)$$

The mentioned coefficients i.e., ω and α are determined based on current user status, service type and network condition through uplink data analysis. Using this method for resource allocation, the self-optimization model satisfies QoS constraints with the minimum cost and low computational load.

6. Distributed Load-Balanced Resource Allocation

Determining the optimal values in the proposed model is not purely based on local node variables. This method solves optimization Lagrange equations iteratively; each node calculates the updated Lagrange coefficients and uses them for the next iteration of the power allocation algorithm. In the system model, it is assumed that the system has N users, and the K^{th} user has a data rate equal to R_k bits per symbol. $C_k^{(c)}$ is the number of bits allocated to the c^{th} class-carrier for the K^{th} user. In the transmission channels, different class-carriers will experience different channel gains, denoted by $\alpha_k^{(c)}$, the magnitude of the c^{th} class-carrier seen by the K^{th} user. It is assumed that N_0 is white noise and is equal for all class-carriers and the same for all users. The goal of this approach is the best assignment of $C_k^{(c)}$ which besides of satisfying total power constraint, the capacity of links has been maximized. Note that this problem can be formulated either to minimize the transmission powers besides satisfying the given QoS requirements or to improve the user QoS parameters for a fixed overall transmission power. The formulation for the second approach can be achieved by changing the class-carrier power levels proportionally using the same set of $C_k^{(c)}$. The enhancement in quality can be demonstrated by the increase in total user transmission rate (R) as follows. Ideal resource allocation based on the network load distribution

is a main QoS affecting factor. In order to minimize load variance, the proposed self-optimizing model utilizes an intelligent resource allocation pattern. Cost constraints and the upper bound of network power limitation must be considered when distributing resources among entities. In order to allocate power to users over time intervals $t = [1, 2, \dots, T]$, information related to flexibility $\omega_i(t)$ and cost component $c(t)$ must be determined by the big data processing engine through analysis of the received data. $P_i(t)$ denotes the power consumption by user i at moment t and P denotes the restriction on network total power. The problem of real time resource assignment can be formulated as follows:

$$\text{maximize } \sum_{k=1}^K \alpha_k R_k \quad \text{subject to: } R_k = \sum_{c=1}^M C_k^{(c)} \quad (8)$$

Replacing $C_k^{(c)}$ with its equivalent in Equation (8) results the formulation of the goal function in Equation (9). The goal of this formula is to maximize the weighted aggregation rate of the network users considering total power constraints. In addition, U and f indicate Utility and Cost functions respectively which are calculated based on network condition and flexibility factor. Also, to achieve optimal solution, variance of allocated resources should be at the minimum possible value.

$$\begin{aligned} \text{maximize } & \sum_{k=1}^K \sum_{c=1}^M \left[\alpha_k \rho_k^{(c)} \log \left(1 + \frac{p_k^{(c)} |h_k^{(c)}|^2}{\Gamma \cdot n_k^{(c)}} \right) + \Phi U(P_i(t), \omega_i(t)) \right. \\ & \left. - \Psi f \left(\sum_{i \in \mathbb{N}} P_i(t) \right) P_i(t) \right] - \phi \frac{\alpha T}{2} \text{Var} \left(\sum_{k \in K} \hat{P}_k \right) \quad (9) \\ \text{bje } & \text{ct to: } \sum_{k=1}^K \sum_{c=1}^M \alpha_k p_k^{(c)} \\ & P_{\text{tot}} \text{ \& } \omega_i(t), \rho_k^{(c)} \geq 0 \end{aligned}$$

In this model the mentioned coefficients i.e., ω and α are determined based on current user status, service type and network condition through uplink data analysis. Using this method for resource allocation, the self-optimization model satisfies QoS constraints with the minimum cost and low computational load where each user is allowed to transmit at a rate associated with α_k which is related user priority and $\rho_k^{(c)}$ a coefficient with values within the interval 0 and 1 associated with the c^{th} class-carrier for $c = 1, 2, \dots, M$. The Lagrange equation in Equation (3) is used to take the problem constraints into account.

The channel coefficient for the k^{th} transmitter node on

the c^{th} class is denoted by $h_k^{(c)}$ and includes the path loss, Rayleigh fading factor, and constant coefficients for the transmitter and receiver antenna. Moreover, Γ indicates the SINR-gap which is function of coding and modulation and the bit error ratio (BER). For example, for the modulation of non-coded QAM, the SINR-gap Γ will be shown as $\Gamma = -\ln(5.BER)/1.5$ and $n_k^{(c)}$ denotes the noise of class c for the node k .

$$L(P, \lambda) = \sum_{k=1}^K \sum_{c=1}^M \left[\alpha_k \rho_k^{(c)} \log \left(1 + \frac{p_k^{(c)} |h_k^{(c)}|^2}{\Gamma n_k^{(c)}} \right) + \varphi U(P_i(t), \omega_i(t)) \right. \\ \left. - \psi f \left(\sum_{i \in N} P_i(t) \right) P_i(t) \right] - \phi \frac{\alpha T}{2} \text{Var} \left(\sum_{k \in K} \bar{P}_k \right) \\ - \lambda \left(\sum_{k=1}^K \sum_{c=1}^M \rho_k^{(c)} p_k^{(c)} - P_{tot} \right) \quad (10)$$

Assuming that the derivation of Equation (10) is equal to zero, the optimal power allocated to each class-carrier can be obtained by Equation (11). For each iteration of the power assignment algorithm, a current power of the class-carrier that does not satisfy the reliability will be modified and the Lagrange coefficient will be updated accordingly. After R iterations, the algorithm provides an optimal transmission power for each class-carrier as demonstrated by $P_k^{(c)*}$.

$$p_k^{(c)*} = \rho_k^{(c)} \left[\frac{\theta_k}{\lambda} - \frac{\Gamma n_k^{(c)}}{|h_k^{(c)}|^2} \right]^+ - v - \frac{\alpha T}{2} (\nabla P) \quad (11)$$

Where λ is a Lagrange coefficient associated with transmission power constraints. Equation (4) can be solved by defining auxiliary variable g as:

$$g_k^{(c)} = \frac{|h_k^{(c)}|^2}{n_k^{(c)}}$$

$$P_k^{(c)*} = \rho_k^{(c)} \left[\frac{\theta_k}{\lambda} - \frac{\Gamma}{g_k^{(c)}} \right]^+ - v - \frac{\alpha T}{2} (\nabla P) \quad (12)$$

The optimal power allocation formulation in Equation (12) is very similar to the common waterfilling problem. In this formulation, power is assigned to nodes based on the difference in their weighting coefficients. Each class-carrier of user k is assigned to a flow level equal to $\frac{\alpha_k}{\lambda}$. After waterfilling, the different users have flow levels that are proportional to their weighting coefficients. The users with the higher weighting factors have higher flow levels and can allocate more power to their class-carriers. The Equation (13) can be used to convert a single level

waterfilling to a multilevel.

$$\frac{P_k^{(c)*}}{\alpha_k} = \rho_k^{(c)} \left[\frac{1}{\lambda} - \frac{\Gamma}{\theta_k g_k^{(c)}} \right]^+ - a_k v - (\nabla P) \frac{\alpha_k T}{2} \quad (13)$$

Starting with small values for initial Lagrange coefficients, the coefficients are modified in each iteration so that the data rate constraints of different users are satisfied in each node. Each node is treated in turn using the new allocated power until the SINR in the output of the links with temporary failure reach at a minimum level of sensitivity. When the link is recovered, the possibility of obtaining a solution sub-graph in the BD-SON algorithm will increase. In this way, the data rate constraint and dedicated power constraint for all nodes are satisfied and the algorithm will converge.

$$g(\lambda) = \max_{P_k^{(c)}} L(P, \lambda) \approx \text{minimize } g(\lambda); \lambda \geq 0 \quad (14)$$

The solution to Equation (14) leads to optimal values for maximizing $L(P, \lambda)$. The gradient method can be used to solve the problem to obtain a distributed solution. According to the steepest descent lemma, we have Equation (15):

$$\lambda(t+1) = [\lambda(t) - \gamma \nabla g(\lambda(t))]^+ \quad (15)$$

where $g > 0$ is the step size and $[Z]^+ = \max\{z, 0\}$. Using Equation (8) and according to dual function derivation, we will have Equation (16).

$$\nabla g(\lambda(t)) = \sum_{k=1}^K \sum_{c=1}^M \rho_k^{(c)} p_k^{(c)*} - P_{tot} (\nabla P) \frac{\alpha T}{2} J \quad (16)$$

Using the Lagrange coefficient (λ), the class-carrier powers in the next iteration can be calculated as in Equation (17):

$$P_k^{(c)*} = \rho_k^{(c)} \left[\frac{\theta_k}{\lambda(t)} - \frac{\Gamma}{g_k^{(c)}} \right]^+ - v - (\nabla P) \frac{\alpha T}{2} = P_k^{(c)}(\lambda(t)) \quad (17)$$

The Lagrange coefficient λ can be updated for the next step in Equation (18) during successive iterations [24].

$$\lambda(t+1) = \left[\lambda(t) - \gamma \left(\sum_{k=1}^K \sum_{c=1}^M \rho_k^{(c)} p_k^{(c)}(\lambda(t)) - P_{tot} \frac{\alpha T}{2} \text{Var} \left(\sum_{k \in K} \bar{P}_k \right) \right) \right]^+ \quad (18)$$

Based on the algorithm performance, the SINR can be calculated as the reliability of the transmission in the output of each link. By calculating the value of this parameter, the status of the link becomes clear and the temporary failures can be determined with greater confidence. The new SINR can be used to calculate their new capacities as $C_{ij} = C(SINR_{ij})$.

To achieve transmission reliability, the SINR value at the end point of each link is compared with the minimum SINR required for reliable transmission. In fact, the acceptable SINR threshold is the sensitivity level of the node. If the calculated SINR value is lower than the sensitivity, temporary failure is considered to have occurred for that link and the link will be removed from the set of potential sub-graphs. It is evident that, frequent link failure decreases the possibility of finding a solution sub-graph which satisfies the QoS requirements and increases the cost. To prevent link failure, the power control algorithm is used to gradually increase the transmission power of the node located at the beginning point of the failure links. It should be noted that during all the steps of power control, the total power allocated to all nodes must not exceed a pre-determined value.

6.1 Fixed-Power Efficient Resource Management

Non-linear problem P1 is shown as a mixed integer programming (MIP) framework. The problem now needs to be formulated so that the transmission power is assumed to be fixed; hence, the primal problem P1 will be simplified to problem P2.

$$P2: \max_{x, \varepsilon, G} u(x, \varepsilon, G) \quad (19)$$

s.t. C1, C2, C3, C4, C5, C6

The Simplified primary problem P2 has discrete modality and is a combination of several subproblems. To find an efficient solution for P2, an iterative decomposition approach was applied. Using indicators G and ε , P2 can be modified as:

$$P2.1: \max_x U(x) \quad (20)$$

s.t. C1, C2, C4, C5

6.2 Lagrangian Dual Decomposition

Using the goal function, the Lagrangian equation has been formulated to take the problem constraints (P2.1) into account as:

$$L(x, \lambda, \theta) = U(x) - \sum_{j=1}^N \lambda_j \left(\bar{\tau}_{min} - \sum_{m=1}^{M+1} x_{jm} \tau_{jm} \right) - \sum_{m=1}^{M+1} \theta_m \left(\sum_{j=1}^N x_{jm} P_{jm} - P_m \right) \quad (21)$$

in which λ_j and θ_m are the Lagrange coefficients with positive values. The dual function can be defined as:

$$g(\lambda, \theta) = \begin{cases} \max_x L(x, \lambda, \theta) \\ \text{s.t. } C2, C5 \end{cases} \quad (22)$$

Using the primal-dual principles, the dual problem can be

Algorithm 1: Efficient UA Algorithm

Step 1: From Subscriber's side

1: **Begin**

2: **if** t = 0

3: **Input:** $\lambda_j(t)$, $\forall j$. Each user equipment evaluates imposed inter-cell interference by checking reference signal of neighbor base stations and the user equipment choose the base station with highest CINR level.

4: **else**

5: j^{th} user equipment finds the levels of μ_{jm} and τ_{jm} through base stations.

6: Selecting the dominant base station (m) based on $m^* = \operatorname{argmax}_m(\mu_{jm})$

7: Update $\lambda_j(t)$ based on (16).

8: **end if**

9: $t \leftarrow t + 1$.

10: The request of the user equipment will be feedback towards selected base station and degree of $\lambda_j(t)$ will be broadcast accordingly.

Step 2: From Base Station Perspective

1: **Begin**

2: **if** t = 0

3: Input $\theta_m(t)$, $\forall m$.

4: **else**

5: Consider the matrix x as the uptodate user association indicator

6: Updating $\theta_m(t)$ exactly based on (17), respectively.

7: All base stations compute μ_{jm} and τ_{jm} according to Non-orthogonal multiple access.

8: **end if**

9: $t \leftarrow t + 1$.

10: All base stations multicast the degree of μ_{jm} and τ_{jm} used to simply produce the solution. Using P2.1, the dual problem can be defined as shown in Eq. (13) as:

$$\min_{\lambda, \theta} g(\lambda, \theta) \quad (23)$$

Using the dual Lagrangian coefficients λ_j and θ_m , the optimum value of parameter x for the Lagrange formula can be calculated as:

where, in Eq. (14), $m^* = \operatorname{argmax}_m(\mu_{jm})$ with:

$$x_{jm}^* = \begin{cases} 1, & \text{if } m = m^* \\ 0, & \text{otherwise} \end{cases}, \quad (24)$$

The optimal solution in Equation (24) means that subscribers choose base stations (which supply the maximum achievable throughput) according to the grid power consumption. Because the goal of the dual function is not differentiable, the subgradient method was applied to achieve the solution (λ^*, θ^*) with maximum optimality of the dual problem. This can be expressed as:

$$\lambda_j(t+1) = [\lambda_j(t) - \delta(t) \left(\sum_{m=1}^{M+1} x_{jm} \tau_{jm} - \bar{\tau}_{min} \right)]^+, \quad (25)$$

$$\theta_m(t+1) = [\theta_m(t) - \delta(t) \left(P_m - \sum_{j=1}^N x_{jm} P_{jm} \right)]^+, \quad (26)$$

In Equations (25) and (26), $[a]^+ = \max\{a, 0\}$, t is the indicator of iteration and $\delta(t)$ denotes the step size. Of the various step size patterns available, such as fixed and decreasing step sizes, in this study, decreasing step size was applied as introduced by Zhang [25]. After achieving the optimal values (λ^*, θ^*) using Eqs. (25) and (26), the optimal value of index x will be the response to main problem P2:1. Using the iterative decomposition method, user association can be designed in both centralized and decentralized modes, which this a specific capability of the proposed approach. The centralized user association system needs an intensive controller which has access to global channel state information and is aware that the subscriber is served by a specific base station. This article suggests a decentralized user association approach in which there is no requirement for centralized control data using algorithm 1. Because the convergence requirements (described by in [25]) are satisfied through the proposed algorithm, convergence is definite.

For each iteration, the proposed algorithm has complexity order $O((M+1)N)$. Convergence of the resource management algorithm appears to be fast because convergence occurs in less than 40 repetitions. This is significantly less than the Brute Force approach with complexity order $O((M+1)^N)$. The broadcast operations applied in the proposed model have little effect on the order of time complexity.

6.3 Genetic-based UA Algorithm

Next, a genetic algorithm (GA) based on user association is proposed to solve main problem P2.1. The aim is to compare the results of proposed algorithm 1 with a genetic-based algorithm. As stated by Abdelaziz [30], a genetic-based algorithm has good functionality if the number of potential solutions is adequate. In particular, each chromosome represents a feasible solution which meets the requirements of problem P2.1 and is formulated as:

$$D_i = \{[m_{1i}], [m_{2i}], \dots, [m_{Ni}]\}, i \in \{1, \dots, K\}, \quad (27)$$

In Equation (27), m_{ij} denotes the gene for the base station to which user equipment j is connected, with a variable amount between interval $[1 \ M+1]$. K denotes the density indicator of the population. In any production process, all chromosomes will be assessed based on compatibility to allows selection of the most compatible chromosomes and generates the most compatible children. In the goal of primal problem P2.1, the compatibility of chromosome D_i is computed as:

In this evaluation, all chromosomes having rank r are ranked according to their fitness and compatibility. For a chromosome, the possibility of producing child is equal to $\rho_s(r) = \frac{q(1-q)^{r-1}}{1-(1-q)^K}$ with predefined value q that has been defined by in [38]. During all production stages, a monotonous crossover action with possibility ρ_c is applied for generation of a child by exchanging or merging genes using the generator chromosomes. A monotonous mutation action with probability ρ_m has been applied. The generation method is repeated until the highest amount of production is achieved as shown in algorithm 2.

Considering the highest amount of production and a constant population density equal to K , the computational complexity order of the proposed framework is equal to $O(\Omega K \log(K))$ [39].

The performance of the user association based on genetic-based algorithm depends upon the number of generations and the size of the population [38]. The simulation results confirm that the effectiveness of algorithm 1 is greater than genetic-based algorithm 2. When the density of the population in the genetic algorithm is not sufficient, it has lower computational complexity.

Algorithm 2: Genetic-based UA

1: if $t = 0$
2: Input set of possible chromosomes $\{D_i\}$ by population density equal to K and the topmost number of production t_{max} .
3: else
4: Ordering $\{D_i\}$ according to the degree of compatibility roaming in (19).
5: According to the selection possibility $\rho_s(r)$, chromosomes have been selected to generate offspring by identical jumping operations.
6: If in case of exceeding the upper bound of generation
7: Consider $x_{jm}^* = \{D_i^*\}$, where $\{D_i^*\}$ indicates the possible chromosome with maximum degree of compatibility
8: break
9: else
10: $t \leftarrow t + 1$.
11: end if
12: end if

The aforesaid approach obtains an optimal user association framework for P2.1. By achieving the optimal value of user association $X = [x_{jm}^*]$, parameters (G, ϵ) are achievable according to linear-based programming (LP) method in Eq. (28):

$$P2.2: \min_{\epsilon, G} \sum_{m=1}^{M+1} G_m \quad (28)$$

s.t. C3.C6.

P2:2 is effectively solvable by applying software tools, such as CVX tool.

If power sharing is not permitted, as for $\varepsilon_{mm'} = 0, \forall m$, the optimal amount of grid requested power (G) is for P2.2 based on user association solution $X = [x_{jm}^*]$. This can be calculated using Eq. (29) as:

$$G_m^* = [P_m - E_m]^+, \quad (29)$$

where $P_m = \sum_{j=1}^N x_{jm}^* P_{jm}$.

Using the solutions obtained for sub-problems P2.1 and P2.2, algorithm 3 is introduced as an optimal framework for solving P2 iteratively.

7. Result

7.1 Mistakes Amount of Gathered & Analyzed Data

The performance of our proposed approach was evaluated under different scenarios having specific assumptions to simplify. For this purpose, BD-SON algorithm was compared with current self-optimization solutions and SOTA schemes with non-self-organization framework. SOTA refers to previous schemes to find efficient and optimal solution by various approaches. Some of the main SOTA approaches mentioned in the reference part. Also, we have compared the proposed approach with most compatible SOTA to the described model.

In these scenarios, channel Drop Rate (DR), Downlink Quality and Throughput were applied as target indicators.

It should be mentioned that we applied some various software planes to assess the proposed approach. For example, pre-process part of the model is done by MATLAB and we achieved KPI results by some network planning tools which they are able to monitor networks as real time. Also, some parts of the network modeling like as network configuration definition is done bvia network simulator software.

The volume of data required by the BD-SON is significantly higher than for the SOTA. Moreover, the volume of data stored has a significant relationship with the density of eNBs and UEs. According to Figure 4, this value for SOTA is relatively constant based on the problem assumption in which the volume of the data gathered by SOTA is somewhat related to the density of the UEs, not the density of the eNBs. It should be noted that the processing speed of BD-SON is directly related to the volume of the data stored in the register and the computational complexity of data frame decoding.

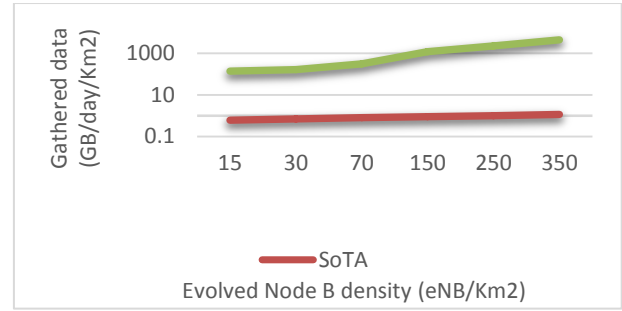


Figure 4. Amount of gathered and analysed data for decision-making in BD-SON with comparison to SOTA

7.2 Channel Quality Estimation:

Our introduced approach not only reduce the interference of its specified cell, but also increase the network functionality by alleviating interference to adjacent cell areas. Figure 5 demonstrates the coverage probability considering SINR values based on BD-SON functionality in comparison with Q-Learning SON scheme [24] and the SOTA schemes with non-self-organization feature.

We have evaluated the performance of the network in a cluster having 15 sites in the presence and the absence of the SON engine. As shown in Figure 5, the level of DCR and the signalling drop rate (SD_Drop_Rate) have significantly degradation after self-optimization model activation.

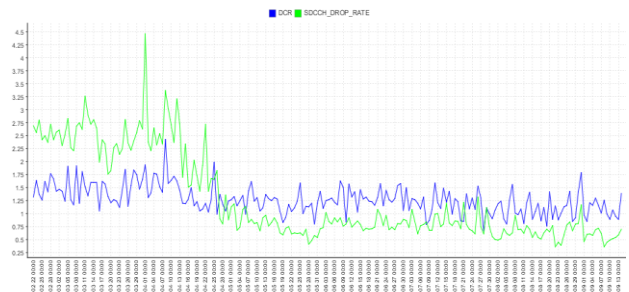


Figure 5. Decreasing the Drop Rate, by enabling the self-optimization model

The vertical axis of the plot indicates the percent of Drop Call Rate and the horizontal axis denotes the Decreasing the Drop Rate, by enabling the self-optimization model

Downlink quality will also increase when the SON model is enabled. As shown in Figure 6, when the self-optimization scheme was applied in the BSS layer, the user quality of service is stable without any considerable fluctuation.

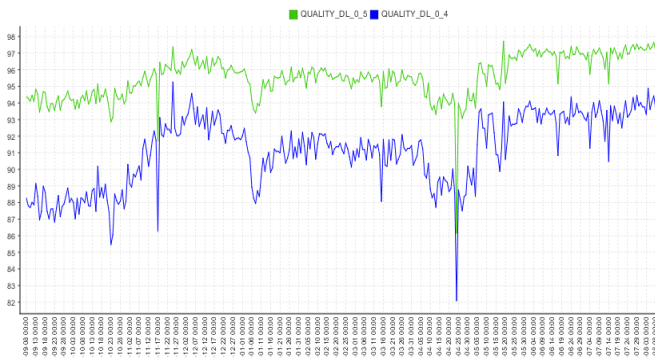


Figure 6. Stable downlink quality, by enabling the self-optimization model

7.3 Timing Complexity:

The vertical axis of the plot indicates the percent of Quality DL/UL and the horizontal axis shows the Stable downlink quality, by enabling the self-optimization model

Then, by evaluating the functional timing of the proposed model under three distinct modes in a general manner, solely based on learning, and self-optimization based on learning and recommender system, we tried to evaluate the effects of using state space reduction technique on reducing the time required for the decision-making process.

As the outputs in figure 7 show, in proportion to the lower number of network parameters, the decision-making time is solely dependent on learning algorithms, and using the recommender system reduces the required time. However, by increasing the number of parameters, statistical analyses effectively reduce the number of parameters influencing the target indicators and the decision-making process becomes simpler and quicker. The obtained outputs indicate that in the small state space, using feature extraction and parameter selection modules will not have a significant impact on the performance of the self-optimization engine, and it will increase the volume of computations and, in turn, the response time. On the other hand, by increasing the number of network parameters, the presence of these modules will effectively reduce the time required for the decision-making process.

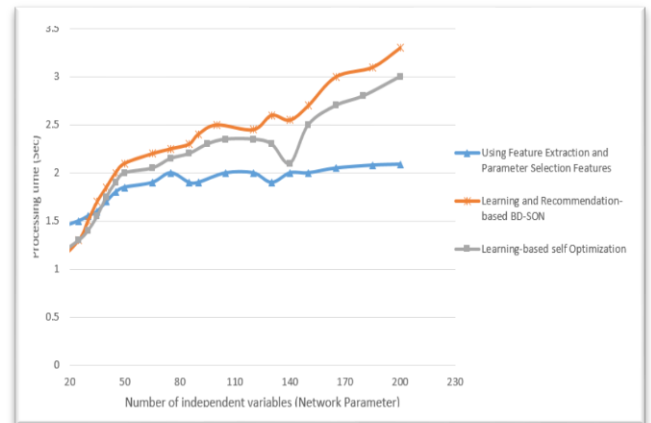


Fig.7 The effect of engine’s component on timing complexity

Moreover, using the recommender system, along with the learning algorithm based on support vector, will add an approximately constant time to the processing duration. This constant value is related to the passing of the components of the set of commands through the rule-based filter. If we use inference engine to increase the capability of the recommender system, this time difference will obviously increase.

7.4 Accuracy Evaluation:

In this section of assessing the self-optimization model, we try to evaluate the accuracy and recall of the learning section, which is used for predicting the target efficacy indicators.

As mentioned earlier, the learning tool used in this study is the support vector machine. However, the reason behind selecting this tool as the main unit for estimating the status of the efficacy measures is the higher level of accuracy and recall than other learning methods. As can be seen from the figure 8, the value of the ROC indicator is somewhat higher for the learning method based on support vector compared to other learning methods. Therefore, using this learning method will allow for reaching decisions with a higher level of accuracy. The ROC indicator used is related to the ratio of correct true positive decisions to incorrect true positive decisions, which is a valuable criterion for determining the accuracy level of the network’s decision-making. However, if we want to use a more powerful criterion, we can use the F-measure.

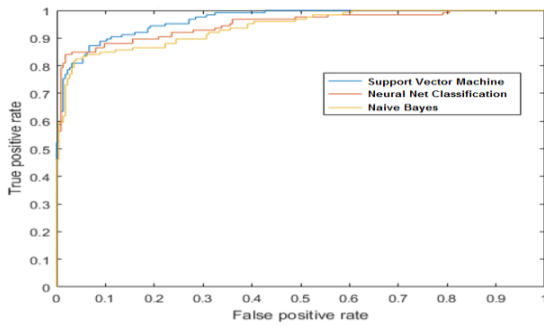


Fig.8. SVM accuracy in comparison with other ML methods

As can be seen from the figure below, support vector-based learning method creates a bigger area under the curve than the other two learning methods do, thus indicating the higher accuracy level of decision-making in this method for this type of data. Then, we evaluate the performance of these three machine learning methods in the real-life mobile network data platform. In this scenario, these three machine learning methods are analysed using three important criteria—precision, recall, and F-measure. The obtained results confirm the findings of previous schemes, presented in the following figure.

As can be seen from the table 1, besides precision and recall factors, the highly accurate F-measure is used also for assessing the performance accuracy of the three learning methods, and the results indicate the superiority of the support vector learning method over the other two methods based on the detection accuracy level.

Table 1. SVM accuracy level in comparison other ML methods

It should be noted that Precision, Recall and F-Measure factors are accessible via following formulas:

$$\text{Precision} = \frac{t_p}{t_p + f_p}$$

$$\text{Recall} = \frac{t_p}{t_p + f_n}$$

$$F_{\text{measure}} = 2 \cdot \frac{\text{Precision} \cdot \text{Recall}}{\text{Precision} + \text{Recall}}$$

Which these factor's components are defined as below:

Recall ~ Sensitivity

Precision ~ Positive Predictive Value (PPV)

t_p : True Positive Rate

f_p : False Positive Rate

f_n : False Negative Rate

t_n : True Negative Rate (accuracy)

Based on the assessments, the support vector learning method is used for predicting the target efficacy indicator in the monitoring and learning modules.

In this scenario, the feature extraction and parameter selection are evaluated as the basic modules in the process of data analysis. In order to evaluate the results of the proposed scheme regarding the network's intelligence in selecting parameters influencing the target indicator, we want to analyse the output from implementing the proposed method in a cluster involving five basic stations and 15 cells under KPI mode and drive test mode. In this scenario, the throughput index, as the target efficacy indicator, is below expectations. Therefore, it should be determined what kind of solution based on the proposed self-optimization model can be utilized to improve this indicator. To begin with, we consider the feature extraction component. In this section, the system identified the parameters whose values were directly related to the throughput indicator. In this section, about 50 parameters with satisfactory significance level are selected. Out of the selected indicators, transmission power, transmission mode, neighbourhood threshold, and various timing factors are related to the 'Idle' and 'Dedicated' modes.

KPI control:

In the next stage, by carrying out a linear multiple regression model on the current state space, the level of relations and the effects of the extracted parameters on the values of the throughput indicator were identified. The relations between some of the parameters and the target

	Precision (%)	Recall (%)	F-measure (%)
SVM	91.04	87.16	89.05
Naive Bayes	89.46	87.79	88.61
Neural Net Classification	79.64	81.27	80.44

indicator were logarithmic, and some were exponential. After identifying the impact coefficients, about 10 main parameters were selected from among all the parameters

based on the obtained impact factor. It is interesting that, several parameters, selected in the feature extraction phase with a high correlation coefficient, obtained a low impact factor during the assessment of the effects of parameters on the throughput measure and were thus eliminated. We can particularly mention the transmission mode indicator and the physical characteristic of antenna E-tilt, which generally have a direct impact on the level of throughput. The reason for this can be related to the unstable state of the network, as well as the effects of the network parameters on the impact of a certain network parameter on the efficacy indicator. In the statistical tests, only the correlation of the parameters and the efficacy indicator is

measured. In the regression analysis, the effects of each parameter on the general state and the presence of other network parameters on the target indicator will be evaluated.

In the support vector-based learning unit, the selected parameters are used as inputs. In this phase, the predicted throughput level is considered, which was lower than the threshold value. Therefore, the decision-making operation is continued by determining a set of specific commands.

While the number of handover requests has significantly come down, the handover success rate (HOSR) has only reduced as much as a few hundredth of a per cent. As can be seen from the figure 9, this reduction will not have a negative impact on the network's efficiency. In fact, a 0.5% reduction in the handover success rate is the negative impact of the decision made by the self-optimization engine for increasing the throughput. However, this degradation is not high enough to get the efficiency indicator of handover success rate out of the acceptable range.

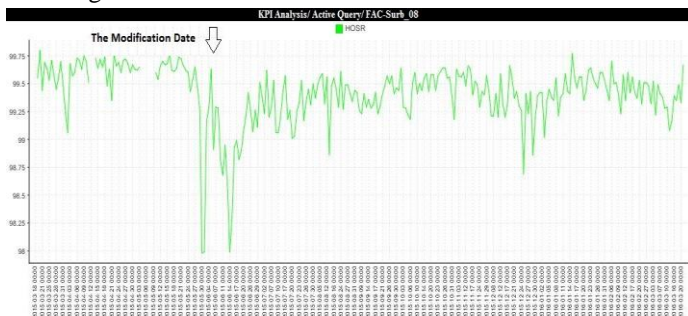


Figure 9. HO success rate, by enabling the self-optimization model

Figure 9 which is relevant to Stable downlink quality, by enabling the self-optimization model, the vertical axis of the plot indicates the percent of Handover Success rate and the horizontal axis shows the timing of the algorithm execution.

On the other hand, the main impact of tightening the handover conditions is a reduction in the traffic load of the network's signalling. The figure 10 shows that, after applying this change in the network, the traffic load of network's signalling is degraded 30%. This can be very useful in reaching an optimal network. Under these conditions, unnecessary network signalling resources can be allocated to the data transmission traffic channels.

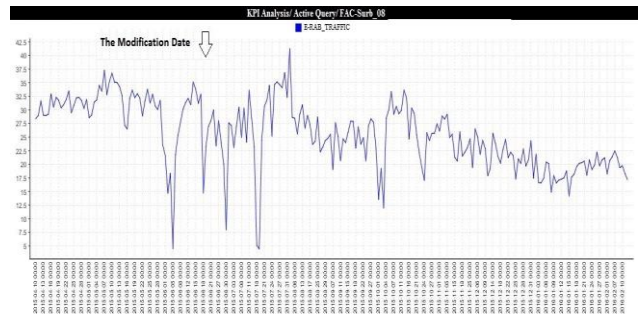


Figure 10. Decreasing of signaling rate, by enabling the self-optimization model

Figure 10 which is relevant to Decreasing of signaling rate, by enabling the self-optimization model, the vertical axis of the plot indicates the amount of the traffic and the horizontal axis shows the timing of the algorithm execution.

One of the issues that should be considered is that, by reducing the control signals, the conditions of the network regarding service retainability and service quality must not be changed. One of the effective measures in providing services with SLA is the quality level of the communication channels from the viewpoints of uplink and downlink. In this scenario, by changing the ranges of the predefined network parameters, we will look at the levels of these measures with respect to the quantitative aspects as well as stability.

As can be seen from the figure 11, there is no negative change in the quality of uplink and downlink links. However, this is also related to the reduction in the number of clients. Moreover, the stability in the quality level of uplink radio frequency channels is one of the results of applying the decisions of the proposed self-optimization engine, which has a positive impact on the synchronous communication between UE and the network core through Backhaul.

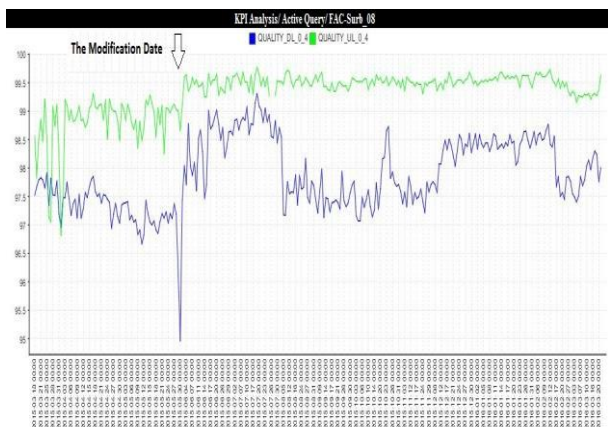


Figure 11. Quality stability after enabling the self-optimization model

Figure 11 which is relevant to horizontal axis shows the

Quality stability after enabling the self-optimization model, the vertical axis of the plot indicates the Quality and the horizontal axis shows the timing of the algorithm execution.

However, by assessing all the important efficiency indicators influencing the network, we tried to quantitatively analyse the reaction of the network status to the decisions of the self-optimization engine. As has been seen so far, the decisions for increasing the level of the network's throughput rate do not have significant negative impacts on the other efficiency indicators of the network, and the positive effects of introducing the recommender module in the structure of the self-optimization engine are obvious. In the following, the effects of the output of the self-optimization model on the target indicator of throughput rate are discussed and evaluated.

As can be seen from the figure 12, by allocating radio signalling resources to the traffic channels of data transmission, the data transmission rate, particularly in the uplink direction, is significantly increased. Of course, the reduction in the number of clients is also important in this regard. However, this increase in the rate and in the level of traffic resources is obvious. Allocating a larger number of resource blocks to traffic connections will lead to a service with a higher throughput rate and an average 20% increase is clearly seen.

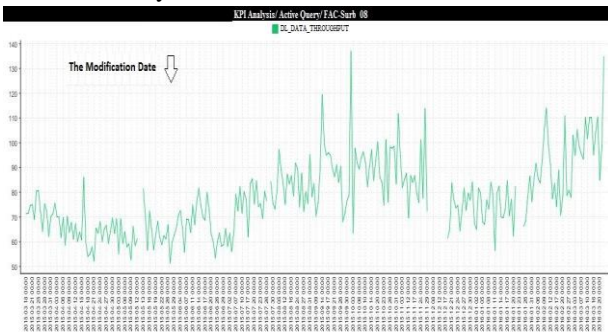


Figure 12. Throughput enhancement, by enabling the self-optimization model

Figure 12 which is relevant to Throughput enhancement, by enabling the self-optimization model, the vertical axis of the plot indicates the throughput level and the horizontal axis shows the timing of the algorithm execution.

Therefore, it can be concluded that the performance of the self-optimization engine in this scenario is highly satisfactory, and that using this model, the system will be able to change the parametric structure of the network for a target indicator in a way that the value of this indicator is increased to a satisfactory level without any significant

negative impact on the other indicators. It is worth mentioning at this point that the basis for the functioning of the proposed self-optimization model is iterative. The value of the target indicator after the change is observed and based on the new value of the indicator after the changes are applied to the network parameters in each cycle, the decision-making process is repeated so that the target indicator's value reaches a satisfactory level.

In this section, we tried to evaluate the changes in the levels of the network's efficiency indicators by implementing the self-optimization model. It can be concluded, that under normal conditions, the predictions for the performance of the model accurately depict the correct functioning of the model. However, in order to prove the positive impact on the model, it should be assessed in larger-scale networks as well. In the next section, we try to evaluate the performance of the proposed model with similar well-known schemes.

7.5 Coverage Assessment:

Our introduced approach not only reduce the interference of its specified cell, but also increase the network functionality by alleviating interference to adjacent cell areas. Figure 13 demonstrates the coverage probability considering SINR values based on BD-SON functionality in comparison with Q-Learning SON scheme [24] and the SOTA schemes with non-self-organization feature.

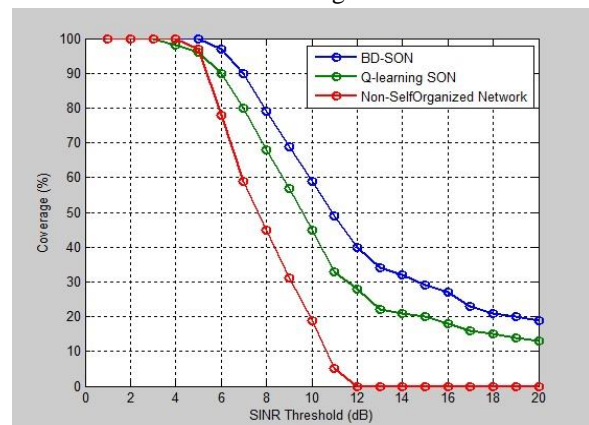


Figure 13. Coverage probability of Q-Learning SON, BD-SON and Non-Self Organized network based on needed SINR

Figure 14 shows the effects of the proposed model on throughput based on number of layers defined for the network. As expected, the self-optimization model using big data increased the throughput. Also, the network capacity has been approached to the maximum theoretical capacity. Using this model, the SINR indicator for macro users was maintained at an ideal level and the throughput of each cell was improved by increasing the number of layers.

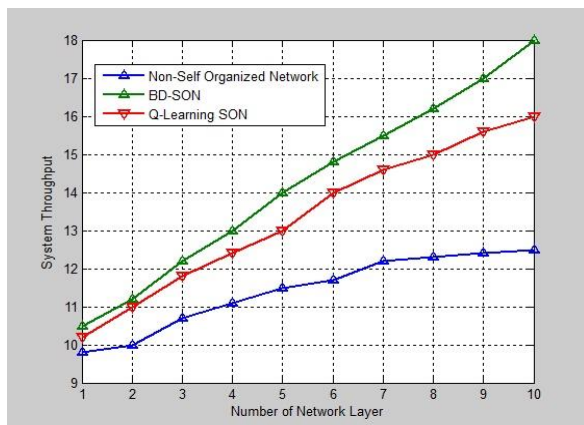


Figure 14. Increasing throughput by increasing the number of layers in BD-SON in comparison with Q-Learning

8. Conclusion and Future Works

This study introduced self-optimization technique as a powerful tool for distributed network management, consistent with next-generation wireless networks. In proposed method, coded flow multicasting has been utilized for guaranteeing the QoS constraints by finding an optimal sub-graph in a flow-based optimization framework. The load balanced gradient power allocation (L-GPA) algorithm was also applied for the QoS-aware multicast model to accommodate the effect of transmission power level based on load distribution to increase link resistance to temporal failure caused by interference and noise. In comparison to other schemes proposed method can better satisfy the QoS requirements of multicast sessions. The simulation results prove that using introduced approach considerably increases the chance of finding an optimal sub-graph. Also, Experimental results show that the proposed method can improve the throughput and quality of service in next-generation wireless networks. A further study with more focus on other requirements of next generation wireless networks are therefore recommended. Also, further research might investigate determining the self-healing intelligently based on environmental conditions. From KPI perspective, experimental results prove that despite the tremendous volume of the analyzed data – which is hundreds of times bigger than usual methods – it is possible to improve the KPIs, such as throughput, up to 30 percent by optimal resource allocation and reducing the signaling load. Also, uplink quality improvement and 15-percent increment of the coverage area under satisfied SINR conditions can be considered as outcome of the proposed scheme. Also, computational complexity analysis will be one of the appropriate ideas as the future works of the scheme.

References

- [1] A. Imran, A. Zoha and A. Abu-Dayya, "Challenges in 5G: how to empower SON with big data for enabling 5G," *IEEE Network*, Vol. 28, No. 2, 2014, pp. 27–33.
- [2] N. Baldo, L. Giupponi and J. Mangues-Bafalluy, "Big Data Empowered Self Organized Networks," *European Wireless 2014; 20th European Wireless Conference*, 2014, pp. 1-8.
- [3] R. Murugeswari, S. Radhakrishnan, and D. Devaraj, "A multi-objective evolutionary algorithm based QoS routing in wireless mesh networks," *Applied Soft Computing*, Vol. 40, No C, 2016, pp. 517–525.
- [4] Jun, Ersin Uzun, and Jose J. Garcia-luna-aceves. "NETWORK CODING FOR CONTENT-CENTRIC NETWORK." U.S. Patent 20,160,065,685, issued March 3, 2016..
- [5] H. Zhang, C. Jiang, R. Q. Hu and Y. Qian, "Self-organization in disaster-resilient heterogeneous small cell networks," *IEEE Network*, vol. 30, No. 2, 2016, pp. 116-121.
- [6] S. Berger, M. Simsek, A. Fehske, P. Zanier, I. Viering, and G. Fettweis, "Joint Downlink and Uplink Tilt-Based Self-Organization of Coverage and Capacity Under Sparse System Knowledge," *IEEE Transactions on Vehicular Technology*, Vol. 65, No. 4, 2016, pp. 2259–2273.
- [7] M. Huang and XU. Zhang, "Enhanced automatic neighbor relation function for 5G cellular systems with massive MIMO," *2017 IEEE International Conference on Communications (ICC)*, 2017, PP 1-6. 2017.
- [8] K.-L. Yap and Y.-W. Chong, "Software-Defined Networking Techniques to Improve Mobile Network Connectivity: Technical Review," *IETE Technical Review*, 2017, pp.1-13.
- [9] Gebremichail and C. Beard, "Fade Duration Based Neighbor Cell List Optimization for Handover in Femtocell Networks," *International Journal of Interdisciplinary Telecommunications and Networking*, Vol. 9, No. 2, 2017, pp. 1–15.
- [10] T. Han and N. Ansari, "Network Utility Aware Traffic Load Balancing in Backhaul-Constrained Cache-Enabled Small Cell Networks with Hybrid Power Supplies," *IEEE Transactions on Mobile Computing*, Vol. 16, No. 10, 2017, pp. 2819–2832.
- [11] Guita, José, Luis M. Correia, and Marco Serrazina. "Balancing the Load in LTE Urban Networks via Inter-Frequency Handovers." M.S. thesis, Instituto Superior Técnico ,University of Lisbon, Lisbon, Portugal, 2016.
- [12] K. Zheng, Z. Yang, K. Zhang, P. Chatzimisios, K. Yang, and W. Xiang, "Big data-driven optimization for mobile networks toward 5G," *IEEE Network*, Vol. 30, No. 1, 2016, pp. 44–51.
- [13] S, L, B. Iwan, R. Nicolas, Q. Ripault, J.R. Andrade, S. Han, H. Kim, "Self-optimization of plasmonic nanoantennas in strong femtosecond fields." *Optica*, Vol.4, No.9, 2017, pp. 1038-1043.
- [14] Z. Dawy, W. Saad, A. Ghosh, J. G. Andrews, and E. Yaacoub, "Toward Massive Machine Type Cellular Communications," *IEEE Wireless Communications*, Vol. 24, No. 1, 2017, pp. 120–128..
- [15] Gillot, David, and John Yue Jun Jiang. "Method and system for providing roaming intelligence (RI) to a host network operator for its roaming traffic." U.S. Patent 9,338,663, 2016.
- [16] S. Fong, C. Fang, N. Tian, R. Wong, B. W. Yap, "Self-Adaptive Parameters Optimization for Incremental Classification in Big Data Using Neural Network." In *Big Data Applications and Use Cases* Springer International Publishing, 2016.

- [17] Agrawal, Himanshu, and Krishna Asawa. "New Architecture for Dynamic Spectrum Allocation in Cognitive Heterogeneous Network using Self Organizing Map." arXiv preprint arXiv, 2016.
- [18] G. Foster, S. Vahid, and R. Tafazolli, "SON Evolution for 5G Mobile Networks," *Fundamentals of 5G Mobile Networks, USA*, Wiley, 2015.
- [19] H. Goudarzi and M. Pedram, "Hierarchical SLA-Driven Resource Management for Peak Power-Aware and Energy-Efficient Operation of a Cloud Datacenter," *IEEE Transactions on Cloud Computing*, Vol. 4, No. 2, 2016, pp. 222–236.
- [20] C. Segura, C. Coello, G. Valladares, C. Leon, "Using multi-objective evolutionary algorithms for single-objective constrained and unconstrained optimization." *Annals of Operations Research*, Vol.240, No.1, 2016, pp. 217-250.
- [21] Z. M. Fadlullah, D. M. Quan, N. Kato, and I. Stojmenovic, "GTES: An Optimized Game-Theoretic Demand-Side Management Scheme for Smart Grid," *IEEE Systems Journal*, Vol. 8, No. 2, 2014, pp. 588–597,.
- [22] Y. Liu, C. Yuen, S. Huang, N. Ul Hassan, X. Wang and S. Xie, "Peak-to-Average Ratio Constrained Demand-Side Management With Consumer's Preference in Residential Smart Grid," *IEEE Journal of Selected Topics in Signal Processing*, Vol. 8, No. 6, 2014, pp. 1084-1097.
- [23] A. De Waegenaere, J. L. Wielhouwer, "A breakpoint search approach for convex resource allocation problems with bounded variables." *Optimization Letters*, Vol.6, No.4, 2012, pp. 629-640.
- [24] A. Galindo-Serrano, "Self-organized Femto-cells: A Time Difference Learning Approach," Ph.D. thesis, Universitat Politècnica de Catalunya (UPC), Barcelona, Spain, 2013.
- [25] Y. Jiang, Q. Liu, F. Zheng, X. Gao and X. You, Energy-efficient joint resource allocation and power control for communications, *IEEE Transactions on Vehicular Technology* 65(8) (2016), 6119–6127

Abbas Mirzaei received the B.S. degree in Computer Engineering from Azad University, Gazvin Branch, Iran in 2006, and M.S. degree in Computer Engineering from Azad University, Tabriz Branch, Iran, in 2008, and Ph.D. degree in Computer Engineering from Malek Ashtar University of Technology, Tehran, Iran in 2018. He currently works as an assistant professor at the Department of Computer Engineering, Islamic Azad University, Ardabil Branch. His research interests include Computer security and reliability, Artificial intelligence, Computer communications (networks), Cellular network optimization, Heterogeneous networks, Data mining, and Wireless resource allocation.

Amir Rahimi received the B.S. degree in Computer Engineering from Sabalan University, Ardabil, Iran in 2015 and M.S. degree Computer Engineering from Moghadas Ardabil University, Ardabil, Iran, in 2019. His area research interests include Artificial intelligence, Cellular network optimization, and Data mining.

Assessing the Company's E-Readiness for implementing Mobile-CRM System: Case A Nationwide Distribution Company

Alireza Kamanghad

Department of Management, Islamic Azad University, Central Tehran Branch, Iran
ali.kamanghad.mng@iauctb.ac.ir

Gholamreza Hashemzadeh Khorasgani*

Department of Management, Islamic Azad University, Central (South) Tehran Branch, Iran
gh_hashemzadeh@azad.ac.ir

Mohammadali Afshar Kazemi

Department of Management, Islamic Azad University, Central Tehran Branch, Iran
dmafshar@gmail.com

Nosratollah Shadnoosh

Department of Management, Islamic Azad University, Central Tehran Branch, Iran
n.shadnoosh@iauctb.ac.ir

Received: 01/May/2019

Revised: 22/Aug/2019

Accepted: 28/Sep/2019

Abstract

In today's world, most of companies are trying to survive in a competitive environment which has been increased in recent years. This competition has raised the customer power to select desired products and services among different suppliers and providers. So the importance of customer satisfaction and loyalty has been increased dramatically for companies and businesses. This is more important for distributor companies which deal with a lot of customers in a B2B market. Mobile-CRM has emerged new opportunities on customer satisfaction and loyalty. However, implementing a Mobile-CRM system is a complicated large project that affects all aspects of an organization and needs a huge investment which increases the risk of failure. To avoid this risk, the assessing of company's E-Readiness before starting main project is necessary but the vital question is that how companies can assess their E-Readiness level for implementing a M-CRM system and improve it. Since there was not introduced before a suitable model to help companies for achieving this, in this research we have investigated different models and selected VERDICT as a suitable model for assessing the E-Readiness of a company willing to implement a Mobile-CRM system. A large distributor company is the case study of this research. The research is conducted based on a descriptive-survey method using questionnaire tools for extracting the experts' opinion and determining the company's E-Readiness level. The results show that the level of E-Readiness of the case company for implementing Mobile-CRM, is in an acceptable situation based on all four main factors including Management, Information Technology, People, and Process. Additionally, the VERDICT model is recommended to those distribution companies that are planning to implement Mobile-CRM system to help them to prevent the risk of project failure.

Keywords: M-CRM, Mobile-CRM; E-Readiness; Distribution Companies.

1. Introduction

In today's world, most of companies are trying to survive in a competitive environment which has been increased in recent years. This competitive environment has affected also the distributor companies who play an important role in supply chain networks. The diversity of goods and quality of their distribution services has increased significantly the selection power of customers for select desired products and services among different distributors. In this situation, CRM should be considered by distribution companies as one of the most important key success factors for survival in competitive market. The CRM concept has evolved in such a way to maintain a long-term relationship with the customers. The use of CRM systems is becoming increasingly important to improve customer life time value [1] and is more important in such companies that have a wide relationship with customers and deal with a large number of customers

especially in a B2B market such as wholesale distribution companies. By leveraging the internet for customer management we get the new structure of CRM known as E-CRM [2]. Then many organizations have identified the need to become more customer-facing with increased global competition. So E-CRM has become an essential for many organizational strategies [3]. In recent years, mobile technology has evolved drastically over the years and mobile phones have become the essential part of customer's life style. In the quest to retain existing customers as well as attracting new, companies are developing innovative mobile customer relationship management (M-CRM) strategies [4]. But the implementation of E-CRM projects (including M-CRM systems) which have a major and key role in the organization is highly risky [5]. The potential risk factors in implementation this kind of project can cause serious failures either in project phase or in go-live phase. To

* Corresponding Author

eliminate, prevent or control this risk, companies have to assess their E-Readiness and prepare required infrastructure [3].

E-Readiness is a relatively new concept that has been given impetus by the rapid rate of internet penetration throughout the world, and the dramatic advance in the use of IT (Information Technology) in business and industry [6]. E-Readiness is a measure of the degree to which a country, nation or economy may be ready, willing or prepared to obtain benefits which arise from information and communication technologies [7].

There are some efforts that have carried out in the field of assessing the E-Readiness of industries and organizations, but we couldn't find a special and proper model for Mobile-CRM implementation readiness assessment in an organization. This research aims to propose a suitable model for assessing the E-Readiness to those distributor companies willing to implement Mobile-CRM system. The case study of this research is one of the largest distribution companies of Iran which is among the national top 100 companies ranked by IMI100. Mobile-CRM implementation is one of the main strategies of this company which deals with about Seventy thousand B2B customers across the country. Obviously, the implementation of such a big project in such a large and complex organization is too costly and risky. So before spending, an assessment should be made to ensure that the organization is ready to implement the project.

The main research questions are "which is the suitable E-Readiness assessment model for distribution companies to implement a Mobile-CRM system?" And "what is the E-Readiness level of the case company for implementing Mobile-CRM system based on the selected model?"

2. Literature Review

2.1 Customer Relationship Management (CRM)

CRM which has introduced in recent years and got attention strongly by companies is a comprehensive approach for creating, maintaining and expanding customer relationships [8]. CRM aims at developing sustainable, long lasting affiliations between companies and customers [2].

CRM systems help organizations interact effectively with customers enabling the creation of customer profiles, analyzing customer data and understanding customers' needs. This leads to improved customer loyalty and enhanced customer experience [9]. The purpose of CRM is to identify, acquire, serve, and retain profitable customers by interacting with them in an integrated way across a range of communication channels [10]. CRM is touted as an imperative strategy to enhance a firm's competitive advantage [11]. Various authors have proposed diverse conceptualizations of CRM, taking the basic premise that companies should develop customer management practices to maximize

their value during the relationship's entire lifecycle. Recent literature explained CRM conceptualizations according to specific implementation dimensions with each dimension representing a set of business activities [12].

It seems that the internet is creating tremendous impact on businesses also in interacting, nurturing, maintaining their customer bases. The impact of the process of managing and interacting customers via the internet has affected CRM too. By Leveraging, the internet for customer management we get the new structure of CRM known as E-CRM. E-CRM is all about managing customers online using internet as the primary channel of interaction [2]. E-CRM refers to CRM using internet technology plus a database, OLAP, data warehouse, data mining, etc. [13]. E-CRM is a dominant paradigm in the world of customer relationship management [14]. So more and more businesses begin to attach great importance to electronic customer relationship management, which focuses on customers instead of products or services, that is, considering customer's needs in all aspects of a business, ensuring customers' satisfaction [1].

2.2 Mobile Computing Technology and Mobile-CRM

Mobile Computing is a technology that allows transmission of data, via a computer, without having to be connected to a fixed physical link [15]. It is a computing paradigm designed for workers who travel outside the boundaries of their organizations such as salespeople who were able to make proposals at customers' offices. This, enables a real-time connection between a mobile device and other computing environments, such as the Internet or an intranet. This innovation is creating a revolution in the manner in which people use computers [16]. Nowadays, smartphones have numerous information and communication technology functions (or apps) that are comparable to those of old computers. It is estimated that the global revenues from apps will reach US\$80 billion in 2020, indicating abundant business opportunities [17]. Current smartphones and tablets contain more computing power than many of the formerly known supercomputers, which used to fill an entire room [18]. As technology is progressing to miniaturize devices, increase computing power and, especially, decrease the price of electronics, smartphone adoption will only accelerate [19]. In 1985, the Cray-2 supercomputer was the fastest machine in the world. The iPhone 4, released in June 2010, had the power equivalent to the Cray-2; now, the Apple Watch has the equivalent speed of two iPhone 4s just five years later. With the consumer retail price of smartphones tumbling to below \$50, processing power skyrocketing and adoption in emerging markets accelerating, nearly everyone will soon have a literal supercomputer in their pocket [18].

With the development of wireless technology, mobile devices, such as smartphones and smart watches, are

becoming the most effective tools for communication in human's daily life. The popularity and availability of mobile devices can help mobile users enrich experience of various services provided by mobile applications without the constrain of time and place [20]. One primordial capacity needed for implementing a CRM strategy is the ability to communicate with customers on an individual basis. For that reason, mobile technologies represent an appealing additional channel which can complement the existing channels. Among the advantages of the mobile channel which are highly relevant to CRM are the personal character of mobile devices which allows an individual customer reach, the interactivity brought by its quick message delivery and response, its reachability and ubiquity. It is the only medium enabling a spontaneous, interactive, direct and targeted interaction with customers, anytime, anywhere. For that reason, the future CRM solutions is envisaged to combine traditional, Internet and mobile channels [21]. Mobile Customer Relationship Management (Mobile-CRM) system is one of the recent advancements in CRM systems [22]. M-CRM has been defined as the communication, bilateral or unilateral, that is related to marketing activities via mobile phone in order to build and maintain relationships between the consumer and the company [23]. The ubiquity of mobile computing devices, such as smartphones and tablets, and the proliferation of mobile customer relationship management applications, may lead to increased CRM adoption and higher returns on CRM technology investments [24]. With the popularity of smart phones and other mobile handheld devices, various vendors have introduced mobile CRM applications that provide a high level of portability. Implementing these applications involves huge investments and additional applications escalate costs but the additional expense is negligible compared to benefits it provides to any organization [9].

2.3 E-Readiness Concept and Models

The first efforts in defining E-Readiness were undertaken in 1998 by the Computer Systems Policy Project (CSPP) when it developed the first E-Readiness assessment tool known as Readiness Guide for Living in the Networked World [25]. There are several definitions for E-Readiness. The CSPP model defines an 'e-ready' community as one that has high-speed access in a competitive market; with constant access and application of ICT in schools, government offices, businesses, healthcare facilities and homes; user privacy and online security; and government policies which are favorable to promoting connectedness and use of the network. The Asian Pacific Economic Cooperation (APEC) group defines a country as e-ready that is 'ready' for e-commerce, has free trade, industry self-regulation, ease of exports, and compliance with international standards and trade agreements. McConnell International defines E-Readiness as the capacity of nations to participate in the digital economy [26] and finally Readiness, as the

Economist Intelligence Unit (EIU) defines it, is the measure of a country's ability to leverage digital channels for communication, commerce and government in order to further economic and social development [27].

Over the last years, a number of models and tools for E-Readiness assessment of countries on the macro level have been developed by different organizations [26] including third-party reports, position papers and survey results [28]. On the surface, each model gauges how ready a society or economy is to benefit from information technology and electronic commerce [26]. There has been a proliferation of E-Readiness assessment measures in recent years that each one has a certain objective [6]. Largely, all the E-Readiness tools measure the E-Readiness phenomena at national level across key sectors of the economy. Diverted from global perspective, a second wave of E-Readiness studies has been introduced to specific ICT-related areas. Thus, in the context of electronic banking, E-Readiness is conceived as the function of the ability to pursue value creation opportunities and within electronic trade, E-Readiness is presented as a resource to be implemented in any organization. The choice of E-Readiness tool largely depends on the purpose and goals for which a particular assessment is meant to achieve. In a general classification, E-Readiness assessment tools and models can be divided into two main categories: those that focus on basic infrastructure or a nation's readiness for business or economic growth, and those that focus on the ability of the overall society to benefit from ICT [29]. In another classification, E-Readiness assessment tools can be divided into two categories. While some of tools focus on assessing readiness of countries, governments and policies for adopting Internet technologies (such as CSPP, APEC, McConnell, Mosaic, WITSA), some others e.g. SCALES (Supply Chain Assessment and Lean Evaluation System) assess the readiness to adopt different concepts or approaches for engineering and was developed for a specific industry sector [30]. In The following, it has mentioned to some of tools and models that was designed to assess a company's readiness.

Mutula and Brakel Model: This tool is designed around five major segments, namely; information readiness, enterprise readiness, human resources readiness, ICT readiness and external environment readiness.

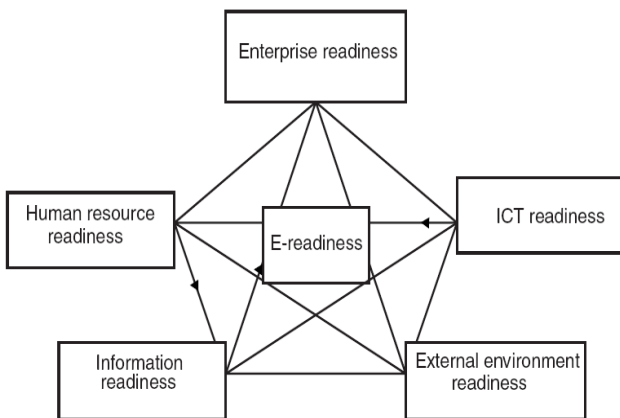


Fig. 1 An integrated information rich E-Readiness assessment tool [21]

Around each of these segments there are a set of variables to measure the degree of E-Readiness within organizations, communities or countries. This information rich E-Readiness tool is premised on the fact that information and digital literacy competencies are needed for an individual to effectively partake in an information society [25]. The Mutula and Brakel model is illustrated in fig. 1.

STOPE Model: Past studies have considered "technology: T", with "organization: O" and "people: P" as main domains to investigate technology in society. Bakry considered the "TOP" domains, and added two complementary domains that is "strategy: S", and "environment: E". The result was the STOPE framework that was used by Bakry and his colleagues for various studies including: e-business, e-government, ERP, applications of information services and security management standards [31]. The STOPE model is illustrated in fig. 2.

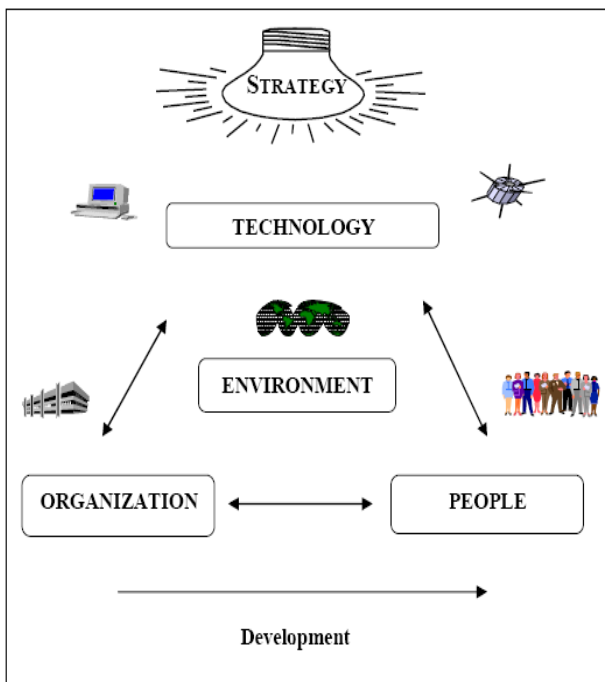


Fig. 2 STOPE E-Readiness assessment framework [31]

SCALES: Supply Chain Assessment and Lean Evaluation System assess the readiness to adopt different concepts or approaches for engineering (e.g. readiness assessment tools for concurrent engineering). SCALES was developed for a specific industry sector—the manufacturing industry. It was designed to assess a company's (especially SMEs) readiness for adopting Lean Manufacturing techniques [30].

RACE: This is a Readiness Assessment tool for Concurrent Engineering (CE) and is widely used in the software engineering, automotive and electronic industries.

BEACON Model: Benchmarking and Readiness Assessment for Concurrent Engineering in Construction, assesses the readiness of construction companies to improve their project delivery processes through the implementation of concurrent engineering. It consists of four elements, which are Process, People, Project and Technology. A commercial software tool has been developed to automate the process of CE readiness assessment for construction organizations [30].

IQ Net Readiness Scorecard: This was developed by CISCO and is a Web-based application that assesses an organization's ability to migrate to an Internet Business model. It is based on the book Net Ready, which gauges the readiness of IT service providers. Similar to the BEACON model, companies are required to respond to the statements and on completion; they are presented with an IQ Net Readiness Profile [30].

VERDICT MODEL: VERDICT is an Internet-based prototype application that assesses the overall E-Readiness of end-user companies and profiles the companies in this regard, based on their responses. VERDICT was developed to aid construction sector end-users to gauge their E-Readiness for using e-commerce technologies such as Web-based collaboration tools. It can be used to assess the E-Readiness of construction companies, departments within a company, or even individual work groups within a department. Several research publications and articles indicate that people, processes and technology are the three key aspects that need to be considered for successful implementation of technologies. It has mentioned in this model that the people, processes, and technology need a leader - just as Fan orchestra needs a conductor. The Conductor in this case is the management. To successfully implement and use any new technology it requires management in order to plan and drive policies and strategies. Thus a fourth category, management is necessary.



Fig. 3 Four key elements of VERDICT model [30]

The VERDICT Model has been so structured that for an organization to be e-ready it must have: Management that believes in the technology and takes strategic measures to drive its adoption, implementation and usage in order to derive business benefits from the technology; Processes that enable and support the successful adoption of the technology; People who have adequate skills, understanding of, and belief in the technology; and finally technology tools and infrastructure necessary to support the business functions [30]. Fig. 3 shows the four key elements of VERDICT model.

For selecting the most suitable model to conduct this research, two points were considered. Firstly, the goal of this research is to assess the E-Readiness of a company rather than a country or society. Secondly, considering the key success factors of CRM implementation is very important in selecting proper model process. After studying on various E-Readiness assessment tools and models, the VERDICT model selected as a compatible model with research goals. There are some reasons for this selection. The VERDICT is one of tools that has designed to assess E-Readiness in organizational level which harmonize with the research subject. Furthermore, based on many studies, managing a successful CRM implementation requires an integrated and balanced approach to key dimensions of "technology", "process", and "people" [32]. These three key dimensions are completely harmonized with VERDICT's main dimensions. Based on VERDICT model we evaluate the level of a company in these three dimensions plus another dimension which holds a coordination role and supplement the other three dimensions. This fourth dimension is "management".

3. Research Methodology

A survey research method was applied to drive this study. For collecting primary data, the questionnaire method was used in this research. To answer the main research questions, two questionnaires were designed based on VERDICT model. In this way, 44 questions were included in the first questionnaire to elicit the expert's opinions on the importance of each of indicators and categories of selected model for assessing E-Readiness of the case company and the second questionnaire based on a five-point Likert scale (1-"strongly disagree" and 5-"strongly agree") was designed to measure the level of every indicator of categories in that case company.

The group of experts relating to indicators importance subject were among decision makers and directors of sales, distribution and IT department of the case company. Similarly, the research population relating to indicators evaluation were head-office managers, branch managers and all operational department supervisors of the company. Since the number of respondents was limited and all of them were accessible, the census method was used. The survey questionnaires were answered by 77 responders including senior managers, supervisors and ICT experts.

4. Data Analysis

Based on VERDICT model as the proper model for doing this research which includes four categories like Management, Information Technology (IT), People and Process, the questionnaires were designed, distributed, coded and analyzed by statistical features of MS-Excel software. In the first step, all answers to the first questionnaire were entered to the Excel software and then weighted average of each indicator (relative importance of each indicator) was calculated by using the Sumproduct and Sum function of Excel. Subsequently the weighted average of related category of the model were determined using the Excel statistical functions. The results are summarized in the tables below.

Table 1 -Importance of each indicator of management category

No.	Rep.	Indicators of Management	Weighted Average
1	M1	The recognition of the benefits of using mobile-commerce tools	3.90
2	M2	The senior management awareness of the potential rewards and risks of using mobile-commerce tools	4.273
3	M3	Having a well-defined strategy for adopting Mobile-CRM tools	4.455
4	M4	Developing strategies to migrate users of existing services to mobile-based applications	4.091
5	M5	Generalizing our Mobile-CRM strategy at all levels within the organization	3.819
6	M6	Existence of e-business mind approach in all levels of management in organization	4

7	M7	Active participation of senior management in developing and implementing the company's Mobile-CRM strategy	4.363
8	M8	The culture of being at the forefront of technology adoption	4.273
9	M9	Adoption of Mobile-CRM tools to improve overall business development	3.7273
10	M10	Comparison of the firm's use of Mobile-CRM tools with competitors	3.545
11	M11	Existence of a flexible approach to accommodate new and emerging technologies	3.636
12	M12	Commitment to allocating adequate resources in terms of time, staff and budget required to implement and use Mobile-CRM tools	4.363
13	M13	Allocating a suitable and independent budget for using Mobile-CRM tools	3.818
14	M14	Staff training to efficient use of Mobile-CRM tools	4
15	M15	Defining key indicators for evaluation the effectiveness of using Mobile-CRM tools	4.091
16	M16	Preparing a platform in organization for sharing people experiences in mobile-commerce tools	3.727
Average			4.001

Table One shows that in Management category, the most important indicator is "Having a well-defined strategy for adopting Mobile-CRM tools".

Table 2- Importance of each indicator of IT category

No.	Rep.	Indicators of Information Technology	Weighted Average
17	IT1	Well definition of IT Policy	3.637
18	IT2	Having adequate IT support (in house or external)	4.364
19	IT3	Having adequate IT infrastructure for supporting staff and current business process	4.273
20	IT4	Flexibility of current IT systems to accommodate rapid change and scalability	3.909
21	IT5	Regularly upgrading the IT systems to meet changing business/market needs	3.909
22	IT6	Existence of a network and communication platform for data transferring and information sharing across the company	4.273
23	IT7	Easy access to required mobile hardware and software resources by IT department experts	3.909
24	IT8	Widespread use of electronic communication tools in organization	4.091
25	IT9	Widespread use of internet for search and information gathering in organization	3.636
26	IT10	Suitable knowledge of technical support for smartphones in IT department staff	3.727
Average			3.972

Table Two shows that in Information Technology category, the most important indicator is "Having adequate IT support (in house or external)".

Table 3- Importance of each indicator of people category

No.	Rep.	Indicators of People	Weighted Average
-----	------	----------------------	------------------

27	H1	Having people with the ability to implement change and move quickly to adopt and use any new technology	3.727
27	H2	Identification and clearly definition the roles and responsibilities of staff who use (or will use) the Mobile-CRM tools	3.727
29	H3	Having an organizational structure and culture that provides a well suited environment for Mobile-CRM adoption and use	4
30	H4	Having staff with the necessary levels of IT literacy, functional expertise and skills to use Mobile-CRM tools	3.727
31	H5	Recognition the importance and benefits of using Mobile-CRM tools by staff	3.909
32	H6	Having business management staff (or decision makers) with adequate IT knowledge	4.182
33	H7	Having IT staff with adequate knowledge of business processes	4
34	H8	Existence of an incentive plan for motivating people to use mobile-commerce tools and new technologies	4.273
35	H9	Identifying barriers to the use of Mobile-CRM tools by employees	3.909
Average			3.939

Table Three shows that in People category, the most important indicator is "Existence of an incentive plan for motivating people to use mobile-commerce tools and new technologies".

Table 4- Importance of each indicator of Process category

No.	Rep.	Indicators of Process	Weighted Average
36	P1	Identifying the bottlenecks and inefficiencies in current business processes	3.637
37	P2	Having flexible processes to accommodate Mobile-CRM tools	3.727
38	P3	Previous attempts to design new technologies-enabled processes	4.273
39	P4	Dealing with the same customers within the supply chain	3.909
40	P5	Widespread use of a communication software for exchanging all documents within the organization	3.727
41	P6	Previous attempts to process reengineering and adopt mobile-commerce tools to automate existing processes	3.727
42	P7	Having well-defined current business processes	4.273
43	P8	Believing That mobile-commerce tools can cut processes costs	3.636
44	P9	Attempts to use of new technologies-based tools for covering main processes of organization	3.909
Average			3.869

Table Four shows that in Process category, the most important indicators are two items including "Previous attempts to design new technologies-enabled processes" and "Having well-defined current business processes".

Additionally, by calculating the average of each category's importance, the "Management" is the most

important category in E-Readiness assessment of the case company for Mobile-CRM implementation.

In the second step, we multiplied each indicator's weight to its average score gathered from second questionnaire in order to obtain final scores. The final results of indicators are summarized in table 5. The higher the average score the more likely it is that the company is "e-ready".

The minimum score that can be obtained for each category equals 'zero' where the respondents 'don't know' the answers to any of the questions, and are therefore not 'e-ready'. The scores are averaged, and depending on the average score, the respondents are presented with "traffic light" indicators i.e. red, green and amber lights, to

Table 5- Final results of indicators of assessing E-Readiness of the company for implementing Mobile-CRM

No.	Rep.	Ave. Score	Weight	Final Score	No.	Rep.	Ave. Score	Weight	Final Score	No.	Rep.	Ave. Score	Weight	Final Score
1	M1	3.60	0.061	0.15	17	IT1	4.66	0.092	0.34	32	H6	2.22	0.117	0.25
2	M2	4.56	0.067	0.13	18	IT2	3.26	0.110	0.38	33	H7	3.76	0.112	0.31
3	M3	3.86	0.068	0.17	19	IT3	3.90	0.108	0.26	34	H8	2.24	0.120	0.15
4	M4	3.70	0.064	0.20	20	IT4	2.20	0.98	0.24	35	H9	2.86	0.109	0.14
5	M5	2.56	0.060	0.10	21	IT5	3.94	0.98	0.22	People Average Score 2.62				
6	M6	4.62	0.060	0.16	22	IT6	4.82	0.108	0.41					
7	M7	4.78	0.062	0.24	23	IT7	3.08	0.98	0.34	Information Technology Average Score 3.74				
8	M8	4.22	0.074	0.18	24	IT8	3.71	0.103	0.30					
9	M9	3.71	0.060	0.21	25	IT9	3.93	0.092	0.27	36	P1	2.58	0.104	0.26
10	M10	4.18	0.058	0.11	26	IT10	3.89	0.094		37	P2	2.88	0.107	0.29
11	M11	4.12	0.060	0.17	Management Average Score 3.90					38	P3	3.44	0.123	0.28
12	M12	4.26	0.058	0.17						39	P4	4.45	0.112	0.37
13	M13	3.80	0.067	0.10	27	H1	3.02	0.104	0.38	40	P5	3.98	0.107	0.37
14	M14	2.88	0.057	0.21	28	H2	2.47	0.104	0.14	41	P6	3.12	0.107	0.40
15	M15	3.55	0.055	0.08	29	H3	2.55	0.112	0.25	42	P7	2.12	0.123	0.26
16	M16	4.10	0.058	0.11	30	H4	1.96	0.104	0.19	43	P8	2.34	0.104	0.35
Process Average Score 3.14					31	H5	2.66	0.109	0.28	Process Average Score 3.14				

The results of each category's final score has been summarized in fig. 4.





Category	Average Score	Traffic Light Indicator
Management	3.90	
IT	3.74	
People	2.62	
Process	3.14	

Fig. 4 Average score of each category with traffic light indicators

The minimum score that can be obtained for each category equals 'zero' where the respondents 'don't know' the answers to any of the questions, and are

visually

indicate their e-readiness in each category, where:

- An average score greater than or equal to zero and less than 2.5 is red. Red indicates that several aspects (within a category) need urgent attention to achieve E-Readiness;
- An average score greater than or equal to 2.5 and less than 3.5 is amber. Amber indicates that certain aspects (within a category) need attention to achieve E-Readiness; and
- An average score greater than or equal to 3.5 is green. This indicates that the case company has adequate capability and maturity in these aspects and therefore is e-ready [30].

therefore not 'e-ready'. The scores are averaged, and depending on the average score, the respondents are presented with "traffic light" indicators i.e. red, green and amber lights, to visually indicate their e-readiness in each category, where:

- An average score greater than or equal to zero and less than 2.5 is red. Red indicates that several aspects (within a category) need urgent attention to achieve E-Readiness;
- An average score greater than or equal to 2.5 and less than 3.5 is amber. Amber indicates that certain aspects (within a category) need attention to achieve E-Readiness; and
- An average score greater than or equal to 3.5 is green. This indicates that the case company has adequate capability and maturity in these aspects and therefore is e-ready [30].

It can be found from analyzed data that the case company is in high level of E-Readiness in two categories of the VERDICT model including Management and Information Technology because the score of these categories are greater than 3. Also the company is in moderate level of E-Readiness in other two categories including People and Process because the score of these categories are between 2.5 and 3.5 whilst the People category is in lowest level of E-Readiness.

Based on each category's score, the overall level of E-Readiness assessment of the case study company for implementing a Mobile-CRM system extracted. This has been illustrated in Radar diagram format in fig 5.

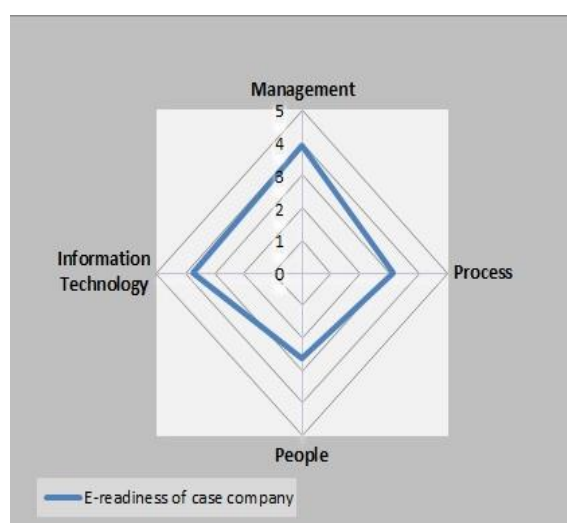


Fig. 5 Final E-Readiness level of the company in Radar diagram format

5. Conclusion

The findings of this research are briefly summarized as follows: **a.** along with the various tools and models for assessing E-Readiness of organizations, the VERDICT model is recommended to those distribution companies that are planning to implement Mobile-CRM system. **b.** The level of E-Readiness of the case study organization for implementing Mobile-CRM, generally is in an acceptable situation based on all four main factors: Management, Information Technology, People, and Process. Since People factor has got the lowest score in comparison with other factors, this factor should be

References

- [1] A. Mishra, and D. Mishra, "Customer Relationship Management: Implementation Process Perspective", *Acta Polytechnica Hungarica*, Vol. 6, No. 4, 2009, pp. 83- 99.
- [2] A. Jafarnejad, C. Loox and A. Monshi, "Towards Electronic Customer Relationship Management: An CRM Solutions Development Mythology", *Iranian Journal of Management Studies (IJMS)*, Vol. 1, No.1, 2007, pp. 73-89.
- [3] P. Forrouhiyehpour, "Assessing the Readiness for implementing CRM in B2B Markets Using AHP Method", M.S. Thesis, Lulea University of Technology, Sweden, 2008.
- [4] R. Shaikh, "Mobile CRM A Case Study of Mobile CRM Strategies", M.S Thesis, Information and Communication Technology, KTH Royal Institute of Technology, Stockholm, Sweden, 2015.
- [5] A. Jafarnejad, S.R. Safavi and M. Ajali "E-Readiness assessment of Gas National company of Iran based on

considered more important for this organization to absorb most attention, investment and improvement. **c.** Based on assessing the E-Readiness assessment of this company, the Management factors has got the highest score but some efforts for improve to desired level is still necessary. **d.** There is more than 1.2 score between the two factors that have the highest and lowest scores which means a considerable gap between various aspects of E-Readiness in this company.

Research findings indicate that E-Readiness of the company for implementing Mobile-CRM is in good condition in terms of Management and IT factors but it is strongly suggested that prior to start a Mobile-CRM implementation project in this company, the decision makers prepare some plans and perform some basic actions for increasing the E-Readiness level of the company especially in People and then Process category. Firstly, by the fact that the lowest score belongs to People factor, they should prepare a comprehensive plan for their employees to develop their knowledge of information technology and provide continuing education, training courses, incentive plans, culture development of using electronic tools, motivators, etc. Secondly, from Business Process perspective the company should carry out several organizational improvement projects to raise its E-Readiness level. A business process reengineering (BPR) approach is recommended in this regard. Then a full review of company's information systems and IT infrastructure is needed to analyze gaps and achieve a suitable compatibility with M-Commerce tools. Additionally, we suggest the VERDICT model for assessing the E-Readiness of the firm to those distribution companies that are willing to implement Mobile-CRM project. E-Readiness is a relatively new concept and most of E-Readiness assessment models that have been introduced so far, are suitable for national level assessment. Corporate level assessment models are few and their abilities are limited to cover many domains. There are many opportunities for further studies to design and propose suitable models for assessing the E-Readiness of companies in different types of businesses and industries. Other fields of further study would be the E-Readiness assessment models for implementing ERP projects, E-Commerce Projects, E-SCM projects and etc.

- AHP and fuzzy logic", 2th international conference of OR, Babolsar, Iran, 2009.
- [6] P. Hanafizadeh, M. Hanafizadeh, and M. Khodabakhshi, "Taxonomy of E-Readiness assessment measures", *International Journal of Information Management*, Vol. 29, 2009, pp. 189-195.
- [7] D. Dada, "E-Readiness for developing countries: Moving the focus from the environment to the users", *EJISDC*, Vol. 27, No. 6, 2006, pp. 1-14.
- [8] K. Anderson, and C. Kerr, "Customer Relationship Management", McGraw Hill Companies, Inc., 2002.
- [9] S. Grandhi and R. Chugh. "Strategic Value of Mobile CRM Application: A Review of Mobile CRM at Dow Corning and Direct TV", *International Conference on Innovation and Information Management (ICIM 2012)*, *IPCSIT* Vol. 36, 2012, pp. 388-393.
- [10] I. Mahdavi, N. Cho, B. Shirazi and N. Sahebjamnia, "Designing evolving user profile in e-CRM with dynamic clustering of web documents." *Data & Knowledge Engineering*, Vol 65, 2008, pp. 355-372.
- [11] R. Lin, R. Chen and K. Shun Chiu, "Customer relationship management and innovation capability: an empirical study", *Industrial Management & Data Systems*, Vol. 110, No. 1, 2010, pp. 111-133.
- [12] I. Dalla Pozza, O. Goetz and J.M. Sahut, "Implementation effects in the relationship between CRM and its performance", *Journal of Business Research*, Vol. 89, 2018, pp. 391-403.
- [13] M. Wang, "Measuring CRM service quality in the library context: a preliminary study", *The Electronic Library*, Vol. 26, No. 6, 2007, pp. 896-911.
- [14] A. Albadvi and M. Enayat tabar, "Customer Relationship Management in electronic environment". 4th international conference of management, Tehran, Iran, 2006.
- [15] S. Kaur, S. Saini and R. Vashisht, "Mobile Computing", *Advance in Electronic and Electric Engineering*, Vol. 3, No. 6, 2013, pp. 675-682.
- [16] A. Turban et al. (2008). *Information Technology for Management: Transforming Organizations in the Digital Economy*, 6th ed., John Wiley & Sons, 2008.
- [17] T. Fan-Chen, P.T.T. Linh, T.C.E. Cheng, and T. Ching, "Enhancing customer loyalty to mobile instant messaging: Perspectives of network effect and self-determination theories", *Telematics and Informatics*, Vol. 35, 2018, pp. 1133-1143.
- [18] S. Klaous, *The Fourth Industrial Revolution*. Penguin Random House, UK, 2017.
- [19] World Economic Forum. "Deep Shift Technology Tipping Points and Societal Impact", 2015, Retrieved from http://www3.weforum.org/docs/WEF_GAC15_Technological_Tipping_Points_report_2015.pdf
- [20] F. Gu, J. Niu, Z. Qi and M. Atiquzzaman, "Partitioning and Offloading in Smart Devices for Mobile Cloud Computing: State of the Art and Future Directions", *Journal of Network and Computer Applications*. Accepted 19 June 2018.
- [21] G. Componovo, Y. Pigneur, A. Rangone and F. Renga, "Mobile Customer Relationship management: An Explorative Investigation of the Italian Consumer Market", Vol 10, No. 1109, *ICMB.2005.63*. pp. 42-48.
- [22] D. Verma and D.S. Verma, "Managing Customer Relationship through Mobile CRM in Organized retail outlets", *International Journal of Engineering Trends and Technology (IJETT)*, Vol. 4, No. 5, 2015, pp. 1697-1701.
- [23] S. San-Martin, N.H. Jimenez, and B. Lopez-Catalan, "The firm's benefits of mobile CRM from relationship marketing approach and the TOE model", *Spanish Journal of Marketing- ESIC* 20, 2016, pp. 18-29.
- [24] M. Rodriguez and K. Trainor, "A conceptual model of the drivers and outcomes of mobile CRM application adoption", *Journal of Research in Interactive Marketing*. Vol. 10, No.1, 2016, pp. 67-84.
- [25] S.M. Mutula, and P. Brakel, "An evaluation of E-Readiness assessment tools with respect to information access: Towards an integrated information rich tool". *International Journal of Information Management*, Vol. 26, 2006, pp. 212-223.
- [26] M. Hourali, M. Fathian, A. Montazeri, and M. Hourali, "A model for E-Readiness assessment of Iranian small and medium enterprises". *Journal of Faculty of Engineering*, Vol. 41, No. 7, 2008, pp. 969-985.
- [27] Economist Intelligence Unit, "E-Readiness rankings", 2008 Retrieved from: http://graphics.eiu.com/upload/ibm_ereadiness_2008.pdf
- [28] Bridges. org., "E-Ready for What E-Readiness in Developing Countries: Current Status and Prospects toward the Millennium Development Goals", 2005, Retrieved from:<http://www.bridges.org/en/Publication.3.html>
- [29] S. Toufani, "E-Readiness assessment in Iranian B2C Enterprises (case: Iranian Book Publishing Companies)", *Master Thesis, Lulea University of Technology, Sweden, 2009*.
- [30] K. Ruikar, C.J. Anumba and P.M. Carrillo, "VERDICT- An e-readiness assessment application for construction companies", *Automation in Construction*, Vol. 15, 2006, pp. 98-110
- [31] K.S. AL-Osami, "Mathematical Models for E-Readiness Assessment of Organizations with Intranets", *Master Thesis, King Saud University, Saudi Arabia, 2007*.
- [32] J. C. Injazz and K. Popovich (2003). "Understanding customer relationship management (CRM) people, process and technology", *Business Process Management Journal*, Vol. 9, 2003, pp. 672-688.

Alireza Kamanghad received the B.S. degree in Computer Engineering from Azad University, South Tehran Branch in 2000, M.S. degree in IT Management from Shahid Beheshti University, Iran in 2011, and Ph.D. degree in IT Management from Azad University, Central Tehran Branch, Iran. His research interests include E-Business, Mobile Computing, Internet of Things, IT Governance, IT strategy and Emerging Technologies. He has presented and published several papers in international conferences and journals including the best paper award in 2nd conference on Iran Distribution Industry.

Gholamreza Hashemzadeh is an associate professor in the faculty of management at Azad University, South Tehran Branch, Iran. He received his Ph.D. degree in Industrial management from Azad university Tehran science and research branch, Iran in 2000. His research is focused on Technology Management, E-Business and Research Methodology.

Mohammadali Afshar Kazemi is an associate professor in the faculty of management at Azad University, Central Tehran Branch. He received his Ph.D. degree in Industrial management from Azad university Tehran science and research branch, Iran in 2003. His research is focused on System Dynamics, Data Mining and Methodologies in Software Engineering.

Nosratollah Shadnoosh is an assistant Professor at Department of Industrial Management, Faculty of Management, Islamic Azad University, Central Tehran Branch, Tehran, Iran. He received his Ph.D. from the faculty of Management, Islamic Azad University, Tehran science and research branch, Iran in 2011.

A New VAD Algorithm using Sparse Representation in Spectro-Temporal Domain

Mohadese Eshaghi

Department of Electrical and Computer Engineering, Science and Research Branch, Islamic Azad University, Tehran, Iran.
eshaghi463@yahoo.com

Farbod Razzazi *

Department of Electrical and Computer Engineering, Science and Research Branch, Islamic Azad University, Tehran, Iran.
razzazi@sbiau.ac.ir

Alireza Behrad

Department of Electrical and Electronic Engineering, Shahed University, Tehran, Iran.
behrad@shahed.ac.ir

Received: 03/Apr/2019

Revised: 25/Aug/2019

Accepted: 16/Sep/2019

Abstract

This paper proposes two algorithms for Voice Activity Detection (VAD) based on sparse representation in spectro-temporal domain. Spectral-temporal components which, in addition to the frequency and time dimensions, have two other dimensions of the scale and rate. Scale means spectral modulation and the rate means temporal modulation. On the other hand, using sparse representation in learning dictionaries of speech and noise, separate the speech and noise segment to be better separated. The first algorithm was made using two-dimensional STRF (Spectro-Temporal Response Field) space based on sparse representation. Dictionaries with different atomic sizes and two dictionary learning methods: NMF (non-negative matrix factorization) and the K-SVD (k-means clustering method), were investigated in this approach. This algorithm revealed good results at high SNRs (signal-to-noise ratio). The second algorithm, whose approach is more complicated, suggests a speech detector using the sparse representation in four-dimensional STRF space. Due to the large volume of STRF's four-dimensional space, this space was divided into cubes, with dictionaries made for each cube separately by NMF (non-negative matrix factorization) learning algorithm. Simulation results were presented to illustrate the effectiveness of our new VAD algorithms. The results revealed that the achieved performance was 90.11% and 91.75% under -5 dB SNR in white and car noise respectively, outperforming most of the state-of-the-art VAD algorithms.

Keywords: Speech Processing; Voice Activity Detector; VAD; Spectro-Temporal Domain Representation; Sparse Representation, NMF, K-SVD.

1. Introduction

Many practical speech processing systems are in use today. Voice activity detection (VAD) unit, which discriminates speech segments from environmental noise segment, is an integral part of a variety of speech communication systems. Speech coding, speech recognition, hands-free telephony, and echo cancellation are some examples of these systems. However, developing a VAD for noisy environments with low signal-to-noise ratios or for any non-stationary noise is still very challenging [1–4].

Recent psycho-acoustical and physiological findings in mammalian auditory systems, however, suggest that the spectral decomposition is only the first stage of transformations in the representation of sound. Specifically, it is thought that neurons in the auditory cortex decompose the spectrogram further into its spectro-temporal modulation contents. This finding has inspired a multi-scale model representation of speech modulations whose usefulness has been demonstrated in speech representation, reproduction, intelligibility, discriminating

* Corresponding Author

speech from non-speech signals, and describing a variety of other psycho-acoustic phenomena [5, 6].

In this model, the primary stage converts the sound waveform into a time-frequency distribution along a logarithmic frequency axis. The cortical stage works as a two-dimensional filter bank on the auditory spectrogram image to investigate efficient clues of different acoustic phenomena. Each filter has a spectro-temporal impulse response (usually called spectro-temporal response field (STRF)) in the form of a Gabor function which is effectively a multi-resolution wavelet filter [7, 8].

STRFs decompose the content of auditory spectrogram into the scale-rate domain. The scale represents the spectral modulation rate with the unit defined as cycles/octave (or cycles/kHz). Also, the rate means temporal modulation variations with the unit being cycles/second (Hz) [9]. This multi-domain representation model of speech is proven to be useful in estimation of speech intelligibility [10]. Our VAD key features are captured by the sparse representation of the above two stages.

Sparse solutions have recently attracted a great deal of attention because of their potential applications in many different areas. They are used, for example, in compressed sensing, under-determined sparse component analysis (SCA), and source separation based on atomic decomposition on over-complete dictionaries [11, 12]. In this article, we present and assess the two new approaches to VAD systems based on sparse nature of information in spectro-temporal domain. In the first approach, separation of speech and noise regions is performed using auditory spectrogram and sparse decomposition.

In the second approach, we transform the input utterance into spectro-temporal domain. Owing to large dimensions in the space, each temporal frame in the new domain is divided into small 3D sub-cubes. Then, using sparse decomposition of the sub-cubes on pre-trained speech and noise dictionaries for each sub-cube, speech and noisy parts are classified by combining the results of sparse classification of the sub-cubes within a time frame.

This paper is organized as follows: Section 2 describes the architecture of the system: sparse representation model and the proposed algorithm. Section 3 evaluates the performance of the proposed algorithm, and finally section 4 concludes the paper.

2. Proposed Algorithms

2.1 System Architecture

The first algorithms were proposed using two-dimensional STRF space and via sparse representation in dictionaries with different atomic sizes and two learning methods of K-SVD (generalizing the K-means clustering process) and NMF.

The second algorithm, which is more complicated than the first algorithm, suggests a speech detector in the STRF four-dimensional domain. Due to the large volume of STRF's four-dimensional space, this space was divided into cubes, with dictionaries created for each cube separately by NMF learning method. The results indicate a better performance of the proposed method in STRF space.

2.1.1 The First Algorithm using Auditory Model

In this method, first the input speech is converted to two-dimensional components of time-frequency space. Then, the speech and non-speech frames of the input signal are separated by the sparse method as well as speech and noise dictionaries. Fig. 1 displays the block diagram of this method.

The input signal is converted to two-dimensional auditory spectrogram $y(t,f)$. Then, the sliding window method [13] is used for the continuous speech signal owing to the presence of multiple concatenated phonemes. This two-dimensional signal is converted to windows with T_w length. Δ ($1 < \Delta < T_w$) represents the extent of overlap between the windows. Larger step sizes

of Δ reduce the computational demand, but can decrease its accuracy.

Y Character vector, y_w is the two-dimensional matrix of each window, w denotes the number index of windows, A_s is the matrix of components of the speech dictionary, and A_n shows the components matrix of the noise dictionary. \hat{Y}_w^s and \hat{Y}_w^n indicate the speech and noise estimates of each window using speech and noise dictionaries respectively, and α is the activation coefficient vector of each window whose maximum value is zero.

Fig. 2 illustrates the VAD results of the first proposed algorithm on a sample voice. Fig. 2(a) presents clear speech and the VAD output of the clean speech.

The spectrogram of clean speech is demonstrated in Fig. 2(b) (30 s of silence were added to a clear speech utterance). Fig. 2(c) illustrates the mixed speech with white noise and The VAD results of the proposed algorithm. According to the graph, if the value of the output is 1, it is assumed to be speech; otherwise it is assumed to be noise. The speech and noise signals are mixed to obtain SNR of 5 dB for the signal. Fig. 2(d) exhibits the spectrogram of noisy speech.

2.1.2 The Second Algorithm using STRF domain

The architecture of the proposed VAD algorithm is depicted in Fig. 3. As can be observed, after receiving the input raw speech signal samples by a microphone or other sources, it has been divided into the sequence of time frames. Then, the spectral-temporal features of speech are extracted using the auditory model. These features (Z) include four dimensions of Ω scales (cycles/octave), ω rates (Hz), frequency, and time (frame number). In the next step, the representation space is partitioned into small cubes (named sub-cubes) to manipulate the large volume of data in the resultant four-dimensional space, i.e. each time frame is divided into small 3D sub-cubes.

As a result, in each frame, new feature vectors are extracted with smaller dimensions. In the training phase, speech and noise dictionaries are obtained by dictionary learning algorithms for each sub-cube from the training labeled data. Z_j is a four-dimensional representation of each cube, where J is the cube number index, A_s and A_n represent the speech and noise dictionary matrices, \hat{Z}_j^s and \hat{Z}_j^n denote the speech and noise estimates of each sub-cube using speech and noise dictionaries respectively, and α is the activation coefficient vector of each sub-cube resulting from the sparse representation. In the next step, for each sub-cube the speech and noise frames of speech can be classified for each sub-cube using the proposed algorithm. The final step of this system is the combining of the classification results of sub-cubes by majority voting among the classification results of the sub-cubes of each frame [14].

Fig. 4 displays the results on a different test sample. Fig. 4(a) presents the raw signal as well as the speech and noise sections of the clean signal as the ground truth. Fig. 4(b,d) represent the spectrogram of clean and noisy

speech, which is the same as Fig. 3(b,d). The speech signal in Fig. 4(c) was distorted with babble noise to obtain 5dB SNR and the VAD result of the proposed algorithm.

Comparison of the red diagram of Fig. 3(a) (where the speech and non-speech segments have been manually separated according to the text presented by the ‘‘TIMIT’’ database) with the red diagram of Fig. 3(c) (where the speech and noise segments have been separated by the proposed VAD), as well as red diagram of Fig. 4(a) with the red diagram of Fig. 4(c), reveals the good performance of the second proposed VAD in the separation of speech and non-speech segments. It can be observed that in the absence of information on the structure of the speech and noise, these systems have performed accurately and acceptably. The following subsections capture the functions of the blocks in Fig. 1 and Fig. 3.

2.2 The Proposed Algorithms Based on STRF and Sparse Representation

2.2.1 The First Algorithm using Auditory Model

According to the block diagram of the proposed system in Fig. 1, the spectro-temporal features of speech were extracted using the auditory spectrogram. These features (y) include two dimensions, frequency and time (frame number). Then, the sliding window method [12] is

used for the continuous speech signal given the presence of multiple concatenated phonemes. This two-dimensional signal is converted to windows with a T_w length. Δ ($1 < \Delta < T_w$) reflects the extent of overlap between the windows. Larger windows are associated with lighter calculations, while the smaller the window, the more careful the reconstruction will be. Accordingly, in every window, new feature vectors are extracted with smaller dimensions. Then, using sparse representation, speech and noise dictionaries are obtained for each window from the labeled training data.

The sparse formulation for each window subset can be summarized as:

$$\alpha = \operatorname{argmin}\{\|\Delta\tilde{\alpha} - y_w\| + \lambda\|\tilde{\alpha}\|_1\} \quad \tilde{\alpha} \in \mathbb{R}^N \quad (1)$$

$$\hat{y}_w^s = A^s \alpha^s \quad (2)$$

$$\hat{y}_w^n = A^n \alpha^n \quad (3)$$

y_w is the two-dimensional matrix of each window, w is the number index of windows, A_s represents the matrix of components of the speech dictionary, and A_n shows the components matrix of the noise dictionary.

Also \hat{y}_w^s and \hat{y}_w^n are the speech and noise estimates of each window using speech and noise dictionaries respectively, and α denotes the activation coefficient vector of each window whose most value is zero.

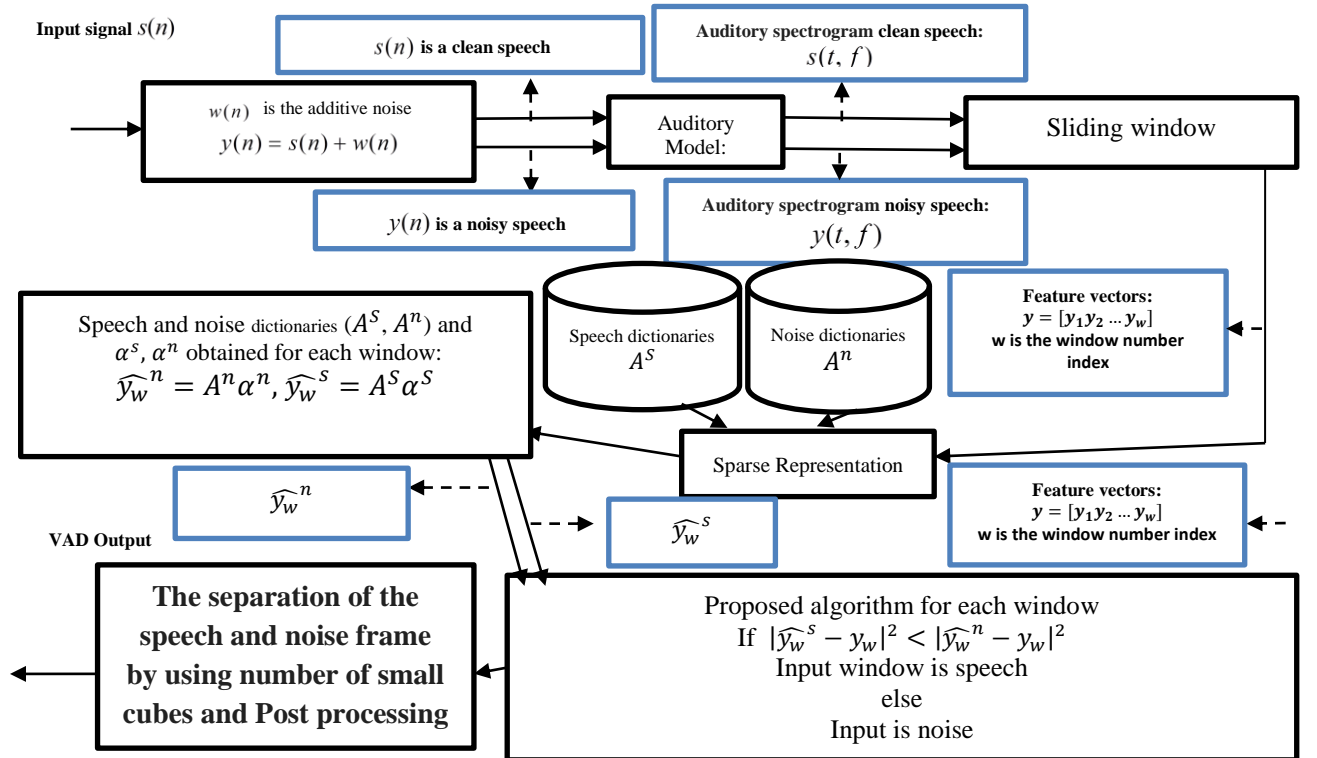


Fig. 1 The block diagram of the proposed first method

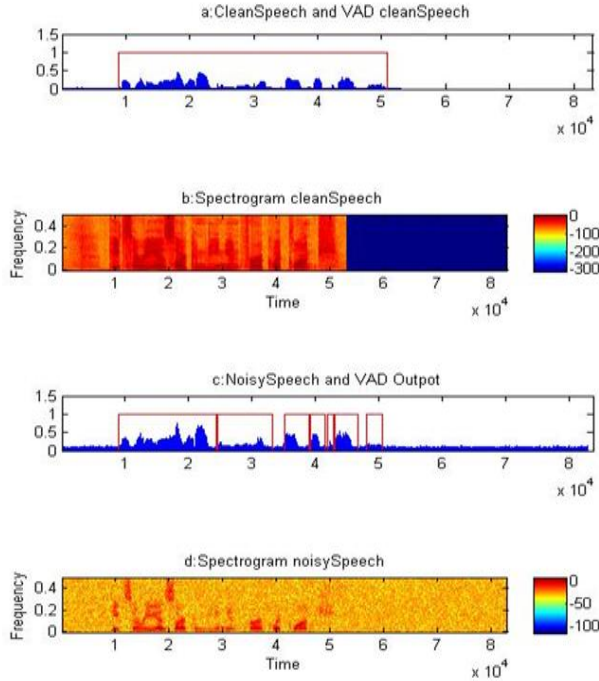


Fig. 2 The VAD results of the proposed first algorithm.

The speech and noise frames of speech can be recognized in each window using the minimum Euclidean distance of the sparse reconstructed signal on two dictionaries. $V(y_w)$ refers to the VAD output of each window. Fig. 5 displays the VAD output decision algorithm of each window.

2.2.2 The Second Algorithm using STRF domain

Based on the block diagram of the proposed system in Fig. 3, initially the spectral-temporal features of speech have been extracted using STRF filter bank. These features (Z) included four dimensions of Ω densities or scales (cycles/octave), ω rates or velocities (Hz), frequency, and time (frame number). The auditory cortical model is obtained using spectral-temporal filter banks, with each of these filters operating within the range of different rates and scales. The space is partitioned into small sub-cubes to manipulate the large volume of data in the four-dimensional space, i.e. each time frame is divided into small cubes (Fig. 6). Hence, in each frame, new feature vectors are extracted with smaller dimensions, after which using sparse representation, speech and noise dictionaries are obtained for each cube from the labeled training data.

The sparse formulation for each cubic subset can be summarized as:

$$\alpha = \underset{\alpha}{\operatorname{argmin}} \{ \|A\tilde{\alpha} - Z_j\| + \lambda \|\tilde{\alpha}\|_1 \} \quad \tilde{\alpha} \in IR^N \quad (4)$$

$$\hat{z}_j^s = A^s \alpha^s \quad (5)$$

$$\hat{z}_j^n = A^n \alpha^n \quad (6)$$

Z_j is a four-dimensional matrix of clean speech each cube, J refers to the cube number index, A_s and A_n

represent the speech and noise dictionary matrices, \hat{z}_j^s denotes the speech estimation of each cube using speech dictionary, \hat{z}_j^n is the noise estimation of each cube using noise dictionary and α shows the activation vector of the cube. Most of the elements of this vector are zero. The speech and noise frames of speech can be recognized in each cube using the minimum Euclidean distance of the sparse reconstructed signal on two dictionaries. $V(Z_j)$ is the VAD output of each sub-cube. Fig. 7 indicates the VAD output decision algorithm of each sub-cube.

In the last step, the decision on the cubes is fused together by majority voting. If the number of speech cubes is greater than the number of noisy cubes within a time frame, the frame is regarded as a speech frame; otherwise it is noise.

2.3 Dictionary learning

Most dictionary learning algorithms use two-step iterative techniques to solve the problem. In the first step, they use a sparse representation algorithm to determine the sparse coefficients given by the dictionary. In the second step, they update the dictionary based on some criteria such as maximizing a likelihood probability or minimizing a cost function [15].

Here, we use two dictionary learning algorithms called NMF [16, 17, 18] and KSVD [19]. Two separate dictionaries are created for signal and noise signals.

2.4 Post-processing

In the post-processing stage, the temporal nature of human speech is considered where speech (both vowel and consonant phonemes) never takes less than 100ms. So, the class of small duration portions of speech and noise, surrounded by the opposing class segments, is inverted. This is because it never occurs to have a speech signal with the length of 32ms between different noisy frames. Similarly, a silence frame with the length of 32ms will not happen either between different speech frames.

A 32ms single frame noise cannot lie between two speech frames. Again, a single 32ms frame of speech cannot be placed between two noise frames either.

If 1 denotes a speech frame and 0 denotes a non-speech frame, and $V(X_t)$ is the VAD output for any time frame, the post-processing algorithm is applied as presented in Fig. 8.

3. Simulation Results

This section provides the simulation results of these proposed algorithms. All training and test clean speech utterances were selected from ‘‘TIMIT’’ database.

Noise samples were taken from ‘‘NOISEX’’ database. The speech and noise signals were mixed in the test bench in order to control the signal-to-noise ratio (SNR).

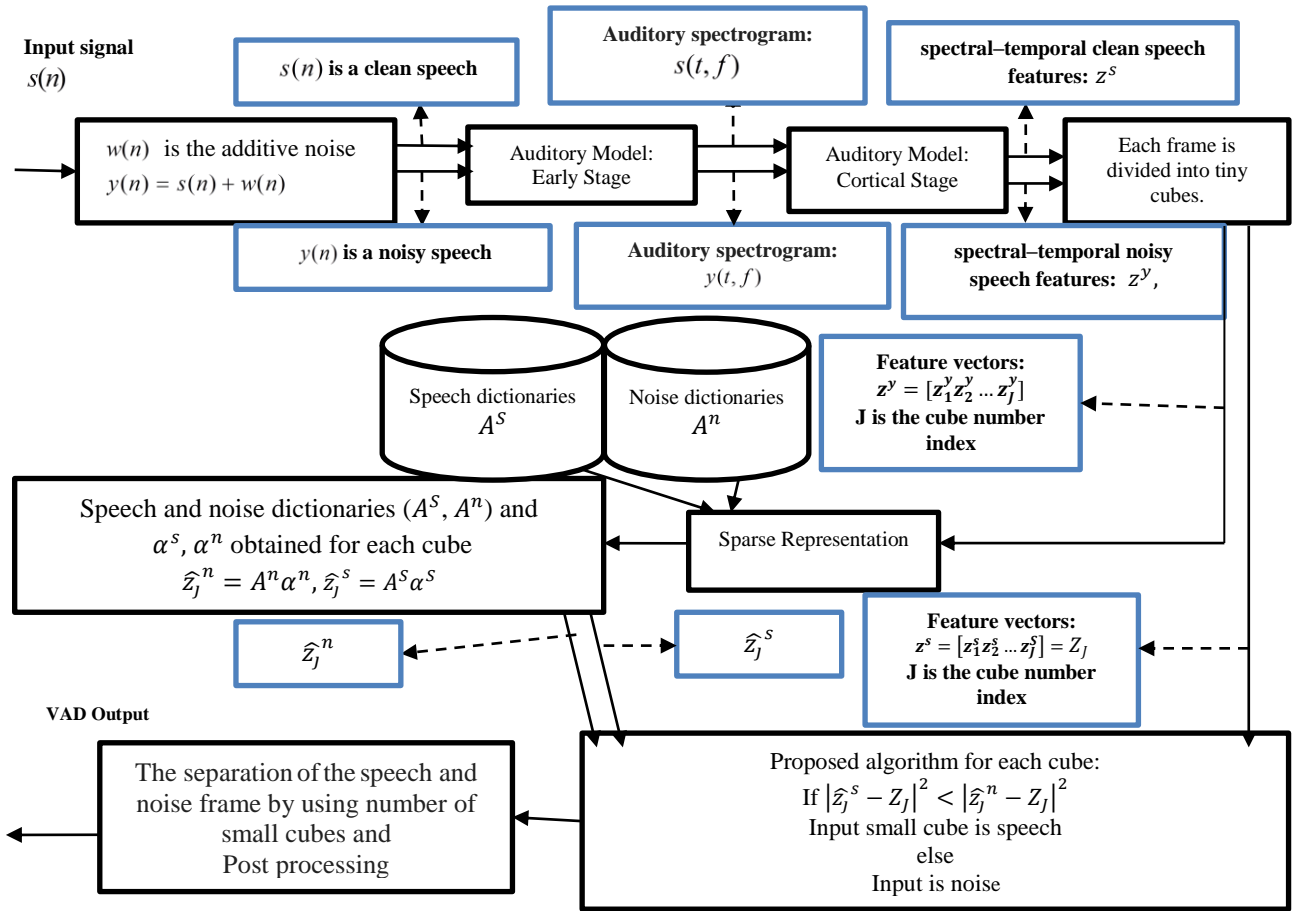


Fig. 3 The block diagram of the proposed second system.

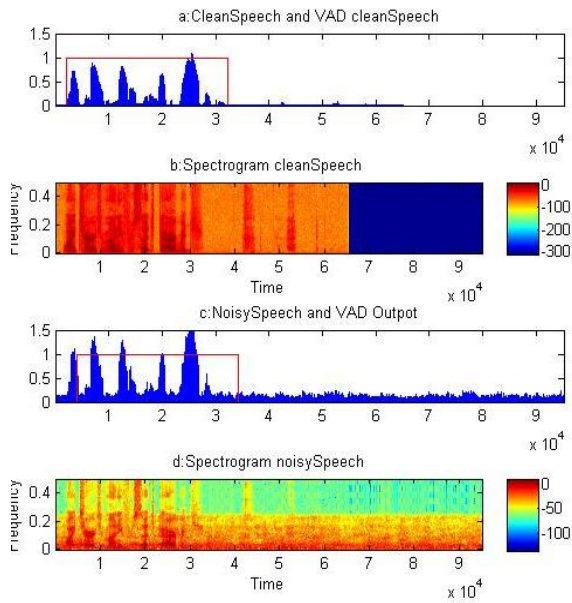


Fig. 4 The VAD results of the proposed second algorithm.

$$\begin{aligned}
 & \text{If } |y_w^s - y_w|^2 < |y_w^n - y_w|^2 \\
 & V(y_w) = 1 \quad //1 \text{ means speech window} \\
 & \quad \text{Otherwise} \\
 & V(y_w) = 0 \quad //0 \text{ means non-speech window} \\
 & \quad \text{end}
 \end{aligned}$$

Fig. 5 The VAD output decision algorithm of each window.

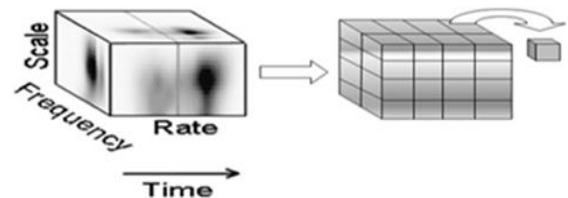


Fig. 6 Each frame 3D spectro-temporal space is divided into tiny cubes.

$$\begin{array}{l}
 \text{If } |\hat{z}_j^s - Z_j|^2 < |\hat{z}_j^n - Z_j|^2 \\
 V(Z_j) = 1 \quad //1 \text{ means speech cube} \\
 \text{Otherwise} \\
 V(Z_j) = 0 \quad //0 \text{ means non-speech cube} \\
 \text{end}
 \end{array}$$

Fig. 7 The VAD output decision algorithm of each cube.

$$\begin{array}{l}
 \text{for } t=3 \text{ to } T-3 \\
 \text{If } V(X_t) = 0 \quad //0 \text{ means non-speech frame} \\
 V(X_t)_{out} = (1 - V(X_t)) \prod_{i=-3}^3 V(X_{t+i}) \\
 \text{If } V(X_t) = 1 \quad //1 \text{ means speech frame} \\
 V(X_t)_{out} = 1 - \left\{ V(X_t) \prod_{i=-3}^3 (1 - V(X_{t+i})) \right\} \\
 \text{end for}
 \end{array}$$

Fig. 8 The VAD post-processing algorithm for any time frame.

The TIMIT corpus of read speech is designed to provide speech data for acoustic-phonetic studies and for the development and evaluation of automatic speech recognition systems. TIMIT contains broadband quality recordings of 630 speakers of eight major dialects of American English, each reading ten phonetically rich sentences. The TIMIT corpus includes 16-bit, 16 kHz speech waveform files for each utterance. [20].

NOISEX database includes airport, babble, car, exhibition, office, restaurant, train, subway, street, and white noises [21].

We applied the proper level of background noise to set the SNR to the desired values.

3.1 Evaluation of the First Algorithm

Table 1 shows the simulation parameters. The most important point in the sparse method is generation of a proper dictionary. The more complete the dictionary, the better the performance of this method will be. Thus, two types of dictionaries are created simultaneously, with the first created from the clean speech of the speech training set and second derived from noise in the noise training set by NMF and KSVD methods. To investigate the effect of the dictionary dimensions, three kinds of speech and noise dictionary with 1000, 500, and 100 atoms were made from 11873 speech data and 9763 noise data, respectively.

Accordingly, there are two categories for the research: i) those whose dictionary was prepared using the NMF method; and ii) the categories whose dictionaries were trained using the K-SVD method. In each category, there are three groups that have different dictionary atoms.

Tables 2 and 3 report the average percent accuracy of the proposed detector in the first two simulation groups at four different noises and different SNRs, respectively.

For computational complexity, the number of atoms in a dictionary should be considered. The larger the dictionary, the more complicated the calculations will be. However, this complexity does not slow down the

simulation. As the computational complexities of three groups are the same, therefore in comparing these three categories the obtained results suggest a better performance of each of the categories and groups. According to Table 2, in the first category, the first group has better results than the other two groups. Thus, the reduction of the dictionary atoms does not only affect the response speed but also reduces accuracy.

Table 3 also suggests that in the first category, the first group has better results compared to the other two groups. Hence, the reduction of the dictionary atoms does not only affect the response speed but also reduces accuracy.

Study of the results indicates that the first group in the second category has better results compared to two other groups.

by compare the best results of both simulations in white, babble, car and factory noises suggests that although the first group of second simulation has better results in white noise, but according to the accuracy criterion, the first category of first simulation, whose dictionary was trained by NMF method, showed better results than the other methods, whose results have been used to be compared with other methods.

Thus, NMF method operates better than K-SVD method in separation. The major difference between these two methods is eliminating negative segments in the non-negative matrix factorization method, which results in better separation of speech and noise segments.

Table 1: Simulation Test bench Parameters.

Parameters	Description
Sampling	16 KHz. 16 bit
frame size	8ms
frame window	40ms
Δ	4
Test utterances	100 TIMIT sentences.
Types of noise	White, babble , car, factory
Noise levels	-10dB to 20dB

3.2 Evaluation of the Second Algorithm

Tables 4 and 5 outline the simulation conditions as well as the characteristics and parameters of simulated cases respectively.

In STRF space, the components of the representation are driven from a three-dimensional space in each frame. The sparse representation in this space is almost impossible due to high dimensionality of the space and lack of sufficient training samples. Therefore, as previously indicated, due to the huge data volume in STRF space, each temporal frame is partitioned into some sub-cubes.

The main issue in this simulation is analysis of the conditions of the cubes: overlapping, non-overlapping or removing the cubes, enlarging and downsizing the cubes, and increasing and decreasing the number of cubes influence the obtained results.

Therefore, three experiments are designed according to the above parameters.

Mesgarani has applied 1-32 as the range for rates and 0.5-8 for the scale [6]. In order to assess the impacts of changes related to rate and scale values in simulations, the mentioned ranges of values were evaluated. It can be said that the ranges of scale and rate affect the number of samples in a cube as well as the number of cubes within a time frame. The number of dictionaries is equal to the number of cubes within a time frame.

After feature extraction, the dictionary is built using Non-Negative Matrix Factorization approach (NMF) [22]

Partitioning the space into cubes leads to emergence of the following questions:

- How to select the appropriate size of the cubes? What is the effect of this size on the performance?
- Should the cubes be overlapped? How the results alter with overlapping cubes?
- Can we ignore some of the cubes? Can we employ a portion of the set of cubes rather than all of them?

The size of cubes was selected according to the selected range for rate and scale. Also, in the first and second simulations, the size of cubes with the same or different segregation sizes on each dimension should be selected such that a time frame could be formed out of the sum of these cubes.

Therefore, the following tests are conducted to achieve the best performance of the system by addressing the answers of the above questions. In each test, the average percentage of correctly detected speech was considered as the measure of performance.

3.2.1 First experiment: Finding the proper size of the cubes

In this section, each time frame was divided into cubes of three different sizes.

In the first and second simulations, the scale and rate change from 0.25-4 cycles/octave and 2-16 Hz, respectively. Nevertheless, the size of the partition of the three dimensions of scale, rate, and frequency in the first case is different, while in the second case it is same.

Finally, in the third case, the rate and scale changes range from 0.5 to 8 cycles/octave and from 1 to 32 Hz, respectively.

The sizes of the partitions are different on the three dimensions.

In the first category, each cube has 168 samples and each time frame is divided into 96 cubes. Thus, 96 dictionaries with 1000 atoms for speech and noise are created for each time frame separately with NMF method. In the second category, each time frame consists of 32 cubes with each cube constituting 504 components.

Thus, 32 dictionaries of 1000 atoms are trained for speech and noise in each frame using the NMF method. In the third category, each cube consists of 792 samples with each time frame composed of 32 cubes. Therefore, 32 dictionaries with 1000 atoms are created for speech and noise at any time using NMF method.

Table 6 summarizes the average percentage of speech/noise detection rate in three cases of the first experiment over 100 utterances.

Studies show that the results of these three groups are not significantly different in the first experiment, though the second category has had better results than the two other groups. It suggests that the speech and noise boundaries are better separated by reducing the range of the scale and rate as well as increasing the size of the cubes, though the same size partition is also effective for the three dimensions. The cubes were partitioned in this space to simplify the calculations of four-dimensional - time spectral space. The larger the cube sizes, the higher the number of iterations of nested loops will be, thereby increasing computational complexity.

The STRF domain is a four-dimensional domain. Due to the complexity of four-dimensional computations, the domain was divided into cubes within a time frame. By increasing the number of samples within each cube, the number of nested loops in the program grows, lengthening the simulation.

Therefore, the time index was assumed fixed in every cube while the other three parameters of frequency, scale, and rate were altered.

If we consider F, R and S as the parameters for frequency, rate and scale respectively. NFq as the magnitude of samples in each cube:

$$NFq = R \times S \times F \quad (7)$$

Thus, a bigger cube will demand more calculations. If we consider the number of cubes as Q within a time frame, NFt is the value of iteration within a time frame, calculated in the following way:

$$NFt = \sum_{i=1}^Q NFq_i \quad (8)$$

Thus, more cubes within a time frame will require a longer time for computations. If we consider T as the time frame in a signal, NF is the number of iterations in a signal:

$$NF = \sum_{i=1}^T NFt_i \quad (9)$$

Hence, the size of cubes affects the complexity of the computations.

The computational complexity of the second and third cases per sample takes about 1.6 times and 3 times longer on average compared to the first category.

The complexities of the second and third cases are proportional to the number of dictionaries. The second case was less complex because of fewer samples in each cube. If the accuracy is the main concern, the overall accuracy of the second case has been slightly better than that of the two other categories, representing a trade-off between speed and accuracy.

3.2.2 Second Experiment: Cubes Overlapping

We conducted the experiments on three new cases using the second cube size of the previous experiment. In these three cases, the cubes overlap with each other within each frame.

Table 2: Performance of the proposed first VAD under four types of noise and different SNR values with NMF dictionary.

case	Number of atoms in dictionary	MEAN VAD ACCURACY (PERCENTAGE TRUE POSITIVE)							
		SNR Noise	20	15	10	5	0	-5	-10
first	1000	White	92.17%	92.10%	92.40%	90.42%	86.58%	81.06%	63.07%
		Babble	95.55%	90.29%	85.10%	81.58%	75.88%	69.64%	60.17%
		Car	95.79%	93.38%	91.81%	89.15%	81.00%	70.29%	65.3%
		Factory	93.72%	91.45%	87.31%	85.27%	80.62%	73.55%	64.93%
second	500	White	92.11%	91.95%	92.15%	90.91%	85.22%	75.45%	65.96%
		Babble	90.23%	86.40%	84.89%	79.78%	72.62%	65.67%	57.00%
		Car	91.44%	91.50%	90.34%	85.15%	79.38%	65.43%	56.20%
		Factory	89.95%	85.22%	82.36%	80.68%	78.15%	67.41%	60.34%
third	100	White	91.43%	92.87%	93.33%	86.76%	84.07%	73.17%	67.21%
		Babble	91.58%	89.29%	86.85%	78.26%	72.64%	66.33%	62.21%
		Car	96.67%	89.92%	83.79%	78.08%	69.19%	61.63%	55.02%
		Factory	90.18%	87.38%	84.65%	79.43%	75.50%	68.98%	65.77%

Table 3: Performance of the proposed first VAD under four types of noise and seven specific SNR values with K-SVD dictionary.

case	Number of atoms in dictionary	MEAN VAD ACCURACY (PERCENTAGE TRUE POSITIVE)							
		SNR Noise	20	15	10	5	0	-5	-10
first	1000	White	95.82%	94.43%	91.26%	90.72%	83.58%	72.29%	60.45%
		Babble	94.25%	87.54%	81.60%	78.46%	68.18%	66.13%	54.68%
		Car	96.10%	92.14%	89.94%	81.34%	70.80%	61.24%	53.58%
		Factory	92.35%	89.23%	85.47%	80.72%	77.15%	69.59%	57.36%
second	500	White	96.27%	95.88%	92.78%	90.16%	84.21%	74.96%	63.58%
		Babble	92.44%	85.67%	81.09%	76.05%	67.15%	58.74%	53.54%
		Car	95.30%	91.54%	88.37%	79.54%	68.61%	59.21%	52.32%
		Factory	90.69%	83.48%	80.56%	78.15%	71.37%	65.28%	58.92%
third	100	White	94.65%	93.98%	90.84%	86.94%	81.64%	71.94%	61.77%
		Babble	93.63%	86.36%	82.49%	76.70%	67.28%	60.51%	53.49%
		Car	95.54%	92.59%	89.48%	79.91%	70.42%	64.56%	57.61%
		Factory	90.15%	85.44%	84.32%	80.57%	73.68%	65.04%	58.92%

Table 4: Simulation Test bench Parameters.

Parameters	Description
Sampling	16 KHz. 16 bit
frame size	32 ms
Test utterances	100 TIMIT sentences.
Types of noise	White, babble , car, factory
Noise levels	-10dB to 20Db

Table 5: The characteristics and parameters of simulated cases.

Experiment	cubes partitioning (in a time frame)	Case	Number of samples of each cube	Number of small cubes of each time frame	Dimensions of speech and noise dictionaries	Range of scale (Cycle/Octave)	Range of rate(HZ)
1	Considering all of cubes	First	168	96	168×1000	0.25 - 4.00	2 - 16
		second	504	32	504×1000	0.25 - 4.00	2 - 16
		Third	792	32	792×1000	0.5 - 8.00	1 - 32
2	Overlapping cubes	First	280	96	280×1000	0.25 - 4.00	2 - 16
		second	504	62	504×1000	0.25 - 4.00	2 - 16
		Third	504	80	504×1000	0.25 - 4.00	2 - 16
3	removing some cubes	First	343	36	343×1000	0.5 - 8.00	1 - 32

Table 6: Performance of the proposed VAD under four types of noise and seven specific SNR values without overlapping.

case	Number of samples of each cube	MEAN VAD ACCURACY (PERCENTAGE TRUE POSITIVE)							
		SNR Noise	20	15	10	5	0	-5	-10
first	168	White	91.61%	91.35%	91.49%	90.91%	87.77%	82.09%	82.92%
		Babble	91.37%	91.76%	90.96%	89.77%	83.73%	78.58%	69.46%
		Car	90.68%	91.29%	90.47%	89.44%	86.67%	77.48%	64.13%
		Factory	90.15%	88.41%	85.27%	85.97%	82.61%	80.02%	73.21%
second	504	White	93.09%	92.45%	92.94%	89.34%	90.48%	90.93%	86.93%
		Babble	94.04%	93.37%	93.39%	95.29%	92.78%	84.57%	75.31%
		Car	93.45%	94.06%	93.85%	95.36%	96.11%	91.87%	82.50%
		Factory	92.54%	91.48%	91.62%	94.10%	93.31%	89.25%	80.96%
third	792	White	92.20%	92.34%	93.27%	88.65%	85.00%	87.84%	86.20%
		Babble	93.34%	93.33%	93.14%	93.55%	90.43%	87.64%	81.20%
		Car	92.90%	92.54%	92.04%	89.50%	92.91%	89.83%	80.69%
		Factory	90.64%	91.01%	90.28%	92.82%	91.51%	88.34%	78.74%

In the first case, the overlapping occurs in three cubes. A total of 96 dictionaries were formed separately for speech and noise. The rate and scale ranges have been as same as the previous second case. The results are presented in Table 7.

The second case overlaps in four cubes. In the case, 62 dictionaries were made separately for speech and noise with 504 attributes for each atom, with Table 7 tabulating the results.

In the third case, the overlap is in five cubes, with each cube composed of 504 samples and each time frame covering 80 cubes. Therefore, 80 dictionaries were made for speech and noise with 1000 atoms.

The segregation sizes of the three dimensions of the scale as well as the rate and the frequency have been different in the first and third case. However, they have been the same in the second case.

Studies suggest that the results of the second case have been better than those of the other two cases. In addition, the increase in the number of overlapping cubes worsens the detection rate. Although overlapping the cubes at SNRs above zero results in better rates in babble noise, increasing the number of overlapping cubes showed no significant effect overall.

On the other hand, if N is the number of overlapping cubes, as with Eq. 7, NF_{qov} is defined as the magnitude of samples in each cube with overlaps:

$$NF_{qov} = N \times R \times S \times F \quad (10)$$

$$NF_{tov} = \sum_{i=1}^Q NF_{qov_i} \quad (11)$$

$$NF_{ov} = \sum_{i=1}^T NF_{tov_i} \quad (12)$$

Therefore, similar to previous section, the size of cubes highly affects the complexity of the computations. The complexity of the algorithm is 25% and 50% greater than that of the first case for the second and third cases respectively.

3.2.3 Third Experiment: Removing some cubes

So far, when using small cubes overlapping, we have considered the whole data with redundancy in the time frame. We now consider only a number of cubes in making the final decision. However, in STRF space, the low frequency, low rate, and low scale portion of the space are considered to be more important [23]. Therefore, we considered low frequencies, low rates, and low scales cubes (36 cubes) with the size 7*7*7. Accordingly, 36 dictionaries were made for speech and noise with 343*1000 dimensions. In this test, the scale

and rate ranged from 0.5 to 8.00 cycles/octave and 1 to 32 Hz, respectively. The results are reported in Table 8.

The results of the second case of the first experiment which has considered all cubes within one time frame, in addition to the first overlapping case of the second experiment demonstrate its superiority. Also, the first case of the third experiment which considers the low portion of the space has been compared in this assessment. According to the comparisons of best result of three experiments, we can conclude that the second case of the first experiment and the first case of the third experiment at beyond 0dB have a better performance with close outputs in relation to the first overlapping case of the second experiment.

The result is in contrast with SNRs below 0dB. Overall, the first case of the third experiment slightly outperforms other cases and will be compared with other competing VADs in the next section. Accordingly, better results were achieved by removing cubes away from the source and keeping the three-dimensional information of scale, rate, and frequency near the source.

3.3 Results Comparison

We proposed two algorithms for the speech detector. The first algorithm was proposed using sparse representation of two-dimensional auditory spectrogram space exploring different atomic sizes of dictionaries and two dictionary learning methods. It presented good results at high SNRs. On the other hand, the second algorithm, which has been more complicated than the first one, suggests a speech detector employing the sparse representation of the STRF four-dimensional space. Due to the large volume of STRF's four-dimensional space, this space was divided into sub-cubes for each time frame, with dictionaries trained based on the conditions of these cubes by NMF training algorithm.

Figs. 9, 10, 11 and 12 compare the best results of both algorithms in white, babble, and car noises, respectively.

Investigation of these three diagrams suggests that although the four-dimensional space of STRF has huge computational complexity, unlike the two-dimensional space which considers the overall frequency behavior, it has used local frequency behaviors, which yielded better characteristics and results.

Therefore, the first case of the third experiment in the second algorithm slightly outperforms other cases and will be compared with other competing VADs.

The superior performance of the proposed VAD is illustrated through nonspeech–speech error (NDS) and

speech–nonspeech error (MSC) [24]. Noise detected as speech (NDS) is the proportion of nonspeech frames misclassified as being speech.

Mid-speech clipping (MSC) is the proportion of speech frames erroneously classified as being non-speech

In comparison, some of up-to-date voice-activity detection methods were compared against the proposed VAD algorithms, which have proved to be noise robust. They are LTSV [2], Sohn [3], G.729B [5], Mesgerani's VAD [6], Harmfreq [25], LTSD [26], LSFM [27], and LTPD [28].

In Fig. 13, the proposed VAD has even a lower error rate under zero SNRs compared to other VADs. Specifically, it should be noted that Mesgerani's VAD considers all noisy speeches as noise at low SNRs (i.e. practically it did not perform any classification). In contrast, our proposed STRF-sparse VAD successfully classified the noise and speech with a low error rate at even low SNRs.

Fig. 14 represents the comparison of our VAD against state-of-the-art VADs. Mesgerani and G729B degrade at low SNRs. At high SNRs, the proposed method error is also the same as Mesgerani's methods.

Totally, comparing the results of these VADs, it can be observed that the proposed VAD outperforms the other state-of-the-art methods compared here.

Because of the similarity of structures of babble noise and speech, at some SNRs, the proposed VAD NDS performance degrades in our method in contrast to MSC performance.

4. Conclusion

In this paper, two new VAD algorithms were proposed based on sparse representation in spectro-temporal domain.

The simulation results indicated that the results of considering total cubes or removing some of them within a time frame are similar and at SNRs below zero, overlapping cubes perform better. However, if we consider the computational complexity, in general, removing some cubes is a better tradeoff than the other two experiments.

The simulation results suggested that our second proposed VAD algorithm is effective in low SNR situations. Our future work focuses on developing a low calculation complexity version of the algorithm to be suitable for real-time processing.

Table 7: Performance of the proposed VAD under four types of noise and seven specific SNR values with overlapping.

case	Number of samples of each cube	MEAN VAD ACCURACY (PERCENTAGE TRUE POSITIVE)							
		SNR noise	20	15	10	5	0	-5	-10
first	280	White	91.94%	89.26%	88.38%	86.91%	87.80%	85.78%	84.56%
		Babble	88.78%	87.33%	87.16%	86.84%	85.55%	81.23%	77.34%
		Car	91.68%	91.06%	90.74%	89.32%	88.83%	83.47%	80.62%
		Factory	90.27%	88.41%	86.98%	87.55%	86.39%	83.61%	79.01%
second	504	White	91.76%	91.80%	91.86%	89.15%	86.26%	86.42%	86.55%
		Babble	91.47%	91.27%	91.27%	90.48%	89.85%	80.72%	75.47%
		Car	93.30%	93.70%	93.96%	90.50%	84.61%	83.72%	81.84%
		Factory	91.55%	91.64%	91.71%	91.07%	88.35%	82.15%	78.92%
third	504	White	86.88%	87.42%	87.64%	89.71%	91.89%	88.92%	86.79%
		Babble	90.64%	90.73%	90.89%	87.24%	80.68%	78.69%	76.05%
		Car	87.43%	85.63%	84.92%	84.17%	83.32%	81.52%	80.19%
		Factory	89.33%	90.12%	90.26%	88.41%	82.09%	79.85%	75.76%

Table 8: Performance of the proposed First case VAD under four types of noise and seven specific SNR values after removing some cubes.

case	Number of samples of each cube	MEAN VAD ACCURACY (PERCENTAGE TRUE POSITIVE)							
		SNR noise	20	15	10	5	0	-5	-10
first	343	White	94.59%	94.82%	95.53%	94.19%	91.42%	90.11%	87.35%
		Babble	94.44%	93.84%	93.12%	89.86%	89.20%	88.43%	76.84%
		Car	95.56%	96.04%	94.41%	94.96%	95.24%	91.75%	82.23%
		Factory	94.98%	94.87%	94.32%	93.51%	92.11%	91.24%	88.69%

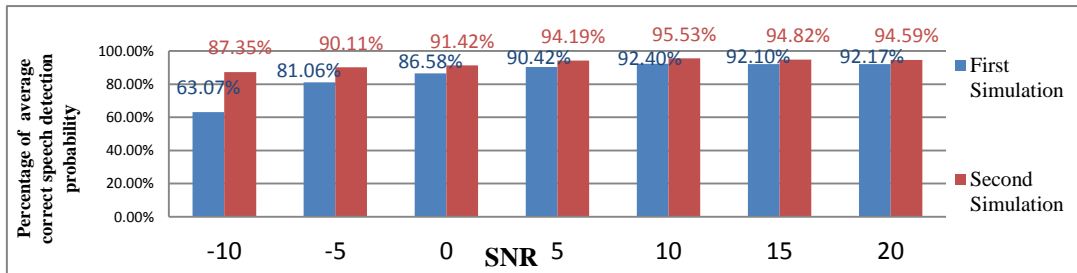


Fig. 9 Comparison of the best results of both simulations in white noise.

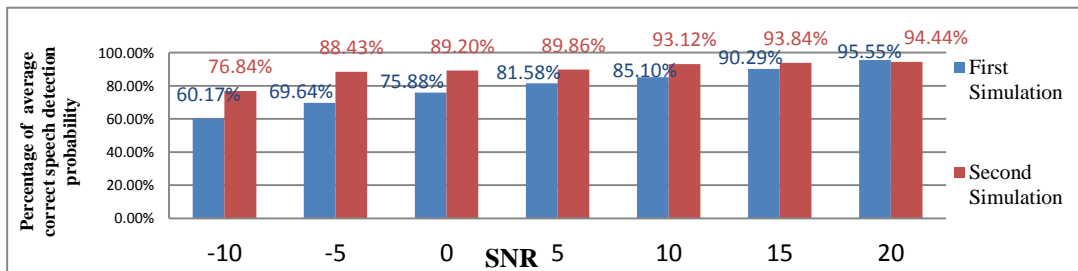


Fig. 10 Comparison of the best results of both simulations in babble noise.

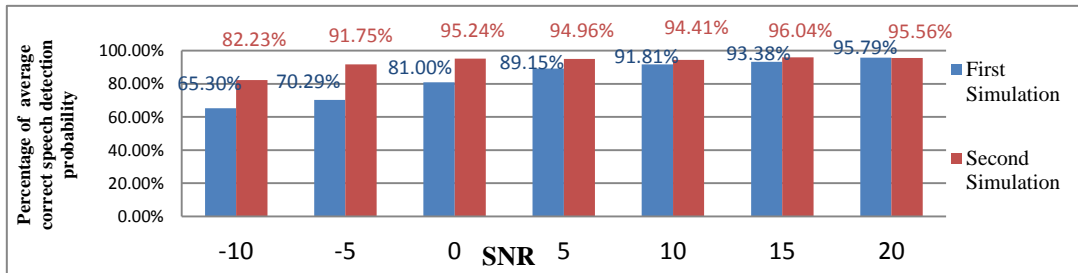


Fig. 11 Comparison of the best results of both simulations in car noise.

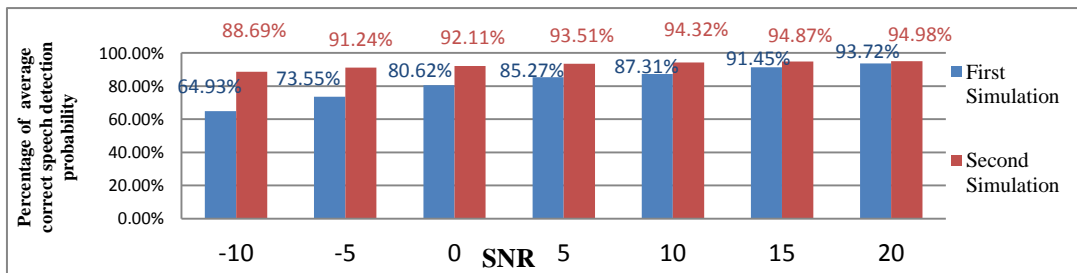


Fig. 12 Comparison of the best results of both simulations in factory noise.

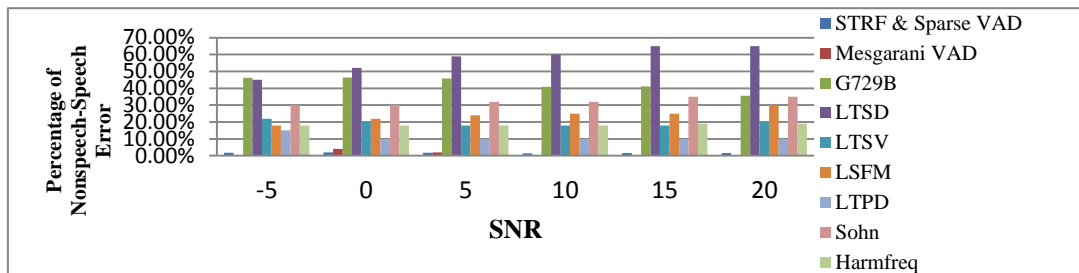


Fig. 13 Nonspeech-speech Error(NDS).

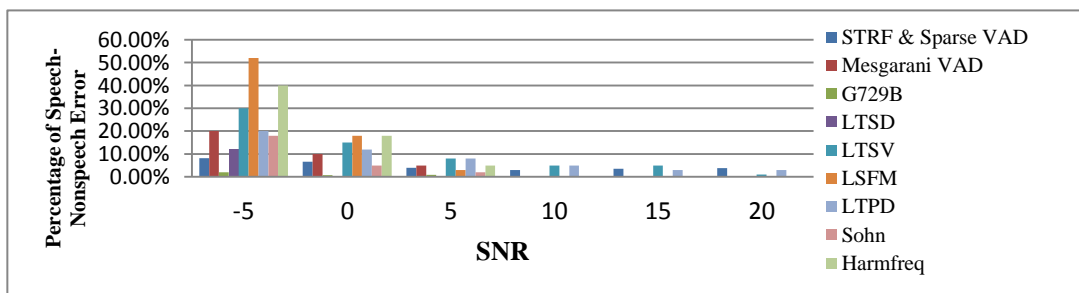


Fig. 14. Speech-nonspeech Error(MSC).

References

[1] M. Graciarena, A. Alwan, D. Ellis, H. Franco, L. Ferrer, J. H. L. Hansen, A. Janin, B. S. Lee, Y. Lei, V. Mitra, N. Morgan, S.O. Sadjadi, T.J. Tsai, N. Scheffer, L.N. Tan and B. Williams, "All for one: feature combination for highly channel-degraded speech activity detection," in *ISCA Interspeech*, pp.709-713, 2013.[2] M. Eshaghi, and M. R. Karami Mollaei, "Voice activity detection based on using wavelet packet," in *Digital Signal Processing*, vol. 20, No. 4, pp. 1102-1115, 2010.

[3] Y. Datao, H. Jiqing, Z. Guibin and Z. Tieran, "Sparse power spectrum based robust voice activity detector," in *IEEE International Conference on Acoustics, Speech and Signal Processing (ICASSP)*, Kyoto, pp. 289-292, 2012

[4] W Hongzhi, X Yuchao and L Meijing, "Study on the MFCC similarity-based voice activity detection algorithm," in *International Conference on Artificial Intelligence, Management Science and Electronic Commerce (AIMSEC)*, Dengleng, 2011.

- [5] S.G. Mallat, "A theory for multiresolution signal decomposition: the wavelet representation," in *IEEE Transactions on Pattern Analysis and Machine Intelligence*, vol.11, No.7, pp. 674-693,1989.
- [6] Nima Mesgarani, and Shihab Shamma, "Denoising in the Domain of Spectro-temporal Modulations", in *EURASIP Journal on Audio, Speech, and Music Processing*, ID. 42357, 8 pages, doi:10.1155/2007/42357,2007.
- [7] Weifeng Li, Yicong Zhou, Norman Poh, Fei Zhou, and Qingmin Liao, "Feature Denoising Using Joint Sparse Representation for In-car Speech Recognition", in *IEEE Transactions on audio, speech, and language processing*, vol.20, No.7, pp. 681-684, 2013.
- [8] N. Mesgarani, S. David, and S.A. Shamma, "Representation of phoneme in primary auditory cortex: how the brain analyzes speech," in *IEEE International Conference on Acoustic, Speech and Signal Processing (ICASSP)*, Hawaii, April, 2007.
- [9] Majid Mirbagheri, Nima Mesgarani, and Shihab Shamma, "Nonlinear filtering of spectrotemporal modulation in speech enhancement," in *IEEE International Conference on Acoustic, Speech and Signal Processing (ICASSP)*, pp. 5478-81, 2010.
- [10] C. Kim, K. Kumar and R. M. Stern, "Binaural sound source separation motivated by auditory processing," in *Acoustics, Speech, and Signal Processing, IEEE International Conference on ICASSP2011*, Prague, 2011.
- [11] C. Mart'inez, J. Goddardb, D. Milone, and H. Rufiner, "Bio inspired sparse spectro-temporal representation of speech for robust classification," in *Computer Speech and Language*, vol.26, No.5, pp. 336-345, 2012.
- [12] Jort Florent Gemmeke, Hugo Van Hamme, Bert Cranen, and Lou Boves, "Compressive Sensing for Missing Data Imputation in Noise Robust Speech Recognition", in *IEEE Journal of selected topics in signal processing*, vol.4, No.2, pp. 272-287, 2010.
- [13] B. K. Natarajan, "Sparse approximate solutions to linear systems," in *Society for Industrial and Applied Mathematics (SIAM J. Computer)*, vol.24, No.2, pp.227-234, 1995.
- [14] Mohadese Eshaghi, Farbod Razzazi, and Alireza Behrad, "A voice activity detection algorithm in spectro-temporal domain using sparse representation," in *International Journal of Machine Learning and Cybernetics*, 2018, DOI: 10.1007/s13042-018-0856-z.
- [15] G. Hosein Mohimani, Massoud Babaie-Zadeh, and Christian Jutten, "A fast approach for overcomplete sparse decomposition based on smoothed L0 norm," in *IEEE Transactions on Signal Processing*, vol.57, No.1, pp.289-301, 2009.
- [16] K. Kreutz-Delgado, J.F. Murray, B.D. Rao, K. Engan, T. Lee, and T.J. Sejnowski, "Dictionary learning algorithms for sparse representation," in *Neural Computer*, vol.15, No.2, pp.349-396,2003.
- [17] P. O. Hoyer, "Non-negative matrix factorization with sparseness constraints," in *Journal of Machine Learning Research*, vol.5, No. 9, pp.1457-1469, 2004.
- [18] R. Zdunek, and A. Cichocki, "Non-negative matrix factorization with quadratic programming," in *Neurocomputing*, vol.71, No.10-12, pp. 2309-2320, 2007
- [19] M. Aharon, M. Elad, A. Bruckstein, "K-SVD: An algorithm for designing over complete dictionaries for sparse representation," in *IEEE Transactions on Signal Processing*, vol.54, No.11, pp.4311-4322, 2006.
- [20] W. M. Fisher, G. R. Doddington, M. Goudie and M. Kathleen, "The DARPA speech recognition research database: specifications and status", in *DARPA Workshop on Speech Recognition*, 1986.
- [21] A. Varga, H. J. M. Steeneken, M. Tomlinson and D. Jones, "The NOISEX-92 study the effect of additive noise on automatic speech recognition", Documentation included in the NOISEX-92 CD-ROMs, 1992.
- [22] B. Raj, T. Virtanen, S. Chaudhure, and R. Singh, "Non-negative matrix factorization based compensation of music for automatic speech recognition," *International Conference on Speech and Language Processing*, 2010.
- [23] N. Mesgarani, S. Shamma, and M. Slaney, "Speech discrimination based on multiscale spectro-temporal modulations," in *IEEE International Conference on Acoustics, Speech and Signal Processing*, vol4, No.1, pp.601-604, 2004.
- [24] Ian Vince McLoughlin, "Super-Audible Voice Activity Detection," in *IEEE Transactions on Speech and Audio Processing*, vol. 22, No.9, pp.1424-1433, 2014.
- [25] L. N. Tan, B. J. Borgstrom, and A. Alwan, "Voice activity detection using harmonic frequency components in likelihood ratio test," in *IEEE International Conference on Acoustics, Speech, and Signal Processing (ICASSP)*, 2010.
- [26] J. Ramirez, J.C. Segura, C. Benitez, A. de la Torre and A. Rubio, "Efficient voice activity detection algorithms using long-term speech information," in *Speech Communication*, vol.42, No.3-4, pp.271-287, 2004
- [27] M. Yanna and A. Nishihara, "Efficient voice activity detection algorithm using long-term spectral flatness measure," in *EURASIP Journal on Audio, Speech and Music Processing*, 2013, DOI: 10.1186/1687-4722-2013-21.
- [28] Xu-Kui Yang, Liang He, Dan Qu and Wei-Qiang Zhang, "Voice activity detection algorithm based on long-term pitch information," in *EURASIP Journal on Audio, Speech, and Music Processing*, 2016, DOI: 10.1186/s13636-016-0092-y.

Mohadese Eshaghi received her B.Sc. and M.Sc. in Electrical Engineering from Mazandaran University in 2005 and 2008, respectively. She received her Ph.D. from Department of Electrical and Computer Engineering, Islamic Azad University, Science and Research Branch in 2019 in Electrical Engineering. Her research interests include Speech enhancement, Image processing, Pattern recognition methods and Data mining.

Farbod Razzazi received his B.Sc. and M.Sc. in Electrical Engineering from Sharif University of Technology in 1994 and 1996, respectively. He received his Ph.D. from Amirkabir University of Technology (Tehran Polytechnic) in 2003 in Electrical Engineering. He is currently an Associate Professor in Department of Electrical and Computer Engineering, Islamic Azad University, Science and Research Branch, Tehran, Iran. His current research interests are signal forensics and anti-forensics, pattern recognition methods and their applications in statistical signal processing systems.

Alireza Behrad received the B.Sc. degree in Electrical Engineering from Tabriz University, Tabriz, Iran, in 1995. In 1998, he received the M.Sc. degree in Electrical Engineering from Sharif University of Technology, Tehran, Iran. He received the Ph.D. degree in Electrical Engineering from Amirkabir University of Technology, Tehran, Iran, in 2004. Currently, he is an associate professor of Engineering Faculty, Shahed University, Tehran, Iran. His research fields are image and video processing, machine vision and digital multimedia authentication.